INDIAN INSTITUTE OF TECHNOLOGY GUWAHATI

UNLOCKING THE MULTI-FACETED REACTIVITY OF 4-HYDROXYTHIOCOUMARIN:

Sustainable Synthesis of Novel Hybrid Heterocyclic Scaffolds with Therapeutic Potential

A Dissertation Submitted to the

Indian Institute of Technology Guwahati

As Partial Fulfilment for the Degree of

Doctor of Philosophy (Ph.D.)

Submitted By

Ujjwal Jyoti Goswami

Roll Number: 196122110

Under Supervision of

Prof. Abu Taleb Khan

Department of Chemistry

Indian Institute of Technology Guwahati

Guwahati-781039, Assam

July-2025

—Dedication—

In loving memory of my **mother**,
whose boundless love and silent sacrifices shaped my life, and whose memory continues to guide me every step of the way.

And to my **father**,
whose quiet strength and unwavering belief laid the foundation of all that I have become.

Indian Institute of Technology Guwahati
Guwahati – 781039, India
e-mail: ujyoti@iitg.ac.com

Ujjwal Jyoti Goswami
Research Scholar

DECLARATION

I, Ujjwal Jyoti Goswami, enrolled in the Ph.D. program in December 2019 in the Department of Chemistry at the Indian Institute of Technology Guwahati. I began my research work under the supervision of Prof. Abu Taleb Khan in October 2021. The delay was primarily due to the extended closure of the Institute for nearly 10 months during the COVID-19 pandemic, which significantly limited access to laboratory facilities. In addition to this, my deteriorating health in the aftermath of the pandemic further affected the continuity of my research, leading to a considerable loss of productive time.

I hereby declare that the work presented in this thesis, titled *"Unlocking the Multi-Faceted Reactivity of 4-Hydroxythiocoumarin: Sustainable Synthesis of Novel Hybrid Heterocyclic Scaffolds with Therapeutic Potential"*, is the result of investigations carried out by me under the supervision of Prof. Abu Taleb Khan in the Department of Chemistry, Indian Institute of Technology Guwahati.

Wherever the work draws upon the insights or findings of other researchers, appropriate acknowledgements have been made in accordance with standard scientific conventions.

Ujjwal Jyoti Goswami

IIT Guwahat
4th July, 2025

Ujjwal Jyoti Goswami
Roll No.: 196122110

Indian Institute of Technology Guwahati
Guwahati – 781039, India
Tel. No.: +91-361-2582343
Fax No.: +91-361-2582349
e-mail: atk@iitg.ac.com

Abu Taleb Khan
Professor of Chemistry

4th July 2025

CERTIFICATE

This is to certify that Mr. Ujjwal Jyoti Goswami has been working in my research group since December 2019 as a regular, registered Ph.D. student in the Department of Chemistry at the Indian Institute of Technology Guwahati. His initial research progress was delayed due to the COVID-19 pandemic, during which the Institute remained closed for nearly ten months. This period, along with subsequent health-related challenges, resulted in the loss of valuable research time. Nevertheless, he has worked with sincerity and perseverance throughout the course of his doctoral program.

I am forwarding his thesis, entitled *"Unlocking the Multi-Faceted Reactivity of 4-Hydroxythiocoumarin: Sustainable Synthesis of Novel Hybrid Heterocyclic Scaffolds with Therapeutic Potential"*, for submission in partial fulfilment of the requirements for the award of the Ph.D. (Science) degree from this Institute.

I certify that he has met all academic and research requirements as per the Institute's regulations, and that the work embodied in this thesis has not been submitted elsewhere for the award of any degree or diploma.

Prof. Abu Taleb Khan
Thesis Supervisor

Acknowledgments

It is with immense gratitude and a deep sense of fulfilment that I acknowledge the many individuals whose support, guidance, and presence have shaped this journey. Completing this Ph.D. has been both a rigorous and transformative experience, and I feel truly fortunate to have received encouragement from such remarkable people along the way.

First and foremost, I express my deepest gratitude to Prof. Abu Taleb Khan, my research supervisor, for his generous support, constant encouragement, and thoughtful mentorship. His scientific vision and clarity of thought have guided every stage of this work. From him, I have learned not only research skills but also patience, perseverance, and a sense of responsibility that will remain with me well beyond this academic pursuit. His personal kindness and steady moral support during difficult phases are something I will always hold close to my heart.

I also extend my sincere thanks to the members of my Doctoral Committee, Prof. L. M. Kundu (Chairman), Dr. K. P. Bhabak, and Prof. C. Mukherjee, for their valuable suggestions, critical evaluations, and academic support throughout my PhD tenure.

I am grateful to the Department of Chemistry, IIT Guwahati, for providing a vibrant academic atmosphere and access to excellent research infrastructure. My sincere thanks to all faculty members and staff of the department for their cooperation and kindness.

I also express special appreciation to Dr. Kalishankar Bhattacharyya and his student Kaushik Soni for their contribution to the computational studies related to my work.

I am also thankful to Dr. Prabal Banerjee, Professor, Department of Chemistry, IIT Ropar, and Dr. Radhakrishnanand P, Professor at NIPER Guwahati, for their support in providing HRMS data. I extend my appreciation to their students as well, for their kind assistance in recording the HRMS data of the organic compounds.

I gratefully acknowledge the financial support provided by the Indian Institute of Technology Guwahati, and the various instrumental facilities extended by the Department of Chemistry including 400 and 500 MHz NMR, IR, UV–Vis and fluorescence spectroscopy, and X-ray diffraction. I also extend my thanks to the Central Instrument Facility for access to the 600 MHz NMR and HRMS facilities, and to the North East Centre for Biological Sciences and Healthcare Engineering for the use of the 400 MHz NMR facility.

I would like to sincerely thank Dr. Babulal Das for his invaluable help with XRD data analysis and for his constant support during my teaching assistantship. I am also thankful to Mr. Imdadul Islam for his patient instruction on the operation of the 500 MHz NMR machine. I am equally grateful to the many NMR instrument operators, who often stepped in to help me troubleshoot problems and taught me something new along the way.

My warmest thanks to my wonderful labmates in Prof. Khan's group, both past and present. The countless discussions, shared frustrations, laughter, and support have been integral to my experience. In particular, I wish to mention Dr. Md. Belal, Dr. Santa Mondal, Dr. Saghir Ali, Dr. Sabina Yashmin, Anjela Xalxo, Dr. Arnab Mandal, Ahmad Ali, Dr. Simra Faraz, Mukesh

Kumar, Anil R Pawar, Satyajit Singh, Eman Ali, Nisha Rani, Halida Khatun, Devendra Kumar, Somesh Shekhar Chaugule, Afzal, and Dr. Gyani Yumnum. Your presence made the lab more than just a place of work. Each of them has, in some way or another, contributed to my learning and to the spirit of cooperation in the lab.

I have also had the opportunity to work with a number of dedicated M.Sc. and summer trainees, Mapleleaf Basumatary, Kusum, Raihan Ahmed, Sayan Sarkar, Pranami Barman, Mehnaz Farhin, and Arunabh Sarmah, whose interest and involvement added to the overall momentum of our group.

I extend my deepest gratitude to some of the most wonderful people I had the pleasure of meeting outside the lab: Dr. Sandeep Kumar, Mithu Roy, Sangay Moktan, and Jyoti Gangwar. Your steady companionship, encouragement, and sense of perspective throughout this journey were invaluable. I would also like to acknowledge Hirak, Pallav, Surjya, Aditya, and Jagajivan, whose kindness and occasional conversations, encountered along the way, added warmth to the everyday rhythm of campus life.

I am grateful to Sandeep Kumar for his invaluable assistance in resolving crystallographic structures and for helping me to learn fluorescence studies, and to Sabina Yashmin for helping me to learn UV-Vis spectroscopy.

I remain especially indebted to Sabina Yashmin, Anjela Xalxo, and Ahmad Ali for standing firmly by my side through the most trying phases of this endeavour, offering unwavering support and empathy when I needed it most. I am thankful to someone who, even unknowingly, inspired moments of reflection and growth during this journey.

I am also thankful to someone who, even unknowingly, inspired moments of reflection and growth during this journey, reminding me of the strength that comes from sincerity and patience.

I offer my deepest and most heartfelt gratitude to my late mother, whose love, strength, and sacrifices continue to shape who I am. To my father, I am profoundly grateful, not only for his enduring support, but also for the immense sacrifices he has made silently and selflessly throughout my life. His quiet strength and unshakeable belief in me have been a constant source of motivation. To my elder sister, I remain grateful for her quiet encouragement and affection. And to my two beloved little ones: my nephew Baby Om and my niece Baby Idha, your presence brought unspoken comfort, light, and laughter into my life during some of its most difficult days. A special and heartfelt note of gratitude goes to my elder brother, whose strength and guidance have shaped every step of my journey. Through every joy and hardship, his unwavering presence has been my greatest blessing.

Lastly, I am forever grateful to the Almighty for granting me the strength, clarity, and patience to persevere through this long and demanding journey.

Ujjwal Jyoti Goswami

Abstracts

The following sections present chapter-wise abstracts summarizing the key scientific findings, synthetic strategies, and conceptual developments described in each chapter of the thesis. Each abstract is accompanied by a graphical representation, where applicable, to provide a concise visual overview of the core transformations and outcomes. Together, these summaries offer a self-contained view of the research progression and highlight the thematic connections between chapters.

Chapter 1

4-Hydroxycoumarin and its derivatives are well-established scaffolds in medicinal chemistry, valued for their reactivity and biological activity. Replacing oxygen with sulfur yields thiocoumarins, which exhibit distinct electronic properties and synthetic potential, yet remain underexplored. This chapter reviews the structural features, reactivity patterns, and medicinal relevance of 4-hydroxythiocoumarins and their dithio analogs, highlighting literature examples and also discussing molecular hybridization strategies relevant to drug design. It also outlines synthetic approaches to 4-hydroxythiocoumarin derivatives, including a revised methodology, reaction optimization, and compound characterization. These foundational insights form the basis of the design and synthesis of thiocoumarin-derived hybrids discussed in later chapters.

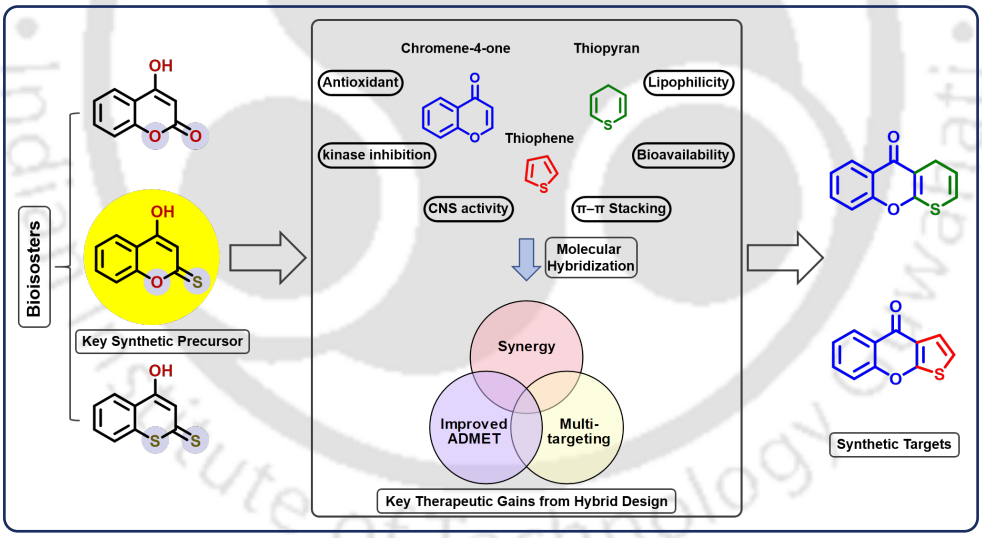

Chapter 2

A series of previously unreported pentacyclic-dione derivatives containing three heteroatoms within a fused ring system were synthesized from 4-hydroxythiocoumarins and aryl (heteroaryl) or alkyl aldehydes *via* a pseudo-three-component reaction. The transformation proceeds under solvent- and catalyst-free conditions through Knoevenagel condensation of 4-hydroxythiocoumarin with aldehyde, followed by Michael addition with another molecule of 4-hydroxythiocoumarin, with the elimination of H_2S to furnish the final product. The method offers mild conditions, good yields, broad substrate scope, and avoids chromatographic purifi-

cation. Its excellent atom economy and minimal waste generation reflect strong alignment with key principles of green chemistry.

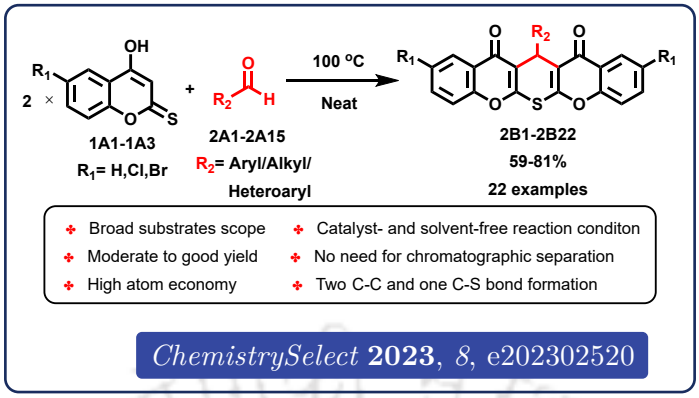

Chapter 3

The alkylation of 4-hydroxythiocoumarins was carried out using a range of allyl and propargyl bromides in the presence of potassium carbonate in anhydrous acetone at room temperature, yielding the corresponding *S*-alkylated derivatives with high regioselectivity. These intermediates underwent thio-Claisen rearrangement to furnish novel sulfur-containing heterocycles, with the outcome of the rearrangement notably influenced by the solvent in the case of *S*-propargyl ethers. Additionally, a direct cyclization protocol was developed wherein 4-hydroxythiocoumarins reacted with 2-methylbut-3-yn-2-ol in the presence of catalytic *p*-toluenesulfonic acid in nitromethane at elevated temperature, providing the cyclised products efficiently. Density Functional Theory (DFT) calculations were employed to explore the mechanistic pathways and rationalize the formation of solvent-dependent products. Overall, the methodology offers good to excellent yields, high regioselectivity, and favorable atom economy under relatively mild and metal-free conditions.

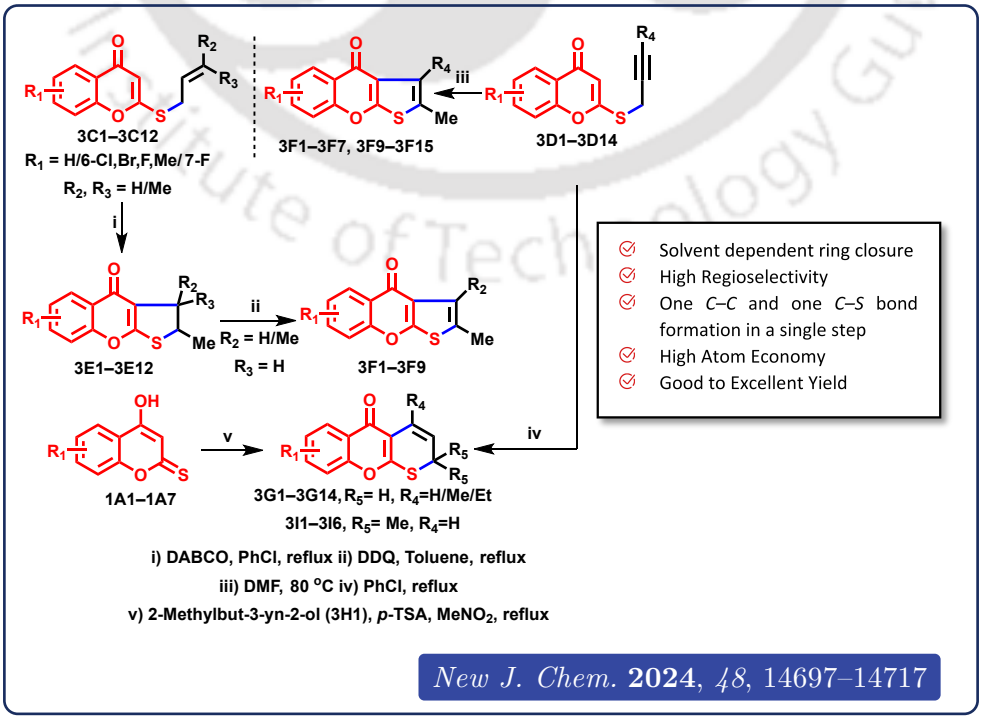

Chapter 4

A mild and efficient one-pot three-component strategy was developed for the synthesis of substituted thieno[2,3-*b*]chromen-4-one derivatives bearing pendant imine functionalities. The transformation involves the reaction of 4-hydroxythiocoumarin, salicylaldehyde (or aryl aldehydes), and *trans*-β-nitrostyrene. The reaction proceeds *via* a Michael addition between 4-hydroxythiocoumarin and *trans*-β-nitrostyrene, followed by intramolecular cyclization through nucleophilic attack. Notably, the protocol features an unusual oxime-to-amine conversion *via* a disproportionation pathway that occurs without the need for external reagents, proceeding to Schiff base formation with the aldehyde component. The methodology exhibits excellent regioselectivity and enables the concurrent formation of one C—C, one C—S, and two C—N bonds in a single operation. The process avoids metal catalysts, minimizes waste, and proceeds under mild conditions, reflecting good alignment with green chemistry principles.

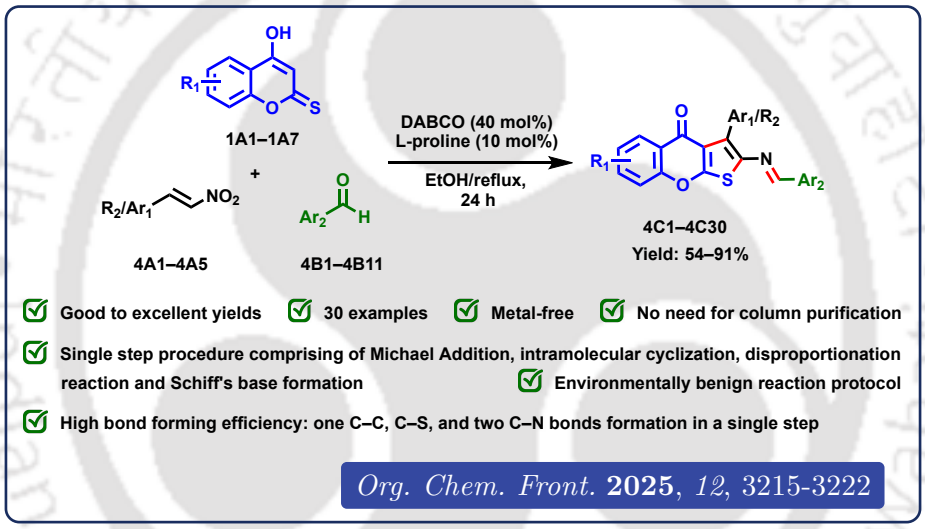

Table of contents

List of Abbreviations

5-HT – 5-Hydroxytryptamine or Serotonin

NaH – Sodium hydride

A549 – Human alveolar basal epithelial cell line derived from lung carcinoma

ADMET – Absorption, Distribution, Metabolism, Excretion, and Toxicity

ALR2 – Aldose Reductase

ATR – Attenuated Total Reflectance

CCDC – Cambridge Crystallographic Data Centre

$\mathbf{CDCl_3}$ – Deuterated Chloroform

CE – Crown ether

COSY – Correlation Spectroscopy

$\mathbf{CS_2}$ – Carbon disulfide

CSA – Camphorsulfonic acid

DABCO – 1,4-Diazabicyclo[2.2.2]octane

DDQ – 2,3-Dichloro-5,6-dicyano-1,4-benzoquinone

DFT – Density Functional Theory

DKHDA – Domino-Knoevenagel-hetero-Diels–Alder reaction

DMF – *N*,*N*-Dimethylformamide

DMSO – Dimethyl Sulfoxide

DMSO-d_6 – Deuterated Dimethyl Sulfoxide

DNA – Deoxyribonucleic Acid

DNA-PK – DNA dependent protein kinase

EDG – Electron-Donating group

E-factor – Environmental Factor (mass of waste per mass of product)

ESI – Electrospray Ionization

EWG – Electron-Withdrawing group

FT – Fourier Transform

$\mathbf{H_2S}$ – Hydrogen sulfide

$\mathbf{H_2SO_4}$ – Sulfuric acid

HIV – Human Immunodeficiency Virus

HOMO – Highest Occupied Molecular Orbital

HRMS – High-Resolution Mass Spectrometry

HSQC – Heteronuclear Single Quantum Coherence

IL-6 – Interleukin 6

iNOS – Inducible Nitric Oxide Synthase

IR – Infrared

Lawesson's reagent – 2,4-Bis(4-methoxyphenyl)-1,3,2,4-dithiadiphosphetane 2,4-disulfide

LUMO – Lowest Unoccupied Molecular Orbital

MCF-7 – Michigan Cancer Foundation-7

m-CPBA – *meta*-Chloroperoxybenzoic Acid

MCR – Multicomponent Reaction

MeCN – Acetonitrile

$\mathbf{NEt_3}$ – Triethylamine

$\mathbf{NH_4OAc}$ – Ammonium acetate

NMR – Nuclear Magnetic Resonance

OFET – Organic Field-Effect Transistor

OLED – Organic Light Emitting Diode

OPV – Organic Photovoltaic

ORTEP – Oak Ridge Thermal Ellipsoid Plot

$\mathbf{P_2S_5}$ – Phosphorus pentasulfide

PK – Protein Kinase

ppm – Parts Per Million

PTC – Phase Transfer Catalyst

p-TSA – *para* -Toluenesulfonic acid

rt – Room Temperature

SAR – Structure–Activity Relationship

SFRC – Solvent-free reaction conditions

$\boldsymbol{KO^tBu}$ – Potassium *tert*-butoxide

TBHP – *tert*-Butyl Hydroperoxide

THF – Tetrahydrofuran

TLC – Thin Layer Chromatography

TMS – Tetramethylsilane

TNF-α – Tumor Necrosis Factor alpha

TS – Transition State

VKOR – Vitamin K Epoxide Reductase

General Remarks

The experimental work described in this thesis was carried out at the Department of Chemistry, Indian Institute of Technology Guwahati, Guwahati–781039, Assam, during the period from October 2021 to April 2025, under the supervision of Prof. Abu Taleb Khan.

All analytical samples were dried using a high vacuum pump at ambient temperature, unless otherwise specified. Thin-layer chromatography (TLC) was used for monitoring reactions, employing either silica gel G or silica gel GF254 (SRL) as the stationary phase. For purification of crude products, column chromatography was performed using silica gel (60–120 mesh, Merck or SRL).

Solvent removal was generally achieved with rotary evaporators (Büchi R-300). Melting points were measured using a Büchi B-540 melting point apparatus and are reported without correction. Infrared (IR) spectra were recorded using a PerkinElmer Spectrum Two instrument. Deuterated solvents $CDCl_3$ and DMSO-d_6 were used for recording NMR spectra.

^{1}H and ^{13}C NMR spectra were acquired on Bruker spectrometers operating at 400, 500, or 600 MHz for ^{1}H and at 100, 125, or 150 MHz for ^{13}C, with tetramethylsilane (TMS) serving as the internal standard. Chemical shift values are reported in parts per million (δ, ppm). The reported ^{1}H NMR data include signal multiplicity, proton count, and coupling constants (J, in Hz), with standard notations: s = singlet, d = doublet, t = triplet, q = quartet, m = multiplet, brs = broad singlet, dd = doublet of doublets, dq = doublet of quartets, dt = doublet of triplets, and ddt = doublet of doublet of triplets.

High-resolution mass spectra (HRMS) were obtained using an electrospray ionization-time of flight (ESI-TOF) setup. Single-crystal X-ray diffraction data were collected at 296 K using a Bruker SMART APEX-II CCD diffractometer equipped with graphite-monochromated MoKα radiation (λ = 0.710 73 Å).

Compound Numbering Convention Used in This Thesis

In this thesis, a systematic alphanumeric code is used to name compounds and derivatives across different chapters to maintain clarity and consistency in tracking synthetic relationships.

The naming convention follows the pattern: XLY, where:

- X = Chapter number (e.g., 4 for Chapter 4)
- L = Series or structural class identifier (A, B, C…)
- Y = Compound number within that class (1, 2, 3…)

For example:

- 1A1: First compound of series A described in Chapter 1.
- 3C2: Second compound of series C in Chapter 3.
- 4D3: Third compound of series D in Chapter 4.

Chapter 1

Foundations of 4-hydroxycoumarins, Thio-analogs, and Hybrid Heterocyclic Scaffolds in Medicinal Chemistry

Graphical Abstract

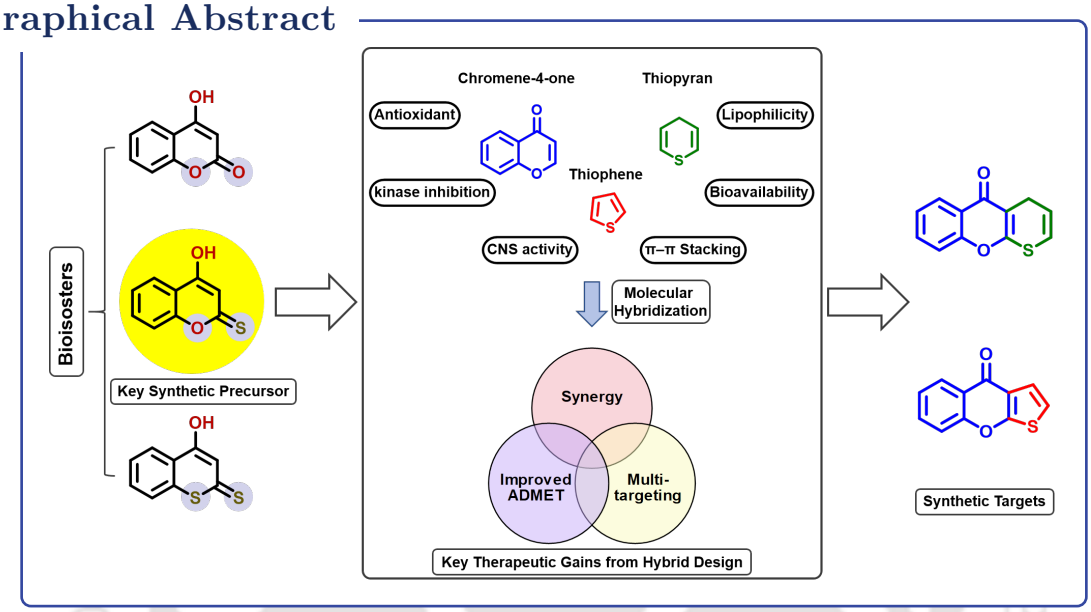

Table of contents

Part 1A
Structure, Relevance and Reactivity

1A.1 4-Hydroxycoumarin and Its Derivatives

1A.1.1 Structure and Chemical Properties of 4-Hydroxycoumarin

4-Hydroxycoumarin is a derivative of benzopyran-2-one. It has a hydroxy group at the C-4 position of the coumarin structure, formally called 4-hydroxy-2*H*-chromen-2-one (A). The molecule consists of a fused benzene and α-pyrone ring system, which imparts significant conjugation and aromatic character. The hydroxyl group at C-4 is essential for the compound's reactivity. It also plays a key role in tautomerism and contributes to the biological activity seen in many of its derivatives.

1A.1.1.1 Tautomerism and electronic structure

4-Hydroxycoumarin exhibits keto–enol tautomerism, existing primarily as the 4-hydroxy-2*H*-chromen-2-one (**A**) form, but also interconverting with the 2,4-chromandione (**B**) and 2-hydroxy-4-chromenone (**C**) tautomers (**Scheme 1A.1**).[1] The predominance of the 4-hydroxy form in solution has been established by NMR and computational studies, yet the equilibrium with the diketone and 2-hydroxy forms is important for understanding both reactivity and isotope exchange at C-3.[2]

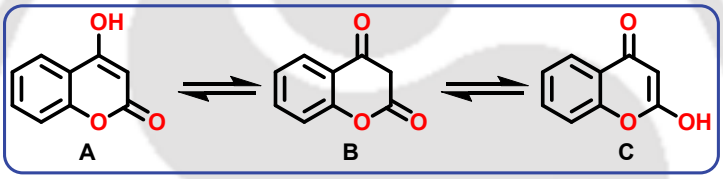

Scheme 1A.1: Structures and tautomeric forms of 4-hydroxycoumarin.

1A.1.1.2 Chemical reactivity

The reactivity of 4-hydroxycoumarin is governed by both its electron-rich aromatic system and the nucleophilicity of the C-3 position, which is activated by the adjacent carbonyl and hydroxy groups.[3,4] Electrophilic substitution, alkylation, and condensation reactions occur preferentially at C-3,[5,6] while the hydroxyl group at C-4 is susceptible to acylation and alkylation.[6] The molecule thus acts both as a nucleophile and an electrophile in various organic transformations.

1A.1.2 Biological and Pharmacological Relevance

4-Hydroxycoumarin and its derivatives constitute a privileged class of bioactive molecules. They are widely recognized for their diverse pharmacological properties and longstanding clinical significance.[7] The core 4-hydroxycoumarin scaffold is central to the structure of several major anticoagulant drugs, most notably warfarin, acenocoumarol, phenprocoumon, and coumatetralyl, which have been mainstays in the management of thromboembolic disorders for decades.[8] These agents act as vitamin K antagonists, inhibiting the Vitamin K Epoxide Reductase (VKOR) enzyme in hepatic microsomes, thereby blocking the regeneration of reduced vitamin K and ultimately suppressing the γ-carboxylation of key clotting factors.[9] The enolic hydroxyl group at C-4 is critical for this mechanism of action, and structural

modifications at this position or the adjacent C-3 site can dramatically influence both potency and pharmacological profile.

The clinical impact of 4-hydroxycoumarin-based anticoagulants is substantial: warfarin remains the most commonly prescribed oral anticoagulant worldwide, with proven efficacy in reducing the incidence of stroke, myocardial infarction, and venous thromboembolism.[10] Second-generation derivatives such as brodifacoum, difenacoum, and flocoumafen, often termed "superwarfarins", have been developed as rodenticides due to their greater potency and prolonged biological half-life.[11]

Beyond their anticoagulant activity, 4-hydroxycoumarin derivatives show a wide range of other biological activities. Numerous synthetic and natural analogs exhibit anti-inflammatory, analgesic, antibacterial, antifungal,[12] antiviral, anticancer, antioxidant, and anti-arthritic activities.[13] Some of these compounds have also demonstrated cytotoxic and chemopreventive effects in cancer studies,[14] as well as the ability to inhibit enzymes involved in neurodegenerative[15] and metabolic diseases.[16] A few representative examples are shown in **Figure 1A.1**.

The widespread presence of coumarins in nature underscores their significant biological roles. Among them, 4-hydroxycoumarin occurs naturally in various plants, typically as a component of secondary metabolites. It is especially well known for its association with dicoumarol, a natural anticoagulant that was first discovered in spoiled sweet clover (Melilotus species). Dicoumarol is formed through microbial transformation of plant-derived coumarins. This finding not only emphasized the biological relevance of 4-hydroxycoumarin derivatives but also paved the way for the development of synthetic anticoagulants such as warfarin.[17]

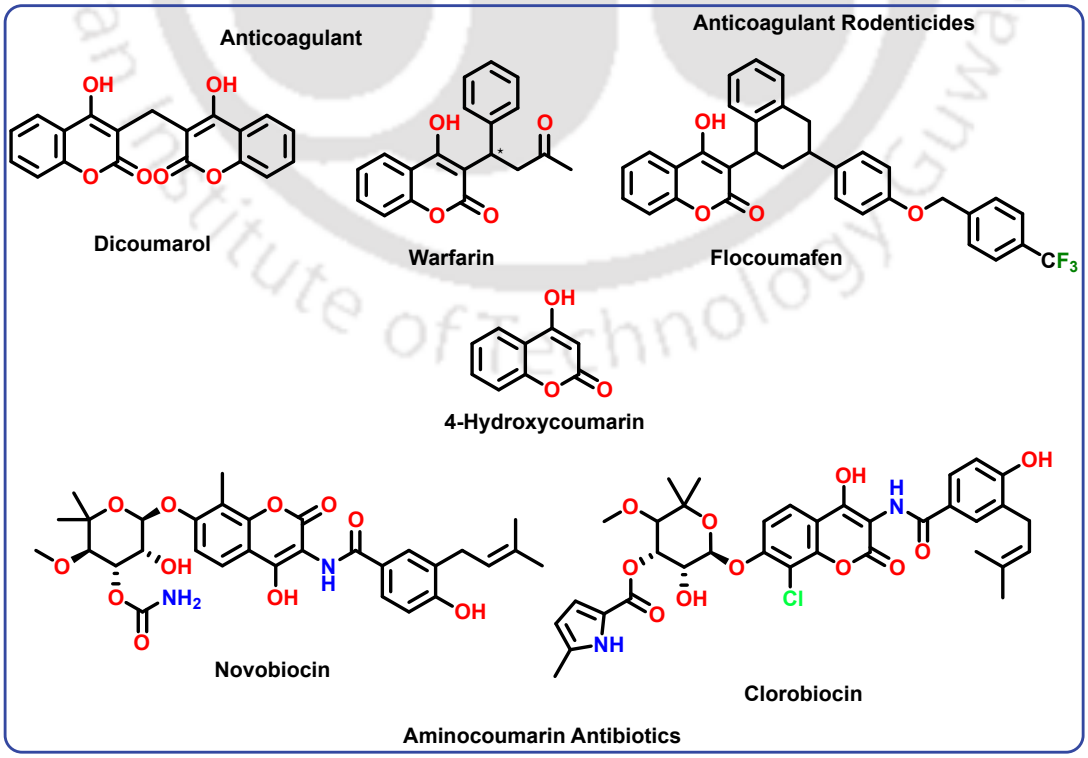

Figure 1A.1: Structures of key 4-hydroxycoumarin-based bioactive molecules.

Summary: The 4-hydroxycoumarin scaffold is a cornerstone of both natural and synthetic bioactive chemistry, forming the basis for several essential therapeutic agents. Its continued significance in medicinal chemistry shows its structural flexibility and ability to participate in various biological processes.

1A.2 Bioisosterism and Its Significance in Drug Design

Bioisosterism is a fundamental concept in medicinal chemistry that involves the replacement of atoms or groups within a molecule with alternative moieties possessing similar physicochemical or spatial properties, while retaining or improving biological activity. Researchers frequently use this strategy to optimize pharmacokinetic profiles, improve target selectivity, lower toxicity, and address metabolic issues.[18,19]

Notable examples include (**Figure 1A.2**):

- **Glycine antagonists:** Chlorine substitution in kynurenic acid reduced IC_{50} from 41,000 nM to 560 nM, significantly enhancing potency.[20]
- **5-Hydroxytryptamine or Serotonin (5-HT) reuptake inhibitor:** Trifluoromethyl addition to the lead compound led to fluoxetine (Prozac), improving efficacy and reducing side effects.[21]
- **Mitotic inhibitor:** O/S replacement and demethylation of colchicine yielded 3-demethyl-thiocolchicine, retaining activity with reduced toxicity.[22]
- **Antidiabatic Drug:** Incorporation of a *para*-chlorine substituent in place of a methyl group on the phenyl ring, along with shortening of the alkyl side chain in Tolbutamide, produced Chlorpropamide, offering a longer half-life and slower metabolism.[23]

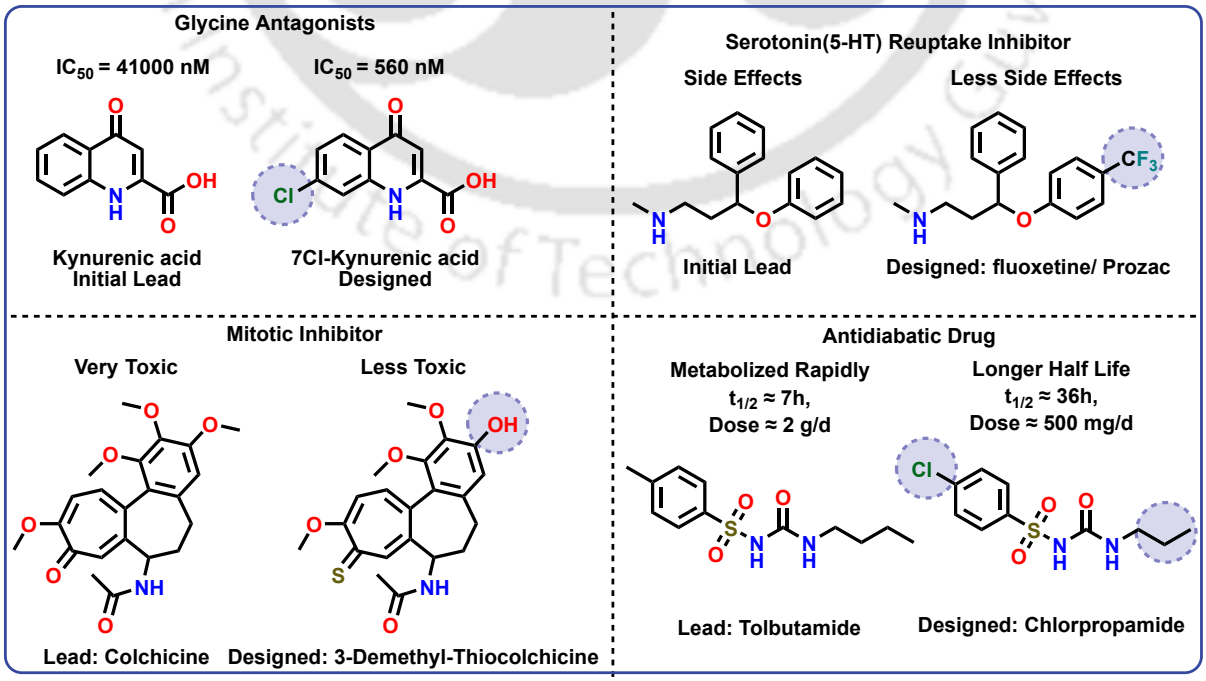

Figure 1A.2: Representative examples of bioisosters.

Note: The result of a bioisosteric substitution often relies on the specific molecular and biological context. A group that works well in one situation may not work well in another. Using this strategy effectively demands careful thought about the target's biology and the wider impacts of structural changes. Despite this complexity, bioisosterism is still a valuable and vital tool for creating drug candidates with better safety, effectiveness, and development potential.[18,24]

1A.3 Transition to Thio Analogs

While 4-hydroxycoumarins are extensively studied for their various reactivities, synthetic utilities as well as biological activities, there is growing interest in exploring sulfur-containing analogs as a means to access new chemical space and tunable pharmacological properties. In line with the principles of bioisosterism, the replacement of oxygen with sulfur within the coumarin scaffold can significantly influence electronic distribution, lipophilicity, and reactivity, thereby offering opportunities for the development of novel compounds with distinct or enhanced bioactivity. This thesis therefore shifts focus to the synthesis and study of 4-hydroxythiocoumarin and related thio analogs, aiming to expand the repertoire of heterocyclic scaffolds available for medicinal chemistry.

1A.4 Thio-Analogs of 4-Hydroxycoumarin

The significance of 4-hydroxycoumarin and its derivatives has already been outlined in the preceding sections. In contrast, their thio analogs, namely, 4-hydroxy-1-thiocoumarin (**I**), 4-hydroxydithiocoumarin (**II**), and 4-hydroxy-2-thiocoumarin (**III**), have remained comparatively underexplored. Among these, structure **III**, more accurately referred to as 4-hydroxy-2*H*-chromene-2-thione, is of particular interest. This compound will be the central focus of the present research and will be discussed in detail throughout this section as well as in subsequent chapters. For brevity, it will hereafter be referred to as **4-hydroxythiocoumarin** (**Figure 1A.3**).

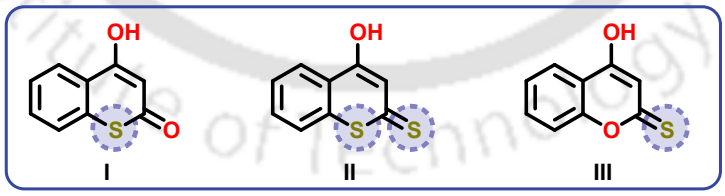

Figure 1A.3: Thio analogs of 4-Hydroxycoumarin.

1A.4.1 Structure and Tautomerism

4-Hydroxythiocoumarin comprises a benzopyranone core in which the carbonyl oxygen at position 2 of the coumarin scaffold is replaced by a sulfur atom, forming a thiocarbonyl (C═S) group. The compound features a fused bicyclic system, consisting of a benzene ring fused to a six-membered heterocyclic γ-pyrone ring, which in this case is better described as a benzopyran-2-thione. Notably, 4-hydroxythiocoumarin can exist in three

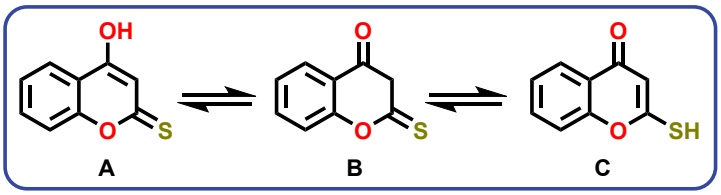

Scheme 1A.2: Tautomeric forms of 4-hydroxythiocoumarin.

tautomeric forms: 4-hydroxy-2*H*-chromene-2-thione (**A**), 2-thioxochroman-4-one (**B**), and 2-mercapto-4*H*-chromen-4-one (**C**) (**Scheme 1A.2**).

1A.4.2 Synthesis and Chemical Properties

1A.4.2.1 Key chemical reactivity and functionalization patterns

4-Hydroxythiocoumarin is a structurally rigid heteroaromatic scaffold featuring three distinct nucleophilic centers: a soft sulfur at C-2, an active methylene at C-3, and a phenolic hydroxyl at C-4. Its reactivity, therefore, is shaped not only by the positions of these centers but also by differences in their chemical nature, influencing the types of transformations they can undergo and offering opportunities for strategic functional group interconversions during synthesis.

We can conceptually divide the literature reports on 4-hydroxythiocoumarin into three fundamental reaction types, each reflecting a distinct synthetic strategy:

Type I: Functionalization *via* nucleophilic substitution (soft sulfur center at C-2)

The sulfur at C-2 behaves as a soft nucleophile in the thiolactone ring, and its reactivity is heavily exploited for displacement-type transformations. These proceed *via* two distinct but related strategic approaches:

(a) Direct substitution of sulfur after activation

One of the earliest and simplest approaches involves alkylating the sulfur atom, typically *via* ethylation or methylation, to enhance its leaving group ability. Subsequent substitution under harsh thermal conditions enables its replacement by various nucleophiles such as amines, phenols, or other heteroatoms. This method enables the sulfur to serve as a temporary placeholder, directing reactivity and later being replaced.

In Leahy's work (2004), such sulfur substitution enabled the installation of morpholine substituents at the 2-position of 6-bromo-4-hydroxythiocoumarin, generating a library of DNA-dependent protein kinase (DNA-PK) inhibitors, a target implicated in DNA repair mechanisms. The sulfur center was effectively a latent leaving group, directing substitution selectively at C-2 (**Scheme 1A.3**).[25]

(b) Oxidation-activated substitution *via* sulfones

In a more refined strategy, the sulfur atom is first alkylated, and the resulting thioether is subsequently oxidized (commonly with *m*-chloroperbenzoic acid (*m*-CPBA)) to a sulfoxide or sulfone. These oxidized intermediates are more electrophilic, facilitating substitution by nucleophiles under milder reaction conditions. This method provides better functional group compatibility and often leads to improved yields.

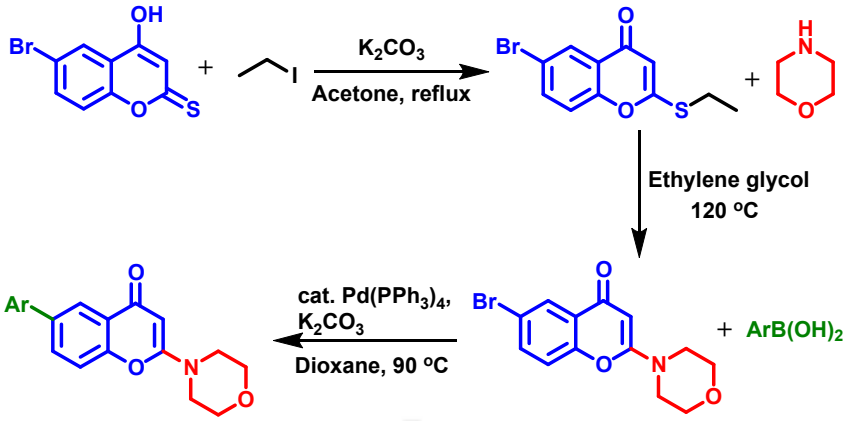

Scheme 1A.3: Synthesis of 2-morpholino-6-aryl-4*H*-chromen-4-one libraries.

Costantino *et al.* (2001) employed two complementary approaches: (i) direct substitution of sulfur with a polar nucleophile (4-aminophenol), and (ii) a two-step transformation involving oxidation of the *S*-ethyl intermediate to sulfoxide, followed by nucleophilic displacement with 4-hydroxythiophenol (**Scheme 1A.4**). Their synthesized derivatives were evaluated for Aldose Reductase (ALR2) inhibitory activity. The Structure–Activity Relationship (SAR) revealed that the sulfur-containing compound (**V**) retained good activity. At the same time, the nitrogen analog (**IV**) displayed significant loss of activity, indicating the importance of the sulfur's electronic characteristics.[26]

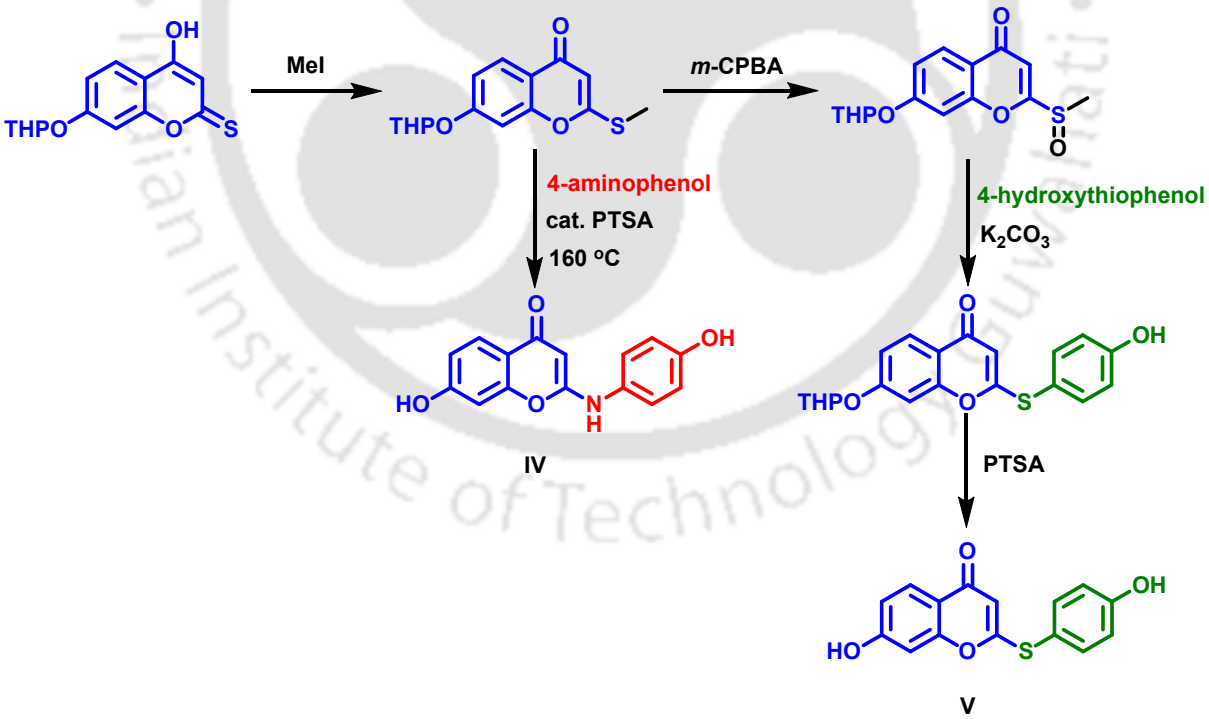

Scheme 1A.4: Synthesis of 7-hydroxy-2-(4'-hydroxyphenylamino)-4*H*-chromen-4-one (**IV**) and 7-hydroxy-2-(4'-hydroxyphenylthio)-4*H*-chromen-4-one (**V**).

Yuan Feng Tong *et al.* (2007) demonstrated a similar strategy utilizing *m*-CPBA for the oxidation of *S*-ethyl intermediates to sulfones. These sulfones were subsequently displaced by

phenols. This method was instrumental in synthesizing **6-demethoxycapillarisin**, a natural product with known ALR2 inhibition properties (**Scheme 1A.5**).[27]

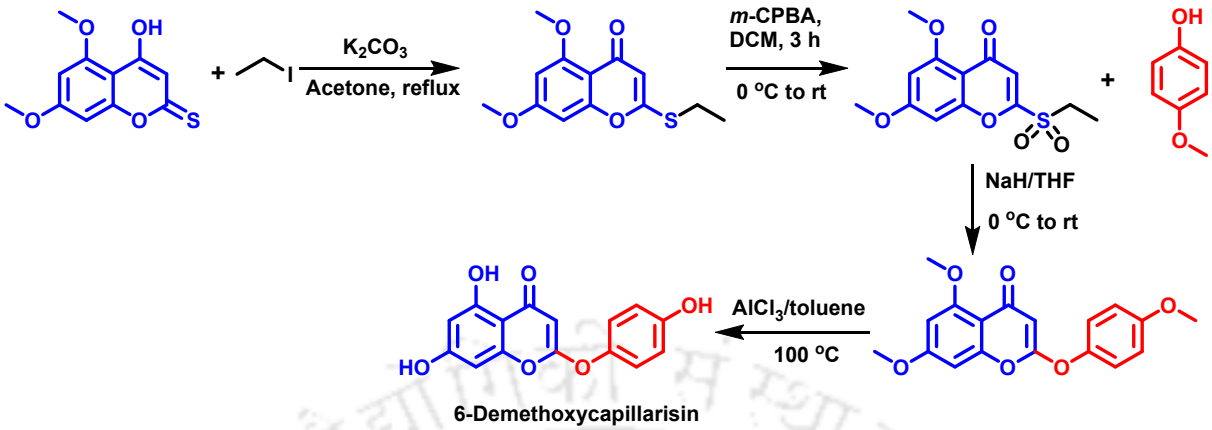

Scheme 1A.5: Synthesis of 6-Demethoxycapillarisin.

Hatnapure *et al.* (2012) adopted the same sulfone-based substitution strategy to prepare a new class of 6-methoxy-2-(piperazin-1-yl)-chromen-4-one derivatives. These compounds showed significant antimicrobial activity and reduced levels of inflammatory cytokines Tumor Necrosis Factor alpha (TNF-α) and Interleukin 6 (IL-6), highlighting their therapeutic potential (**Scheme 1A.6**).[28]

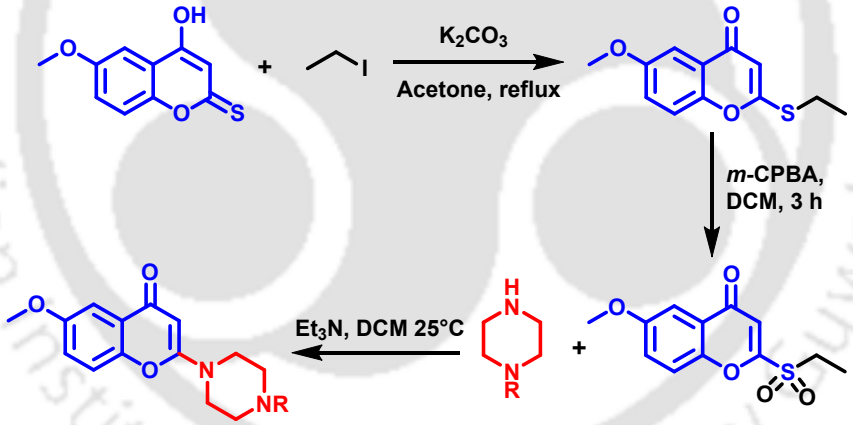

Scheme 1A.6: Synthesis of 6-methoxy-2-(piperazin-1-yl)-4*H*-chromen-4-one derivatives.

In a later study, **Balboa and co-workers (2016)** synthesized chromones with amino or *N*-substituted carboxamide groups at position-2, demonstrating selective inhibition of certain transport proteins associated with drug resistance (e.g., ABCC1). Their potential as pharmacological tools for overcoming chemoresistance in cancer was also emphasized (**Scheme 1A.7**).[29]

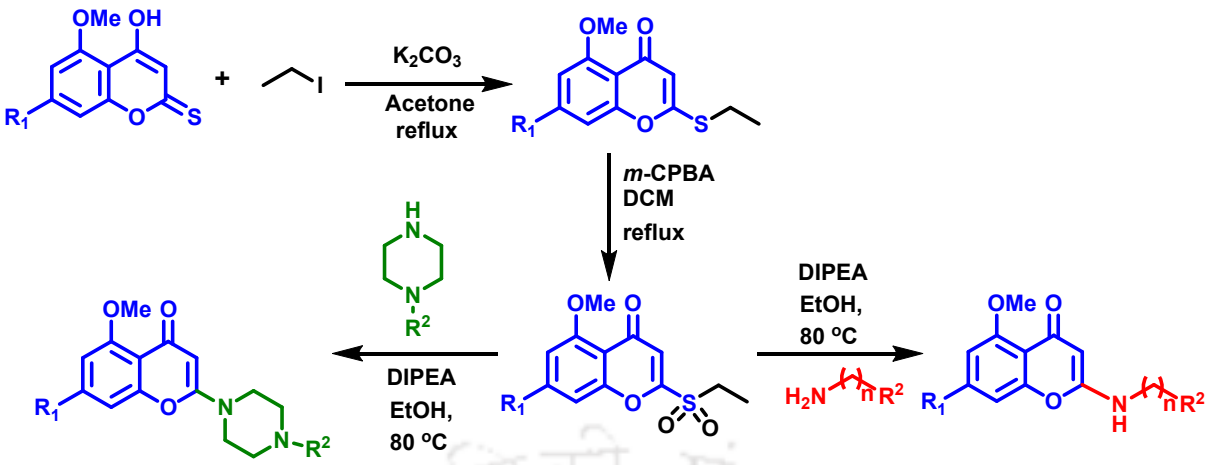

Scheme 1A.7: Synthesis of 2-amino- and 2-carboxamide-substituted 4*H*-chromen-4-one derivatives.

Type II: O-Nucleophile reactivity and peripheral modification at the 4-hydroxy group

The hydroxyl functionality at position 4 is another reactive center, though less explored than the C-2 sulfur center. This site is primarily targeted for **etherification**, especially *via* allylation, to diversify the 4-position and extend molecular complexity.

Avetisyan and Alvandzhyan (2004) reported the allylation of 4-hydroxythiocoumarin using electrophiles like allyl bromide, 1,3-dichlorobut-2-ene, and 1,1,3-trichloroprop-1-ene. The resulting ethers displayed substitution at the 4-OH site and provided valuable intermediates for further derivatization (**Scheme 1A.8**). This transformation underscores the moderate reactivity of the phenolic OH group and its potential for *O*-alkylation.[30]

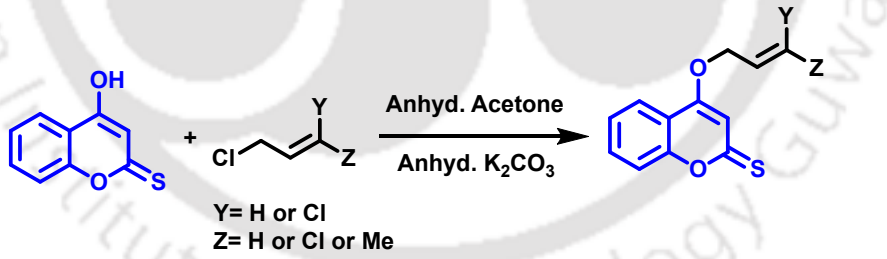

Scheme 1A.8: Reaction at 4-OH position of 4-hydroxythiocoumarin.

Despite its synthetic utility, the 4-OH group remains less frequently exploited compared to the sulfur at position 2, perhaps due to its greater electronegativity and harder nucleophilic character.

Type III: Conjugation-driven reactions at the activated methylene (C-3)

The C-3 methylene group lies flanked by two electron-withdrawing centers, a carbonyl and a thiocarbonyl, making it highly acidic and enabling base-catalyzed condensations. This gives rise to reactions governed by enolate chemistry, prominently:

- **Knoevenagel condensations** with aldehydes or ketones
- **Tandem pericyclic rearrangements** following condensation

These transformations not only extend conjugation but also enable fusion of additional ring systems, giving rise to fused tricyclic frameworks with promising pharmacological relevance.

Cravotto *et al.* (2007) showcased this in a cascade Knoevenagel–electrocyclic reaction of 4-hydroxycoumarin and 4-hydroxythiocoumarin with *trans*,*trans*-farnesal, yielding unexpected regioselectivity. Substituting oxygen with sulfur in the coumarin ring dramatically reversed regioselectivity, highlighting the subtle yet significant influence of sulfur on conjugation and overall reaction topology. (**Scheme 1A.9**).[31]

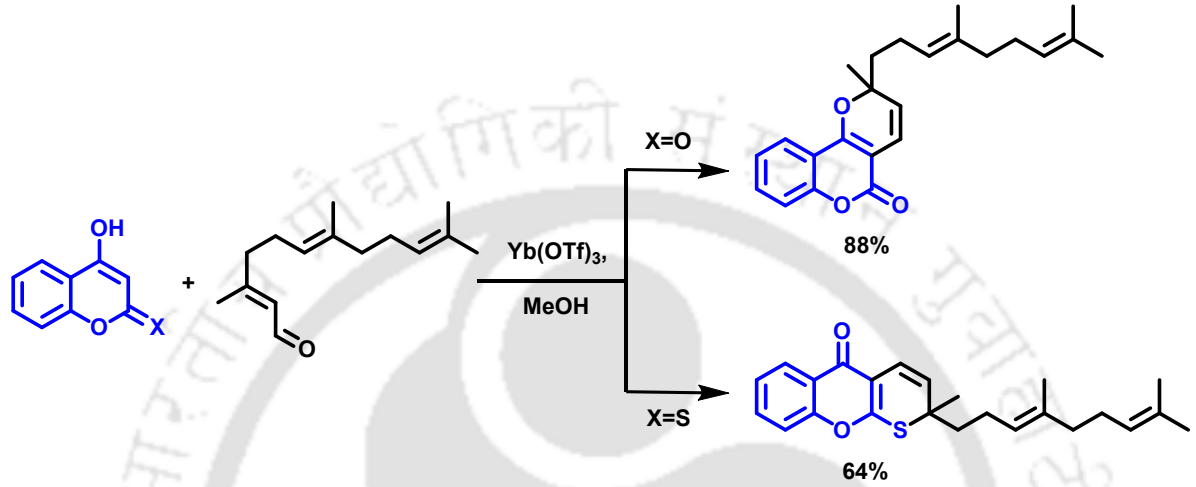

Scheme 1A.9: Influence of O–S isosterism on cyclization regioselectivity.

Interplay of reactive centers

What sets 4-hydroxythiocoumarin apart is not merely the presence of multiple reactive sites, but the way they interact. Engaging one center in a reaction often influences, or even limits, the reactivity of the others:

- **Substitution or alkylation at sulfur (C–2)** eliminates enolizability at C–3 by forming a C=C double bond between C-2 and C-3.
- **Nucleophilic attack by C–3** generates an intermediate that tautomerizes to restore the thiol at C–2, retaining sulfur nucleophilicity for further intramolecular reactions.
- **Oxidation of sulfur (e.g., to sulfoxide or sulfone)** changes electron density around C–2, suppressing nucleophilicity at C–3 while introducing new electrophilic sites for substitution.

Insight: The reactivity must be planned in a stepwise and coordinated manner, with consideration for the interplay between different electronic effects.

Summary: The literature clearly establishes 4-hydroxythiocoumarin as a chemically versatile scaffold featuring three nucleophilic centers (**Figure 1A.4**):

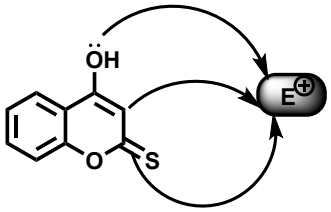

Figure 1A.4: Visual overview of 4-hydroxythiocoumarin reactivity.

- **Sulfur at position 2:** The most chemically manipulated site; reactions include alkylation, oxidation to sulfoxide/sulfone, and substitution with nitrogen/sulfur nucleophiles. This site has been crucial for introducing pharmacophoric groups and generating biologically active chromone analogs.
- **Hydroxyl group at position 4:** Primarily involved in alkylation (e.g., allylation), providing access to *O*-functionalized derivatives with potential for further transformations.
- **Methylene carbon at position 3:** Acts as a soft nucleophile participating in condensation reactions, notably the Knoevenagel condensation, often followed by electrocyclizations to yield fused or extended ring systems.

Scope for Further Exploration

Despite existing research, the synthetic potential of 4-hydroxythiocoumarin remains significantly underexplored. The scaffold's inherent capacity for modification at multiple reactive sites enables its use as a versatile core for constructing a wide variety of hybrid heterocyclic architectures. Further exploration of this framework under alternative activation strategies, especially under sustainable or metal-free conditions, is likely to yield novel structures with valuable physicochemical and biological properties. This forms the foundation of the present study, which seeks to exploit the multi-nucleophilic nature of 4-hydroxythiocoumarin in the synthesis of structurally diverse heterocyclic frameworks.

1A.4.2.2 Reactivity studies of 4-hydroxydithiocoumarin

Although 4-hydroxythiocoumarin has recently begun to attract synthetic interest, the 4-hydroxydithiocoumarin scaffold has been more extensively studied and is included here due to its structural similarity and expected reactivity parallels. Our research group primarily leads the exploration of its reactivity under various conditions, and a number of key transformations have been developed. To provide a contextual foundation for these efforts, a chronological overview of key literature reports on 4-hydroxydithiocoumarin is presented below.

2006 – *S*-Alkylation and sigmatropic rearrangement (Mozumdar *et al.*)

Mozumdar and co-workers reported the *S*-alkylation of 4-hydroxydithiocoumarin with 1-aryloxy-4-chlorobut-2-ynes under Phase Transfer Catalysis. Compared to the classical

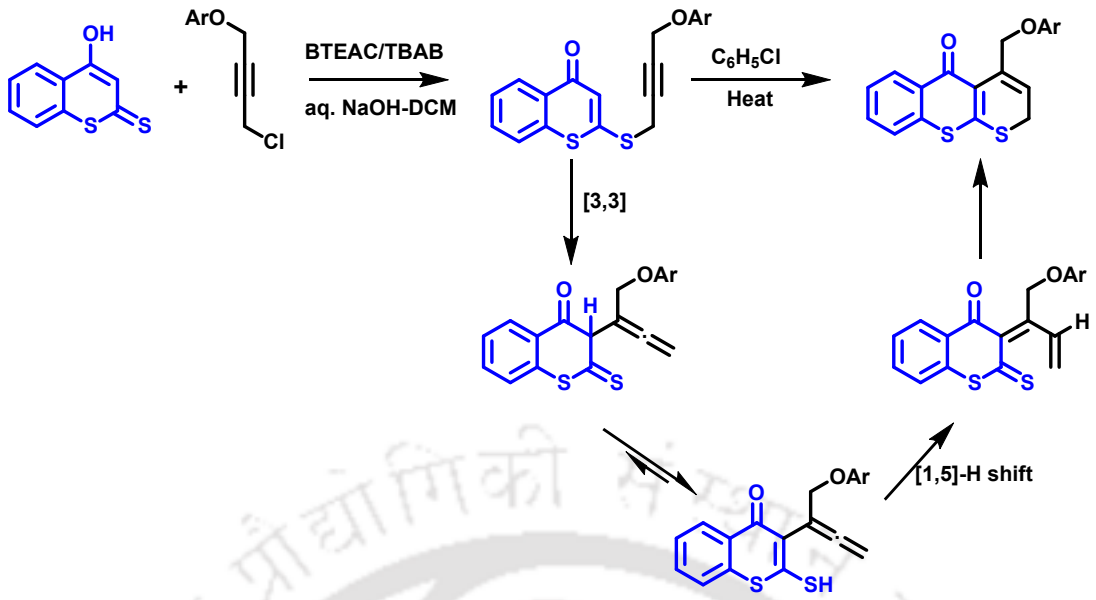

Scheme 1A.10: Regioselective synthesis of thiopyran fused thiocoumarin *via* [3,3]-sigmatropic reaction.

alkylation using K_2CO_3 in acetone, the Phase Transfer Catalyst (PTC) methodology afforded higher yields and accelerated reaction rates. Upon heating the *S*-alkylated intermediates in chlorobenzene, the reaction proceeded *via* a [3,3]-sigmatropic rearrangement, followed by a [1,5]-hydride shift and intramolecular cyclization, resulting in the formation of 4-(aryloxymethyl)thiopyrano[2,3-*b*]benzothiopyran-5(2*H*)-ones (**Scheme 1A.10**). Notably, the C═S bond participated in the proton shift, contrasting with the C═O-directed shift observed in oxygen analogs.[32]

2010 – Domino-Knoevenagel-hetero-Diels–Alder reaction (DKHDA) reactions (Mozumdar *et al.*)

In a notable advancement, the same group developed a DKHDA reaction involving 4-hydroxydithiocoumarins and *O*-propargyl salicylaldehyde derivatives, employing water as a solvent (**Scheme 1A.11**).

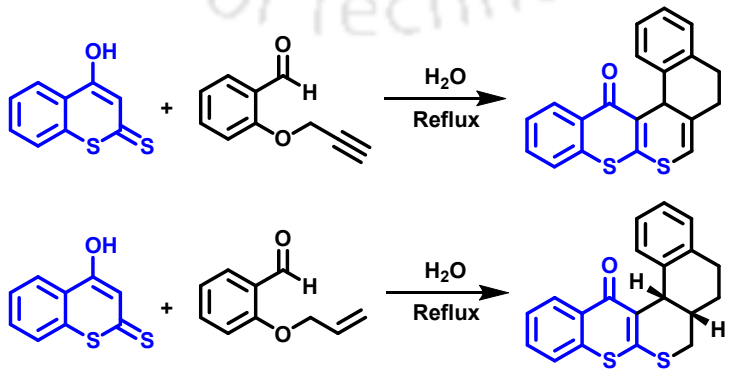

Scheme 1A.11: DKHDA reaction of *O*-propargylated/allylated salicylaldehyde with 4-hydroxydithiocoumarin.

This green approach afforded regioselective [6,6]-fused thiopyrano[2,3-*b*]benzopyran derivatives, favored over the oxygen analogs due to the greater polarizability and reduced HOMO–LUMO gap of sulfur-containing heterodienes. The methodology was later extended to include *O*-allylated salicylaldehydes, which underwent *endo*-selective cycloaddition, evidenced by the formation of *cis*-fused products.[33,34]

2011 – Catalyst-Free Multicomponent Reaction (MCR) (Majumdar *et al.*)

Majumdar and co-workers reported a metal- and catalyst-free MCR involving 4-hydroxydithiocoumarins, aldehydes, and malononitrile in aqueous medium, delivering the desired products in excellent yields. The reaction proceeds *via* a sequential Knoevenagel condensation, Michael addition, followed by regioselective nucleophilic ring closure that preferentially involves the sulfur nucleophile over the oxygen counterpart. The scope of the methodology was further broadened by employing dimedone as an alternative active methylene component (**Scheme 1A.12**).[35]

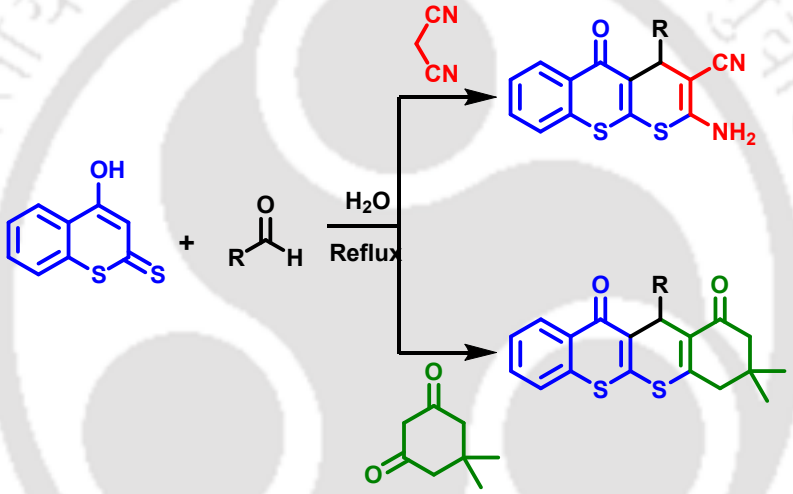

Scheme 1A.12: MCR involving aldehydes, 4-hydroxydithiocoumarin and malononitriles/ dimedones.

2018 – Oxidative Cross-Coupling with nucleophiles (Mahato *et al.*)

Mahato and co-workers explored the oxidative coupling reactivity of 4-hydroxydithiocoumarins with various nucleophiles under metal-free conditions. Utilizing I_2/TBHP as the oxidizing system, the reaction delivered sulfenamides, sulfanes, and disulfides in an atom-economical and operationally simple manner. Several of the synthesized compounds displayed promising antiproliferative activity against the MCF-7 breast cancer cell line, underscoring their potential pharmacological relevance (**Scheme 1A.13**).[36]

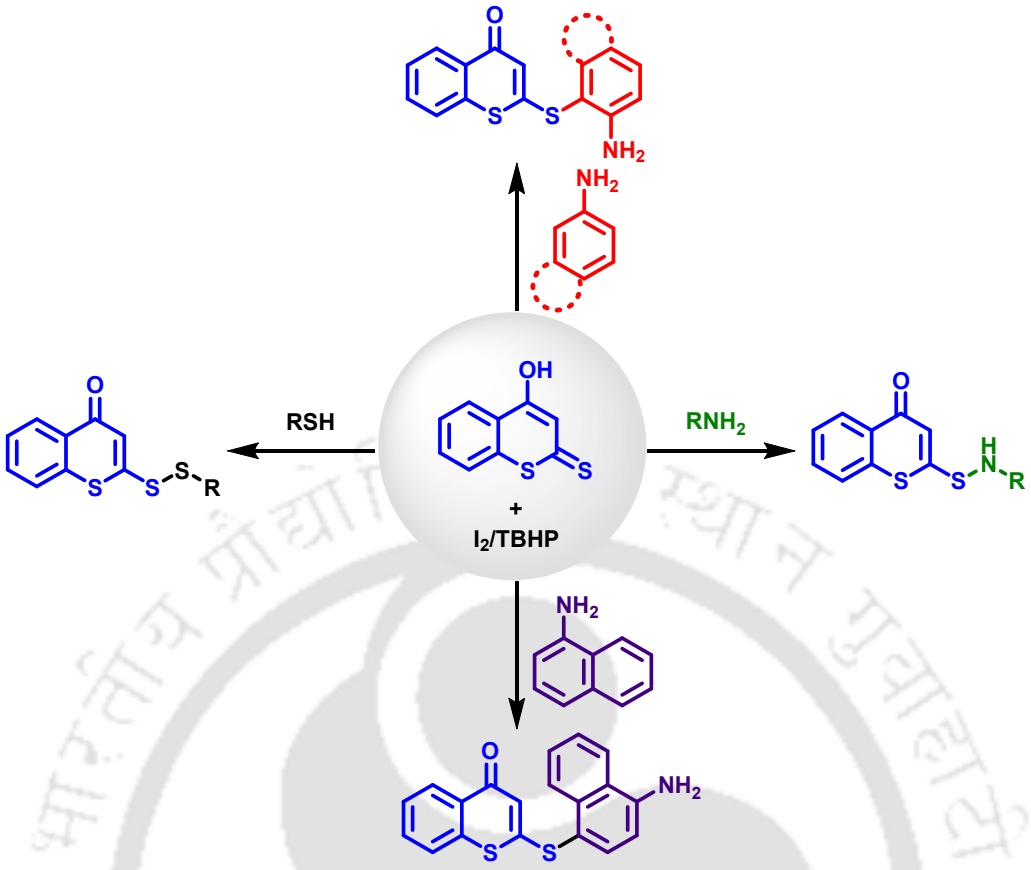

Scheme 1A.13: Iodine/TBHP-mediated oxidative cross-coupling of 4-hydroxydithiocoumarin with nucleophiles.

2021 – Hydrothiolation of alkenes and alkynes

In a more recent endeavor, our group investigated the hydrothiolation of olefins using 4-hydroxydithiocoumarin. The reaction follows an oxidative addition pathway, followed by insertion of alkynes or styrenes and subsequent hydrolysis that affords vinyl thioethers or methylbenzyl thioethers, depending on the olefinic substrate (**Scheme 1A.14**). These derivatives represent promising scaffolds for further medicinal chemistry applications.[37]

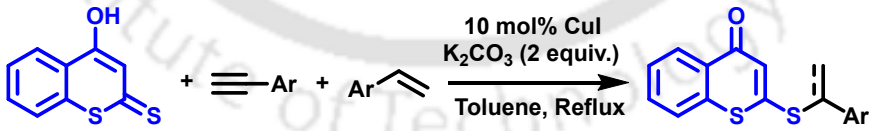

Scheme 1A.14: Hydrothiolation of olefins using 4-hydroxydithiocoumarin.

Other Developments – cyclizations and pericyclic pathways

Beyond the transformations described above, 4-hydroxydithiocoumarin has also been employed in diverse synthetic strategies, including oxidative cyclizations through pseudo-three-component reactions to form 1,3-thiazine-fused chromones, as well as various multicomponent and pericyclic processes, which have been recently reviewed.[38] For the sake of conciseness, these contributions are not detailed here but collectively underscore the scaffold's multifaceted reactivity and synthetic potential. Together with the literature discussed earlier on 4-hydroxythiocoumarin, these studies form a robust platform for the design and development

of novel synthetic strategies aimed at expanding the chemical space of biologically relevant heterocycles.

1A.4.3 Biological and Medicinal Relevance

4-hydroxythiocoumarin derivatives have emerged as promising bioactive compounds in recent times. Thio analogs of flocoumafen, thioflocoumafen, exhibited greater anticoagulant potency and lower toxicity compared to flocoumafen.[39] In 2006, Sharon A. Jackson and her co-workers synthesized a 4-hydroxythiocoumarin derivative, which showed weak inhibition of Inducible Nitric Oxide Synthase (iNOS), which has been linked to a variety of central and peripheral pathophysiological conditions.[40] Molecules synthesized from 4-hydroxydithiocoumarin have been shown to exhibit antiproliferative activity against the breast cancer cell line MCF-7.[36]

1A.5 Selected Heterocyclic Scaffolds Relevant to This Thesis

Heterocyclic compounds play a pivotal role in medicinal chemistry, owing to their structural complexity and broad pharmacological potential. They form the core of numerous natural products, essential biomolecules, and more than 90% of newly approved pharmaceuticals.[41]

This thesis focuses on three representative heterocyclic scaffolds: chromone/coumarin, thiophene/dihydrothiophene, and thiopyran systems. These were selected based on their well-established biological relevance and chemical versatility. The following subsections briefly outline their structural features and medicinal significance, providing context for the synthetic works discussed in this thesis.

1A.5.1 Chromene-4-one (Chromone) Scaffold

Chromone derivatives, featuring a benzene ring fused to a pyrone ring, form a significant class of oxygen-containing heterocycles. They occur widely in natural products and are recognized for their therapeutic relevance, earning them the designation of "privileged scaffolds" in medicinal chemistry. As structural isomers of coumarins, chromones differ primarily in the position of the carbonyl group: C-4 in the benzo-γ-pyrone system of chromones, versus C-2 in the benzo-α-pyrone system of coumarins, resulting in distinct chemical and biological behaviors.

1A.5.1.1 Established biological significance and medicinal applications[42]

Chromone derivatives are a versatile class of compounds with a wide range of pharmacological activities (**Figure 1A.5**). They have been extensively studied for their potential as therapeutic agents, with modifications to the core structure often enhancing specific biological activities. These compounds can help manage inflammation,[43] inhibit cancer cell growth,[44] combat various pathogens,[45] protect nerve cells in neurodegenerative diseases,[46] and neutralize harmful free radicals.[47] Additionally, some chromones may support antidiabetic therapy by influencing glucose metabolism.[48]

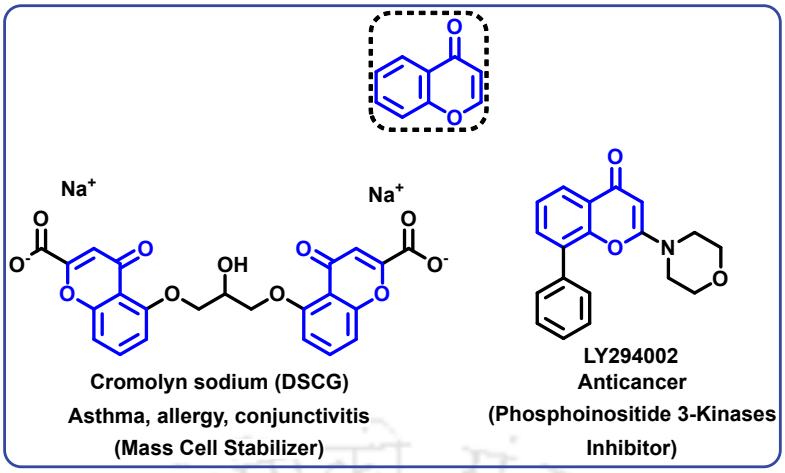

Figure 1A.5: Representative examples of biologically active chromone derivatives.

1A.5.2 Thiophene and Dihydrothiophene Scaffolds

Thiophene, a five-membered aromatic sulfur-containing heterocycle, and its partially saturated analogs, dihydrothiophenes, are important scaffolds in both medicinal chemistry and materials science.

Structurally, thiophene (C_4H_4S) features a five-membered aromatic ring in which sulfur contributes two electrons to the 6π electron system, making it electron-rich and reactive toward electrophilic substitution, especially at the α-positions (C–2 and C–5).[49]

Dihydrothiophenes, such as 2,3- and 2,5-dihydrothiophene, are non-aromatic or weakly aromatic analogs. Their partial saturation imparts allylic sulfide character, enhancing their reactivity in addition and cycloaddition reactions, as well as increased susceptibility to sulfur oxidation compared to aromatic thiophene.[50]

1A.5.2.1 Established biological significance and medicinal applications

Thiophenes:

The thiophene ring is a privileged scaffold in medicinal chemistry, often used as a bioisostere for benzene or other aromatic systems to fine-tune the biological activity and pharmacokinetics. Their aromatic nature enhances π–π stacking interactions, allowing strong binding to biological targets, while their sulfur atom contributes to lipophilicity and metabolic stability, supporting therapeutic potential across multiple domains.

Thiophene derivatives display a broad range of therapeutic activities, including antimicrobial,[51] anticancer,[52] anti-inflammatory,[53] antiviral,[54] and antiparasitic[55] effects. Some thiophene derivatives can cross the blood-brain barrier and act on neurotransmitter systems,[56] showing promise in central nervous system disorders, as well as in antidiabetic,[57] antioxidant, antitubercular,[58] and cardiovascular therapies.[59] The versatility and effectiveness of thiophene-based compounds are reflected in several marketed drugs like Tipepidine, Suprofen, Duloxetine, and Tioconazole, among others, underscoring their significance in modern drug development (**Figure 1A.6**).

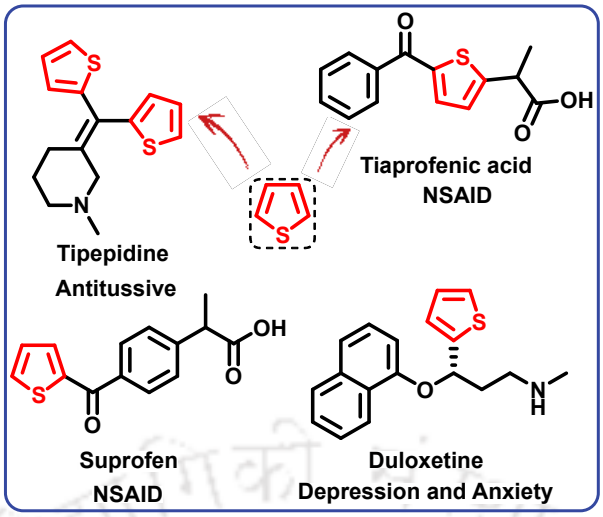

Figure 1A.6: Representative examples of thiophene-containing drugs.

Dihydrothiophenes:

Dihydrothiophenes are recognized primarily as valuable synthetic intermediates for constructing complex pharmacologically active heterocyclic systems, including various fused thienopyrimidines and other thiophene derivatives. While direct therapeutic applications of simple dihydrothiophenes are less common than their aromatic analogs, their structural features contribute to the diversity of bioactive compounds. Some dihydrothiophenes also occur naturally, contributing to the aroma profiles of certain foods.[60]

1A.5.2.2 Role as versatile building blocks in synthesis and materials

Beyond their biological roles, thiophenes are key building blocks in synthesis and materials science. Their ease of functionalization and compatibility with cross-coupling reactions enable the construction of conjugated oligomers and polymers used in organic electronics. Thiophene-based materials exhibit desirable semiconducting, luminescent, and charge transport properties, making them valuable in Organic Field-Effect Transistors (OFETs), Organic Light Emitting Diodes (OLEDs), and Organic Photovoltaics (OPVs).[61]

1A.5.3 Thiopyran Scaffolds

Thiopyrans, six-membered sulfur heterocycles, are emerging privileged scaffolds in medicinal chemistry due to their lipophilicity, DNA-binding potential, and enzyme-targeting abilities, leading to diverse biological activities (**Figure 1A.7**).[62]

These scaffolds have been extensively utilized in the design of natural product analogs exhibiting diverse pharmacological activities, including antibacterial,[63] anti-hyperplasia,[64] antipsychotic,[65] and anticancer effects.[66] However, their high lipophilicity may contribute to suboptimal biomembrane permeability. Additionally, substituted thiopyrans have been identified as potent inhibitors of DNA-dependent protein kinase (DNA-PK), further highlighting their therapeutic potential.[67]

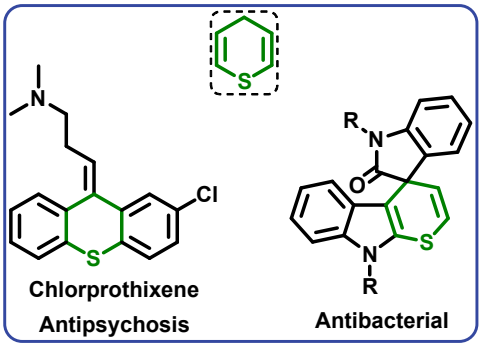

Figure 1A.7: Representative examples of thiopyran-containing bioactive compounds.

1A.5.4 Concluding Remarks: Synergistic Potential of Selected Motifs

The broad biological relevance and synthetic flexibility of chromone, thiophene (including dihydrothiophene), and thiopyran scaffolds make them important building blocks in drug discovery and central to this thesis. While each scaffold possesses distinct pharmacological potential, their combination into hybrid molecular frameworks opens new opportunities for structural innovation and functional enhancement. By combining distinct heterocycles, this research focuses on the design and synthesis of novel hybrid scaffolds with the potential for enhanced activity, broader pharmacological profiles, or new modes of action. The following section introduces core principles of hybrid molecule design, which guide the synthetic strategies developed in this work.

1A.6 Hybrid Heterocyclic Scaffolds

1A.6.1 Hybrid Molecule Design: Concept and Rationale

Hybrid heterocyclic scaffolds mark a shift from single-pharmacophore drug design toward integrating multiple bioactive motifs within one molecule. By covalently linking distinct pharmacophores, often from privileged scaffolds, this approach aims to enhance or broaden biological activity.[68] It is particularly suited for tackling complex diseases involving multiple targets.

1A.6.1.1 Linking patterns in hybrid molecule design

The manner in which pharmacophores are joined in a hybrid molecule significantly influences its biological activity. Three main strategies are commonly used:[69,70]

- **Direct fusion:** Pharmacophores are connected without a linker, often through a shared bond or fused ring. This creates rigid, planar hybrids that may simultaneously bind adjacent sites on a biological target or enable electronic interaction between motifs, ideal when close spatial arrangement is key for activity.
- **Linked hybrids (spacer-based):** Pharmacophores are joined *via* a flexible or rigid linker, whose length, polarity, or cleavability can be tailored. This allows each unit to orient independently, aiding multi-target binding or access to separate pockets on a target protein.

- **Embedded hybrids:** One pharmacophore is structurally integrated into another, forming a new scaffold with properties of both. This can yield unique 3D architectures and binding modes, unlocking novel biological effects.

1A.6.1.2 Rationale: why design hybrid molecules?

1. **Synergistic effects:** Hybrid molecules combine multiple pharmacophores to achieve greater pharmacological effects than their individual components. This synergy results from modulation of related biological pathways, enhanced binding through multi-point interactions, or the ability to trigger complementary mechanisms within a disease process.[71]

2. **Multi-target activity (polypharmacology) and overcoming drug resistance:** Unlike traditional drugs that typically act on a single molecular target, Hybrid molecules are designed for polypharmacology, simultaneously influencing multiple targets or pathways, an advantage in complex diseases like cancer or neurodegenerative disorders with multiple pathology.[72,73] By integrating pharmacophores with different mechanisms, they can broadly engage disease pathways, minimize compensatory biological responses, and help overcome drug resistance. This multi-target approach is especially valuable in antimicrobial and anticancer therapy, where resistance often arises from inhibition of a single pathway and alternative pathways compensate. By targeting multiple sites within a single entity, hybrid molecules can effectively circumvent such resistance mechanisms.[74,75]

4. **Improved pharmacological profiles:** The hybridization strategy allows medicinal chemists to optimize a molecule's pharmacokinetic and pharmacodynamic properties by carefully selecting and linking pharmacophores. This approach can enhance Absorption, Distribution, Metabolism, Excretion, and Toxicity (ADMET) profiles, control drug release with flexible or cleavable linkers,[71] and improve selectivity while minimizing off-target effects.

5. **Simplified therapy and patient compliance:** Hybrid molecules simplify therapy by combining multiple drug actions into one compound, reducing pill burden, lowering the risk of drug–drug interactions,[76] and improving patient compliance, especially important for chronic or complex therapeutic regimens.[77]

6. **Novel biological activities:** Hybridization can also produce new biological activities absent in the parent scaffolds by creating unique structures that interact with new targets or pathways, expanding drug discovery possibilities and potentially leading to first-in-class therapeutics.[78]

Summary: The hybrid heterocyclic approach is a powerful and versatile strategy in drug design, enabling the creation of molecules that can address disease complexity through synergistic, multi-target, and optimized pharmacological actions. The conceptual framework described here set the stage for the diverse applications discussed in the following section.

1A.6.2 Therapeutic Applications of Hybrid Heterocycles

Hybrid heterocycles play a crucial role in drug discovery across diverse therapeutic areas.

Hybrid molecules are valuable in **anticancer drug discovery** for combining pharmacophores with complementary mechanisms. For example, quinazoline-based hybrids (e.g., quinazoline–imidazole,[79] quinazoline–urea[80]) often act as kinase inhibitors. These hybrids typically outperform parent compounds in potency and selectivity. Notably, several hybrids, such as lapatinib, cabozantinib, bosutinib, and palbociclib, have reached clinical trials and approval, highlighting the effectiveness of this strategy in cancer therapy.[81]

As a promising strategy in **antimalarial drug development**, hybrid molecules address drug resistance, improving outcomes. For example, hybrids like trioxaquines, which link a trioxane (artemisinin-like) to an aminoquinoline (chloroquine-like), act through multiple pathways, such as heme alkylation and inhibition of hemozoin formation, showing potent activity against both chloroquine-sensitive and -resistant Plasmodium falciparum strains.[82,83] These hybrids enhance efficacy, reduce resistance risk, and can improve pharmacokinetic profiles compared to traditional therapies.

Hybrid molecules are highly promising in **antibacterial and antiviral drug development**. Examples like pyrazole–tetrazole and indole–triazole hybrids have shown potent antibacterial activity, sometimes surpassing standard drugs,[84,85] while antiviral hybrids targeting multiple HIV enzymes offer greater potency and reduced resistance.[70] The use of specialized linkers further enhances pharmacokinetics and targeted drug release.

Beyond anti-infectives, hybrid scaffolds have proven effective in anti-inflammatory,[86] antidiabetic,[87] neuroprotective,[88] and cardiovascular therapies.[89] Rational design enables improved efficacy, safety, and reduced side effects, highlighting the broad therapeutic potential of molecular hybridization across diverse disease areas. **Figure 1A.8** showcases representative hybrids, demonstrating diverse linking strategies and pharmacophore combinations.

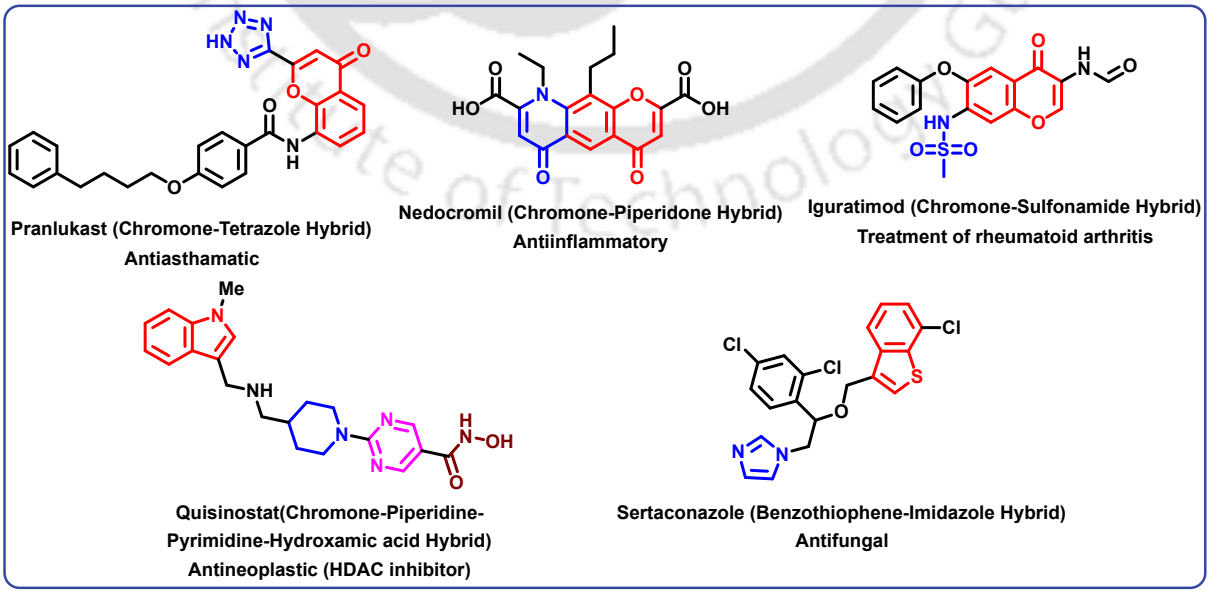

Figure 1A.8: Representative hybrid scaffolds with notable biological activity.

1A.6.3 Hybrid Scaffolds Incorporating Chromone, Thiophene, and Thiopyran Motifs

The strategic combination of chromone and thiophene motifs into hybrid molecular frameworks has garnered significant attention in the quest for novel bioactive compounds.[90] Among the most studied examples are thieno-coumarins, a class of heterocycles in which a thiophene ring is fused to the coumarin or chromone core. Within this family, thieno[3,2-*c*]chromones have been investigated for their diverse biological and pharmacological properties, including anticancer and antimicrobial activities.[90][91] However, the structurally related thieno[2,3-*b*]chromene derivatives remain considerably underexplored. Only a limited number of reports address their synthesis,[92][93] and studies evaluating their biological activities are scarce.[94][95] As a result, the chemical space surrounding these fused scaffolds remains largely untapped, despite their potential as privileged motifs in drug discovery (**Figure 1A.9a**).

In comparison, chromone–thiopyran hybrids are even less represented in both natural and synthetic contexts. To date, the only naturally occurring example reported in the literature is *Preussochromone A*, a rare metabolite isolated from the endolichenic fungus *Preussia africana*. This compound features a chromone moiety fused to a thiopyran ring and has demonstrated notable cytotoxic activity against A549 human lung carcinoma cells (**Figure 1A.9b**).[96,97]

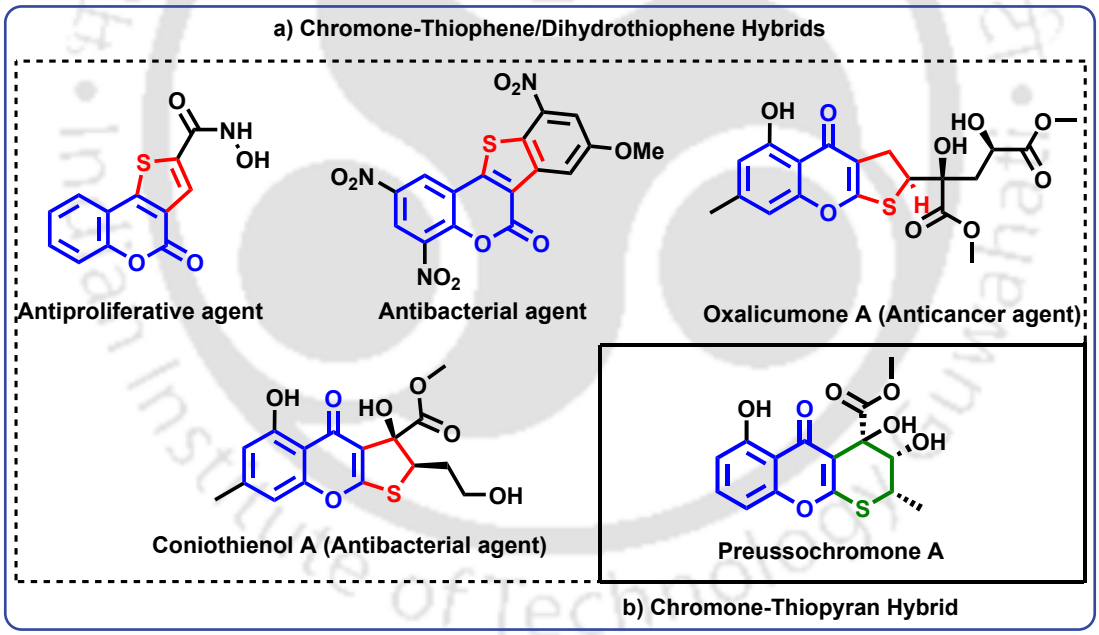

Figure 1A.9: Biologically active thieno-coumarins.

The scarcity of such hybrids in nature and the limited synthetic exploration further highlight the opportunity to develop novel thiopyran-containing chromone derivatives. These structures may offer improved physicochemical and pharmacological properties, owing to the distinct steric and electronic characteristics imparted by the sulfur-containing ring system.

1A.6.4 Concluding Remarks on Current Standing and Future Potential

Molecular hybridization has emerged as a powerful strategy in drug discovery, enabling the development of therapeutics for complex diseases and drug-resistant conditions. Continued

advances in synthetic methods are poised to accelerate progress in creating multi-target agents. The following section explores current challenges and future opportunities in synthesizing hybrid heterocycles built on the core scaffolds central to this research.

1A.6.5 Literature on synthetic strategies

The construction of chromone-thiophene hybrid molecules employs several specific methodologies:

1A.6.5.1 Synthesis of linked chromone-thiophene hybrids (Spacer-Based)

Direct condensation reactions: A straightforward approach for synthesizing hybrids like 2-(2-Thienyl)chromone involves the **Claisen–Schmidt condensation** of 2-hydroxyacetophenone with thiophene-2-carbaldehyde in the presence of acid catalysts (**Scheme 1A.15**). This method generally yields good results within moderate reaction times. Notably, this strategy has been employed to synthesize novel molecules with antiparasitic activity, as discussed in the preceding section.[98]

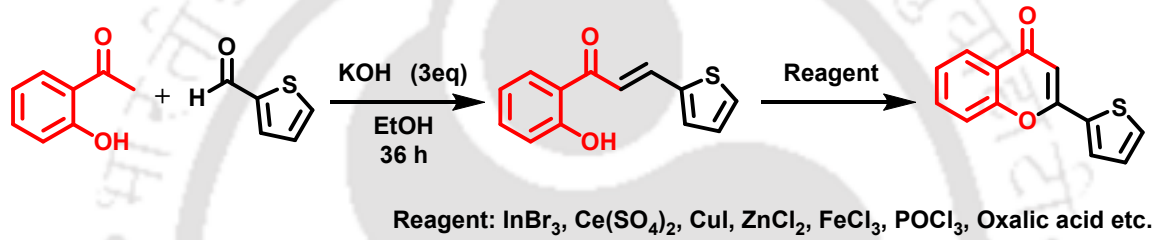

Scheme 1A.15: Chromone-thiophene hybrid synthesis *via* direct condensation reaction.

Conversion from chalcone derivatives: A notable synthetic pathway involves the cyclization of (*E*)-1-(2-hydroxyphenyl)-3-(1-(2,3-dimethylphenyl)-3-(thiophen-2-yl)-1*H*-pyrazol-4-yl) prop-2-en-1-ones (a series of chalcone derivatives) into their corresponding chromone derivatives, specifically 2-(1-(2,3-dimethylphenyl)-3-(thiophen-2-yl)-1*H*-pyrazol-4-yl)-4*H*-chromen-4-ones (**Scheme 1A.16**).[99]

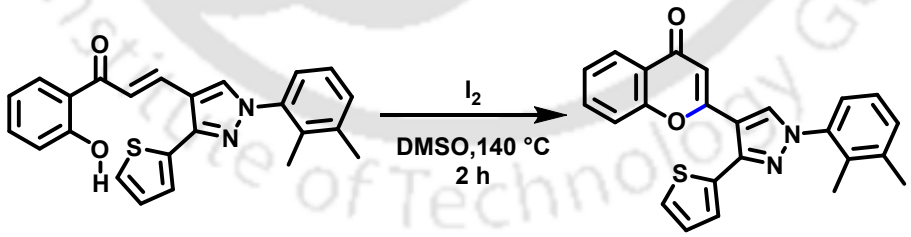

Scheme 1A.16: Chromone-thiophene hybrid synthesis *via* iodine-catalyzed cyclization of chalcone derivatives.

1A.6.5.2 Synthesis of fused chromone-thiophene hybrids

Levchenko *et al.* employed a multi-step synthetic sequence involving (i) acylation, (ii) Baker–Venkataraman rearrangement, and (iii) cyclization, followed by bromination. This was succeeded by thioether formation, intramolecular cyclization, and elimination upon heating with thioacetamide in *N*,*N*-Dimethylformamide (DMF). The process led to the formation of a

thieno[3,4-*b*]chromen-9-one core, representing a fused chromone–thiophene scaffold, with an additional thiophene ring attached via a linker (**Scheme 1A.17**).[100]

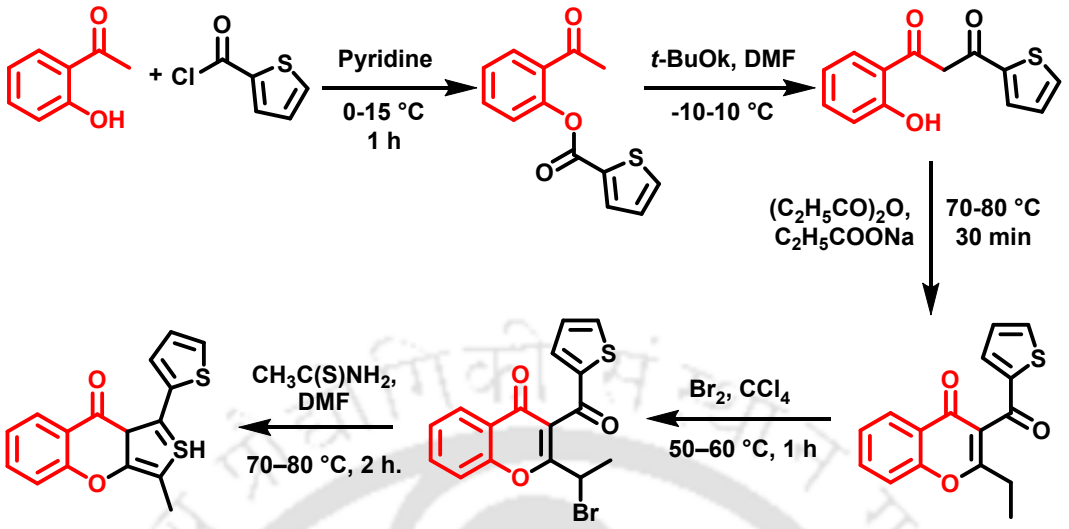

Scheme 1A.17: Synthesis of a fused thieno[3,4-*b*]chromen-9-one scaffold.

Wittine *et al.* carried out a Vilsmeier–Haack formylation of 4-hydroxycoumarin to obtain 4-chloro-3-formylcoumarin, which was then reacted with ethyl 2-mercaptoacetate and triethylamine (Et_3N) in pyridine to afford a tricyclic coumarin[3,2-*c*]thiophene ester (**Scheme 1A.18**). This ester served as a key intermediate for the synthesis of hydroxamic acid and ureido derivatives, which demonstrated potent cytostatic activity.[90]

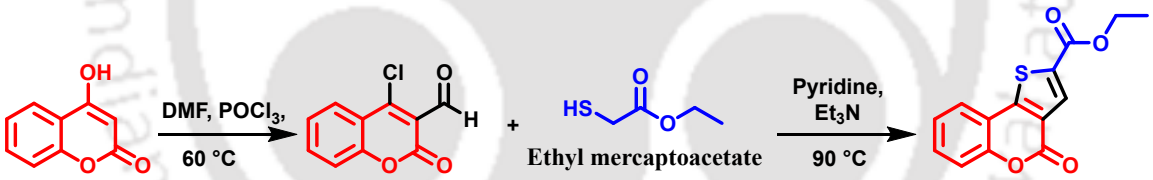

Scheme 1A.18: Formation of a fused tricyclic coumarin[3,2-*c*]thiophene ester.

In addition to the examples presented here, more advanced synthetic approaches for chromone-thiophene hybrids encompass multicomponent reactions,[101] transition-metal-catalyzed cross-coupling, C—H functionalization,[92] and electrochemical cyclization,[98] enabling more efficient and sophisticated molecular assembly. A few of these methods will be discussed in **Chapter 3**, as they are more directly relevant to the themes explored therein.

1A.6.6 Chromone–Thiopyran Hybrids: Importance and Synthetic Methods

Chromone-Pyran Hybrids: A Well-Explored Domain

Chromone-pyran hybrids have been extensively studied owing to their broad pharmacological profiles. These compounds typically comprise a chromone core (a benzopyran-4-one structure) fused or linked to a pyran ring (a six-membered oxygen-containing heterocycle). The literature is rich with examples of such hybrids, including fused systems like pyrano[3,2-*c*]chromenes and spiro-linked architectures. These compounds have attracted considerable attention due to their diverse biological activities, including anticancer,[102] antimicrobial,[103] antidiabetic[104]

and antioxidant properties,[105] as well as their interesting optical characteristics for materials science.[106]

Chromone-Thiopyran Hybrids: An Underexplored Frontier

In contrast, when we look for chromone-thiopyran hybrids, i.e., molecules that contain both a chromone ring and a thiopyran ring (a six-membered ring with a sulfur atom), we find a significant gap in the literature. Unlike the oxygen-oxygen systems of chromone-pyran hybrids, there are no well-documented examples of molecules where a chromone and a thiopyran ring are covalently fused or directly linked within the same framework. Most of the reported compounds either feature a chromone or a thiopyran (or its close relative, thiochromone), but not both in a true hybrid sense. As discussed earlier, *Preussochromone A* remains the only known natural product exemplifying this class,[96,97] highlighting both the rarity and untapped potential of chromone–thiopyran hybrids in drug discovery.

Incorporating a thiopyran ring into chromone-based hybrids offers several potential advantages over their oxygen-containing counterparts.

1. Sulfur substitution increases molecular lipophilicity due to its lower electronegativity and higher polarizability compared to oxygen, which can enhance membrane permeability and bioavailability of the compounds.

2. While sulfur is generally a weaker hydrogen-bond acceptor than oxygen, it can still participate in non-covalent interactions, albeit less effectively, potentially influencing molecular recognition and binding affinity.[107,108]

These attributes underscore the rationale for exploring chromone-thiopyran hybrids in drug discovery and development.

The synthesis of chromone–thiopyran hybrids remains underexplored, with only a few methodologies reported to date. These synthetic strategies will be discussed in detail in **Chapter 3**, aligning with the thematic focus of that chapter.

> **Summary:** While chromone-pyran hybrids are a well-explored area of research, the corresponding chromone-thiopyran hybrids remain unexplored. Addressing this gap could be a fruitful direction for future studies, both to advance synthetic methodology and to explore new frontiers in heterocyclic chemistry.

1A.6.7 Shortcomings and Challenges in Previous Studies

1A.6.7.1 Synthesis challenges for chromone-thiophene hybrid

The synthesis of chromone–thiophene hybrids often employs classical organic reactions such as condensation, cyclization, and acylation, along with more specific catalytic approaches. Each method, while effective in certain contexts, presents its own set of drawbacks:

Condensation reactions:

Lack of selectivity: Classical condensation reactions, such as the Claisen-Schmidt condensation (often used to form chalcone precursors to chromones), can suffer from a lack of

selectivity, leading to mixtures of products or undesired isomers. This necessitates extensive purification steps, thereby reducing overall yield and increasing cost.

Competitive side reactions: Competing reactions, like self-aldol reactions in the context of chalcone synthesis, can lower the yield of the desired product.

Harsh reaction conditions: Many condensation reactions require strong acids or bases, high temperatures, or prolonged reaction times, which can be detrimental to sensitive functional groups present in either the chromone or thiophene precursors, leading to degradation or unwanted side products.

Cyclization reactions:

Use of pre-functionalized coupling partners: Often, cyclization reactions require highly pre-functionalized starting materials, which themselves may involve multi-step syntheses, thereby increasing the overall synthetic complexity and cost.

Catalyst requirements: Cyclization reactions, especially those forming carbon–carbon bonds, often rely on transition metal catalysts like copper or zinc. While these catalysts are effective, they pose challenges in pharmaceutical contexts due to potential toxicity and poor solubility. Moreover, removing residual metals typically necessitates rigorous purification methods, such as expensive nanofiltration membranes or extensive column chromatography, which can be both costly and detrimental to sensitive compounds.

1A.6.7.2 Synthesis challenges for chromone-thiopyran hybrid

The synthesis of chromone–thiopyran hybrids presents a notable challenge, primarily due to the limited availability of established synthetic methodologies. The fusion of chromone and thiopyran moieties demands precise control over reaction conditions to achieve selectivity and acceptable yields, which is often tricky. In particular, the high reactivity of sulfur-containing intermediates can be challenging to control, frequently leading to side reactions, structural rearrangements, or degradation, which hinder the formation of the desired hybrid structure. Together, these factors contribute to the scarcity of chromone–thiopyran hybrids in the literature. A detailed discussion of the few reported synthetic strategies will be provided in **Chapter 3**, in alignment with its focus on methodology.

1A.7 Objectives and Scope of the Thesis

4-Hydroxycoumarin is a well-established scaffold in medicinal chemistry, with its reactivity and applications extensively explored. Similarly, **4-hydroxydithiocoumarin** has also been investigated to a considerable extent, particularly in key transformations such as sigmatropic rearrangements, Diels–Alder reactions, cross-coupling strategies, MCRs, and Michael additions. In contrast, **4-hydroxythiocoumarin** remains significantly underexplored, primarily due to its limited commercial availability and sparse documentation in the synthetic literature.

Despite this, 4-hydroxythiocoumarin shares key structural features with both 4-hydroxycoumarin and 4-hydroxydithiocoumarin, including the presence of multiple nucleophilic centers that can participate in diverse organic transformations. This structural similarity

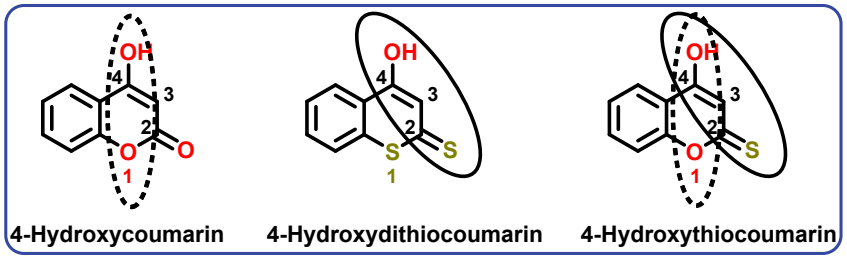

Figure 1A.10: Structural comparison of 4-hydroxycoumarin, 4-hydroxythiocoumarin, and 4-hydroxydithiocoumarin.

suggests the potential for complementary or novel reactivity patterns that have not yet been fully realized.

This thesis aims to compare the reactivity of 4-hydroxythiocoumarin with its oxygenated and dithio analogs, with the goal of uncovering unique and underutilized transformation pathways.

Three nucleophilic centers are identified across these scaffolds:

- **Sulfur at position 2:** The most widely studied site, known for undergoing alkylation (e.g., with methyl or ethyl halides).
- **Carbon at position 3:** Participates in nucleophilic addition reactions such as the Michael and Knoevenagel condensations.
- **Hydroxy group at position 4:** Although structurally present, this group's reactivity has not been properly explored in the literature.

The central focus of this work is to explore the synthetic utility of 4-hydroxythiocoumarin by leveraging its multiple reactive centers for the development of complex and functionally diverse heterocycles. A systematic comparison with its structural analogs will provide insights into how electronic and positional factors govern reactivity, thus contributing to the broader field of heterocyclic synthesis in medicinal chemistry.

Part 1B
Synthesis of 4-Hydroxythiocoumarin

1B.1 Overview of Synthetic Approaches to 4-Hydroxythiocoumarin

Few protocols exist in the literature for the synthesis of 4-hydroxy-2*H*-chromene-2-thione derivatives (**Scheme 1B.1**). One of the protocols utilizes P_2S_5 in pyridine for the synthesis.[30] However, P_2S_5 is a harmful solid and reacts violently with water, releasing toxic, combustible H_2S gas. Also, it requires dry pyridine, which requires distillation, releasing toxic fumes into the air.

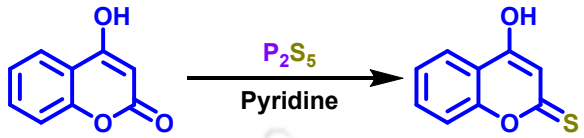

Scheme 1B.1: Preparation of 4-hydroxythiocoumarin using P_2S_5 in pyridine.

While it is a reasonable assumption that Lawesson's reagent might be the ideal method for converting 4-hydroxycoumarin to 4-hydroxythiocoumarin, as a similar reaction has been carried out before,[109] as it turns out, on reacting 4-hydroxycoumarin with Lawesson's reagent in boiling toluene, it gets converted to 4-thiohydroxycoumarin-2-thione (4-mercapto-2*H*-chromene-2-thione) instead (**Scheme 1B.2**).[110]

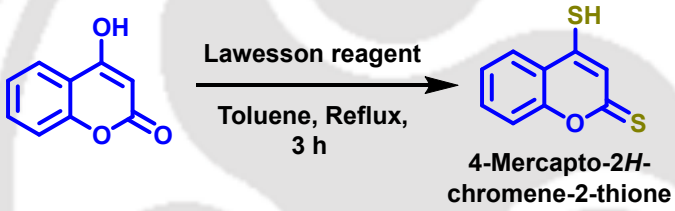

Scheme 1B.2: Reaction of 4-hydroxycoumarin with Lawesson's reagent.

1B.2 Current Strategy and Reaction Optimization

Thus, with the goal of achieving good yield and environmental compatibility, carbon disulfide (CS_2) was chosen as the sulfur-containing reagent for thionation. The earlier reported procedures include base-catalysed cyclisation of acetophenone with carbon disulfide in dry Tetrahydrofuran (THF), which resulted in poor yield due to poor proton abstraction by the base.[26] Here we have slightly modified the procedure by using 18-crown-6 ether. It has been found that adding a catalytic amount of this phase transfer catalyst (PTC) improved the basic character of potassium *tert*-butoxide.

Crown ethers (CEs) are heterocyclic compounds known for their strong and selective binding affinity toward specific cations. They are widely used as PTCs in organic synthesis. Notably, previous studies have reported the *in situ* formation of the [K(18-C-6)(O^tBu)] complex when crown ether is combined with potassium tert-butoxide (KO^tBu). This complexation enhances the solubility, nucleophilicity, and basicity of the tert-butoxide anion, thereby improving reaction efficiency.[111]

Accordingly, this thesis employs a base-catalyzed synthesis method assisted by 18-crown-6 ether to efficiently produce 4-hydroxythiocoumarin, which serves as the key starting material

for all subsequent synthetic transformations (**Scheme 1B.3**). The methodology has been further extended to synthesize several derivatives of 4-hydroxythiocoumarin.

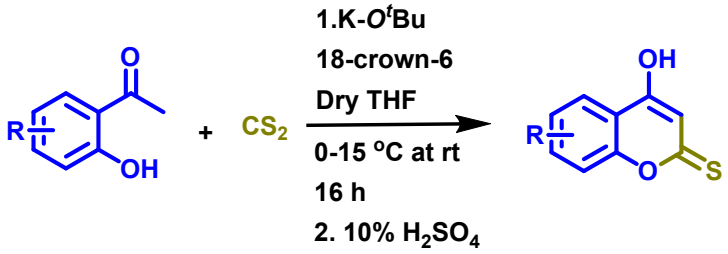

Scheme 1B.3: Base-catalyzed synthesis of 4-hydroxythiocoumarin assisted by 18-crown-6 ether.

Optimization of the reaction conditions was carried out using 2'-hydroxyacetophenone and carbon disulfide as model substrates, with the results summarized in **Table 1B.1**. The initial reaction performed in dry benzene without any catalyst afforded the product **1A1** in only 5% yield (**Table 1B.1**, entry **1**). The structure of **1A1** was confirmed by ^{1}H and ^{13}C NMR spectroscopy and HRMS analysis. Switching the solvent to dry toluene resulted in a modest improvement in yield to 10% (**Table 1B.1**, entry **2**), while further enhancement to 17% was achieved using dry THF (**Table 1B.1**, entry **4**).

To further enhance the yield, 10 mol% of crown ether (relative to base) was introduced under otherwise identical conditions in dry THF, which significantly increased the product yield

Table 1B.1: Optimization of the reaction conditions for the synthesis of 4-hydroxythiocoumarins.[a]

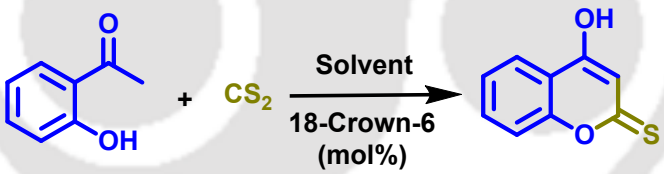

Sl No.	Solvent	Base	Temp	Crown ether (mole%) w.r.t base	1A1 (Yield (%)[b])
1	Dry Benzene	KO^{t}Bu	r.t	0	5
2	Dry Toluene	KO^{t}Bu	r.t	0	10
3	Dry Toluene	KO^{t}Bu	r.t	10	41
4	Dry THF	KO^{t}Bu	r.t	0	17
5	**Dry THF**	**KO^{t}Bu**	**r.t**	**10**	**50**
6	DMF	NaH	r.t	0	NR
7	Dry THF	KO^{t}Bu	r.t	50	19
8	Dry THF	KO^{t}Bu	r.t	100	23

[a]Reactions were carried out using 2'-hydroxyacetophenone (1 equiv), carbon disulfide (1 equiv), KO^{t}Bu (3 equiv), and 18-crown-ether (10 mol% w.r.t base). [b]Isolated Yield.

to 50% (**Table 1B.1**, entry **5**). A similar reaction in dry toluene provided a slightly lower yield of 41% (**Table 1B.1**, entry **4**). Attempts to use sodium hydride in DMF did not afford any significant improvement (**Table 1B.1**, entry **6**). Notably, increasing the crown ether loading to 50% and 100% relative to base led to reduced yields of 19% and 23%, respectively (**Table 1B.1**, entries **7** and **8**).

Based on the data presented in **Table 1B.1**, the use of 10 mol% crown ether proved optimal for maximizing the reaction yield. Under these conditions, 4-hydroxythiocoumarin was synthesized efficiently (50% yield). The protocol was further extended to various 6-substituted derivatives, including chloro, bromo, methyl, and methoxy groups, as well as 6- and 7-fluoro analogs. All derivatives were obtained in good yields, ranging from 55% to 67% (**Table 1B.2**). All compounds were fully characterized by ^{1}H and ^{13}C NMR spectroscopy, which had not been reported in previous literature.

Table 1B.2: Synthesis of 4-hydroxy-2-thiocoumarin derivatives.[a][b]

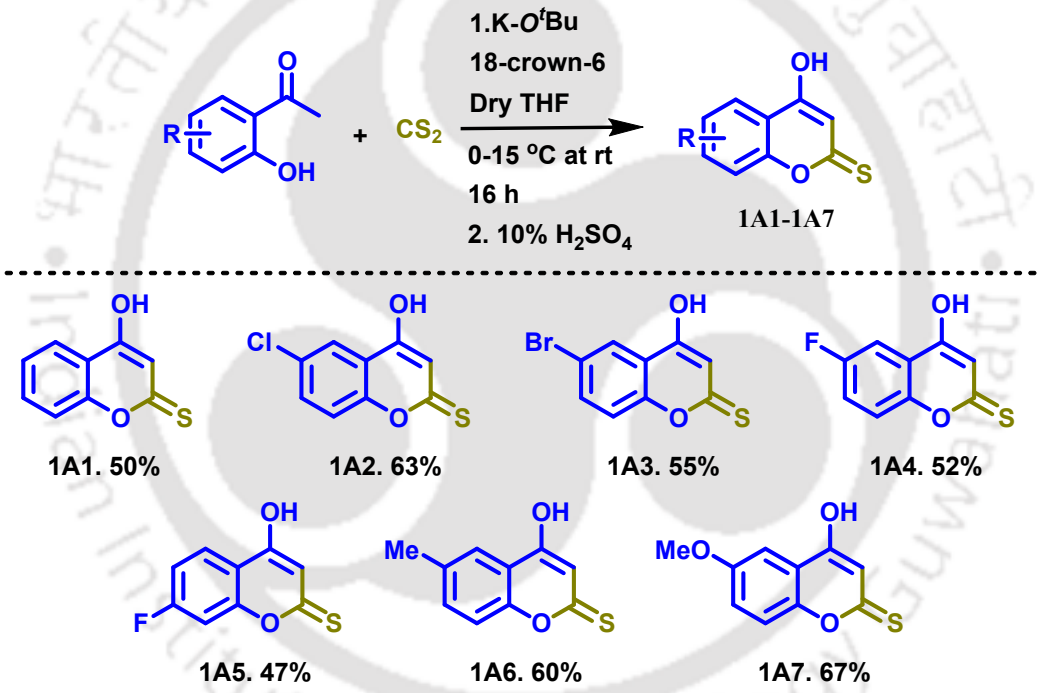

[a]**Reagents and conditions:** 2'-hydroxyacetophenone (5 mmol), carbon disulfide (5 mmol), KO^{t}Bu (15 mmol), 18-crown-6 (30 mol%), dry THF (15 mL), stirred at 0 – 15 °C for 1 h and then at room temperature for 16 h. [b]Isolated yields are provided.

The compounds synthesized using this protocol served as the foundational substrates for all subsequent synthetic studies carried out in the course of this doctoral work.

1B.3 Experimental Protocol

General procedure for the synthesis of compound 1A1–1A7

4-Hydroxythiocoumarin (**1A1**) was synthesized following a modified version of the previously reported procedure.[26] Potassium tertiary butoxide (15 mmol) and 18-crown-6 ether (1.5 mmol) were taken in 7 mL of anhydrous THF in an oven-dried round-bottomed flask. The mixture

was purged with N_2 and cooled to 0 °C in an ice bath. 5 mmol of 2'-hydroxyacetophenone was added dropwise, followed by the addition of carbon disulfide (5 mmol) to the reaction mixture, resulting in the formation of a yellow precipitate. The reaction was stirred at 0 – 15 °C for another 1 h, then brought to room temperature, and stirring was continued at this temperature for 16 h. The reaction was quenched by adding 5 mL of water and then washing the water layer with ethyl acetate (2×5 mL). The aqueous layer was then acidified with 10% H_2SO_4 until pH was adjusted to 4 – 5, and the mixture was stirred for another 16 h. A yellow precipitate was formed, which was collected by vacuum filtration and washed with petroleum ether several times to obtain the desired product as a yellow solid. The other substituted 4-hydroxythiocoumarins (**1A2**–**1A7**) were synthesized following a similar protocol.

1B.4 Characterization Data for Compounds 1A1–1A7

4-hydroxy-2*H*-chromene-2-thione (1A1)

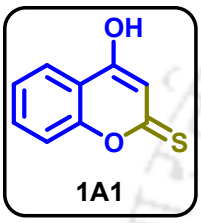

Yellow solid (0.445 g, 50%); **mp** 215 – 218 °C; **^{1}H NMR (400 MHz, DMSO-d$_6$)** δ 7.88 (dd, J = 7.9, 0.9 Hz, 1H), 7.77 – 7.68 (m, 1H), 7.54 (d, J = 8.3 Hz, 1H), 7.43 (t, J = 7.6 Hz, 1H), 6.66 (s, 1H); **^{13}C{^{1}H} NMR (125 MHz, DMSO-d$_6$)** δ 196.97 (1C), 162.08 (1C), 157.06 (1C), 133.58 (1C), 125.38 (1C), 123.38 (1C), 116.92 (1C), 116.57 (1C), 108.03 (1C); **IR (KBr)** ν_{max}/cm^{-1} 3436 (O–H), 1019 (C=S); **HRMS (ESI)** calcd for $C_9H_7O_2S^+$ 197.0161 M+H$^+$ found 197.0157.

6-Chloro-4-hydroxy-2*H*-chromene-2-thione (1A2)

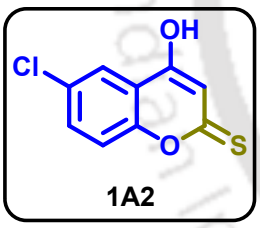

Yellow solid (0.670 g, 63%); **mp** 256 – 257 d*c*; **^{1}H NMR (400 MHz, DMSO-d$_6$)** δ 7.82 (d, J = 2.5 Hz, 1H), 7.74 (dd, J = 2.6, 8.9 Hz, 1H), 7.58 (d, J = 8.9 Hz, 1H), 6.62 (s, 1H); **^{13}C{^{1}H} NMR (125 MHz, DMSO-d$_6$)** δ 196.25 (1C), 161.68 (1C), 155.65 (1C), 133.07 (1C), 129.32 (1C), 122.60 (1C), 119.00 (1C), 118.78 (1C), 108.63 (1C); **IR (KBr)** ν_{max}/cm^{-1} 3070 (O–H), 1105 (C=S); **HRMS (ESI)** calcd for $C_9H_6ClO_2S^+$ 212.9772 M+H$^+$ found 212.9762.

6-Bromo-4-hydroxy-2*H*-chromene-2-thione (1A3)

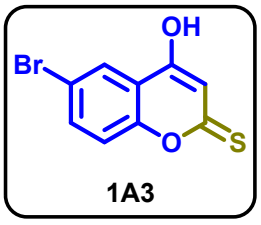

Yellow solid (0.707 g, 55%); **mp** 248 – 249 °C; **^{1}H NMR (500 MHz, DMSO-d$_6$)** δ 7.95 (d, J = 2.4 Hz, 1H), 7.83 (dd, J = 2.4, 8.8 Hz, 1H), 7.47 (d, J = 8.8 Hz, 1H), 6.54 (s, 1H); **^{13}C{^{1}H} NMR (100 MHz, DMSO-d$_6$)** δ 196.59 (1C), 160.72 (1C), 155.95 (1C), 135.89 (1C), 125.43 (1C), 118.91 (1C), 118.87 (1C), 117.23 (1C), 108.54 (1C); **IR (KBr)** ν_{max}/cm^{-1} 3034 (O–H), 1100 (C=S); **HRMS (ESI)** calcd for $C_9H_6BrO_2S^+$ 256.9267 M+H$^+$ found 256.9254.

6-Fluoro-4-hydroxy-2*H*-chromene-2-thione (1A4)

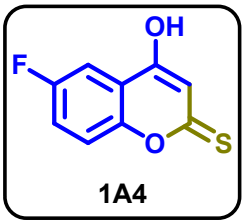

Yellowish brown solid (519 mg, 52 %), mp 218–220 °C; **mp** 218 – 220 °C; **^{1}H NMR (500 MHz, DMSO-d$_6$)** δ 7.63 – 7.61 (m, 1H), 7.60 (d, J = 3.5 Hz, 1H), 7.58 (d, J = 2.9 Hz, 1H), 6.67 (s, 1H); **^{13}C{^{1}H} NMR (125 MHz, DMSO-d$_6$)** δ 196.3, 162.3, 159.6, 157.6, 153.6, 120.9 (d, J = 26.0 Hz), 119.0, 118.8 (d, J = 3.4 Hz), 108.7 (d, J = 24 Hz); **IR (KBr)** ν_{max}/ cm^{-1} 3090 (O−H), 1081 (C=S); **HRMS (ESI)** calcd for $C_9H_6FO_2S^+$ 197.0067 M+H$^+$ found 197.0061.

7-Fluoro-4-hydroxy-2*H*-chromene-2-thione (1A5)

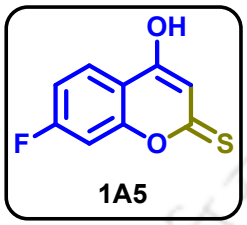

Yellowish brown solid (470 mg, 47 %), mp 212–214 °C; **mp** 212 – 214 d*c*; **^{1}H NMR (500 MHz, DMSO-d$_6$)** δ 7.93 (dd, J = 8.9, 6.2 Hz, 1H), 7.56 (dd, J = 9.6, 2.5 Hz, 1H), 7.33 (td, J = 8.7, 2.5 Hz, 1H), 6.63 (s, 1H); **^{13}C{^{1}H} NMR (125 MHz, DMSO-d$_6$)** δ 196.9, 164.7 (d, J = 250.6 Hz), 161.1, 158.0 (d, J = 13.6 Hz), 125.6 (d, J = 10.5 Hz), 113.9, 113.4 (d, J = 23.0 Hz), 107.4, 104.0 (d, J = 25.7 Hz); **IR (KBr)** ν_{max}/ cm^{-1} 3098 (O−H), 1076 (C=S); **HRMS (ESI)** calcd for $C_9H_6FO_2S^+$ 197.0067 M+H$^+$ found 197.0062.

1B.5 Copies of ^{1}H NMR, ^{13}C{^{1}H} NMR and HRMS spectra of Compounds

Figure 1B.1a: ^{1}H NMR (400 MHz, DMSO-d_6) spectrum of compound **1A1**.

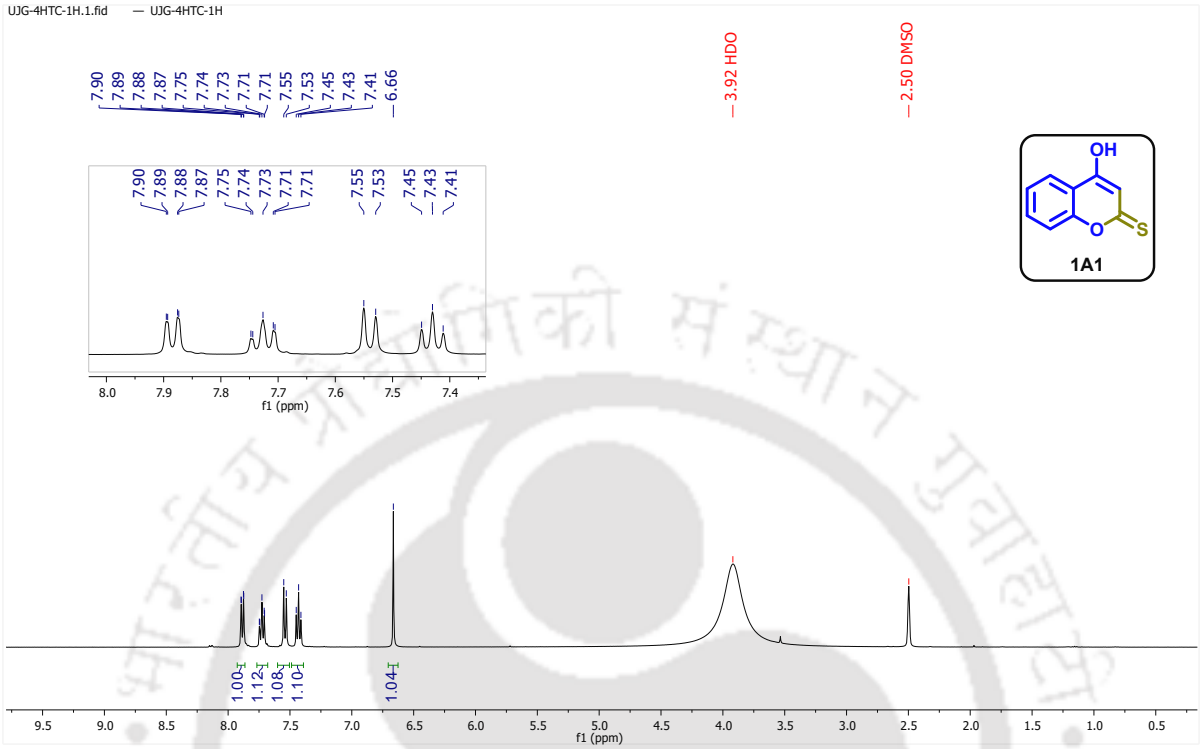

Figure 1B.1b: ^{13}C{^{1}H} NMR (125 MHz, DMSO-d_6) spectrum of compound **1A1**.

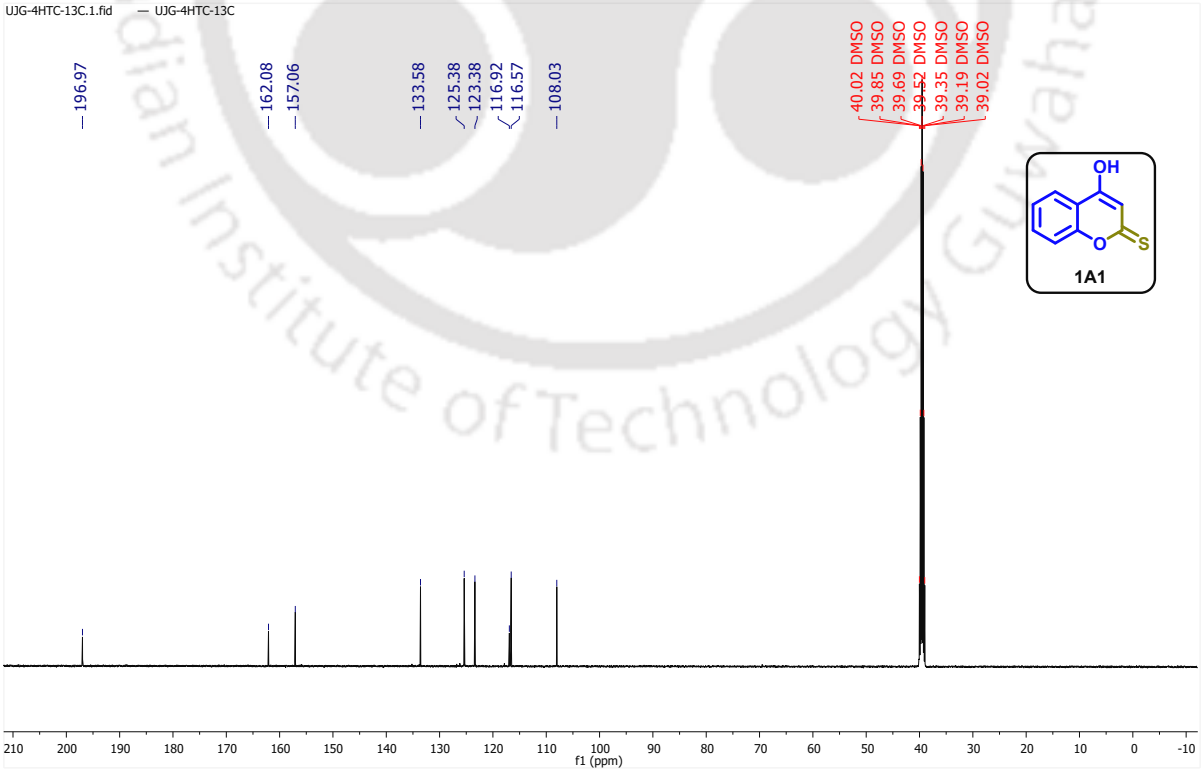

Figure 1B.2a: ^{1}H NMR (400 MHz, DMSO-d_6) spectrum of compound **1A2**.

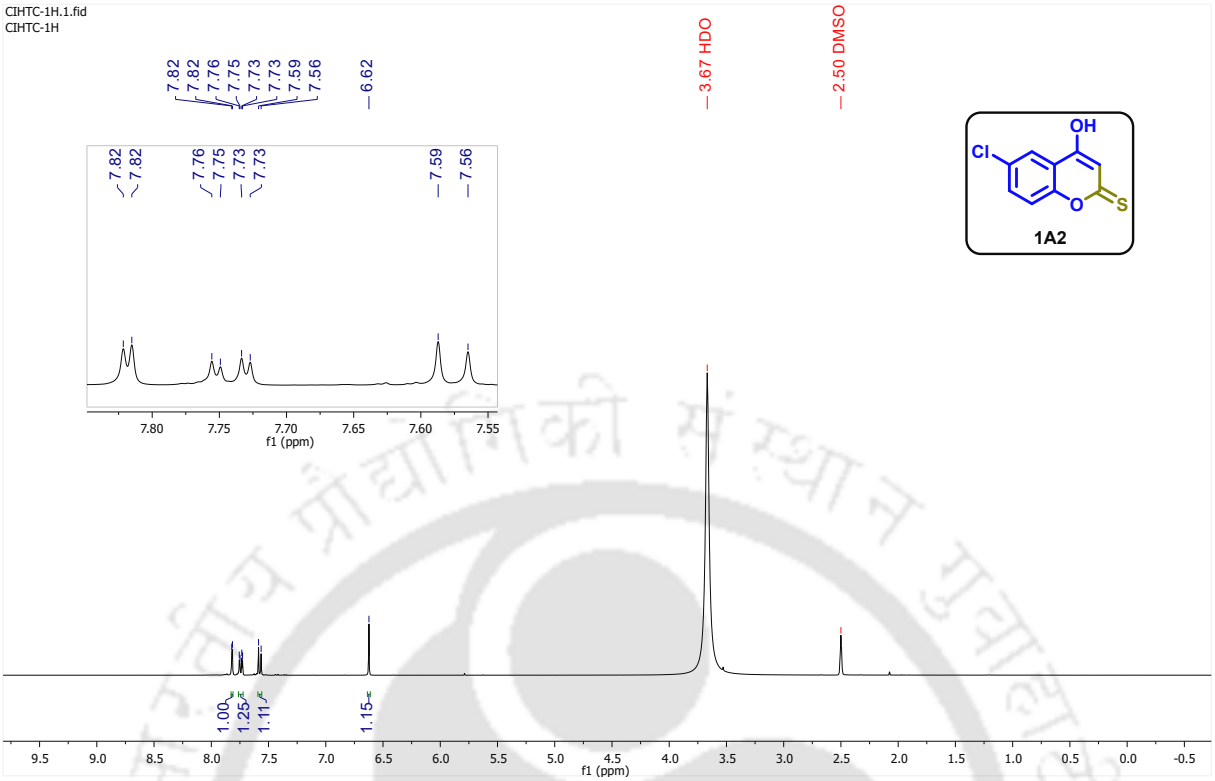

Figure 1B.2b: ^{13}C{^{1}H} NMR (100 MHz, DMSO-d_6) spectrum of compound **1A2**.

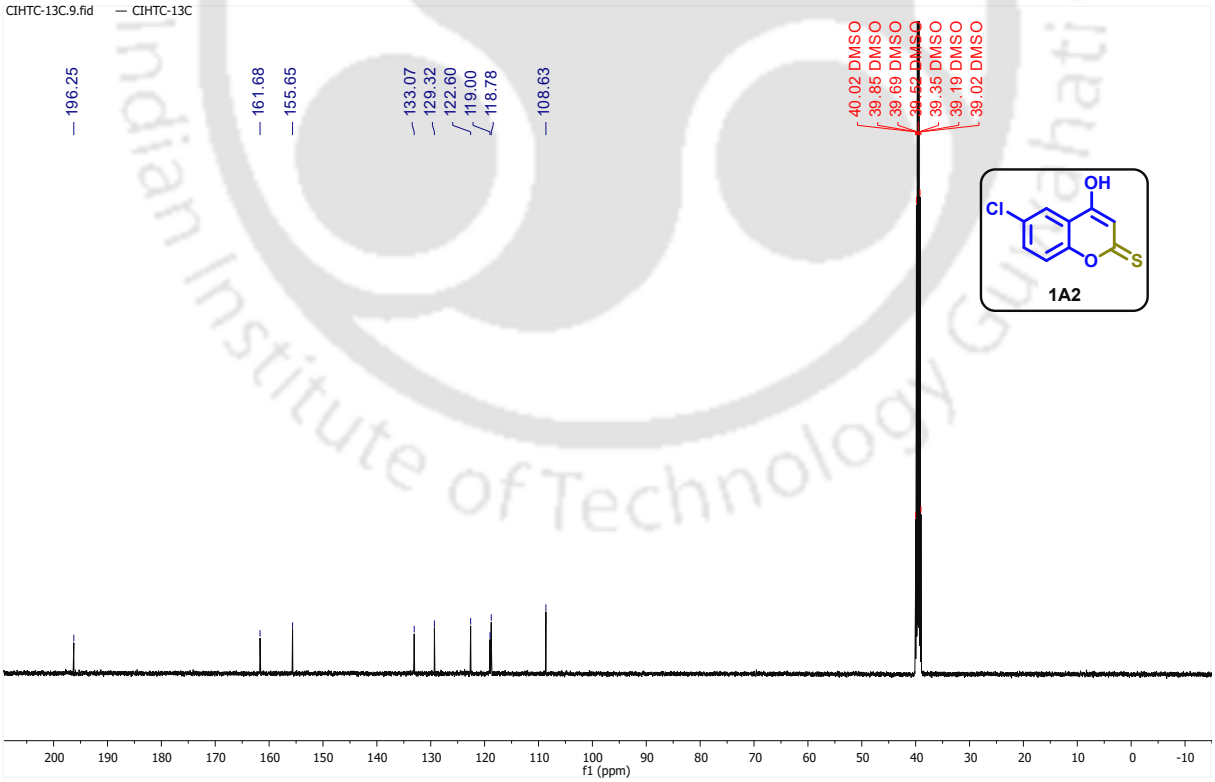

Figure 1B.2c: HRMS spectrum of compound **1A2**.

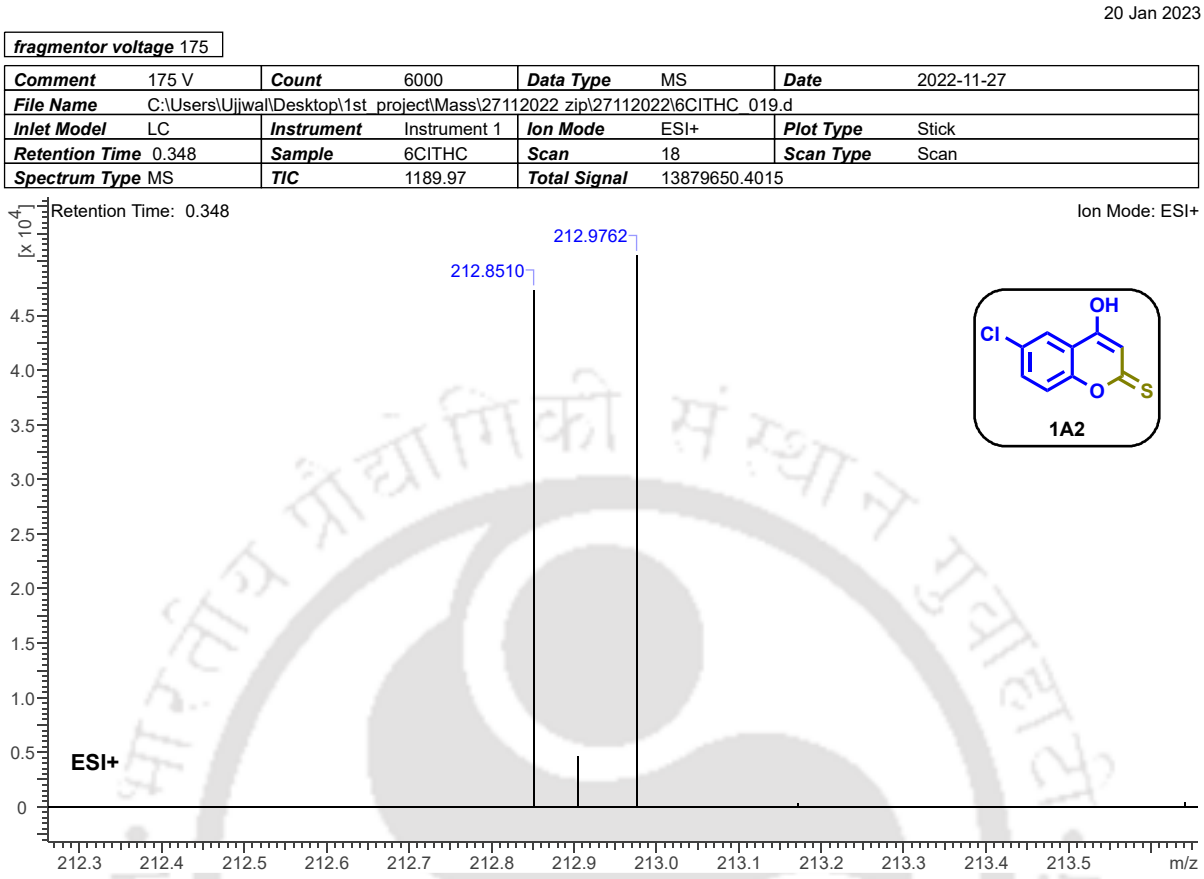

References

[1] M. M. Abdou, R. A. El-Saeed, S. Bondock, *Arab. J. Chem.* **2019**, *12*, 88–121.

[2] V. F. Traven, V. V. Negrebetsky, L. I. Vorobjeva, E. A. Carberry, *Can. J. Chemistry* **1997**, *75*, 377–383.

[3] M. M. Abdou, *Arab. J. Chem.* **2017**, *10*, S3664–S3675.

[4] I. Cortés, L. J. Cala, A. B. J. Bracca, T. S. Kaufman, *RSC Adv.* **2020**, *10*, 33344–33377.

[5] Q. Su, H. Qian, Z. Li, X. Sun, Z. Wang, *Asian J. Org. Chem.* **2017**, *6*, 512–515.

[6] V. Narayana, R. Varala, P. Zubaidha, *Int. J. Org. Chem.* **2012**, *2*, 287–294.

[7] J.-C. Jung, O.-S. Park, *Molecules* **2009**, *14*, 4790–4803.

[8] M. Gebauer, *Bioorgan. Med. Chem.* **2007**, *15*, 2414–2420.

[9] N. Au, A. E. Rettie, *Drug Metab. Rev.* **2008**, *40*, 355–375.

[10] W. R. Porter, *J. Comput.-Aided Mol. Des.* **2010**, *24*, 553–573.

[11] B. E. Watt, A. T. Proudfoot, S. M. Bradberry, J. A. Vale, *Toxicol. Rev.* **2005**, *24*, 259–269.

[12] R. Z. Batran, M. A. Khedr, N. A. Abdel Latif, A. A. Abd El Aty, A. N. Shehata, *J. Mol. Struct.* **2019**, *1180*, 260–271.

[13] J. Kaur, P. Famta, N. Khurana, M. Vyas, G. L. Khatik, in *New and Future Developments in Microbial Biotechnology and Bioengineering*, Elsevier, **2020**, pp. 209–218.

[14] Y. Wu, J. Xu, Y. Liu, Y. Zeng, G. Wu, *Front. Oncol.* **2020**, *10*, 592853.

[15] Z.-M. Wang, S.-S. Xie, X.-M. Li, J.-J. Wu, X.-B. Wang, L.-Y. Kong, *RSC Adv.* **2015**, *5*, 70395–70409.

[16] Z. Soleimani, M. Mohammadi, M. Halimi, S. Safapoor, N. Dastyafteh, E. Safaie, S. Mojtabavi, M. A. Faramarzi, M. Bozorgi-Koushalshahi, B. Larijani, M. Mohammadi-Khanaposhtani, M. Mahdavi, *Sci. Rep.* **2024**, *14*, 18693.

[17] C. Sun, W. Zhao, X. Wang, Y. Sun, X. Chen, *Pharmacol. Res.* **2020**, *160*, 105193.

[18] N. A. Meanwell, *J. Med. Chem.* **2011**, *54*, 2529–2591.

[19] G. A. Patani, E. J. LaVoie, *Chem. Rev.* **1996**, *96*, 3147–3176.

[20] J. A. Kemp, A. C. Foster, P. D. Leeson, T. Priestley, R. Tridgett, L. L. Iversen, G. N. Woodruff, *Proc. Natl. Acad. Sci.* **1988**, *85*, 6547–6550.

[21] D. T. Wong, F. P. Bymaster, E. A. Engleman, *Life Sci.* **1995**, *57*, 411–441.

[22] P. Kerkes, P. N. Sharma, A. Brossi, C. F. Chignell, F. R. Quinn, *J. Med. Chem.* **1985**, *28*, 1204–1208.

[23] A. Melander, G. Sartor, E. Wahlin, B. Schersten, P.-O. Bitzen, *Br. Med. J.* **1978**, *1*, 142–144.

[24] N. A. Meanwell, *J. Agr. Food Chem.* **2023**, *71*, 18087–18122.

[25] J. J. J. Leahy, B. T. Golding, R. J. Griffin, I. R. Hardcastle, C. Richardson, G. C. M. Smith, *Bioorg. Med. Chem. Lett.* **2004**, *14*, 6083–6087.

[26] L. Costantino, A. Del Corso, G. Rastelli, J. M. Petrash, U. Mura, *Eur. J. Med. Chem.* **2001**, *36*, 697–703.

[27] Y. F. Tong, S. Chen, Y. H. Cheng, S. Wu, *Chinese Chem. Lett.* **2007**, *18*, 407–408.

[28] G. D. Hatnapure, A. P. Keche, A. H. Rodge, S. S. Birajdar, R. H. Tale, V. M. Kamble, *Bioorg. Med. Chem. Lett.* **2012**, *22*, 6385–6390.

[29] E. Obreque-balboa, Q. Sun, G. Bernhardt, K. Burkhard, A. Buschauer, *Eur. J. Med. Chem.* **2016**, *109*, 124–133.

[30] A. A. Avetisyan, A. G. Alvandzhyan, *Russ. J. Org. Chem.* **2006**, *42*, 1063–1067.

[31] G. Palmisano, L. Toma, R. Annunziata, S. Tagliapietra, A. Barge, G. Cravotto, *J. Heterocyclic Chem.* **2007**, *44*, 411–418.

[32] K. C. Majumdar, A. T. Khan, S. Saha, *Synthetic Commun.* **1992**, *22*, 901–912.

[33] K. Majumdar, A. Taher, S. Ponra, *Tetrahedron Lett.* **2010**, *51*, 2297–2300.

[34] K. Majumdar, A. Taher, S. Ponra, *Synthesis* **2010**, *2010*, 4043–4050.

[35] K. C. Majumdar, S. Ponra, T. Ghosh, *RSC Adv.* **2012**, *2*, 1144–1152.

[36] K. Mahato, N. Arora, P. Ray Bagdi, R. Gattu, S. S. Ghosh, A. T. Khan, *Chem. Commun.* **2018**, *54*, 1513–1516.

[37] S. Mondal, S. Yashmin, A. T. Khan, *Org. Biomol. Chem.* **2021**, *19*, 9223–9230.

[38] M. Belal, S. Mondal, S. Yashmin, A. T. Khan, *Org. Biomol. Chem.* **2022**, *20*, 715–726.

[39] J. C. Jung, J. C. Kim, O. S. Park, B. S. Jang, *Arch. Pharm. Res.* **1999**, *22*, 302–305.

[40] S. A. Jackson, S. Sahni, L. Lee, Y. Luo, T. R. Nieduzak, G. Liang, Y. Chiang, N. Collar, D. Fink, W. He, A. Laoui, J. Merrill, R. Boffey, P. Crackett, B. Rees, M. Wong, J.-P. Guilloteau, M. Mathieu, S. S. Rebello, *Bioorgan. Med. Chem.* **2005**, *13*, 2723–2739.

[41] D. Thakur, *Int. J. Res. Appl. Sci.* **2023**, *11*, 351–357.

[42] A. T. Benny, S. D. Arikkatt, C. G. Vazhappilly, S. Kannadasan, R. Thomas, M. S. N. Leelabaiamma, E. K. Radhakrishnan, P. Shanmugam, *Mini-Rev. Med. Chem.* **2022**, *22*, 1030–1063.

[43] C. F. M. Silva, D. C. G. A. Pinto, A. M. S. Silva, *ChemMedChem* **2016**, *11*, 2252–2260.

[44] R. Islam, M. S. Hossain, P. Y. Mock, S. W. Leong, K. W. Lam, *Med. Chem. Res.* **2023**, *32*, 1017–1038.

[45] Y. Qiu, J. Lu, C. Zhao, Y. Xiang, A. Wu, L. Shen, H. Jiang, *J. Mol. Struct.* **2025**, *1334*, 141887.

[46] K. Sharma, *ChemistrySelect* **2022**, *7*, e202200540.

[47] P. Yadav, B. Parshad, P. Manchanda, S. Sharma, *Curr. Top. Med. Chem.* **2014**, *14*, 2552–2575.

[48] A. M. Serry, O. M. Abdelhafez, W. K. Khalil, K. A. Hamed, M. I. Mabrouk, M. B. Shalaby, E. Y. Ahmed, *Top. Curr. Chem.* **2025**, *159*, 108338.

[49] R. Taylor, in *Chemistry of Heterocyclic Compounds: A Series Of Monographs* (Ed.: S. Gronowitz), Wiley, **1986**, pp. 1–117.

[50] M. G. A. Shvekhgeimer, *Chem. Heterocycl. Com.* **1998**, *34*, 1101–1122.

[51] G. Roman, *Arch. Pharm. (Weinheim)* **2022**, *355*, 2100462.

[52] Archna, S. Pathania, P. A. Chawla, *Top. Curr. Chem.* **2020**, *101*, 104026.

[53] R. M. D. Da Cruz, F. J. B. Mendoņca-Junior, N. B. De Mélo, L. Scotti, R. S. A. De Araújo, R. N. De Almeida, R. O. De Moura, *Pharmaceuticals* **2021**, *14*, 692.

[54] M. Morales-Tenorio, F. Lasala, A. Garcia-Rubia, E. Aledavood, M. Heung, C. Olal, B. Escudero-Pérez, C. Alonso, A. Martínez, C. Muñoz-Fontela, R. Delgado, C. Gil, *J. Med. Chem.* **2024**, *67*, 16381–16402.

[55] J. P. A. D. Sousa, J. M. S. D. Sousa, R. R. L. Rodrigues, T. A. D. L. Nunes, Y. A. A. Machado, A. C. D. Araujo, I. G. M. Da Silva, K. B. Barros-Cordeiro, S. N. Báo, M. M. D. M. Alves, F. J. B. Mendoņca-Junior, K. A. D. F. Rodrigues, *Int. Immunopharmacol.* **2023**, *123*, 110750.

[56] A. Deep, B. Narasimhan, S. Aggarwal, D. Kaushik, A. K. Sharma, *Cent. Nerv. Syst. Agents Med. Chem.* **2016**, *16*, 158–164.

[57] R. Vijayakumar, R. Tamilarasan, K. Jayamoorthy, M. V. Perumal, *J. Mol. Struct.* **2025**, *1334*, 141829.

[58] C. L. Meena, P. Singh, R. P. Shaliwal, V. Kumar, A. Kumar, A. K. Tiwari, S. Asthana, R. Singh, D. Mahajan, *Eur. J. Med. Chem.* **2020**, *208*, 112772.

[59] J. Meneyrol, M. Follmann, G. Lassalle, V. Wehner, G. Barre, T. Rousseaux, J.-M. Altenburger, F. Petit, Z. Bocskei, H. Schreuder, N. Alet, J.-P. Herault, L. Millet, F. Dol, P. Florian, P. Schaeffer, F. Sadoun, S. Klieber, C. Briot, F. Bono, J.-M. Herbert, *J. Med. Chem.* **2013**, *56*, 9441–9456.

[60] C. Liu, J. Zhang, Z. Zhou, Z. Hua, H. Wan, Y. Xie, Z. Wang, L. Deng, *Food Nutr. Sci.* **2013**, *4*, 305–314.

[61] G. Barbarella, M. Melucci, G. Sotgiu, *Adv. Mater.* **2005**, *17*, 1581–1593.

[62] M. I. Hegab, *Phosphorus, Sulfur, Silicon Relat. Elem.* **2024**, *200*, 1–11.

[63] M. J. Brown, P. S. Carter, A. E. Fenwick, A. P. Fosberry, D. W. Hamprecht, M. J. Hibbs, R. L. Jarvest, L. Mensah, P. H. Milner, P. J. O'Hanlon, A. J. Pope, C. M. Richardson, A. West, D. R. Witty, *Bioorg. Med. Chem. Lett.* **2002**, *12*, 3171–3174.

[64] W. Quaglia, M. Pigini, A. Piergentili, M. Giannella, F. Gentili, G. Marucci, A. Carrieri, A. Carotti, E. Poggesi, A. Leonardi, C. Melchiorre, *J. Med. Chem.* **2002**, *45*, 1633–1643.

[65] L. A. Van Vliet, N. Rodenhuis, D. Dijkstra, H. Wikström, T. A. Pugsley, K. A. Serpa, L. T. Meltzer, T. G. Heffner, L. D. Wise, M. E. Lajiness, R. M. Huff, K. Svensson, S. Sundell, M. Lundmark, *J. Med. Chem.* **2000**, *43*, 2871–2882.

[66] M. Rajabi, M. A. Khalilzadeh, J. Mehrzad, *DNA Cell Biol.* **2012**, *31*, 128–134.

[67] J. J. Hollick, B. T. Golding, I. R. Hardcastle, N. Martin, C. Richardson, L. J. Rigoreau, G. C. Smith, R. J. Griffin, *Bioorg. Med. Chem. Lett.* **2003**, *13*, 3083–3086.

[68] L. F. Tietze, H. P. Bell, S. Chandrasekhar, *Angew. Chem. Int. Ed.* **2003**, *42*, 3996–4028.

[69] R. Morphy, C. Kay, Z. Rankovic, *Drug Discov. Today* **2004**, *9*, 641–651.

[70] W. Liman, N. Ait Lahcen, M. Oubahmane, I. Hdoufane, D. Cherqaoui, R. Daoud, A. El Allali, *Pharmaceuticals* **2022**, *15*, 1092.

[71] B. Meunier, *Accounts Chem. Res.* **2008**, *41*, 69–77.

[72] P. De Sena Murteira Pinheiro, L. S. Franco, T. L. Montagnoli, C. A. M. Fraga, *Expert Opin. Drug Discovery* **2024**, *19*, 451–470.

[73] V. Ivasiv, C. Albertini, A. E. Goṇcalves, M. Rossi, M. L. Bolognesi, *Curr. Top. Med. Chem.* **2019**, *19*, 1694–1711.

[74] M. Szumilak, A. Wiktorowska-Owczarek, A. Stanczak, *Molecules* **2021**, *26*, 2601.

[75] V. Gupta, P. Datta, *Indian J. Med. Res.* **2019**, *149*, 97.

[76] R. R. Ramsay, M. R. PopovicNikolic, K. Nikolic, E. Uliassi, M. L. Bolognesi, *Clin. trans. med.* **2018**, *7*, e3.

[77] S. Bangalore, G. Kamalakkannan, S. Parkar, F. H. Messerli, *Am J Med* **2007**, *120*, 713–719.

[78] A. K. Mishra, K. Prakash, N. Tiwari, *Int. J. Pharm. Sci.* **2025**, *3*, 1683–1704.

[79] W. Cheng, S. Zhu, X. Ma, N. Qiu, P. Peng, R. Sheng, Y. Hu, *Eur. J. Med. Chem.* **2015**, *89*, 826–834.

[80] H.-Q. Zhang, F.-H. Gong, J.-Q. Ye, C. Zhang, X.-H. Yue, C.-G. Li, Y.-G. Xu, L.-P. Sun, *Eur. J. Med. Chem.* **2017**, *125*, 245–254.

[81] A. K. Singh, A. Kumar, H. Singh, P. Sonawane, H. Paliwal, S. Thareja, P. Pathak, M. Grishina, M. Jaremko, A.-H. Emwas, J. P. Yadav, A. Verma, H. Khalilullah, P. Kumar, *Pharmaceuticals* **2022**, *15*, 1071.

[82] F. Coslédan, L. Fraisse, A. Pellet, F. Guillou, B. Mordmüller, P. G. Kremsner, A. Moreno, D. Mazier, J.-P. Maffrand, B. Meunier, *Proc. Natl. Acad. Sci.* **2008**, *105*, 17579–17584.

[83] C. Loup, J. Lelièvre, F. Benoit-Vical, B. Meunier, *Antimicrob. Agents Ch.* **2007**, *51*, 3768–3770.

[84] D. Ashok, N. Nagaraju, B. V. Lakshmi, M. Sarasija, *Russ. J. Gen. Chem+.+* **2019**, *89*, 1905–1910.

[85] Y. U. Cebeci,,. Ceylan,,. A. Karaŏglu, *J. Mol. Struct.* **2022**, *1250*, 131799.

[86] P. L. Bosquesi, T. R. F. Melo, E. O. Vizioli, J. L. D. Santos, M. C. Chung, *Pharmaceuticals* **2011**, *4*, 1450–1474.

[87] S. Ghannay, B. S. Aldhafeeri, I. Ahmad, A. E.A.E. Albadri, H. Patel, A. Kadri, K. Aouadi, *Heliyon* **2024**, *10*, e25911.

[88] V. S. Gontijo, F. P. D. Viegas, C. J. C. Ortiz, M. De Freitas Silva, C. M. Damasio, M. C. Rosa, T. G. Campos, D. S. Couto, K. S. Tranches Dias, C. Viegas, *Curr. Neuropharmacol.* **2020**, *18*, 348–407.

[89] H. Singh, D. K. Agrawal, *Bioorgan. Med. Chem.* **2022**, *62*, 116706.

[90] K. Wittine, I. Ratkaj, K. Benci, T. Suhina, L. Mandić, N. Ilić, S. K. Pavelić, K. Pavelić, M. Mintas, *Med. Chem. Res.* **2016**, *25*, 728–737.

[91] F. Havaldar, S. Bhise, S. Burudkar, *J. Serb. Chem. Soc.* **2004**, *69*, 527–532.

[92] J. Sheng, B. Chao, H. Chen, Y. Hu, *Org. Lett.* **2013**, *15*, 4508–4511.

[93] J. W. H. Watthey, M. Desai, *J. Org. Chem.* **1982**, *47*, 1755–1759.

[94] Y.-L. Sun, J. Bao, K.-S. Liu, X.-Y. Zhang, F. He, Y.-F. Wang, X.-H. Nong, S.-H. Qi, *Planta Med.* **2013**, *79*, 1474–1479.

[95] Y. Wang, S. Niu, S. Liu, L. Guo, Y. Che, *Org. Lett.* **2010**, *12*, 5081–5083.

[96] M. P. Beller, K. Harms, U. Koert, *Org. Lett.* **2020**, *22*, 6127–6131.

[97] F. Zhang, L. Li, S. Niu, Y. Si, L. Guo, X. Jiang, Y. Che, *J. Nat. Prod.* **2012**, *75*, 230–237.

[98] T. Gulchatchai, T. N. Thanh Huynh, N. Vijara, T. Khotavivattana, M. Sukwattanasinitt, S. Wacharasindhu, *Eur. J. Org. Chem.* **2023**, *26*, e202300556.

[99] S. D. Mhaske, S. J. Takate, R. N. Dhawale, H. N. Akolkar, P. V. Randhavane, B. K. Karale, *Indian J. Heterocy. Ch.* **2017**, *27*, 179–187.

[100] K. Levchenko, V. Barachevski, O. Kobeleva, O. Venidiktova, T. Valova, A. Bogacheva, K. Chudov, E. Grebennikov, P. Shmelin, N. Poroshin, G. Adamov, V. Yarovenko, M. Krayushkin, *Tetrahedron Lett.* **2015**, *56*, 1085–1088.

[101] L. Pazhanivel, V. Gnanasambandam, *RSC Adv.* **2018**, *8*, 41675–41680.

[102] J. Nagai, H. Shi, Y. Kubota, K. Bandow, N. Okudaira, Y. Uesawa, H. Sakagami, M. Tomomura, A. Tomomura, K. Takao, Y. Sugita, *Anticancer Res.* **2018**, *38*, 4449–4457.

[103] J. Mullaivendhan, A. Ahamed, G. Raman, S. Radhakrishnan, I. Akbar, *Results Chem.* **2023**, *6*, 101175.

[104] E. Farzaneh, M. Mohammadi, P. Raymand, M. Noori, S. Golestani, S. Ranjbar, Y. Ghasemi, M. Mohammadi-Khanaposhtani, M. Asadi, E. Nasli Esfahani, H. Rastegar, B. Larijani, M. Mahdavi, P. Taslimi, *Top. Curr. Chem.* **2024**, *145*, 107207.

[105] T. E. Ali, D. A. Bakhotmah, M. A. Assiri, *Synthetic Commun.* **2020**, *50*, 3314–3325.

[106] S. H. Kurma, R. Somanaboina, L. R. Vanammoole, K. S. Srivishnu, C. R. Bhimapaka, L. Giribabu, *J. Fluoresc.* **2023**, *33*, 1125–1138.

[107] V. Kojasoy, D. J. Tantillo, *Org. Biomol. Chem.* **2023**, *21*, 11–23.

[108] S. Ghosh, P. Chopra, S. Wategaonkar, *Phys. Chem. Chem. Phys.* **2020**, *22*, 17482–17493.

[109] A. A. Fahmy, T. S. Hafez, A. F. El-farargy, M. M. Hamad, *Phosphorus, Sulfur Silicon Relat. Elem.* **1991**, *57*, 211–215.

[110] N. M. Ibrahim, *Phosphorus, Sulfur, Silicon Relat. Elem.* **2006**, *181*, 1773–1784.

[111] S. A. DiBiase, G. W. Gokel, *J. Org. Chem.* **1978**, *43*, 447–452.

Chapter 2

Catalyst- and Solvent-free Synthesis of Pentacyclic-dione Derivatives from 4-Hydroxythiocoumarin and Aldehyde Using Pseudo-Three-Component Reaction

Graphical Abstract

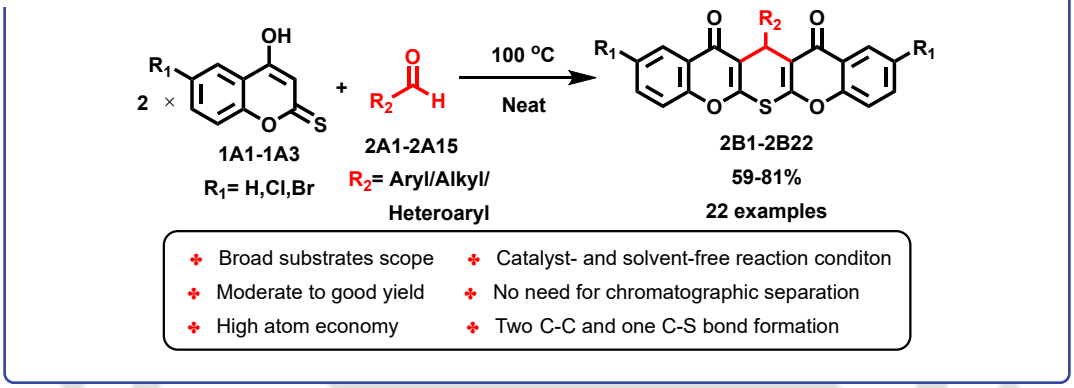

Table of contents

2.1 Context and Significance

Organosulfur compounds are a cornerstone of modern organic chemistry, featuring prominently in pharmaceuticals,[1] agrochemicals,[2,3] natural products,[4–6] and materials science.[7] Their unique reactivity, structural diversity, and biological activities have made them a subject of intense research.

Coumarin derivatives stand out for their anticoagulant, antimicrobial,[8] and anticancer properties,[9] with 4-hydroxycoumarin forming the basis of clinically important drugs such as warfarin[10] and dicoumarol.[11]

While coumarin derivatives are well-established oxygen-containing heterocycles with significant medicinal relevance, their sulfur analogues, thiocoumarins, are a particular class of organosulfur compounds in which one or two oxygen atoms are replaced by sulfur, imparting unique chemical and biological properties. The sulfur analogues, particularly 4-hydroxythiocoumarin, offer intriguing possibilities for new reactivity and biological functions, yet remain underexplored in the literature.

A detailed discussion of the structural, synthetic, and biological aspects of these scaffolds is provided in **Chapter 1**.

2.2 Literature Review: Synthesis of Pentacyclic-Dione Scaffolds

The construction of polycyclic frameworks containing heteroatoms is a central challenge in synthetic organic chemistry,[12,13] as these structures often serve as valuable intermediates or scaffolds for bioactive molecules. Pentacyclic scaffolds, especially those incorporating sulfur, are rare and important motifs that can serve as key intermediates for further functionalization or as potential pharmacophores.[14]

2.2.1 Previous approaches:

1. **4-Hydroxycoumarin and aldehydes:** Traditionally, 4-hydroxycoumarin reacts with aldehydes in the presence of catalysts (e.g., L-proline, piperidine) and solvents (e.g., ethanol, DMF) to yield biscoumarin derivatives *via* Knoevenagel condensation and Michael addition (**Scheme 2.1**).[15–19]

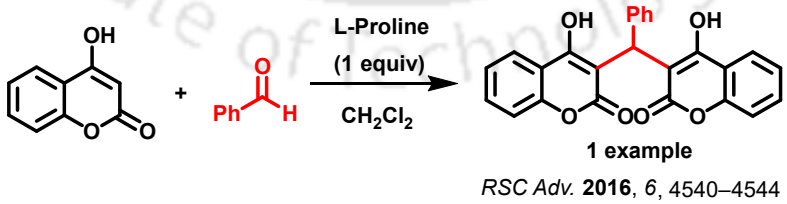

Scheme 2.1: Classical biscoumarin synthesis from 4-hydroxycoumarin and aldehydes.

These reactions, while robust, often require chromatographic purification and generate significant solvent waste.

2. **4-Hydroxydithiocoumarin:** More recently, 4-hydroxydithiocoumarin has been shown to undergo pseudo-three-component reactions with aldehydes, yielding pentacyclic products with three sulfur atoms in the ring (**Scheme 2.2**).[20]

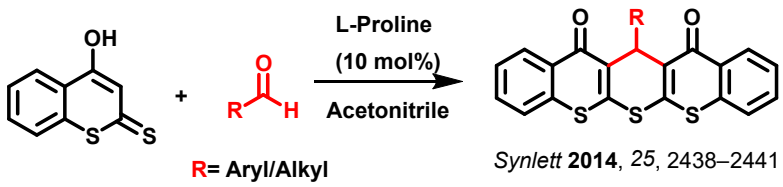

Scheme 2.2: Pentacyclic-dione synthesis from 4-hydroxydithiocoumarin and aldehydes.

This method, however, typically relies on organic solvents and on catalysts, however innocuous, which limit their green credentials.

3. **4-Hydroxythiocoumarin:** Reports on the reactivity of 4-hydroxythiocoumarin are exceedingly rare. Its potential to form pentacyclic-dione scaffolds *via* multicomponent reactions has not yet been explored.

2.2.2 Limitations of Existing Methods

- A significant dependence on catalysts and solvents often increases the overall cost, operational complexity, and environmental burden of these processes.[21]
- The frequent necessity for chromatographic purification makes these methods labor-intensive and contributes to considerable solvent waste.[22]

2.2.3 Present Strategy

The growing emphasis on sustainable and environmentally benign methodologies in organic synthesis has intensified the search for alternatives to conventional organic solvents.[23] One such alternative gaining attention is the use of solvent-free reaction conditions (SFRC), which offer a promising strategy to minimize ecological impact.[24] Among the various synthetic approaches, Multicomponent Reactions (MCRs) stand out due to their inherent advantages, including high atom economy, operational simplicity, reduced waste generation, and the ability to rapidly access structurally diverse, biologically relevant molecules.[25] In light of these benefits, this study presents a catalyst-free and solvent-free protocol for the synthesis of substituted pentacyclic-dione derivatives *via* a pseudo-three-component reaction involving 4-hydroxythiocoumarin and aldehydes (**Scheme 2.3**).

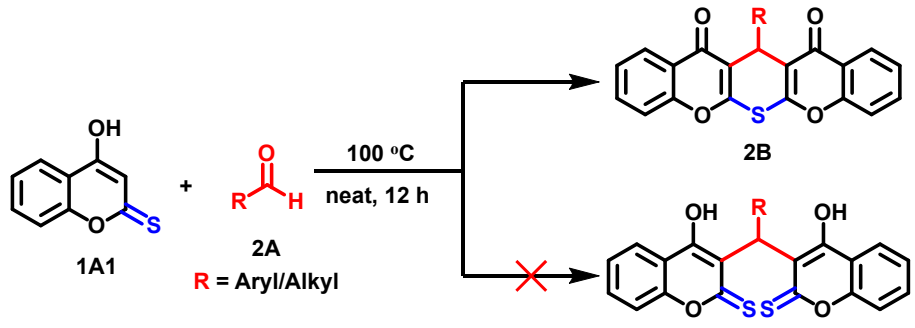

Scheme 2.3: Overview of the green, catalyst- and solvent-free protocol developed in this work.

2.3 Green Chemistry Considerations in This Work

The principles of green chemistry[21] have become a guiding framework for the development of modern synthetic methodologies. These principles emphasize the reduction or elimination of hazardous substances, minimization of waste, increased atom economy, and the use of safer solvents and reaction conditions.

In the context of this research, the methodology was designed to be inherently green by:

- Employing a catalyst- and solvent-free protocol, thereby reducing both chemical waste and the environmental footprint of the process.
- Utilizing a MCR to enhance atom economy and operational simplicity, allowing for the efficient construction of complex heterocyclic frameworks in a single step.[26]
- Avoiding chromatographic purification to minimize solvent consumption and waste.

A detailed evaluation of the protocol's alignment with green chemistry principles is presented in ***Section 2.5.5****.*

2.4 Rationale and Objectives for This Work

The synthesis of pentacyclic-dione derivatives presents a compelling opportunity due to their structural novelty and potential applications. However, current synthetic methodologies often rely on unsustainable practices. Therefore, to address these limitations, this work focuses on developing a green, catalyst- and solvent-free protocol, addressing the following key points:

- Thiocoumarin, particularly 4-hydroxythiocoumarin, represents an underexplored starting material with significant synthetic potential.
- There is a need for more sustainable access to novel heterocyclic frameworks, utilizing reaction conditions that are mild, scalable, and environmentally benign.
- It is crucial to demonstrate the feasibility of efficiently constructing complex molecular architectures, minimizing hazardous reagents and purification steps.

Based on these considerations, the specific objectives of this study are as follows:

1. To synthesize a series of novel pentacyclic-dione derivatives using 4-hydroxythiocoumarin and a variety of aldehydes.
2. To optimize the reaction conditions to establish a high-yielding, solvent-free, and catalyst-free protocol.
3. To determine the substrate scope of the reaction with respect to different aldehyde classes (aromatic, heteroaromatic, aliphatic) and substituted 4-hydroxythiocoumarins.
4. To propose a plausible reaction mechanism based on experimental observations.
5. To evaluate the developed protocols against green chemistry principles.
6. To characterize the synthesized compounds using spectroscopic techniques (NMR, IR, HRMS) and, where possible, X-ray crystallography.

2.5 Results and Discussion

2.5.1 Optimization of Reaction Conditions

The optimization of reaction conditions was a pivotal step in developing an efficient and sustainable protocol for the synthesis of pentacyclic-dione derivatives from 4-hydroxythiocoumarin and aldehydes. Taking 2 equiv of 4-hydroxythiocoumarin and 1 equiv of *p*-tolualdehyde as model substrates, various parameters, including solvent, catalyst, temperature, and reaction time, were systematically investigated to identify the most effective combination, and results are summarized in **Table 2.1**.

When the reaction was carried out **in organic solvents** such as acetonitrile or ethanol, catalytic activation was essential for product formation (**Table 2.1**, entries **1**–**7**). In the absence of a catalyst, no reaction was observed (**Table 2.1**, entry **1**), even at elevated temperatures. Among the catalysts tested, L-proline proved uniquely effective, affording high yields (75%) in both MeCN (**Table 2.1**, entry **2**) and EtOH (**Table 2.1**, entry **6**) in short reaction times. Other acid catalysts, such as *para* -Toluenesulfonic acid (*p*-TSA) (**Table 2.1**, entry **3**), Camphorsulfonic acid (CSA) (**Table 2.1**, entry **4**), and Ammonium Chloride (NH_4Cl) (**Table 2.1**, entry **5**), were significantly less efficient, and the use of THF as solvent led to poor yields even with L-proline (**Table 2.1**, entry **7**). These results demonstrate that while efficient, the use of both solvent and catalyst is required for high conversion under these conditions, which detracts from the overall greenness and simplicity of the protocol.

In contrast, under **solvent-free ("neat") conditions**, the reaction could be promoted solely by thermal activation, eliminating the need for any catalyst (**Table 2.1**, entries **8**–**12**). No product was obtained at room temperature (rt) (**Table 2.1**, entry **8**), but yields increased steadily with temperature, reaching a maximum (81%) at 100 °C after 12 h (**Table 2.1**, entry **13**). Further increases in temperature did not enhance the yield and could lead to minor decomposition (**Table 2.1**, entry **14**).

To compare with the conventional batch heating process, the reaction employing identical substrates was also subjected to microwave irradiation at 100 °C for 20 min and 30 min intervals (**Table 2.1**, entries **15** and **16**). However, these trials produced notably low yields, thereby highlighting the greater effectiveness of batch heating for this synthesis.

Summary: Taken together, these results highlight a clear trade-off: while solvent/catalyst systems are efficient, they compromise the sustainability of the process. The neat, catalyst-free protocol at 100 °C for 12 h achieves comparable yields or better without the use of hazardous reagents or solvents, aligning perfectly with green chemistry principles and offering a much simpler and more environmentally friendly approach.

Table 2.1: Optimization of the reaction condition.[a]

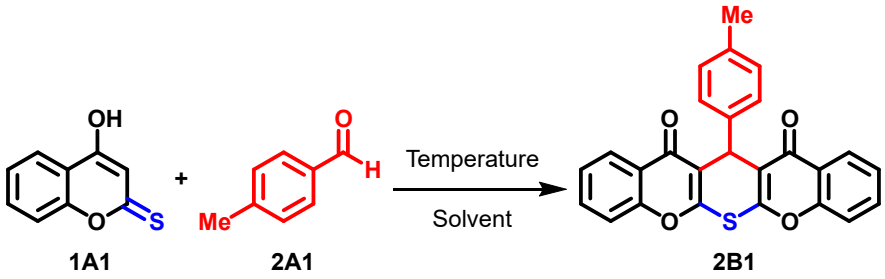

Entry	Catalyst (mol%)	Solvent	Temp (°C)	Time (h)	Yield (%)[b]
1	–	MeCN	80	16	NR
2	L-Proline (10)	MeCN	80	1	75
3	PTSA (10)	MeCN	80	16	16
4	CSA (10)	MeCN	80	16	15
5	NH_4Cl (10)	MeCN	80	16	42
6	L-Proline (10)	EtOH	78	1.5	75
7	L-Proline (10)	THF	65	16	33
8	–	Neat	rt	16	NR
9	–	Neat	40	16	16
10	–	Neat	50	16	28
11	–	Neat	60	16	42
12	–	Neat	80	16	63
13	–	**Neat**	**100**	**12**	**81**
14	–	Neat	110	12	80
15[c]	–	Neat	100	20 min	14
16[c]	–	Neat	100	30 min	16

[a]Reactions were carried out using 4-hydroxythiocoumarin (2 equiv) and *p*-tolualdehyde (1 equiv). [b]Isolated Yield. [c]Reactions were done under Microwave Irradiation (150 W).

2.5.2 Substrate Scope and Limitations

With the optimized reaction conditions in place, the next phase of the study explored the generality of the protocol by examining a wide range of aldehydes, as well as substituted 4-hydroxythiocoumarins. The results, summarized in **Table 2.2**, **Table 2.3**, and **Table 2.4**, revealed several important trends and limitations:

Aromatic aldehydes with an electron-withdrawing substituents, such as nitro (**Table 2.2**, **2B5**) and halogen groups (**Table 2.2**, **2B3** and **2B9**), consistently provided higher yields of the pentacyclic-dione products. For instance, reactions employing *p*-nitrobenzaldehyde (**Table 2.2**, **2B5**) or *p*-fluorobenzaldehyde (**Table 2.2**, **2B9**) proceeded smoothly

Table 2.2: Substrate scope for the synthesis of 13-aryl substituted pentacyclic-diones.[a][b]

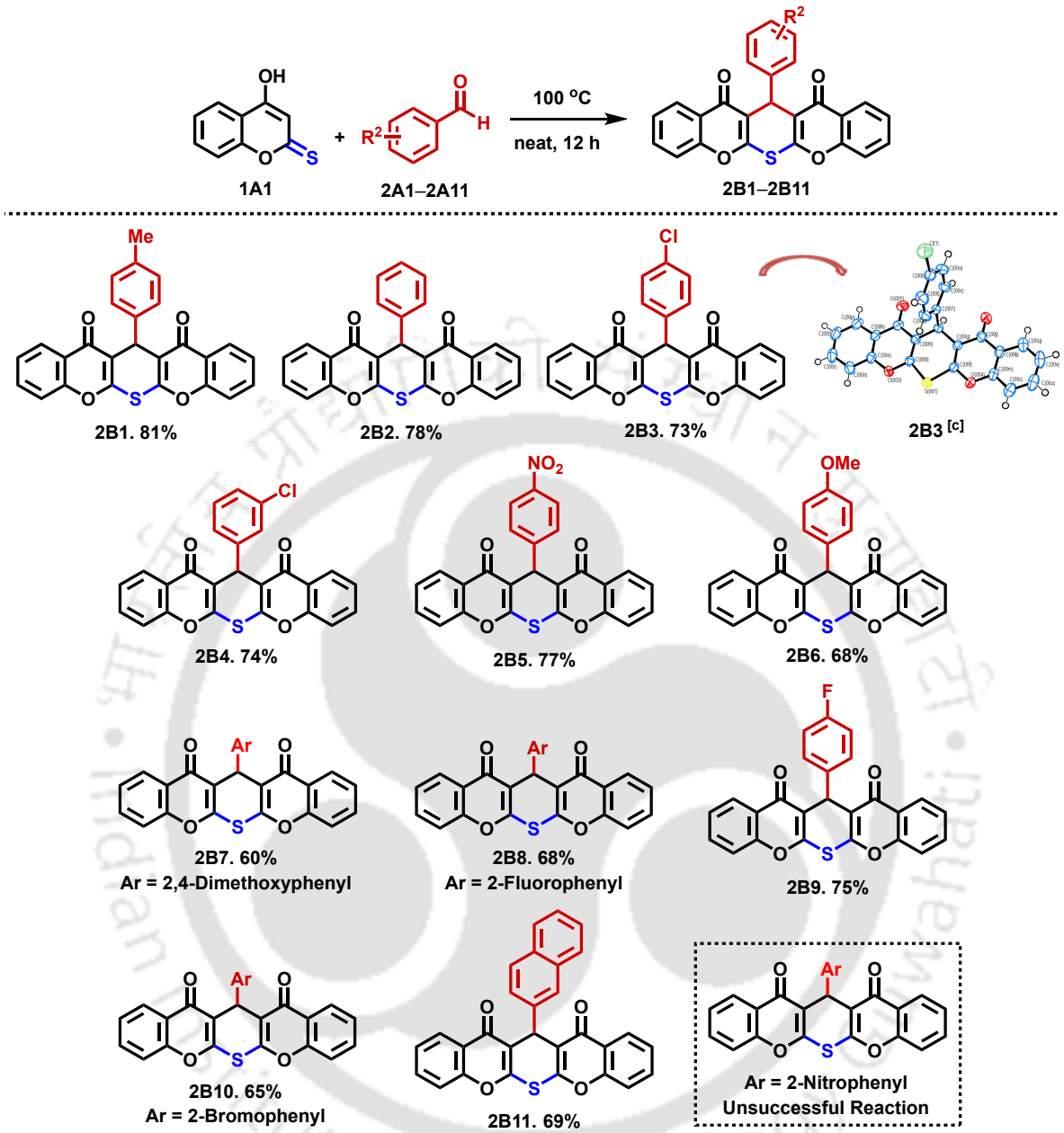

[a]**Reagents and conditions:** 4-hydroxythiocoumarin (0.2 mmol), benzaldehyde (0.1 mmol), neat, stirred at 100 °C for 12 h. [b]Isolated yields are provided. [c]ORTEP diagram of **2B3**. CCDC 2236859.

and resulted in excellent isolated yields. This suggests that increased electrophilicity of the aldehyde carbonyl facilitates the initial condensation step, thereby improving overall efficiency.

Aromatic aldehydes bearing an electron-donating group (EDG), including methoxy substituents (**Table 2.2**, **2B6**, **Table 2.3**, **2B15**), also participated in the reaction but generally afforded slightly lower yields. The decreased reactivity in these cases can be

attributed to the reduced electrophilicity of the aldehyde, which slows down the condensation and subsequent cyclization steps.

***Ortho*-substituted aromatic aldehydes**, such as 2,4-dimethoxy- (**Table 2.2**, **2B7**, **Table 2.3**, **2B16**, **2B18**), 2-bromo- (**Table 2.2**, **2B10**), and 2-fluorobenzaldehyde (**Table 2.2**, **2B8**), exhibited noticeably reduced reactivity. The corresponding pentacyclic-dione products were obtained in low yields or, in some cases (e.g., 2-nitrobenzaldehyde), not at all. This observation is likely due to steric hindrance that impedes the approach of 4-hydroxythiocoumarin to the aldehyde carbonyl, thus hampering the reaction.

Substituted 4-hydroxythiocoumarins were also tested, including those bearing chloro or bromo groups on the aromatic ring. These derivatives participated efficiently in the reaction, affording the corresponding pentacyclic-dione products in yields comparable to the parent compound. This finding highlights the robustness of the protocol with respect to modifications on the thiocoumarin core (**Table 2.3**).

Table 2.3: Substrate scope for the synthesis of 2,10-dihalo-13-aryl substituted pentacyclic-diones.[a][b]

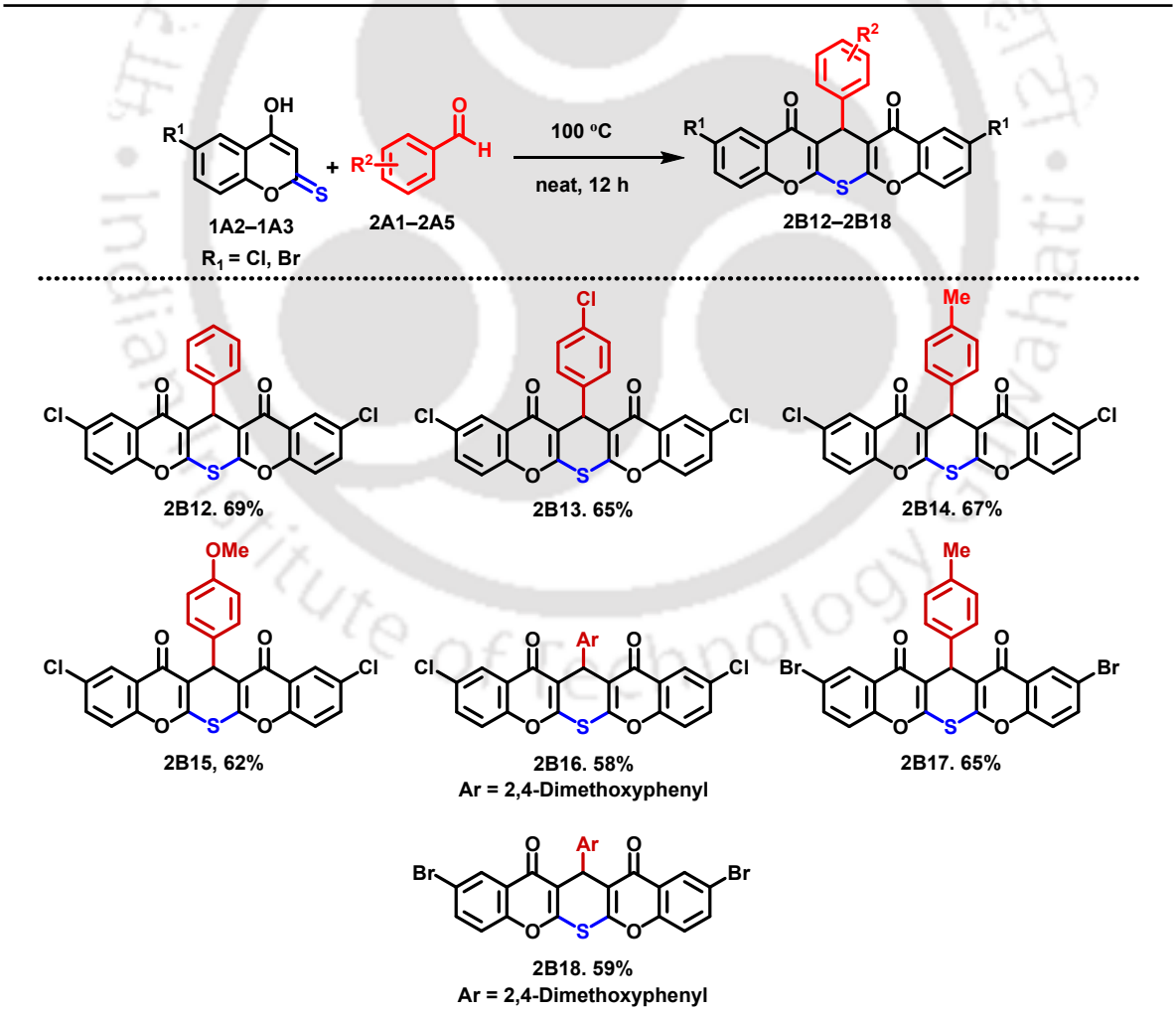

[a]**Reagents and conditions:** 6-halo-4-hydroxythiocoumarin (0.2 mmol), benzaldehyde (0.1 mmol), neat, stirred at 100 °C for 12 h. [b]Isolated yields are provided.

Heteroaromatic aldehydes, including indole-2- and thiophene-2-carboxaldehyde, were found to be compatible with the reaction conditions. These substrates yielded the desired pentacyclic-dione products in moderate to good yields, demonstrating the method's tolerance for heteroatoms in the aromatic ring (**Table 2.4**, entries **2B19** and **2B20**).

Aliphatic aldehydes, in contrast, generally gave lower yields compared to their aromatic counterparts. While some aliphatic aldehydes, such as butyraldehyde and hexanal (**Table 2.4**, entries **2B21** and **2B22**), could be converted to the desired products under the optimized conditions, others, like heptanal, were unreactive. This limitation may be due to both reduced electrophilicity and increased conformational flexibility of aliphatic aldehydes, which may make them less amenable to the condensation and cyclization steps.

Table 2.4: Substrate scope for the synthesis of 13-heteroaryl/alkyl substituted pentacyclic-diones.[a][b]

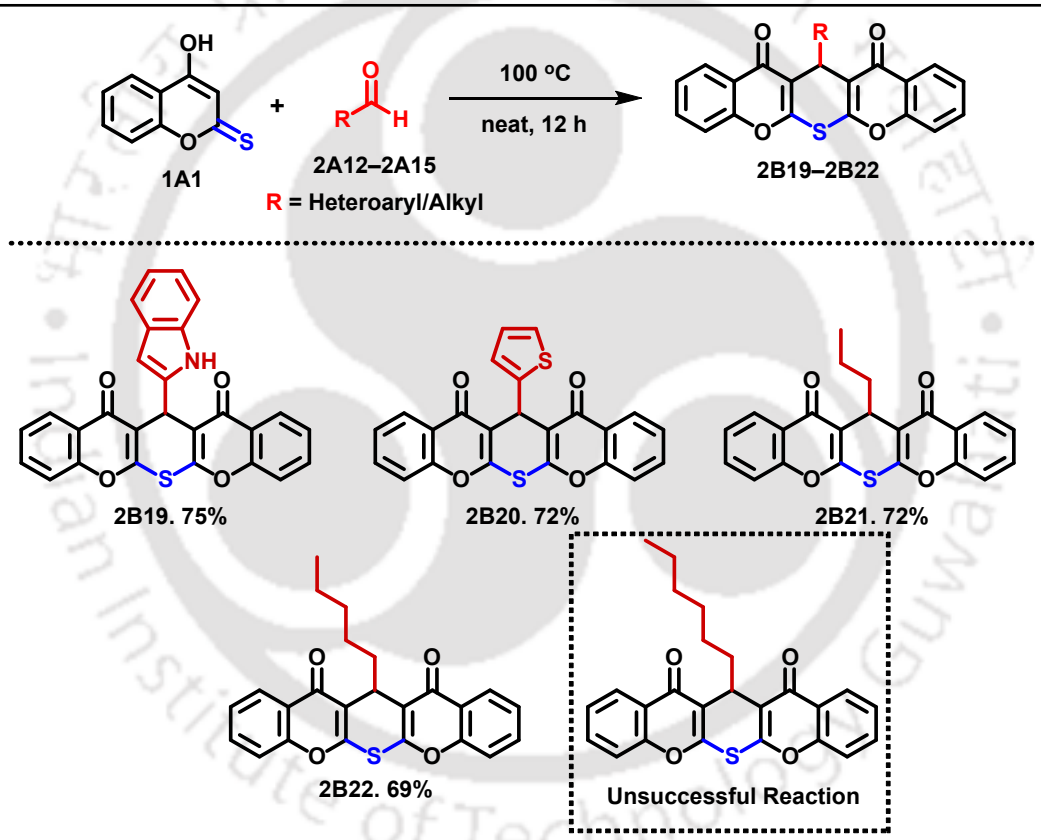

[a]**Reagents and conditions:** 4-hydroxythiocoumarin (0.2 mmol), aldehyde (0.1 mmol), neat, stirred at 100 °C for 12 h. [b]Isolated yields are provided.

Summary: The substrate scope study demonstrates that the developed methodology is broadly applicable to a range of aromatic and heteroaromatic aldehydes, with certain limitations for sterically hindered or aliphatic substrates. The protocol is also tolerant of various substitutions on the 4-hydroxythiocoumarin ring, further underscoring its versatility. However, limited success was observed with *ortho*-substituted aromatic and longer-chain aliphatic aldehydes.

2.5.3 Mechanistic Insights

A deeper understanding of the reaction mechanism was sought through a combination of experimental observations and comparison with related literature precedents.[27,28] The data support a plausible sequence of steps leading to the formation of the pentacyclic-dione product (**Scheme 2.4**).

Step 1: The reaction is proposed to initiate with a **Knoevenagel Condensation** between 4-hydroxythiocoumarin (**1A1**) and the aldehyde **2A1**, generating an α,β-unsaturated intermediate **B**. This step is facilitated by the inherent nucleophilicity of the 4-hydroxythiocoumarin enolate and the electrophilicity of the aldehyde carbonyl.

Step 2: A second equivalent of 4-hydroxythiocoumarin then undergoes a **Michael addition** to the activated intermediate **B** to furnish intermediate **C**, forming a new C—C bond. This step is critical for the construction of the pentacyclic framework and is likely promoted by the high concentration of reactants under solvent-free conditions.

Step 3: Intramolecular cyclization follows, accompanied by the elimination of hydrogen sulfide (H_2S), to yield the final pentacyclic-dione product **2B1**. The evolution of H_2S was experimentally confirmed by the blackening of lead acetate paper held above the reaction mixture, providing direct evidence for this mechanistic step.

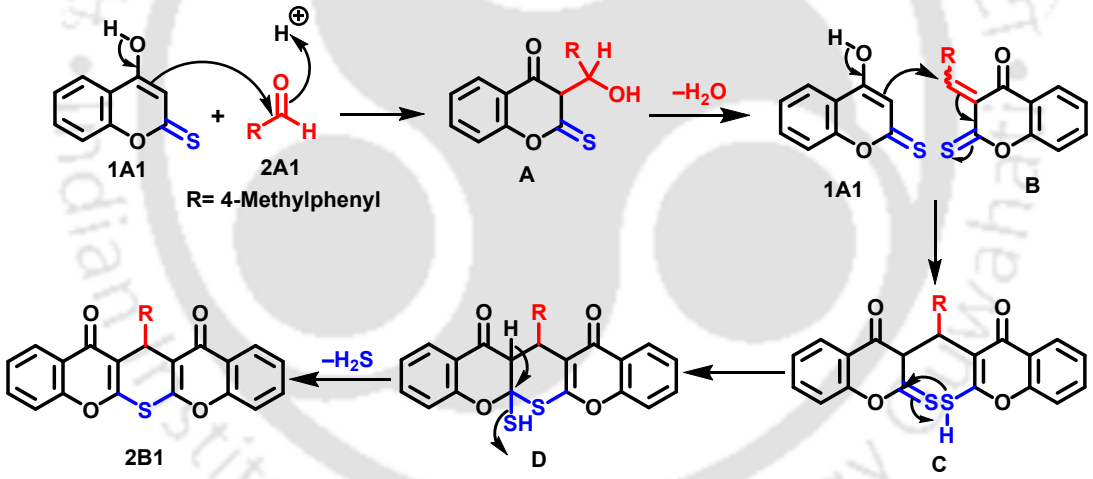

Scheme 2.4: A plausible mechanism for the formation of pentacyclic-dione **2B1**.

> **Insight:** Attempts to isolate or observe reaction intermediates by TLC or NMR were unsuccessful, suggesting that the cyclization and elimination steps proceed rapidly once the Michael addition has occurred. This observation is consistent with the high yields and clean reactions observed under the optimized conditions.

2.5.4 Product Characterization and Structural Analysis

Comprehensive characterization of the synthesized pentacyclic-dione derivatives **2B1**–**2B22** was performed using a combination of spectroscopic and crystallographic techniques, ensuring the unambiguous assignment of product structures.

^{1}H NMR spectra of the products consistently displayed singlet resonances corresponding to the benzylic (methine) proton formed during cyclization. For compound **2B1**, a singlet at δ 6.16 ppm was observed, attributed to this benzylic proton at the newly formed ring junction. The methyl group from the *p*-methylphenyl substituent, derived from *p*-tolualdehyde, appeared as a singlet at δ 2.22 ppm. Due to the molecular symmetry, only half the number of expected proton peaks were observed, as chemically equivalent environments give rise to single resonances. The aromatic region further reflected the substitution patterns of both the aldehyde and thiocoumarin components, with all observed chemical shifts and coupling patterns supporting the proposed structure.

^{13}C NMR spectra for compound 2B1 revealed characteristic signals for the carbonyl, benzylic, methyl, and aromatic carbons within the pentacyclic core. The carbonyl carbon appeared at δ 173.29 ppm, a value typical for conjugated carbonyls in such frameworks. The benzylic carbon was observed at δ 36.95 ppm, and the methyl carbon of the *p*-methylphenyl group appeared at δ 21.18 ppm. As with the proton spectrum, molecular symmetry resulted in only half the number of expected carbon signals being present.

Heteronuclear Single Quantum Coherence (HSQC) experiments provided further confirmation by correlating all observed protons with their directly attached carbons, including the benzylic (methine) proton at δ 6.16 ppm with its carbon at δ 36.95 ppm, and the methyl protons at δ 2.22 ppm with their carbon at δ 21.18 ppm. The aromatic C–H pairs were similarly assigned. No correlation was observed for the carbonyl carbon at δ 173.29 ppm, as expected for a quaternary carbon without directly attached protons. This comprehensive spectral analysis conclusively established the structure and symmetry of compound **2B1** and, by analogy, the other pentacyclic-dione derivatives.

Infrared (IR) spectra of the products provided key evidence for the presence of various characteristic functional groups. For example, **2B1** exhibited strong absorptions in the carbonyl stretching region (1650 cm^{-1}), along with bands attributable to aromatic C−H (3061 cm^{-1}), aliphatic C−H (2925 cm^{-1}), and aromatic C=C stretching vibrations (1620 and 1464 cm^{-1}). These features corroborate the formation of the dione moiety and the retention of aromatic character.

High-Resolution Mass Spectrometry (HRMS) provided molecular weight confirmation for all products, with observed $[M+H]^+$ ions matching the calculated values to within acceptable error margins. For example, for compound **2B1**, the calculated m/z was 425.0842, and the found value was 425.0844.

Single-crystal X-ray diffraction analysis was conducted for compound **2B3**, and the resulting ORTEP diagram unambiguously confirmed the pentacyclic framework and revealed an overall molecular geometry consistent with the proposed structure.

2.5.5 Evaluation of the Current Protocol against Green Chemistry Principles

A critical evaluation of the developed methodology in comparison to existing protocols highlights its advantages in terms of sustainability, efficiency, and operational simplicity.

- Unlike traditional methods that rely on external catalysts and organic solvents, the present protocol operates under truly green conditions, eliminating the need for hazardous reagents and minimizing chemical waste.
- The atom economy of the reaction is high, as all major reactants are incorporated into the final product, and the only byproduct is H_2S, which can be easily detected and managed.
- This efficiency is further enhanced by the avoidance of chromatographic purification, which not only saves time and resources but also further decreases solvent use, enhancing the environmental friendliness and operational simplicity of the synthesis.

> **Note:** While a detailed quantitative assessment of green chemistry metrics (e.g., E-factor) was not performed, the qualitative reduction in reagent and solvent use and waste generation clearly demonstrates the improved sustainability of this approach compared to previous protocols.

Overall, the developed protocol represents a significant advance in the sustainable synthesis of sulfur-containing pentacyclic-dione derivatives, offering both environmental and practical benefits over existing methods.

2.5.6 Limitations and Future Directions

While the methodology developed in this study offers numerous advantages, certain limitations and opportunities for further research remain.

- The reaction is less effective for sterically hindered or unreactive aliphatic aldehydes, which either provide poor yields or fail to yield the desired products under the optimized conditions. Addressing this limitation may require the development of modified protocols or the identification of alternative activation strategies.
- Mechanistic studies, while supportive of the proposed pathway, could be further enhanced by the isolation or detection of key intermediates, as well as computational modeling to explore the energetics of each step. Such investigations would provide deeper insight into the factors governing reactivity and selectivity in this system.
- The biological activity and further functionalization of these novel pentacyclic-dione derivatives represent promising avenues for future research. Given their structural similarity to bioactive coumarin analogues such as dicoumarol, these compounds may possess interesting pharmacological properties and thus warrant detailed biological evaluation.

In conclusion, the work presented here lays a strong foundation for both synthetic and mechanistic exploration of pentacyclic-dione organosulfur compounds, with significant potential for future development and application.

2.6 Conclusion

In this chapter, a green, catalyst- and solvent-free protocol for the synthesis of pentacyclic-dione derivatives from 4-hydroxythiocoumarin and aldehydes has been successfully developed and demonstrated. The optimized reaction conditions, namely, heating the reactants at 100 °C under neat conditions for 12 h, enabled the efficient formation of a wide range of pentacyclic-dione products without the need for external catalysts, solvents, or chromatographic purification.

The methodology was shown to be broadly applicable to various aromatic, heteroaromatic, and alkyl aldehydes and was tolerant of different substituents on the 4-hydroxythiocoumarin ring. Electron-withdrawing groups on the aldehyde generally enhanced reactivity and yield, while *ortho*-substitution and long-chain aliphatic aldehydes presented greater challenges. Mechanistic investigations supported a tandem Knoevenagel condensation, Michael addition, and cyclization sequence, with the evolution of H_2S as the only byproduct.

Comprehensive spectroscopic characterization confirmed the structures of all new compounds, with single-crystal X-ray analysis providing unambiguous evidence for the pentacyclic-dione framework. Compared to previously reported protocols, the present method offers significant advantages in terms of sustainability, atom economy, operational simplicity, and environmental impact.

Despite its strengths, the methodology exhibits some limitations with certain sterically hindered or unreactive substrates. Future work may focus on expanding the substrate scope, probing the mechanism in greater detail, and exploring the biological activity and further functionalization of these novel organosulfur heterocycles. Overall, this work demonstrates the successful integration of green chemistry principles into the synthesis of complex sulfur-containing heterocycles, providing a valuable platform for future research and application in the field of organosulfur chemistry.

2.7 Experimental Section

This section details the procedures and analytical methods employed for the synthesis and characterization of the pentacyclic-dione derivatives described in this chapter. All chemicals and solvents were purchased from commercial suppliers and used as received unless otherwise specified. The syntheses of 4-hydroxythiocoumarin **1A1**, the key precursor and its derivatives, are described in **Chapter 1, Section 1B**.

2.7.1 General Procedure for the Synthesis of Pentacyclic-Dione Derivatives

In a typical experiment, 4-hydroxythiocoumarin (0.2 mmol, 2 equivalents) and the selected aldehyde (0.1 mmol, 1 equivalent) were placed in a dry, 10 mL round-bottom flask. No solvent or external catalyst was added. The vessel was sealed and heated at 100 °C in an oil bath for 12 h. The progress of the reaction was monitored by thin-layer chromatography (TLC) using an appropriate eluent system (1:9 ethyl acetate/hexane). Upon completion, the reaction mixture was allowed to cool to room temperature. The resulting solid was triturated with acetonitrile (3 × 2 mL) and then washed with cold ethanol (2 × 2 mL) to remove unreacted

starting materials and byproducts. The solid product was collected by filtration, dried under vacuum, and weighed. In most cases, the crude product was analytically pure and required no further purification.

2.7.2 Representative Experimental Procedure

Synthesis of 2B1:

4-Hydroxythiocoumarin (**1A1**, 0.2 mmol, 35.6 mg) and *p*-tolualdehyde (**2A1**, 0.1 mmol, 12.02 mg) were placed in a dry, small round-bottom flask. The mixture was heated at 100 °C for 12 h under solvent-free conditions. After cooling to room temperature, the solid was washed with acetonitrile (3 × 2 mL) and cold ethanol (2 × 2 mL), filtered, and dried under vacuum to afford compound **2B1** as a white solid (34 mg, 81% yield).

Comprehensive spectroscopic and analytical data for all synthesized pentacyclic-dione derivatives (**2B1**–**2B22**) are provided in **Section 2.9**. This includes ^{1}H and ^{13}C NMR, IR, and HRMS data, as well as melting points for each compound. ^{1}H, ^{13}C, and HRMS Spectra for a few representative examples are given in **Section 2.10**.

2.8 Crystallographic Analysis

Single crystals suitable for X-ray diffraction were obtained for compound **2B3** by slow evaporation from a mixture of chloroform and ethanol. The crystallographic data confirmed the pentacyclic-dione structure, with bond lengths and angles in agreement with the proposed structure. ORTEP diagram (**Figure 2.1**) was generated using ORTEP-3 for Windows.[29]

The CCDC deposition number 2236859 (for **2B3**) contains the supplementary crystallographic data for this paper, which can be obtained from the joint Cambridge Crystallographic Data Centre and Fachinformationszentrum Karlsruhe https://www.ccdc.cam.ac.uk/structures/

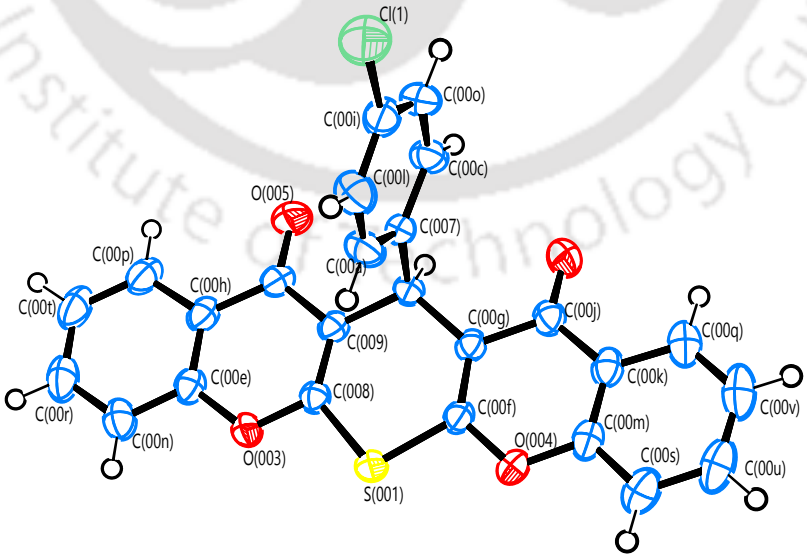

Figure 2.1: ORTEP diagram for compound **2B3**

Table 2.5: Crystallographic data and structure refinement for compound **2B3**.[a]

Entry	Identification Code	Compound 3I1
01	Empirical formula	$C_{25}H_{13}ClO_4S$
02	Formula weight	444.86
03	Temperature	297 K
04	Wavelength	0.71073 Å
05	Radiation type	Mo K\α
06	Radiation system	Fine-focus sealed tube
07	Crystal system	Monoclinic
08	Space group	$P2_1/n$
09	Cell length	a 7.7808(17) Å b 12.199(3) Å c 20.448(5) Å
10	Cell angle	α 90° β 92.209(6)° γ 90°“
11	Cell volume	1939.4(7) $Å^3$
12	Density	1.524 $Mg\,m^{-3}$
13	Completeness to theta	99.6
14	Absorption correction	multi-scan
15	Refinement method	Full-matrix least-squares on F^2
16	Index ranges	−9≤h≤9, −15≤k≤15, −25≤l≤25
17	Reflection number	3834
18	Theta range	2.767 – 26.076°
19	Cell formula units Z	4
20	CCDC no.	2236859

[a]The full .cif file and additional crystallographic data are available from the CCDC.

2.9 Characterization Data for All New Compounds

13-(*p*-tolyl)-12*H*,13*H*,14*H*-thiopyrano[2,3-*b*:6,5-*b*']dichromene-12,14-dione (2B1)

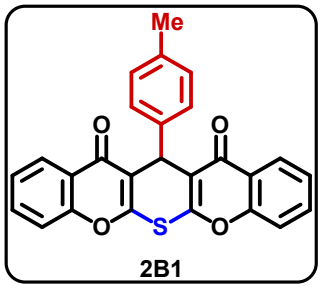

2B1

White solid (0.034 g, 81%); **mp** 291 – 293 °C; **^{1}H NMR (500 MHz, $CDCl_3$)** δ 8.16 (d, J = 7.9 Hz, 2H), 7.64 (t, J = 7.8 Hz, 2H), 7.52 (d, J = 7.7 Hz, 2H), 7.42 (d, J = 8.4 Hz, 2H), 7.37 (t, J = 7.6 Hz, 2H), 7.04 (d, J = 7.8 Hz, 2H), 6.16 (s, 1H), 2.22 (s, 3H); **^{13}C{^{1}H} NMR (125 MHz, $CDCl_3$)** δ 173.29 (2C), 157.18 (2C), 156.50 (2C), 138.68 (1C), 137.20 (1C), 133.91 (2C), 129.33 (2C), 128.19 (2C), 126.64 (2C), 125.71 (2C), 123.73 (2C), 119.02 (2C), 117.43 (2C), 36.95 (1C), 21.18 (1C); **IR (KBr)** ν_{max}/cm^{-1} 3061 (C=C−H), 2925 (C−H),

1650 (C=O), 1620 and 1464 (aromatic C=C); **HRMS (ESI)** calcd for $C_{26}H_{17}O_4S^+$ 425.0842 M+H$^+$ found 425.0844.

13-Phenyl-12*H*,13*H*,14*H*-thiopyrano[2,3-*b*:6,5-*b*']dichromene-12,14-dione (2B2)

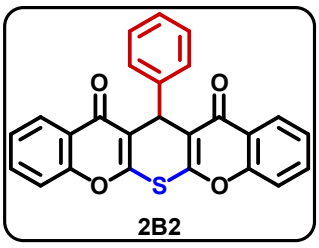

2B2

White solid (0.032 g, 78%); **mp** 303 – 304 °C; **^{1}H NMR (500 MHz, CDCl$_3$)** δ 8.17 (d, J = 7.4 Hz, 2H), 7.66 – 7.62 (m, 4H), 7.43 (d, J = 8.3 Hz, 2H), 7.38 (t, J = 7.3 Hz, 2H), 7.23 (t, J = 7.3 Hz, 1H), 7.15 (t, J = 6.9 Hz, 1H), 6.20 (s, 1H); **^{13}C{^{1}H} NMR (125 MHz, CDCl$_3$)** δ 173.28 (2C), 157.32 (2C), 156.49 (2C), 141.56 (1C), 133.96 (2C), 128.63 (2C), 128.31 (2C), 127.53 (1C), 126.61 (2C), 125.76 (2C), 123.67 (2C), 118.89 (2C), 117.45 (2C), 37.29 (1C); **IR (KBr)** ν_{max}/cm^{-1} 3071 (C=C−H), 2958 (C−H), 1647 (C=O), 1625 and 1464 (aromatic C=C); **HRMS (ESI)** calcd for $C_{25}H_{14}NaO_4S$ +$^+$ 433.0505 M+Na$^+$ found 433.0519.

13-(4-Chlorophenyl)-12*H*,13*H*,14*H*-thiopyrano[2,3-*b*:6,5-*b*']dichromene-12,14-dione (2B3)

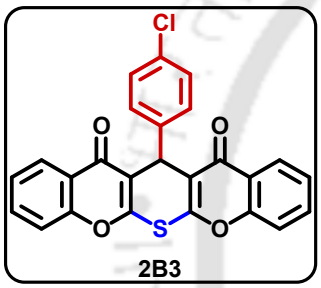

2B3

White solid (0.032 g, 73%); **mp** 289 – 290 °C; **^{1}H NMR (400 MHz, CDCl$_3$)** δ 8.16 (dd, J = 1.6, 8.0 Hz, 2H), 7.67 (ddd, J = 1.7, 7.2, 8.7 Hz, 2H), 7.59 – 7.55 (m, 2H), 7.44 (d, J = 8.2 Hz, 2H), 7.42 – 7.38 (m, 2H), 7.21 – 7.18 (m, 2H), 6.14 (s, 1H); **^{13}C{^{1}H} NMR (100 MHz, CDCl$_3$)** δ 173.25 (2C), 157.29 (2C), 156.49 (2C), 140.12 (1C), 134.12 (2C), 133.32 (1C), 129.77 (2C), 128.76 (2C), 126.58 (2C), 125.91 (2C), 123.57 (2C), 118.47 (2C), 117.49 (2C), 36.99 (1C); **IR (KBr)** ν_{max}/cm^{-1} 3061 (C=C−H), 2926 (C−H), 1649 (C=O), 1622 and 1464 (aromatic C=C); **HRMS (ESI)** calcd for $C_{25}H_{14}ClO_4S^+$ 445.0296 M+H$^+$ found 445.0291.

13-(3-Chlorophenyl)-12*H*,13*H*,14*H*-thiopyrano[2,3-*b*:6,5-*b*']dichromene-12,14-dione (2B4)

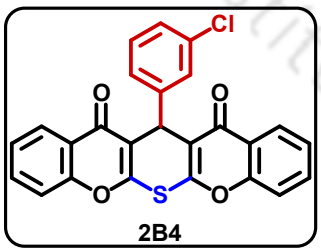

2B4

White solid (0.032 g, 72%); **mp** 269 – 271 °C; **^{1}H NMR (400 MHz, CDCl$_3$)** δ 8.17 (dd, J = 1.5, 7.9 Hz, 2H), 7.67 (ddd, J = 1.7, 7.2, 8.7 Hz, 2H), 7.59 (dt, J = 1.4, 7.6 Hz, 1H), 7.53 (t, J = 1.8 Hz, 1H), 7.47 – 7.43 (m, 2H), 7.43 – 7.37 (m, 2H), 7.18 (t, J = 7.8 Hz, 1H), 7.14 – 7.12 (m, 1H), 6.16 (s, 1H); **^{13}C{^{1}H} NMR (100 MHz, CDCl$_3$)** δ 173.23 (2C), 157.47 (2C), 156.51 (2C), 143.46 (1C), 134.34 (1C), 134.13 (2C), 129.84 (1C), 128.06 (1C), 127.83 (1C), 127.12 (1C), 126.61 (2C), 125.92 (2C), 123.58 (2C), 118.33 (2C), 117.53 (2C), 37.21 (1C); **IR (KBr)** ν_{max}/cm^{-1} 3061 (C=C−H), 2925 (C−H), 1649 (C=O), 1623 and 1464 (aromatic C=C); **HRMS (ESI)** calcd for $C_{25}H_{14}ClO_4S^+$ 445.0296 M+H$^+$ found 445.0296.

13-(4-Nitrophenyl)-12*H*,13*H*,14*H*-thiopyrano[2,3-*b*:6,5-*b*']dichromene-12,14-dione (2B5)

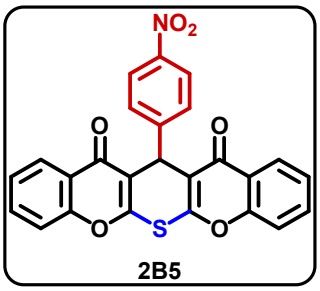

2B5

White solid (0.035 g, 77%); **mp** 300 – 302 °C; **^{1}H NMR (400 MHz, $CDCl_3$)** δ 8.15 (dd, J = 1.5, 8.0 Hz, 2H), 8.13 – 8.08 (m, 2H), 7.84 – 7.79 (m, 2H), 7.69 (ddd, J = 1.7, 7.2, 8.7 Hz, 2H), 7.46 (d, J = 8.1 Hz, 2H), 7.44 – 7.39 (m, 2H), 6.24 (s, 1H); **^{13}C{^{1}H} NMR (100 MHz, $CDCl_3$)** δ 173.21 (2C), 157.65 (2C), 156.51 (2C), 148.80 (1C), 147.26 (1C), 134.37 (2C), 129.47 (2C), 126.54 (2C), 126.14 (2C), 123.91 (2C), 123.43 (2C), 117.74 (2C), 117.57 (2C), 37.76 (1C); **IR (KBr)** ν_{max}/cm^{-1} 3075 (C=C–H), 2925 (C–H), 1649 (C=O), 1623 and 1464 (aromatic C=C) 1347 and 1518 (N=O); **HRMS (ESI)** calcd for $C_{25}H_{14}NO_6S^+$ 456.0536 M+H$^+$ found 456.0536.

13-(4-Methoxyphenyl)-12*H*,13*H*,14*H*-thiopyrano[2,3-*b*:6,5-*b*']dichromene-12,14-dione (2B6)

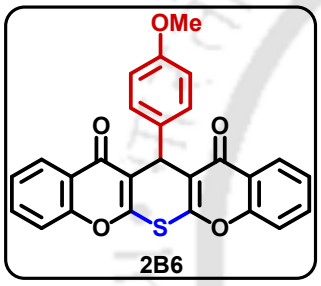

2B6

White solid (0.030 g, 68%); **mp** 279 – 281 °C; **^{1}H NMR (400 MHz, $CDCl_3$)** δ 8.16 (dd, J = 1.6, 8.0 Hz, 2H), 7.65 (ddd, J = 1.7, 7.2, 8.7 Hz, 2H), 7.59 – 7.53 (m, 2H), 7.42 (d, J = 8.0 Hz, 2H), 7.40 – 7.36 (m, 2H), 6.79 – 6.74 (m, 2H), 6.13 (s, 1H), 3.70 (s, 3H); **^{13}C{^{1}H} NMR (100 MHz, $CDCl_3$)** δ 173.31 (2C), 158.93 (1C), 156.99 (2C), 156.48 (2C), 133.93 (2C), 133.91 (1C), 129.40 (2C), 126.60 (2C), 125.72 (2C), 123.69 (2C), 119.02 (2C), 117.44 (2C), 113.99 (2C), 55.30 (1C), 36.60 (1C); **IR (KBr)** ν_{max}/cm^{-1} 3063 (C=C–H), 2835 (C–H), 1649 (C=O), 1618 and 1464 (aromatic C=C); **HRMS (ESI)** calcd for $C_{26}H_{16}NaO_5S^+$ 463.0611 M+Na$^+$ found 463.0607.

13-(2,4-Dimethoxyphenyl)-12*H*,13*H*,14*H*-thiopyrano[2,3-*b*:6,5-*b*']dichromene-12,14-dione (2B7)

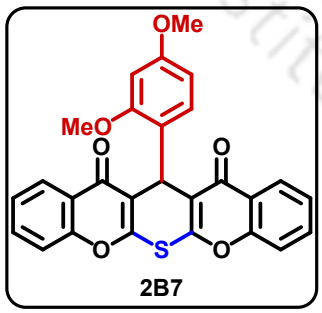

2B7

White solid (0.028 g, 60%); **mp** 264 – 265 °C; **^{1}H NMR (500 MHz, $CDCl_3$)** δ 8.12 (dd, J = 1.7, 7.9 Hz, 2H), 7.84 (d, J = 8.4 Hz, 1H), 7.61 (ddd, J = 1.7, 7.0, 8.6 Hz, 2H), 7.39 (d, J = 8.4 Hz, 2H), 7.34 (t, J = 7.5 Hz, 2H), 6.51 (dd, J = 2.4, 8.4 Hz, 1H), 6.34 (d, J = 2.4 Hz, 1H), 6.05 (s, 1H), 3.75 (s, 3H), 3.72 (s, 3H); **^{13}C{^{1}H} NMR (125 MHz, $CDCl_3$)** δ 173.55 (2C), 160.16 (1C), 159.50 (1C), 158.14 (2C), 156.24 (2C), 134.35 (1C), 133.55 (2C), 126.55 (2C), 125.43 (2C), 123.90 (2C), 120.92 (1C), 117.31 (2C), 116.38 (2C), 104.18 (1C), 99.01 (1C), 55.39 (1C), 55.37 (1C), 36.88 (1C); **IR (KBr)** ν_{max}/cm^{-1} 3068 (C=C–H), 2927 (C–H), 1648 (C=O), 1614 and 1464 (aromatic C=C); **HRMS (ESI)** calcd for $C_{27}H_{18}NaO_6S^+$ 493.0716 M+Na$^+$ found 493.0717.

13-(2-Fluorophenyl)-12*H*,13*H*,14*H*-thiopyrano[2,3-*b*:6,5-*b*']dichromene-12,14-dione (2B8)

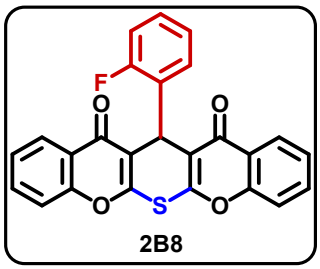

2B8

White solid (0.029 g, 68%); **mp** 296 – 298 °C; **^{1}H NMR (500 MHz, $CDCl_3$)** δ 8.12 (dd, J = 1.7, 8.0 Hz, 2H), 7.88 (td, J = 2.0, 7.6 Hz, 1H), 7.64 (ddd, J = 1.7, 7.1, 8.7 Hz, 2H), 7.42 (d, J = 8.4 Hz, 2H), 7.39 – 7.34 (m, 2H), 7.16 – 7.07 (m, 2H), 6.95 – 6.89 (m, 1H), 6.18 (s, 1H); **^{13}C{^{1}H} NMR (125 MHz, $CDCl_3$)** δ 173.30 (2C), 161.89 (d, J = 247.2 Hz, 1C), 157.73 (d, J = 1.9 Hz, 2C), 156.36 (2C), 133.91 (2C), 133.22 (d, J = 4.3 Hz, 1C), 129.17 (d, J = 8.3 Hz, 1C), 127.58 (d, J = 13.2 Hz, 1C), 126.49 (2C), 125.74 (2C), 124.02 (d, J = 3.2 Hz, 1C), 123.66 (2C), 117.42 (2C), 116.46 (2C), 115.90 (d, J = 22.0 Hz, 1C), 35.29 (1C); **^{19}F NMR (471 MHz, $CDCl_3$)** δ -114.36; **IR (KBr)** ν_{max}/cm^{-1} 3069 (C=C–H), 2922 (C–H), 1650 (C=O), 1625 and 1464 (aromatic C=C); **HRMS (ESI)** calcd for $C_{25}H_{13}FNaO_4S^+$ 451.0411 M+Na$^+$ found 451.0413.

13-(4-Fluorophenyl)-12*H*,13*H*,14*H*-thiopyrano[2,3-*b*:6,5-*b*']dichromene-12,14-dione (2B9)

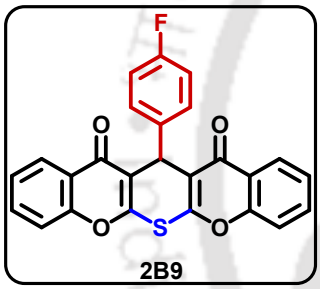

2B9

White solid (0.032 g, 75%); **mp** 291 – 293 °C; **^{1}H NMR (400 MHz, $CDCl_3$)** δ 8.16 (dd, J = 1.6, 8.0 Hz, 2H), 7.66 (ddd, J = 1.7, 7.2, 8.7 Hz, 2H), 7.63 – 7.57 (m, 2H), 7.44 (d, J = 8.1 Hz, 2H), 7.42 – 7.37 (m, 2H), 6.95 – 6.88 (m, 2H), 6.15 (s, 1H); **^{13}C{^{1}H} NMR (100 MHz, $CDCl_3$)** δ 173.27 (2C), 162.18 (d, J = 244.1 Hz, 1C), 157.20 (2C), 156.50 (2C), 137.44 (d, J = 3.2 Hz, 1C), 134.08 (2C), 129.98 (d, J = 8.1 Hz, 2C), 126.58 (2C), 125.86 (2C), 123.61 (2C), 118.73 (2C), 117.49 (2C), 115.43 (d, J = 21.3 Hz, 2C), 36.79 (1C); **^{19}F NMR (471 MHz, $CDCl_3$)** δ -115.17; **IR (KBr)** ν_{max}/cm^{-1} 3079 (C=C–H), 2927 (C–H), 1643 (C=O), 1626 and 1464 (aromatic C=C); **HRMS (ESI)** calcd for $C_{25}H_{14}FO_4S^+$ 429.0591 M+H$^+$ found 429.0597.

13-(2-Bromophenyl)-12*H*,13*H*,14*H*-thiopyrano[2,3-*b*:6,5-*b*']dichromene-12,14-dione (2B10)

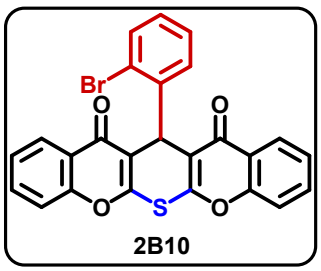

2B10

White solid (0.032 g, 65%); **mp** 306 – 307 °C; **^{1}H NMR (400 MHz, $CDCl_3$)** δ 8.14 (dd, J = 1.5, 8.0 Hz, 2H), 7.78 (dd, J = 1.6, 7.8 Hz, 1H), 7.64 (ddd, J = 1.7, 7.2, 8.7 Hz, 2H), 7.53 (dd, J = 1.2, 8.0 Hz, 1H), 7.41 (d, J = 8.4 Hz, 2H), 7.39 – 7.34 (m, 2H), 7.20 (td, J = 1.3, 7.6 Hz, 1H), 7.00 (td, J = 1.7, 8.0 Hz, 1H), 6.33 (s, 1H); **^{13}C{^{1}H} NMR (100 MHz, $CDCl_3$)** δ 173.40 (2C), 157.32 (2C), 156.15 (2C), 141.16 (1C), 133.98 (2C), 133.87 (1C), 132.34 (1C), 128.83 (1C), 127.33 (1C), 126.63 (2C), 125.80 (2C), 124.34 (1C), 123.60 (2C), 117.82 (2C), 117.29 (2C), 39.90 (1C); **IR (KBr)** ν_{max}/cm^{-1} 3062 (C=C–H), 2925 (C–H), 1651 (C=O), 1622 and 1464 (aromatic C=C); **HRMS (ESI)** calcd for $C_{25}H_{14}BrO_4S^+$ 488.9791 M+H$^+$ found 488.9786.

13-(Naphthalen-2-yl)-12*H*,13*H*,14*H*-thiopyrano[2,3-*b*:6,5-*b*']dichromene-12,14-dione (2B11)

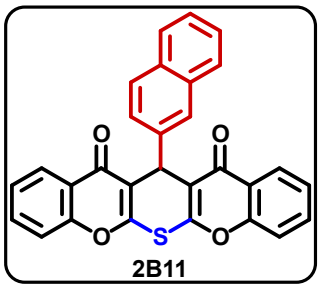

2B11

White solid (0.032 g, 69%); **mp** 298 – 299 °C; **^{1}H NMR (400 MHz, $CDCl_3$)** δ 8.15 (dd, J = 1.5, 8.0 Hz, 2H), 8.03 (s, 1H), 7.82 (dd, J = 1.5, 8.3 Hz, 1H), 7.79 – 7.76 (m, 1H), 7.73 (s, 1H), 7.71 – 7.69 (m, 1H), 7.64 (ddd, J = 1.7, 7.2, 8.7 Hz, 2H), 7.43 (d, J = 8.0 Hz, 2H), 7.40 – 7.33 (m, 4H), 6.35 (s, 1H); **^{13}C{^{1}H} NMR (125 MHz, $CDCl_3$)** δ 173.31 (2C), 157.31 (2C), 156.52 (2C), 139.11 (1C), 133.97 (2C), 133.48 (1C), 132.95 (1C), 128.33 (1C), 128.23 (1C), 127.60 (1C), 126.98 (1C), 126.80 (1C), 126.61 (2C), 125.97 (1C), 125.82 (1C), 125.78 (2C), 123.71 (2C), 118.88 (2C), 117.46 (2C), 37.56 (1C); **IR (KBr)** ν_{max}/cm^{-1} 3070 (C=C−H), 2929 (C−H), 1650 (C=O), 1620 and 1464 (aromatic C=C); **HRMS (ESI)** calcd for $C_{29}H_{17}O_4S^+$ 461.0842 M+H$^+$ found 461.0849.

2,10-Dichloro-13-phenyl-12*H*,13*H*,14*H*-thiopyrano[2,3-*b*:6,5-*b*']dichromene-12,14-dione (2B12)

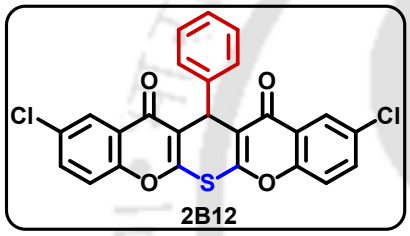

2B12

Light yellow solid (0.033 g, 69%); **mp** 322 – 324 °C; **^{1}H NMR (400 MHz, $CDCl_3$)** δ 8.12 (d, J = 2.6 Hz, 2H), 7.65 – 7.53 (m, 4H), 7.39 (d, J = 8.8 Hz, 2H), 7.23 (d, J = 7.5 Hz, 2H), 7.19 – 7.13 (m, 1H), 6.15 (s, 1H); **^{13}C{^{1}H} NMR (100 MHz, $CDCl_3$)** δ 172.11 (2C), 157.47 (2C), 154.76 (2C), 141.00 (1C), 134.22 (2C), 131.83 (2C), 128.74 (2C), 128.22 (2C), 127.79 (1C), 126.06 (2C), 124.56 (2C), 119.18 (2C), 118.86 (2C), 37.27 (1C); **IR (KBr)** ν_{max}/cm^{-1} 3085 (C=C−H), 2924 (C−H), 1652 (C=O), 1620 and 1465 (aromatic C=C); **HRMS (ESI)** calcd for $C_{25}H_{12}Cl_2NaO_4S^+$ 500.9726 M+Na$^+$ found 500.9727.

2,10-Dichloro-13-(4-chlorophenyl)-12*H*,13*H*,14*H*-thiopyrano[2,3-*b*:6,5-*b*']dichromene-12,14-dione (2B13)

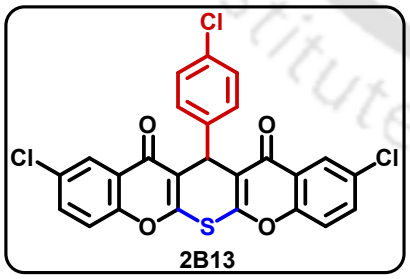

2B13

White solid (0.033 g, 65%); **mp** 345 – 347 °C; **^{1}H NMR (500 MHz, $CDCl_3$)** δ 8.12 (d, J = 2.4 Hz, 2H), 7.61 (dd, J = 2.4, 8.9 Hz, 2H), 7.52 (d, J = 8.4 Hz, 2H), 7.40 (d, J = 8.9 Hz, 2H), 7.20 (d, J = 8.4 Hz, 2H), 6.11 (s, 1H); **^{13}C{^{1}H} NMR (100 MHz, $CDCl_3$)** δ 172.10 (2C), 157.46 (2C), 154.77 (2C), 139.54 (1C), 134.38 (2C), 133.63 (1C), 132.00 (2C), 129.68 (2C), 128.88 (2C), 126.05 (2C), 124.48 (2C), 119.22 (2C), 118.47 (2C), 36.95 (1C); **IR (KBr)** ν_{max}/cm^{-1} 3089 (C=C−H), 2924 (C−H), 1652 (C=O), 1621 and 1465 (aromatic C=C); **HRMS (ESI)** calcd for $C_{25}H_{12}Cl_3O_4S^+$ 512.9516 M+H$^+$ found 512.9516.

2,10-Dichloro-13-(*p*-tolyl)-12*H*,13*H*,14*H*-thiopyrano[2,3-*b*:6,5-*b*']dichromene-12,14-dione (2B14)

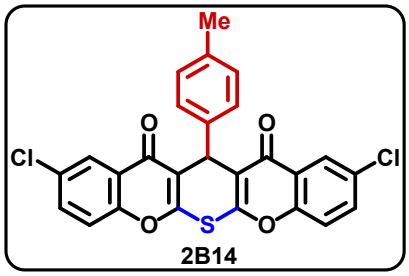

Light brown solid (0.033 g, 67%); **mp** 335 – 337 °C; **^{1}H NMR (400 MHz, $CDCl_3$)** δ 8.12 (d, J = 2.6 Hz, 2H), 7.59 (dd, J = 2.6, 8.9 Hz, 2H), 7.50 – 7.45 (m, 2H), 7.39 (d, J = 8.9 Hz, 2H), 7.04 (d, J = 7.9 Hz, 2H), 6.11 (s, 1H), 2.23 (s, 3H); **^{13}C{^{1}H} NMR (100 MHz, $CDCl_3$)** δ 172.10 (2C), 157.31 (2C), 154.73 (2C), 138.09 (1C), 137.51 (1C), 134.17 (2C), 131.76 (2C), 129.41 (2C), 128.09 (2C), 126.04 (2C), 124.57 (2C), 119.15 (2C), 118.94 (2C), 36.92 (1C), 21.19 (1C); **IR (KBr)** ν_{max}/cm^{-1} 3092 (C=C–H), 2923 (C–H), 1652 (C=O), 1619 and 1465 (aromatic C=C); **HRMS (ESI)** calcd for $C_{26}H_{15}Cl_2O_4S^+$ 493.0063 M+H$^+$ found 493.0063.

2,10-Dichloro-13-(4-methoxyphenyl)-12*H*,13*H*,14*H*-thiopyrano[2,3-*b*:6,5-*b*']dichromene-12,14-dione (2B15)

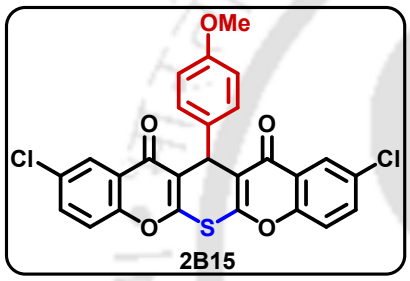

Light yellow solid (0.032 g, 62%); **mp** 355 – 356 °C; **^{1}H NMR (400 MHz, $CDCl_3$)** δ 8.13 (d, J = 2.6 Hz, 2H), 7.60 (dd, J = 2.6, 8.9 Hz, 2H), 7.53 – 7.48 (m, 2H), 7.39 (d, J = 8.9 Hz, 2H), 6.79 – 6.74 (m, 2H), 6.09 (s, 1H), 3.71 (s, 3H); **^{13}C{^{1}H} NMR (100 MHz, $CDCl_3$)** δ 172.15 (2C), 159.18 (1C), 157.18 (2C), 154.80 (2C), 134.19 (2C), 133.32 (1C), 131.82 (2C), 129.35 (2C), 126.10 (2C), 124.64 (2C), 119.17 (2C), 119.07 (2C), 114.14 (2C), 55.35 (1C), 36.61 (1C); **IR (KBr)** ν_{max}/cm^{-1} 3070 (C=C–H), 2925 (C–H), 1651 (C=O), 1622 and 1465 (aromatic C=C); **HRMS (ESI)** calcd for $C_{26}H_{14}Cl_2NaO_5S^+$ 530.9831 M+Na$^+$ found 530.9833.

2,10-Dichloro-13-(2,4-dimethoxyphenyl)-12*H*,13*H*,14*H*-thiopyrano[2,3-*b*:6,5-*b*']dichromene-12,14-dione (2B16)

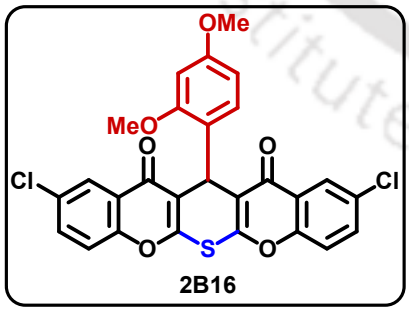

Light Brown solid (0.031 g, 58%); **mp** 315 – 317 °C; **^{1}H NMR (400 MHz, $CDCl_3$)** δ 8.07 (d, J = 2.4 Hz, 2H), 7.79 (d, J = 8.4 Hz, 1H), 7.56 (dd, J = 2.6, 8.9 Hz, 2H), 7.36 (d, J = 8.9 Hz, 2H), 6.51 (dd, J = 2.3, 8.4 Hz, 1H), 6.33 (d, J = 2.1 Hz, 1H), 6.00 (s, 1H), 3.74 (s, 3H), 3.73 (s, 3H); **^{13}C{^{1}H} NMR (100 MHz, $CDCl_3$)** δ 172.38 (2C), 160.34 (1C), 159.43 (1C), 158.29 (2C), 154.49 (2C), 134.32 (1C), 133.80 (2C), 131.44 (2C), 126.00 (2C), 124.75 (2C), 120.26 (1C), 119.04 (2C), 116.30 (2C), 104.15 (1C), 99.04 (1C), 55.40 (1C), 55.36 (1C), 36.85 (1C); **IR (KBr)** ν_{max}/cm^{-1} 3072 (C=C–H), 2955 (C–H), 1652 (C=O), 1620 and 1465 (aromatic C=C); **HRMS (ESI)** calcd for $C_{27}H_{16}Cl_2NaO_6S^+$ 560.9937 M+Na$^+$ found 560.9939.

2,10-Dibromo-13-(*p*-tolyl)-12*H*,13*H*,14*H*-thiopyrano[2,3-*b*:6,5-*b*']dichromene-12,14-dione (2B17)

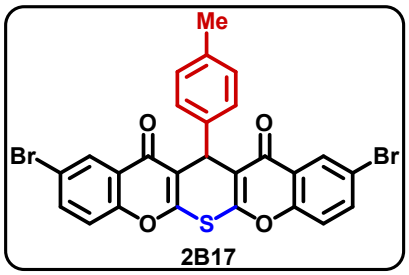

2B17

White solid (0.038 g, 65%); **mp** 333 – 335 °C; **^{1}H NMR (400 MHz, $CDCl_3$)** δ 8.27 (d, J = 2.4 Hz, 2H), 7.73 (dd, J = 2.4, 8.9 Hz, 2H), 7.46 (d, J = 8.1 Hz, 2H), 7.32 (d, J = 8.9 Hz, 2H), 7.04 (d, J = 8.0 Hz, 2H), 6.11 (s, 1H), 2.23 (s, 3H); **^{13}C{^{1}H} NMR (100 MHz, $CDCl_3$)** δ 171.97 (2C), 157.28 (2C), 155.19 (2C), 138.06 (1C), 137.53 (1C), 136.95 (2C), 129.42 (2C), 129.27 (2C), 128.09 (2C), 124.93 (2C), 119.37 (2C), 119.20 (2C), 119.03 (2C), 36.94 (1C), 21.20 (1C); **IR (KBr)** ν_{max}/cm^{-1} 3076 (C=C−H), 2921 (C−H), 1645 (C=O), 1619 and 1460 (aromatic C=C); **HRMS (ESI)** calcd for $C_{26}H_{15}Br_2O_4S^+$ 580.9052 M+H$^+$ found 580.9053.

2,10-Dibromo-13-(2,4-dimethoxyphenyl)-12*H*,13*H*,14*H*-thiopyrano[2,3-*b*:6,5-*b*']dichromene-12,14-dione (2B18)

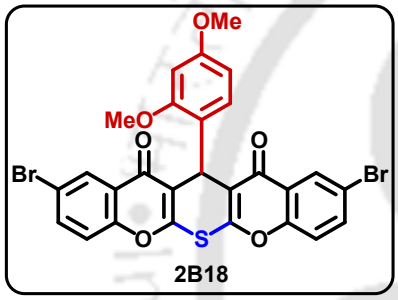

2B18

white solid (0.037 g, 59%); **mp** 307 – 308 °C; **^{1}H NMR (400 MHz, $CDCl_3$)** δ 8.24 (d, J = 2.4 Hz, 2H), 7.79 (d, J = 8.4 Hz, 1H), 7.70 (dd, J = 2.4, 8.8 Hz, 2H), 7.30 (d, J = 8.9 Hz, 2H), 6.51 (dd, J = 2.4, 8.5 Hz, 1H), 6.33 (d, J = 2.3 Hz, 1H), 6.00 (s, 1H), 3.74 (s, 3H), 3.73 (s, 3H); **^{13}C{^{1}H} NMR (100 MHz, $CDCl_3$)** δ 172.25 (2C), 160.35 (1C), 159.43 (1C), 158.27 (2C), 154.94 (2C), 136.58 (2C), 134.32 (1C), 129.23 (2C), 125.11 (2C), 120.21 (1C) , 119.27 (2C), 118.89 (2C), 116.38 (2C), 104.13 (1C), 99.04 (1C), 55.41 (1C), 55.36 (1C), 36.88 (1C); **IR (KBr)** ν_{max}/cm^{-1} 3082 (C=C−H), 2923 (C−H), 1649 (C=O), 1604 and 1460 (aromatic C=C); **HRMS (ESI)** calcd for $C_{27}H_{16}Br_2NaO_6S^+$ 648.8927 M+Na$^+$ found 648.8927.

13-(1*H*-indol-2-yl)-12*H*,13*H*,14*H*-thiopyrano[2,3-*b*:6,5-*b*']dichromene-12,14-dione (2B19)

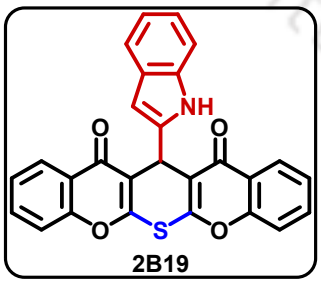

2B19

Yellow solid (0.034 g, 75%); **mp** 304 – 305 °C; **^{1}H NMR (500 MHz, $CDCl_3$)** δ 8.14 (d, J = 7.8 Hz, 2H), 8.06 (s, 1H), 8.01 (dd, J = 3.0, 5.7 Hz, 1H), 7.62 (t, J = 7.3 Hz, 2H), 7.45 (d, J = 2.0 Hz, 1H), 7.41 (d, J = 8.4 Hz, 2H), 7.35 (t, J = 7.5 Hz, 2H), 7.09 (dd, J = 3.1, 5.9 Hz, 2H), 6.54 (s, 1H); **^{13}C{^{1}H} NMR (125 MHz, $CDCl_3$)** δ 173.46 (2C), 156.69 (2C), 156.47 (2C), 136.48 (1C), 133.81 (2C), 126.60 (2C), 126.03 (1C), 125.64 (2C), 124.44 (1C), 123.81 (2C), 121.86 (1C), 120.34 (1C), 119.87 (1C), 118.31 (2C), 117.41 (2C), 115.83 (1C), 111.35 (1C), 29.88 (1C); **IR (KBr)** ν_{max}/cm^{-1} 3064 (C=C−H), 2957 (C−H), 1648 (C=O), 1618 and 1465 (aromatic C=C); **HRMS (ESI)** calcd for $C_{27}H_{15}NNaO_4S^+$ 472.0614 M+Na$^+$ found 472.0602.

13-(Thiophen-2-yl)-12*H*,13*H*,14*H*-thiopyrano[2,3-*b*:6,5-*b*']dichromene-12,14-dione (2B20)

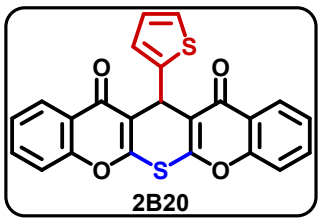

Light brown solid (0.030 g, 72%); **mp** 264 – 265 °C; **^{1}H NMR (400 MHz, $CDCl_3$)** δ 8.22 (dd, J = 1.5, 8.0 Hz, 2H), 7.67 (ddd, J = 1.7, 7.2, 8.7 Hz, 2H), 7.45 (s, 1H), 7.44 – 7.39 (m, 3H), 7.15 – 7.13 (m, 1H), 7.05 (dd, J = 1.2, 5.1 Hz, 1H), 6.84 (dd, J = 3.6, 5.1 Hz, 1H), 6.57 (s, 1H); **^{13}C{^{1}H} NMR (100 MHz, $CDCl_3$)** δ 173.11 (2C), 157.76 (2C), 156.53 (2C), 143.70 (1C), 134.10 (2C), 126.91 (1C), 126.68 (2C), 125.88 (2C), 125.64 (1C), 124.27 (1C), 123.60 (2C), 118.56 (2C), 117.54 (2C), 32.18 (1C); **IR (KBr)** ν_{max}/cm^{-1} 3076 (C=C–H), 2957 (C–H), 1643 (C=O), 1627 and 1463 (aromatic C=C); **HRMS (ESI)** calcd for $C_{23}H_{13}O_4S_2^+$ 417.0250 M+H$^+$ found 417.0251.

13-Propyl-12*H*,13*H*,14*H*-thiopyrano[2,3-*b*:6,5-*b*']dichromene-12,14-dione (2B21)

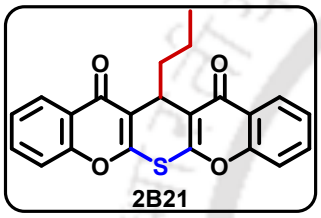

White solid (0.027 g, 72%); **mp** 210 – 212 °C; **^{1}H NMR (400 MHz, $CDCl_3$)** δ 8.25 (dd, J = 1.6, 8.3 Hz, 2H), 7.70 – 7.65 (m, 2H), 7.46 – 7.40 (m, 4H), 5.17 (t, J = 6.3 Hz, 1H), 1.75 – 1.68 (m, 2H), 1.40 – 1.29 (m, 2H), 0.85 (t, J = 7.3 Hz, 3H); **^{13}C{^{1}H} NMR (100 MHz, $CDCl_3$)** δ 173.71 (2C), 157.90 (2C), 156.51 (2C), 133.85 (2C), 126.64 (2C), 125.72 (2C), 123.56 (2C), 119.35 (2C), 117.51 (2C), 35.60 (1C), 31.20 (1C), 19.64 (1C), 14.26 (1C); **IR (KBr)** ν_{max}/cm^{-1} 3071 (C=C–H), 2926 (C–H), 1650 (C=O), 1620 and 1464 (aromatic C=C); **HRMS (ESI)** calcd for $C_{22}H_{17}O_4S^+$ 377.0842 M+H$^+$ found 377.0850.

13-Pentyl-12*H*,13*H*,14*H*-thiopyrano[2,3-*b*:6,5-*b*']dichromene-12,14-dione (2B22)

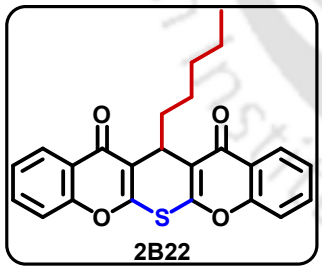

White solid (0.028 g, 69%); **mp** 224 – 226 °C; **^{1}H NMR (400 MHz, $CDCl_3$)** δ 8.24 (dd, J = 1.5, 8.3 Hz, 2H), 7.70 – 7.64 (m, 2H), 7.46 – 7.40 (m, 4H), 5.16 (t, J = 6.3 Hz, 1H), 1.77 – 1.68 (m, 2H), 1.37 – 1.26 (m, 2H), 1.24 – 1.14 (m, 4H), 0.78 (t, J = 6.8 Hz, 3H); **^{13}C{^{1}H} NMR (100 MHz, $CDCl_3$)** δ 173.65 (2C), 157.88 (2C), 156.50 (2C), 133.83 (2C), 126.64 (2C), 125.70 (2C), 123.55 (2C), 119.32 (2C), 117.50 (2C), 33.34 (1C), 32.10 (1C), 31.28 (1C), 25.90 (1C), 22.67 (1C), 14.22 (1C); **IR (KBr)** ν_{max}/cm^{-1} 3070 (C=C–H), 2929 (C–H), 1650 (C=O), 1620 and 1464 (aromatic C=C); **HRMS (ESI)** calcd for $C_{24}H_{21}O_4S^+$ 405.1155 M+H$^+$ found 405.1153.

2.10 Copies of ^{1}H NMR, $^{13}C\{^{1}H\}$ NMR and HRMS spectra of Compounds

Figure 2.2a: ^{1}H NMR (500 MHz, $CDCl_3$) spectrum of compound **2B1**.

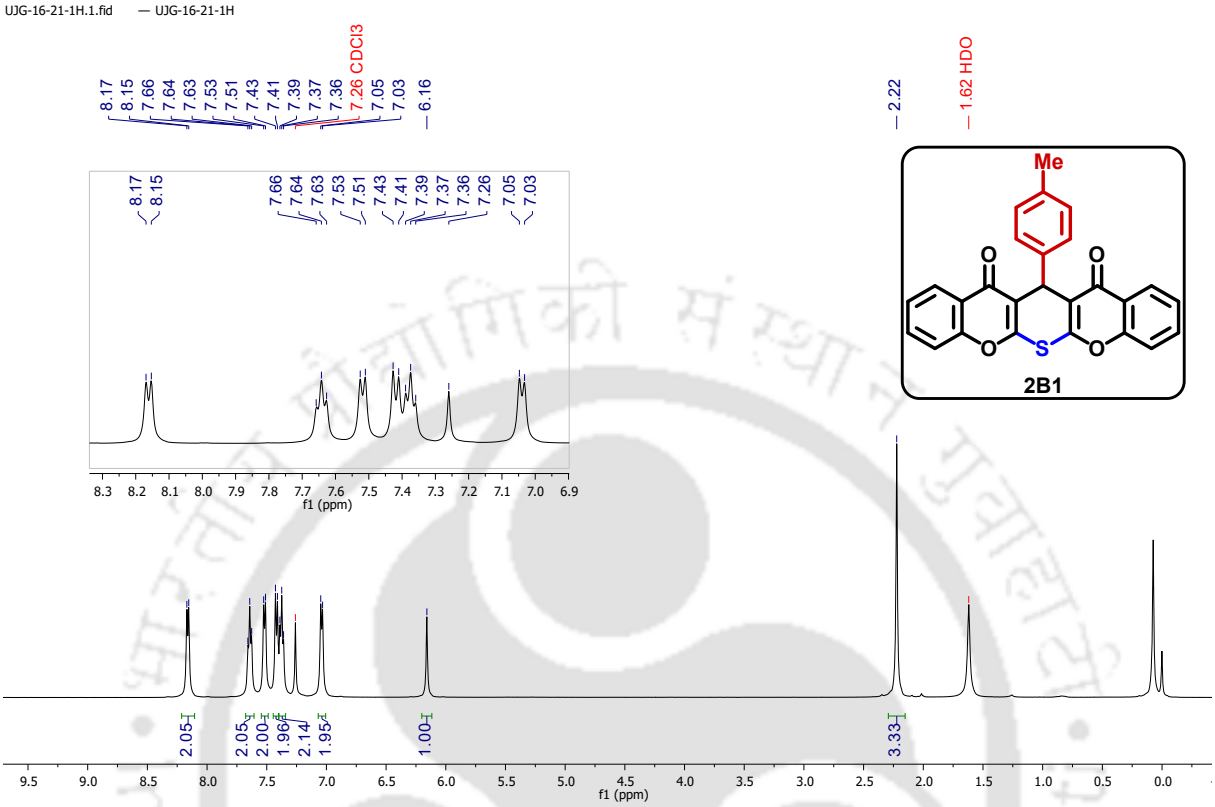

Figure 2.2b: $^{13}C\{^{1}H\}$ NMR (125 MHz, $CDCl_3$) spectrum of compound **2B1**.

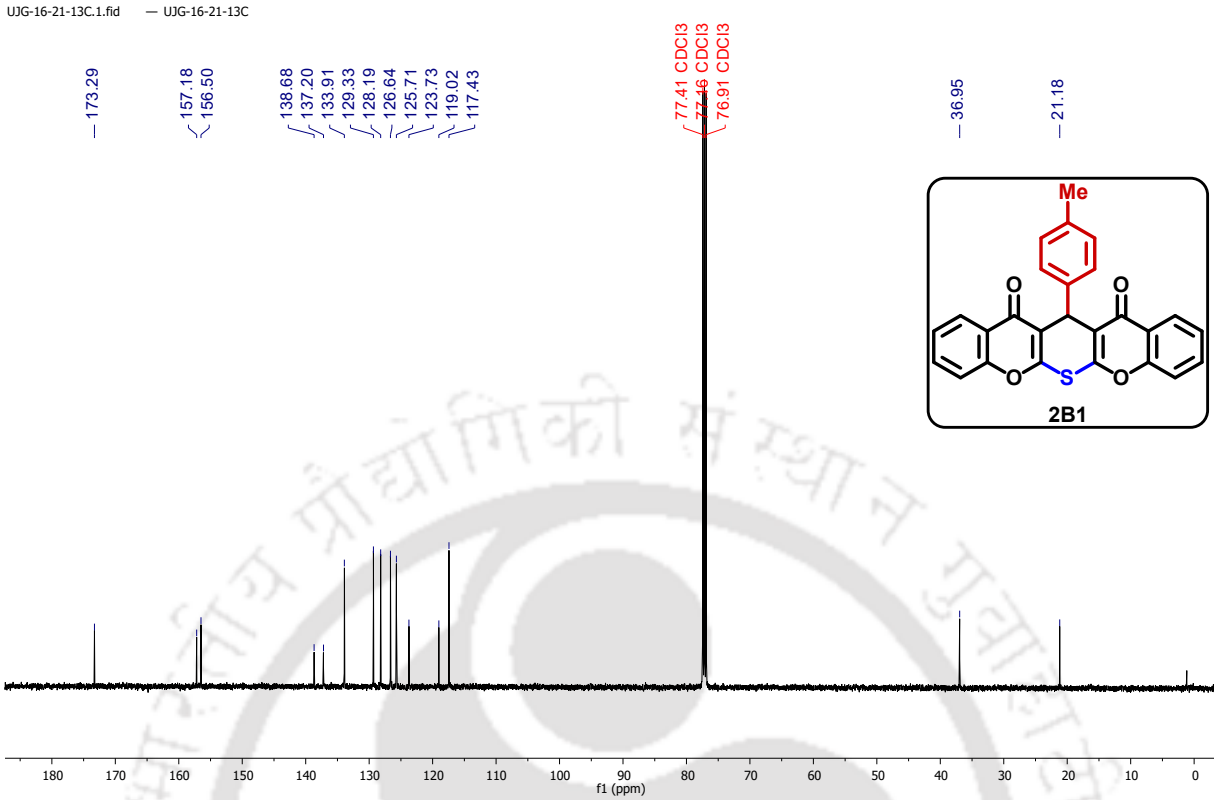

Figure 2.2c: COSY spectrum of compound **2B1**.

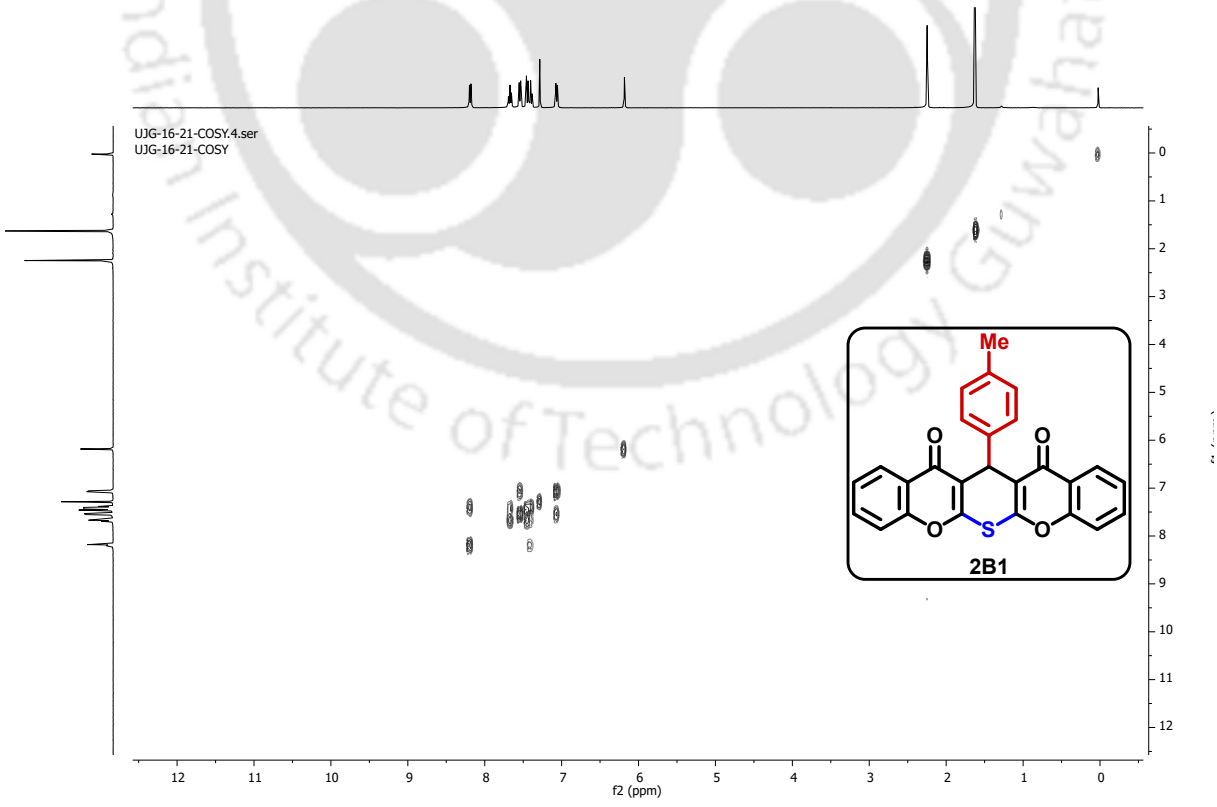

Figure 2.2d: HSQC spectrum of compound **2B1**.

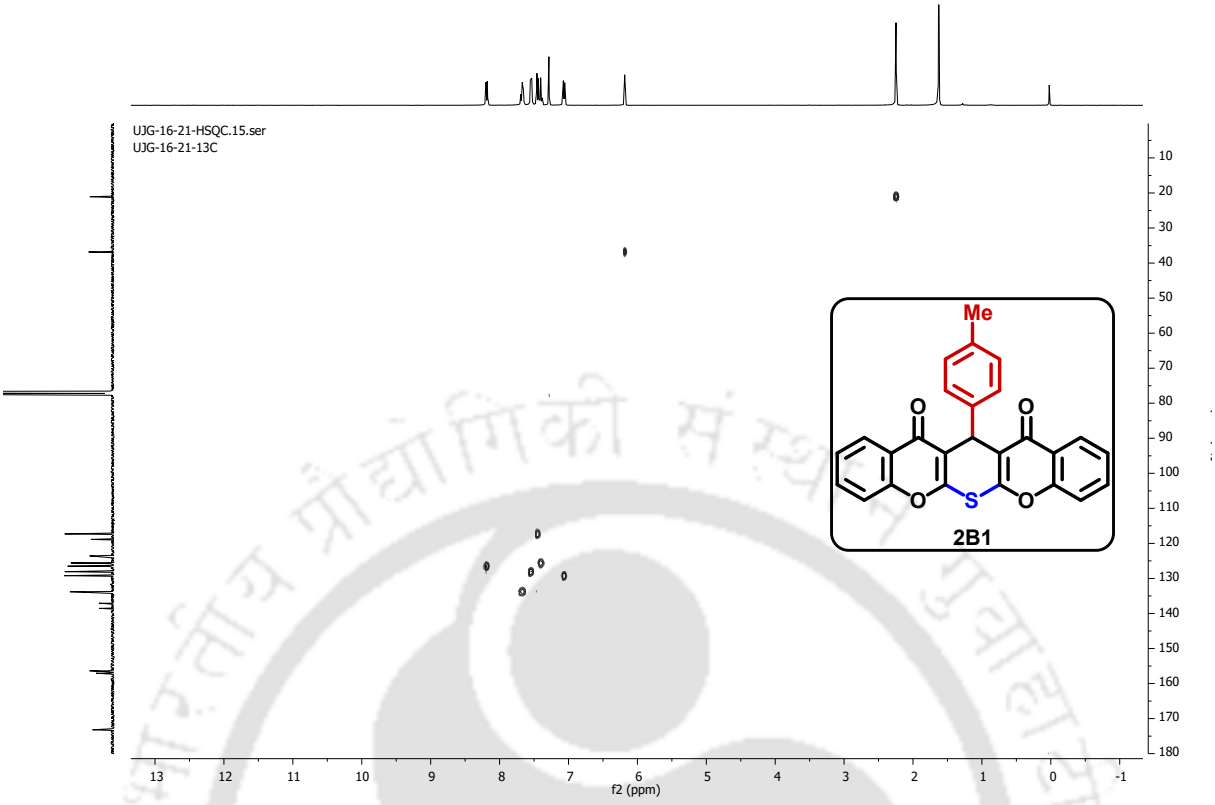

Figure 2.2e: HRMS spectrum of compound **2B1**.

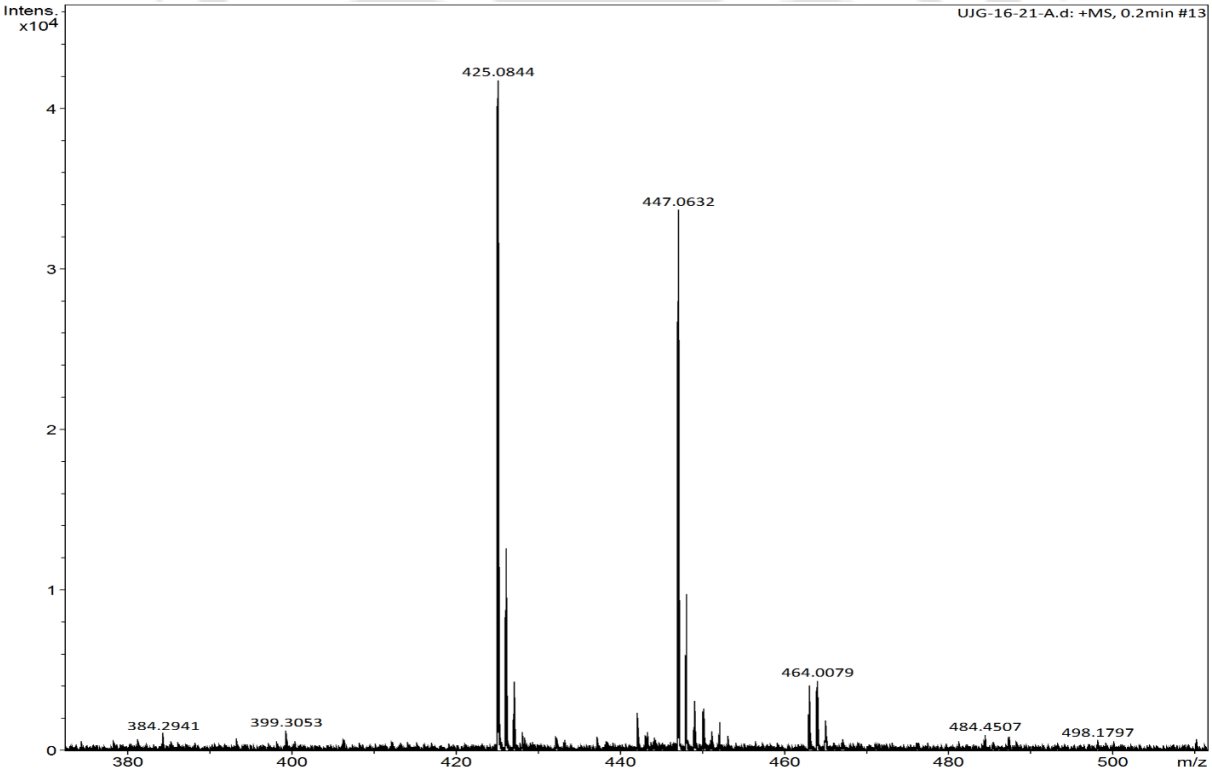

Figure 2.3a: ^{1}H NMR (400 MHz, $CDCl_3$) spectrum of compound **2B14**.

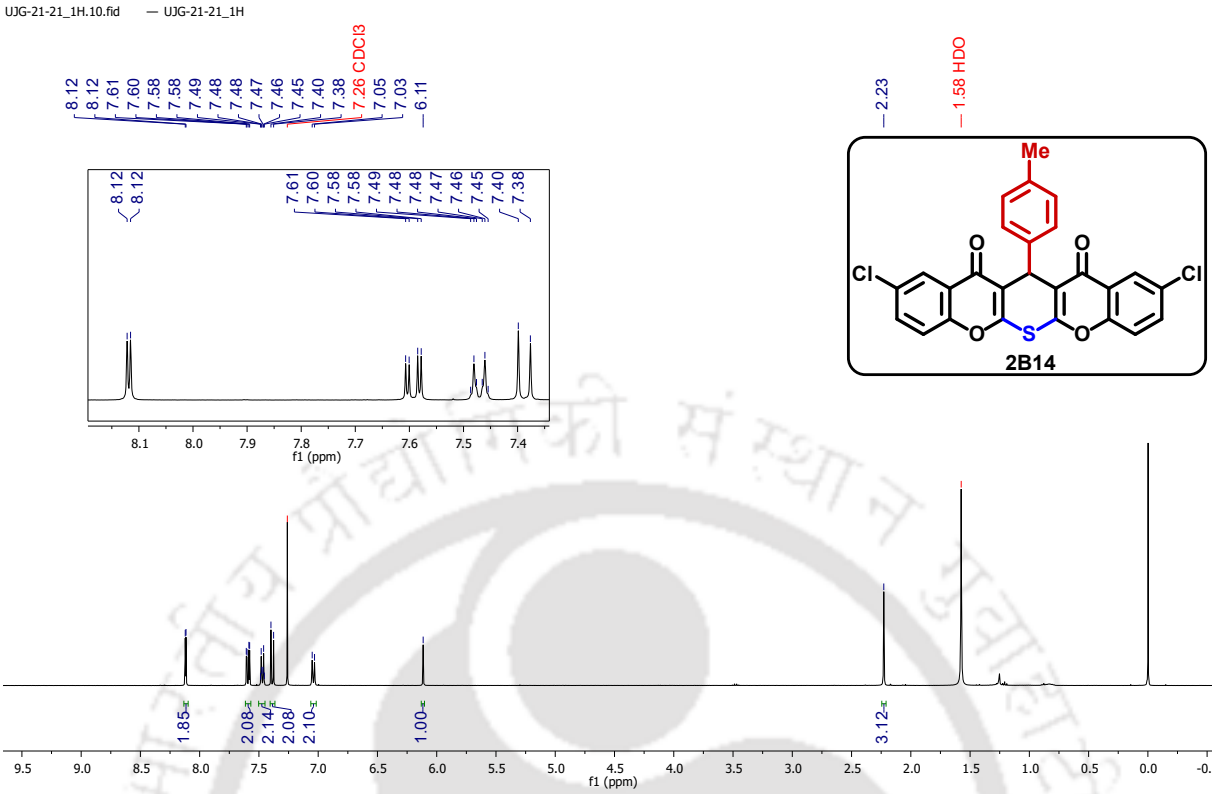

Figure 2.3b: $^{13}C\{^{1}H\}$ NMR (100 MHz, $CDCl_3$) spectrum of compound **2B14**.

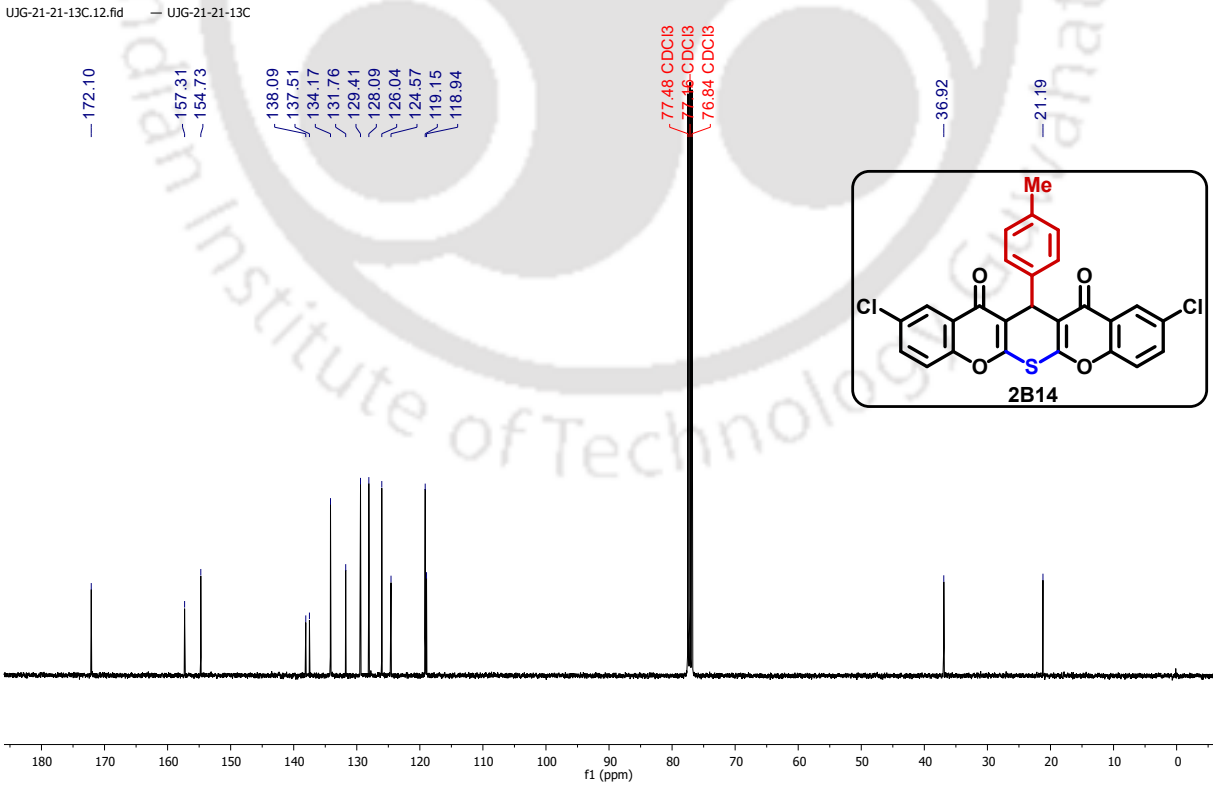

Figure 2.3c: HRMS spectrum of compound **2B14**.

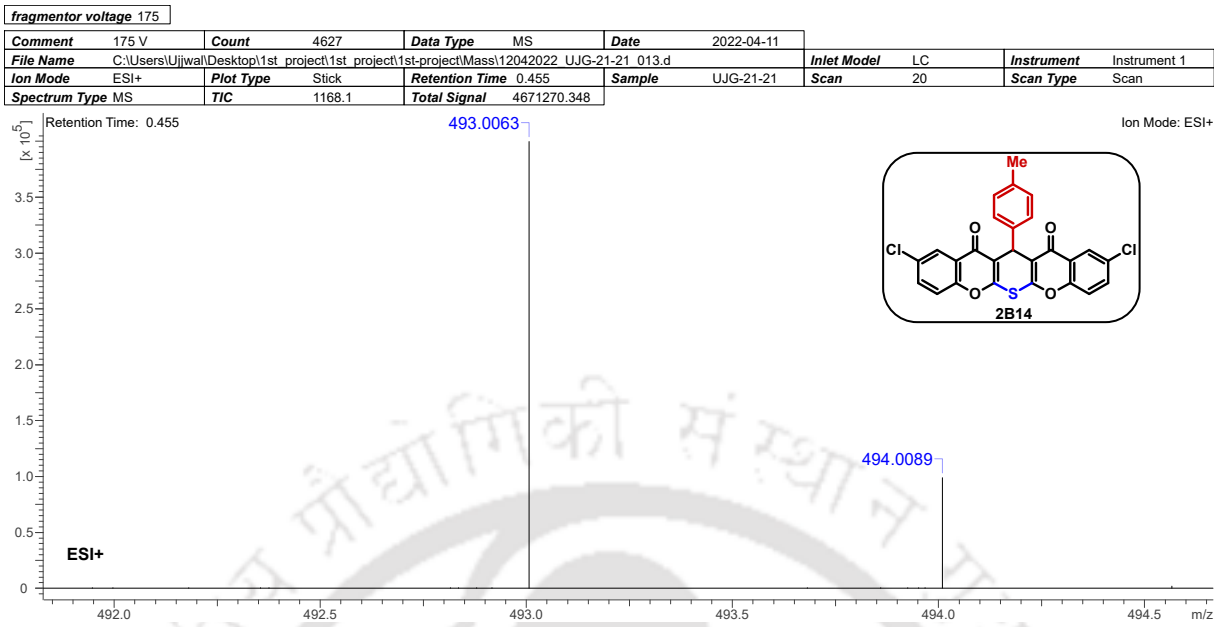

Figure 2.4a: ^{1}H NMR (400 MHz, $CDCl_3$) spectrum of compound **2B22**.

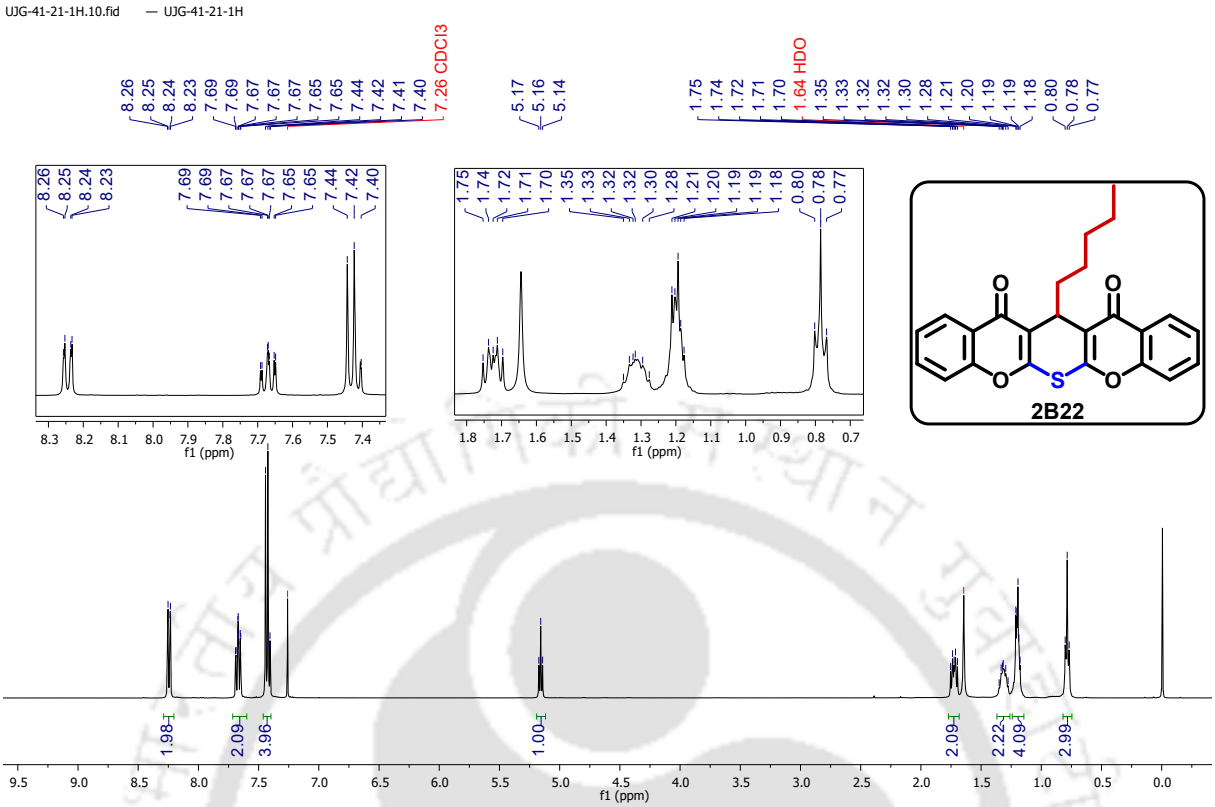

Figure 2.4b: $^{13}C\{^{1}H\}$ NMR (100 MHz, $CDCl_3$) spectrum of compound **2B22**.

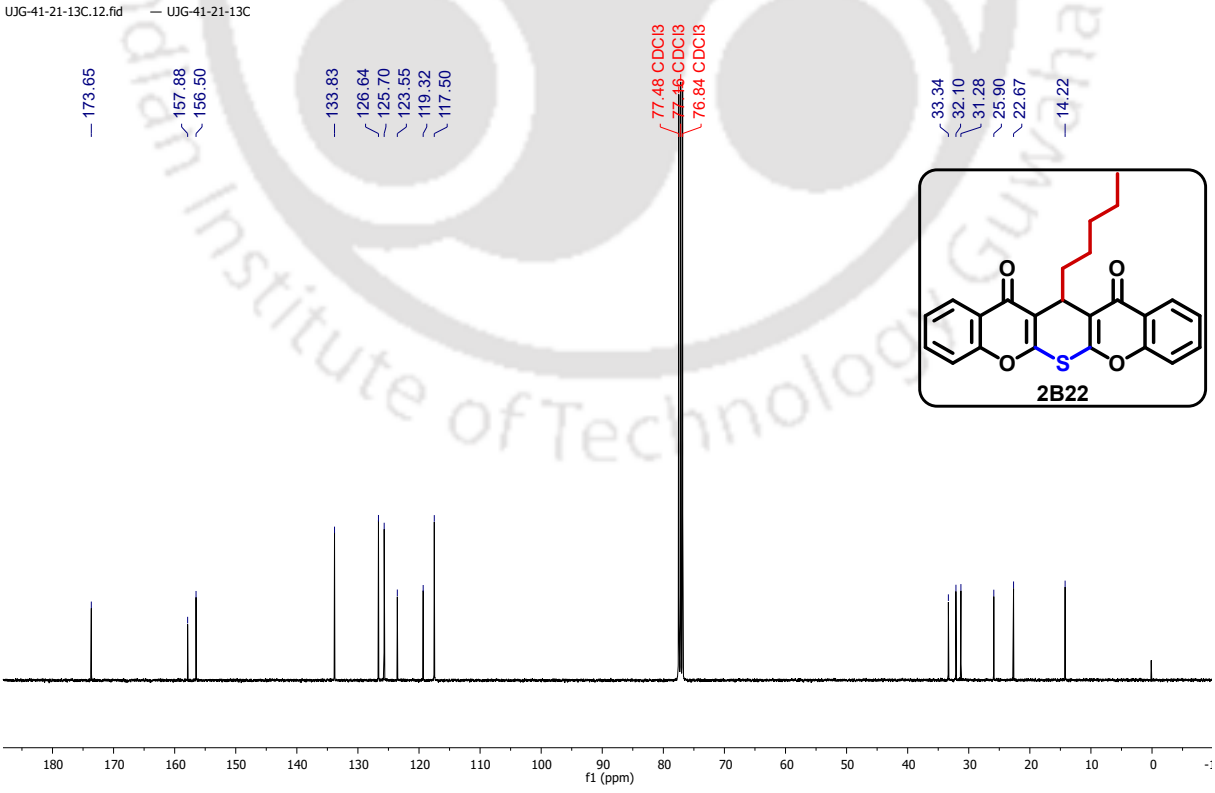

Figure 2.4c: HRMS spectrum of compound **2B22**

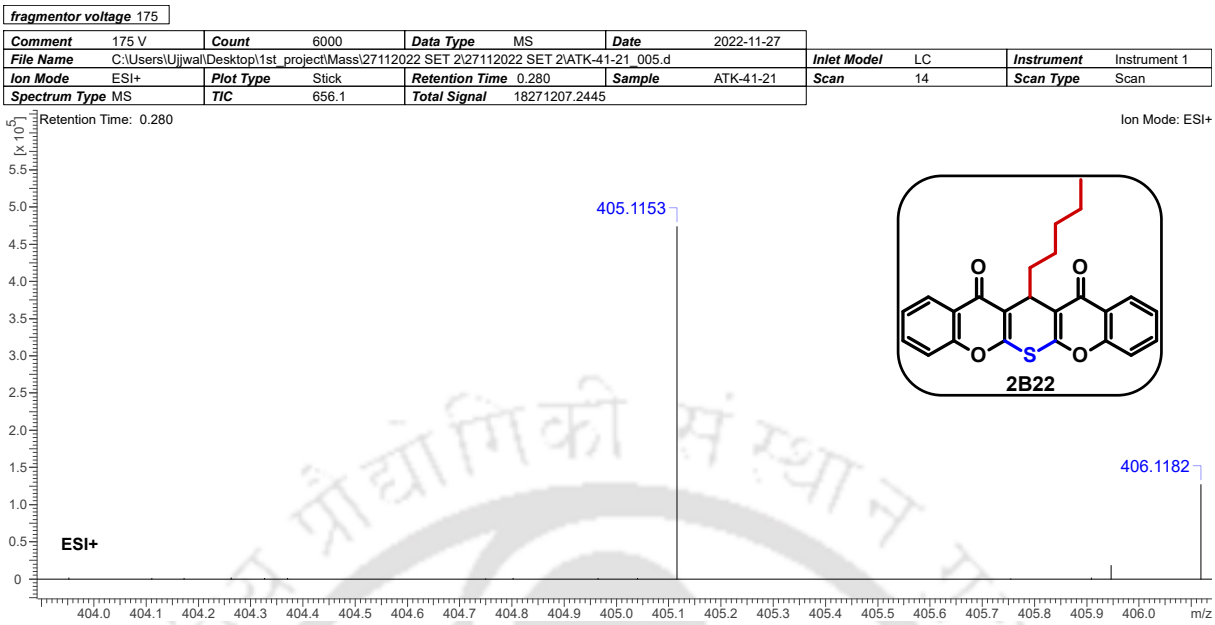

References

[1] K. A. Scott, J. T. Njardarson, *Top. Curr. Chem.* **2018**, *376*, 5.

[2] J. Yu, X. Jiang, *Adv. Agrochem* **2023**, *2*, 3–14.

[3] P. Devendar, G.-F. Yang, *Top. Curr. Chem.* **2017**, *375*, 82.

[4] M. Iciek, I. Kwiecień, L. Włodek, *Environ. Mol. Mutagen.* **2009**, *50*, 247–265.

[5] J. T. Brosnan, M. E. Brosnan, *J. Nutr.* **2006**, *136*, 1636.

[6] C. Sirithanakorn, J. E. Cronan, *FEMS Microbiol. Rev.* **2021**, fuab3.

[7] P. Sang, Q. Chen, D.-Y. Wang, W. Guo, Y. Fu, *Chem. Rev.* **2023**, *123*, 1262–1326.

[8] H.-L. Qin, Z.-W. Zhang, L. Ravindar, K. Rakesh, *Eur. J. Med. Chem.* **2020**, *207*, 112832.

[9] T. Al-Warhi, A. Sabt, E. B. Elkaeed, W. M. Eldehna, *Top. Curr. Chem.* **2020**, *103*, 104163.

[10] M. Gebauer, *Bioorgan. Med. Chem.* **2007**, *15*, 2414–2420.

[11] C. Sun, W. Zhao, X. Wang, Y. Sun, X. Chen, *Pharmacol. Res.* **2020**, *160*, 105193.

[12] E. R. Darzi, J. S. Barber, N. K. Garg, *Angew. Chem-ger. Edit.* **2019**, *58*, 9419–9424.

[13] M. Stępień, E. Gońka, M. Żyła, N. Sprutta, *Chem. Rev.* **2017**, *117*, 3479–3716.

[14] M. Kvasnica, M. Urban, N. J. Dickinson, J. Sarek, *Nat. Prod. Rep.* **2015**, *32*, 1303–1330.

[15] A. Kumar, M. K. Gupta, M. Kumar, *Tetrahedron Lett.* **2011**, *52*, 4521–4525.

[16] A. Montagut-Romans, M. Boulven, M. Lemaire, F. Popowycz, *RSC Adv.* **2016**, *6*, 4540–4544.

[17] M. Gerami, M. Farahi, B. Karami, *J. Mol. Struct.* **2025**, *1328*, 141246.

[18] Y.-P. Zhang, Y.-N. Liang, C. Yang, Y.-S. Yang, H.-C. Guo, H.-R. Zhang, *J. Mol. Liq.* **2024**, *397*, 124111.

[19] N. Wu, X. Li, X. Xu, D. Shi, *J. Chem. Res.* **2007**, *2007*, 561–562.

[20] K. Mahato, P. Ray Bagdi, A. Khan, *Synlett* **2014**, *25*, 2438–2441.

[21] P. T. Anastas, J. C. Warner, *Green Chemistry: Theory and Practice*, Oxford University Press, Oxford, **2000**.

[22] R. A. Sheldon, *Green Chem.* **2023**, *25*, 1704–1728.

[23] B. Nanda, M. Sailaja, P. Mohapatra, R. Pradhan, B. B. Nanda, *Mater. Today:. Proc.* **2021**, *47*, 1234–1240.

[24] S. Zangade, P. Patil, *COC* **2020**, *23*, 2295–2318.

[25] S. E. John, S. Gulati, N. Shankaraiah, *Org. Chem. Front.* **2021**, *8*, 4237–4287.

[26] R. C. Cioc, E. Ruijter, R. V. A. Orru, *Green Chem.* **2014**, *16*, 2958–2975.

[27] M. M. Khan, S. Shareef, S. Saigal, S. C. Sahoo, *RSC Adv.* **2019**, *9*, 26393–26401.

[28] K. Jain, S. Chaudhuri, K. Pal, K. Das, *New J. Chem.* **2019**, *43*, 1299–1304.

[29] L. J. Farrugia, *J. Appl. Crystallogr.* **2012**, *45*, 849–854.

भारतीय प्रौद्योगिकी संस्थान गुवाहाटी
Indian Institute of Technology Guwahati

Chapter 3

Reactivity Study of 4-Hydroxythiocoumarin: A Novel Synthetic Route to Fused Chromono-Thiophene and -Thiopyran Derivatives through Solvent-Dependent Thio-Claisen Rearrangement

Graphical Abstract

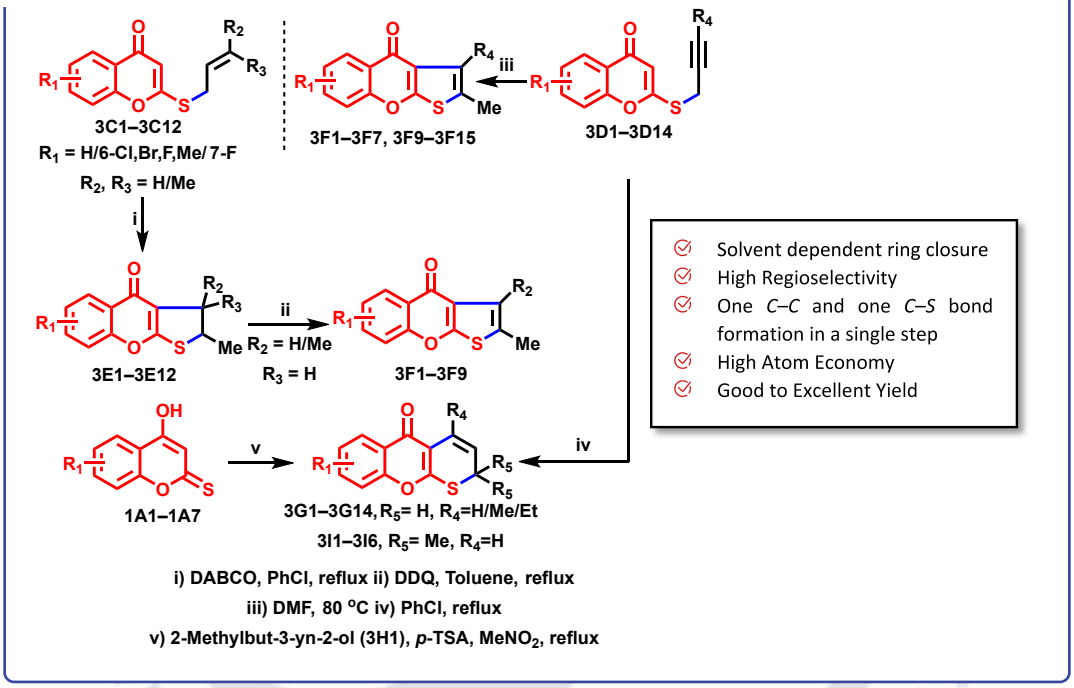

Table of contents

3.1 Context and Significance

The broader context and significance of fused chromone-thiopyran and chromone-thiophene systems, their biological activities, and the unique reactivity of 4-hydroxythiocoumarin are discussed in detail in **Chapter 1**. Readers are referred to that chapter for an in-depth overview of the pharmacological relevance, structural features, and synthetic challenges associated with these heterocyclic frameworks. A very brief overview is presented here.

Fused heterocycles incorporating chromone,[1] thiopyran,[2] and thiophene[3] units are valued for their presence in bioactive compounds and diverse pharmacological properties. Chromones show antibacterial, anticancer, and anti-inflammatory effects,[4] while thiopyran and thiophene cores offer antimicrobial, antitumor, and antidiabetic activity.[5,6] Hybridizing these motifs into single scaffolds can enhance biological potential, making their synthesis a key goal.

3.2 Literature Review: Synthesis of Fused Chromono-Thiophene and -Thiopyran Systems

While chromone and sulfur-containing heterocycles are well established for their diverse biological and pharmacological properties, the synthesis of fused chromono-thiophene and chromono-thiopyran derivatives has received comparatively limited attention.

3.2.1 Previous Approaches and Limitations

Early studies demonstrated that 4-hydroxycoumarin reacts with propargyl bromide in the presence of K_2CO_3 to give *O*-alkylated products,[7] whereas 4-hydroxydithiocoumarin under similar conditions provides cyclized products *via* *S*-alkylation followed by concomitant cyclization.[8] This divergent reactivity highlights the subtle influence of heteroatom positioning on reaction outcomes (**Scheme 3.1**).

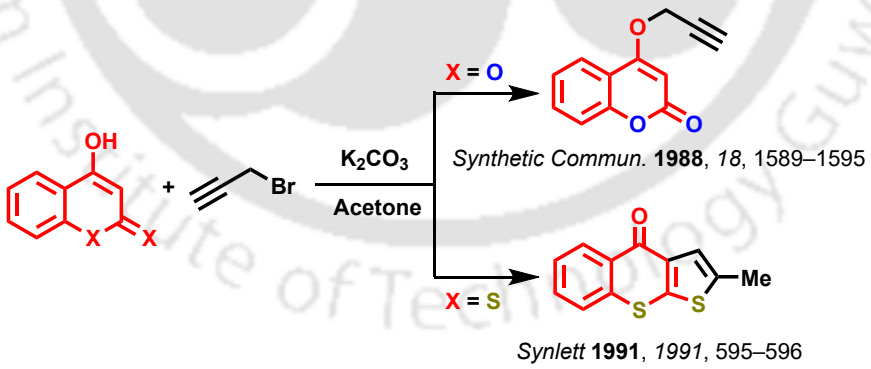

Scheme 3.1: Synthesis of fused chromone-thiophene hybrid.

Efforts to directly access fused chromono-thiophene frameworks have been sparse in the literature.

In an earlier study, Watthey and Desai developed a method based on the regioselective lithiation of 3-(aryloxy/arylthio)thiophenes, followed by carbonation and acid-catalyzed cyclization, to access thieno[3,2-*b*][1]benzopyran-9-one derivatives (**Scheme 3.2**).[9] Although generally effective, the method exhibits incomplete regioselectivity, with minor isomers and dilithiation products occasionally forming. Furthermore, it relies on harsh reaction conditions,

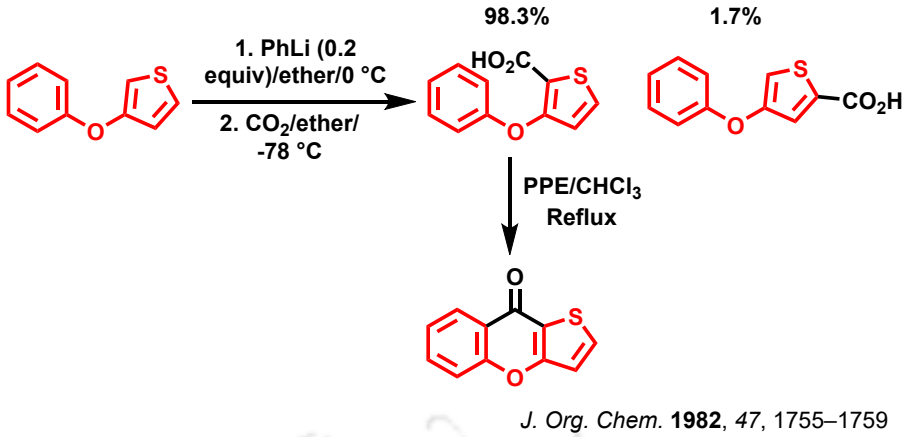

J. Org. Chem. **1982**, *47*, 1755–1759

Scheme 3.2: Synthesis of fused chromone-thiophene hybrid.

hazardous reagents, and demonstrates limited functional group tolerance, making it less suitable for clean, scalable, or structurally diverse synthesis.

One isolated report describes the formation of such fused scaffold through tandem C—H functionalization and C—O bond formation. However, only a single substrate was tested, affording very poor yield of product and no subsequent evaluation of generality (**Scheme 3.3**).[10] This reflects a broader limitation in the field: the absence of robust, broadly applicable methods for these complex fused systems.

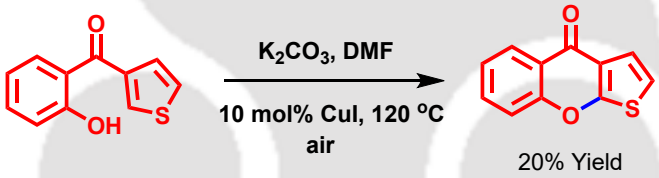

Org. Lett. **2013**, *15*, 4508–4511

Scheme 3.3: Synthesis of fused chromone-thiophene hybrid.

In the context of chromono-thiopyrans, Palmisano and co-workers reported a route involving Knoevenagel condensation between 4-hydroxythiocoumarin and α,β-unsaturated aldehydes, followed by thermal electrocyclization (**Scheme 3.4**).[11] Although mechanistically elegant, this approach is hampered by several drawbacks: it requires expensive and hazardous metal triflates, provides only moderate yields, and is operationally cumbersome. As a result, its practical applicability remains limited.

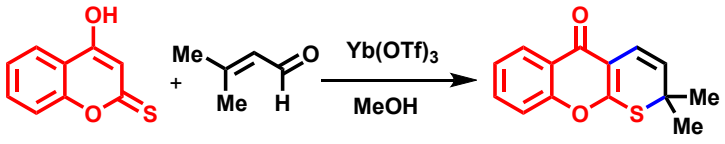

J Heterocycl. Chem. **2007**, *44*, 411–418

Scheme 3.4: Synthesis of fused chromone-thiopyran hybrid.

The thio-Claisen rearrangement has emerged as a versatile and atom-economical strategy for constructing sulfur-containing heterocycles. Seminal work by Majumdar and co-workers

demonstrated the utility of this rearrangement in assembling fused thiophene and thiopyran systems from *S*-allyl and *S*-propargyl ethers,[12–14] inspiring efforts to extend this approach to 4-hydroxythiocoumarin for the synthesis of chromono-thiophene and chromono-thiopyran hybrids (**Scheme 3.5**). However, systematic studies on the reactivity of 4-hydroxythiocoumarin in this context, including substrate scope, mechanistic understanding, and solvent effects, remain lacking.

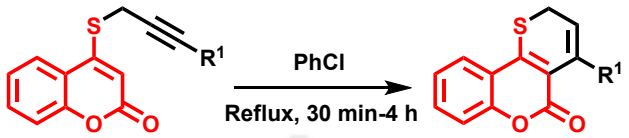

Tetrahedron Lett. **2002**, *43*, 2115–2117

Scheme 3.5: Thio-Claisen rearrangement of *S*-propargyl ethers.

Recent advances in computational chemistry have enabled a deeper mechanistic understanding of rearrangement reactions, yet such studies are rarely integrated with experimental protocol development for these fused systems. Therefore, there remains a significant gap in both methodological innovation and mechanistic insight for the synthesis of fused chromono-thiophene and chromono-thiopyran hybrids.

3.2.2 Present Strategy

Building on the advantages of the thio-Claisen rearrangement and previous literature reports, we employed this strategy for the synthesis of fused chromono-thiophene (**3F1**–**3F15**) and chromono-thiopyran derivatives (**3G1**–**3G14**), as outlined in **Scheme 3.6**.

3.3 Research Objectives

The overarching aim of this chapter is to develop a practical, efficient, and green synthetic methodology for accessing fused chromono-thiophene and chromono-thiopyran derivatives from 4-hydroxythiocoumarin. The specific objectives of this research are as follows:

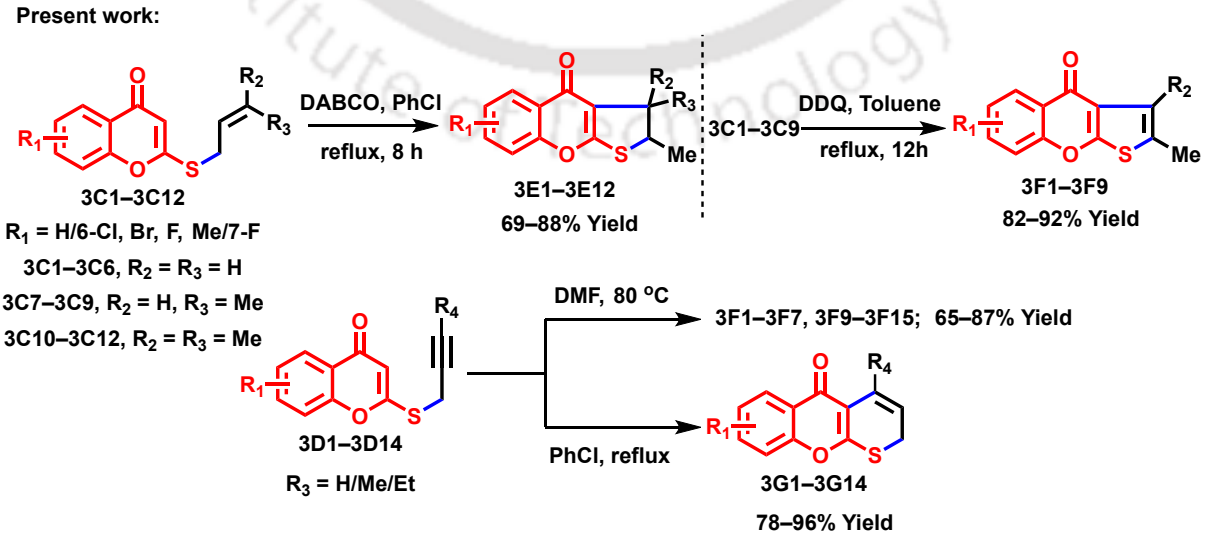

Scheme 3.6: Present work.

1. To systematically investigate the reactivity pattern of 4-hydroxythiocoumarin and to compare its behavior with that of 4-hydroxycoumarin and 4-hydroxydithiocoumarin, particularly in the context of alkylation and subsequent rearrangement reactions.
2. To synthesize a diverse array of *S*-allyl and *S*-propargyl ethers as key precursors.
3. To establish and optimize thio-Claisen rearrangement conditions for these *S*-alkylated ethers, with the goal of achieving efficient and selective cyclization to fused chromono-thiopyran and chromono-thiophene products.
4. To explore the influence of reaction parameters, including solvent, temperature, and catalyst, on the selectivity and outcome of the rearrangement, with particular attention to solvent-dependent product formation.
5. To expand the substrate scope by employing a variety of substituted 4-hydroxythiocoumarins and alkylating agents, thereby assessing the generality and limitations of the developed methodology.
6. To elucidate the mechanisms underlying the observed transformations through experimental studies and Density Functional Theory (DFT) calculations, providing insight into the roles of nucleophilic catalysts and solvent effects.
7. To evaluate the developed protocols against green chemistry principles, aiming for high atom economy, operational simplicity, and minimal environmental impact.
8. To thoroughly characterize all new compounds using spectroscopic techniques such as NMR, IR, HRMS and, where appropriate, single-crystal X-ray diffraction.

> **Note:** By addressing these objectives, this work seeks to provide a comprehensive and sustainable approach to the synthesis and mechanistic understanding of fused chromono-thiophene and chromono-thiopyran frameworks from 4-hydroxythiocoumarin.

3.4 Results and Discussion

3.4.1 Synthesis of Precursors

The synthesis of key precursors for the construction of fused chromono-thiophene and chromono-thiopyran derivatives commenced with the preparation of various *S*-alkylated 4-hydroxythiocoumarin derivatives.

Regioselective *S*-alkylation was achieved by reacting the six previously synthesized 4-hydroxythiocoumarins (**1A1**–**1A6**) with a range of allyl and propargyl bromides in the presence of potassium carbonate (K_2CO_3, 2 equiv) in anhydrous acetone at room temperature. This protocol afforded the corresponding *S*-allyl (**3C1**–**3C6**) and *S*-propargyl (**3D1**–**3D6**) ethers in good yields. Notably, alkylation occurred exclusively at the thione sulfur atom, with no evidence of *O*-alkylation at the 4-hydroxyl position. This selectivity highlights the higher

nucleophilicity of the sulfur atom in 4-hydroxythiocoumarin, distinguishing its reactivity from that of 4-hydroxycoumarin, which typically undergoes *O*-alkylation under similar conditions.

Table 3.1: Synthesis of *S*-allyl and *S*-propargyl chromene-4-one derivatives.[a][b]

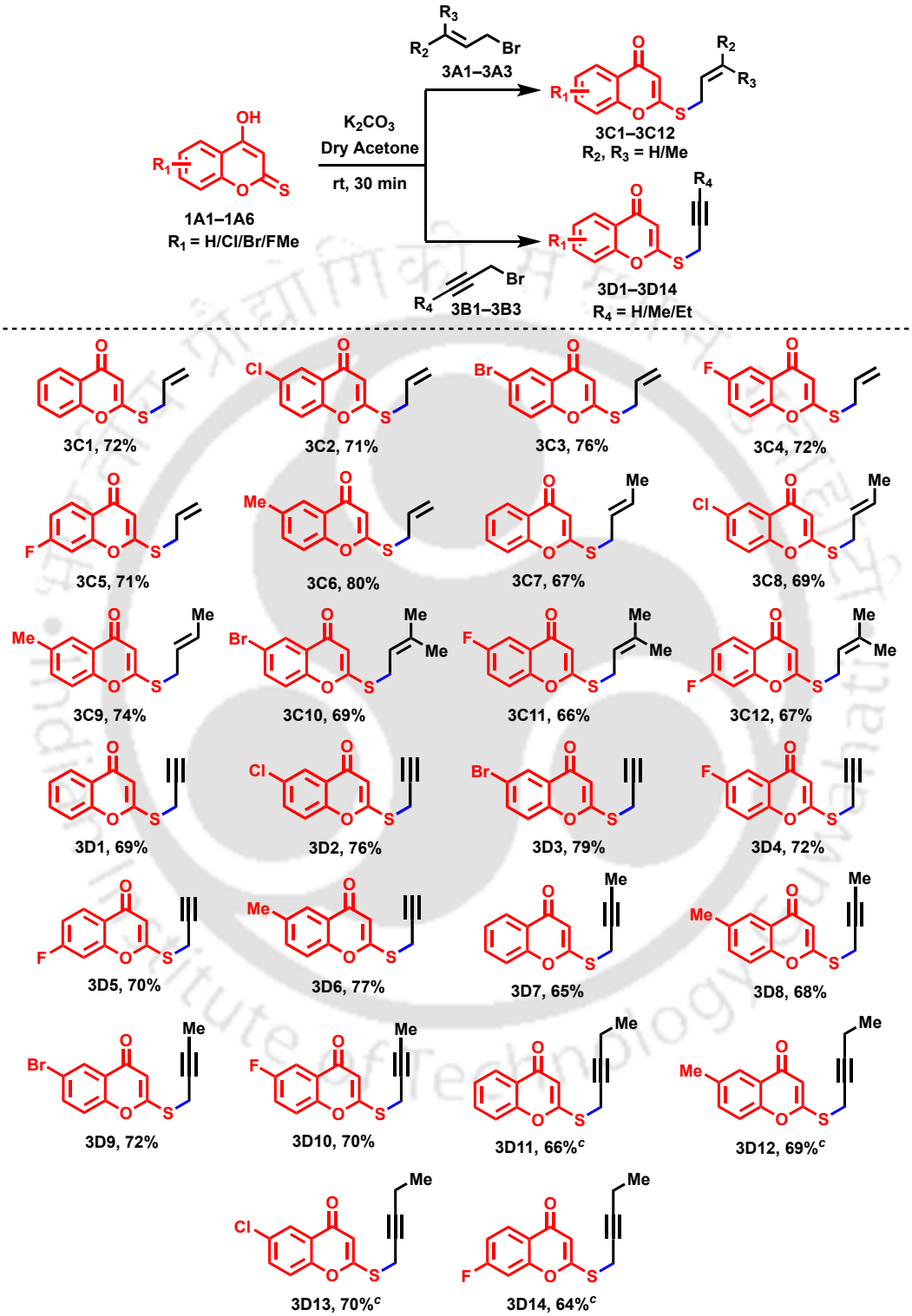

[a]**Reagents and conditions:** 4-hydroxythiocoumarin (1 equiv), allyl/propargyl bromide (1.2 equiv), and K_2CO_3 (2 equiv) in acetone, stirred at rt, 30 min. [b]Isolated yields are provided. [c]Carried out at 0 °C.

Various substituted allyl and propargyl bromides were employed to further diversify the precursor pool, enabling access to a broad array of *S*-ethers (**Table 3.1**). For more sensitive substrates, reactions were performed at 0 °C, while all other conditions remained unchanged (**Table 3.1**, entries **3D11**–**3D14**).

This efficient and regioselective approach to *S*-alkylated 4-hydroxythiocoumarin derivatives provided a robust platform for subsequent thio-Claisen rearrangement studies, enabling systematic exploration of fused chromono-thiophene and chromono-thiopyran construction.

3.4.2 Optimization of Thio-Claisen Rearrangement Conditions for *S*-Allyl Ethers

A systematic optimization of the thio-Claisen rearrangement was undertaken for the *S*-allyl ethers of 4-hydroxythiocoumarins to achieve efficient cyclization to fused chromono-2-methyl-2,3-dihydrothiophene derivatives. The optimization strategy focused on identifying the most suitable catalyst, temperature, and solvent to maximize yield and selectivity.

Initial evaluation of thermal conditions: The model substrate, *S*-allyl ether **3C1**, was first subjected to thermal rearrangement in chlorobenzene at reflux without any catalyst. Under these conditions, only trace amounts of the desired cyclized product **3E1** were obtained, accompanied by significant formation of polymeric byproducts (**Table 3.2**, entry **1**). This highlighted the need for catalytic assistance to promote the rearrangement efficiently.

Catalyst screening: Based on literature precedents for nucleophile-assisted thio-Claisen rearrangements,[15] a variety of nucleophilic catalysts were screened. Triethylamine (10 mol%) in chlorobenzene at reflux and at 150 °C provided moderate conversion, but the yield remained suboptimal (**Table 3.2**, entries **2** and **3**). The introduction of 1,4-diazabicyclo[2.2.2]octane (DABCO) (10 mol%) as a catalyst markedly improved, affording the cyclized product in 82% yield after 8 h (**Table 3.2**, entry **4**). Increasing the DABCO loading to 15 – 20 mol% did not result in further yield enhancement, while lowering the catalyst loading to 5 mol% led to diminished conversion (**Table 3.2**, entries **6,7,** and **8**). Imidazole as a catalyst also promoted the rearrangement but gave slightly lower yields than DABCO (**Table 3.2**, entry **5**). These results established DABCO (10 mol%) as the optimal catalyst for this transformation.

Solvent and Temperature Effects: The choice of solvent was found to be critical for both yield and feasibility. Chlorobenzene at reflux provided the best results, while lowering the temperature to 100 °C significantly reduced the yield (**Table 3.2**, entry **9**). Attempts to conduct the reaction in polar aprotic solvents such as DMF resulted in no product formation (**Table 3.2**, entry **10**).

Summary: Thus, the optimized conditions for the thio-Claisen rearrangement of *S*-allyl ethers of 4-hydroxythiocoumarins involve the use of DABCO (10 mol%) in chlorobenzene at reflux for 8 h, which consistently afforded the desired cyclized product in high yield with minimal byproduct formation.

Table 3.2: Optimization of the reaction condition.[a]

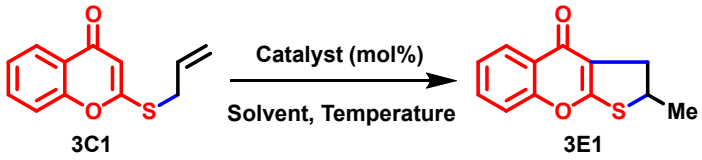

3C1 3E1

Entry	Catalyst (mol%)	Solvent	Temp (°C)	Time (h)	3E1 (%Yield)[b]
1	None	PhCl	Reflux	24	Traces[c]
2	NEt_3(10)	PhCl	Reflux	24	58
3	NEt_3(10)	PhCl	150	24	71
4	**DABCO (10)**	**PhCl**	**Reflux**	**8**	**82**
5	Imidazole (10)	PhCl	Reflux	24	77
6	DABCO (15)	PhCl	Reflux	8	84
7	DABCO (20)	PhCl	Reflux	8	84
8	DABCO (5)	PhCl	Reflux	8	61
9	DABCO (10)	PhCl	100	24	46
10	DABCO (10)	DMF	130	24	NR[d]

[a]Reactions were carried out using *S*-allyl chromene-4-one, **3C1** (1 equiv). [b]Isolated Yield. [c]Some polymeric product obtained. [d]NR= No Reaction.

3.4.3 Extension to Substrate Scope

The optimized conditions were successfully applied to a series of *S*-allyl ethers (**3C1**–**3C12**) derived from various substituted 4-hydroxythiocoumarins and allyl bromides, consistently affording the corresponding fused chromono-2,3-dihydrothiophene derivatives (**3E1**–**3E12**) in good to excellent yields (see **Table 3.3**).

Conversion of fused chromono-2-methyl-2,3-dihydrothiophenes to chromono-2-methylthiophenes *via* DDQ oxidation

The partially saturated chromono-2-methyl-2,3-dihydrothiophenes (**3E1**–**3E9**) obtained *via* thio-Claisen rearrangement of *S*-allyl ethers were oxidized to the corresponding aromatic chromono-2-methylthiophenes (**3F1**–**3F9**) using 2,3-dichloro-5,6-dicyano-1,4-benzoquinone (DDQ). Yields ranged from 82–92%, and functional groups on the chromone ring were well-tolerated (**Table 3.4**).

Table 3.3: Synthesis of fused chromono-2-methyl-2,3-dihydrothiophenes.[a][b]

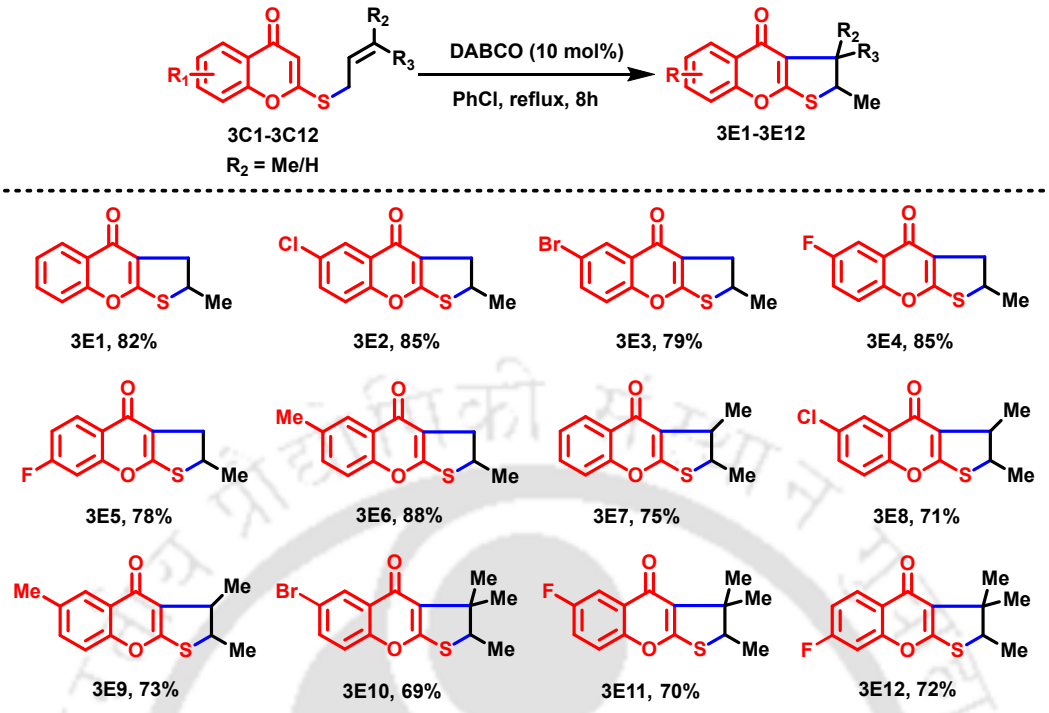

[a]**Reagents and conditions:** 6/7-substituted *S*-allyl chromene-4-ones (1 equiv), and DABCO (10 mol%) in chlorobenzene, stirred at reflux, 8 h. [b]Isolated yields are provided.

Table 3.4: Synthesis of fused chromono-2-methylthiophene derivatives.[a][b]

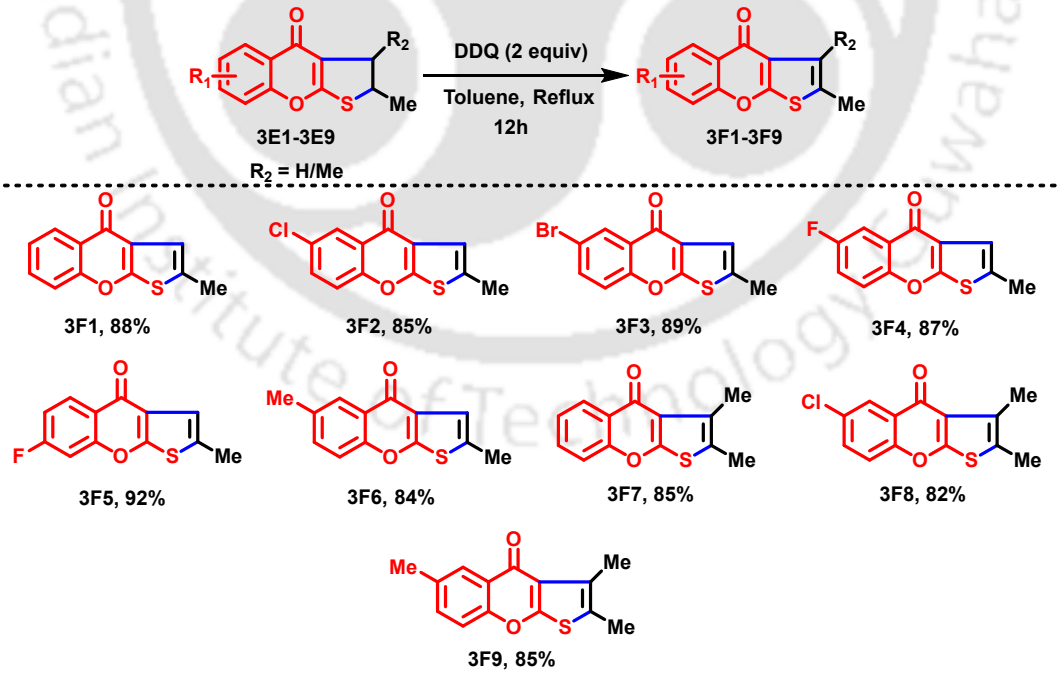

[a]**Reagents and conditions:** 6/7-substituted fused chromono-2-methyl-2,3-dihydrothiophene (1 equiv), and DDQ (2 equiv) in toluene, stirred at reflux, 12 h. [b]Isolated yields are provided.

3.4.4 Optimization of Thio-Claisen Rearrangement Conditions for *S*-Propargyl Ethers

A systematic optimization was conducted to establish efficient and selective conditions for the thio-Claisen rearrangement of *S*-propargyl ethers of 4-hydroxythiocoumarin, aiming to maximize yield and control product selectivity, particularly due to solvent-dependent outcomes observed in preliminary studies.

Initial trials and solvent screening: The model *S*-propargyl ether **3D1** underwent thio-Claisen rearrangement under various solvent conditions (**Table 3.5**). In nonpolar aromatic solvents like toluene (**Table 3.5**, entry **1**) and chlorobenzene (**Table 3.5**, entry **2**), reflux conditions led to exclusive formation of the chromono-thiopyran **3G1** in good to excellent yields (70 % and 94 %, respectively). In contrast, polar aprotic solvents such as DMF (**Table 3.5**, entry **4**) and Dimethyl Sulfoxide (DMSO) (**Table 3.5**, entry **5**) favored the formation of the chromono-2-methylthiophene **3F1**, with DMF giving the best result (83%). Solvents of intermediate polarity or protic nature, THF (**Table 3.5**, entry **6**), MeCN (**Table 3.5**, entry **7**), ethanol (**Table 3.5**, entry **8**), and dioxane (**Table 3.5**, entry **9**) led to incomplete conversion or product mixtures, reducing both selectivity and yield.

Table 3.5: Optimization of the reaction condition.[a]

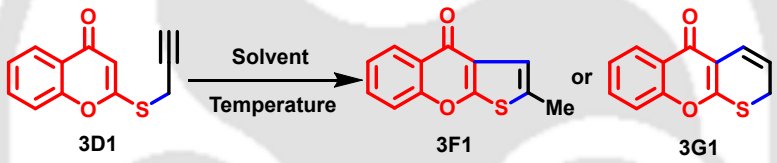

Entry	Solvent	Temp (°C)	Time (h)	3F1(%Yield)[b]	3G1(%Yield)[b]
1	Toluene	Reflux	8	0	70
2	**PhCl**	**Reflux**	**7**	**0**	**94**
3	PhCl	100	7	0	73
4	DMF	100	16	76	0
5	DMSO	100	16	62	0
6	THF	Reflux	16	0	35
7	MeCN	Reflux	16	0	54
8	EtOH	Reflux	16	16	48
9	Dioxane	Reflux	8	18	60
10	**DMF**	**80**	**16**	**83**	**0**
11	DMF	60	24	73	0

[a]Reactions were carried out using *S*-propargyl chromene-4-one, **3D1** (1 equiv). [b]Isolated Yield.

Temperature and reaction time optimization: For fused-thiopyran **3G1** formation in chlorobenzene (**Table 3.5**, entry **2**), reflux at ~132 °C for 7 h was optimal. Lowering the temperature (**Table 3.5**, entry **3**) resulted in incomplete conversion and reduced yield. For selective fused-thiophene **3F1** formation in DMF, 80 °C for 16 h (**Table 3.5**, entry **10**) gave the best outcome. Further reduction to 60 °C (**Table 3.5**, entry **11**) caused a marked decline in yield, indicating the necessity of moderately elevated temperatures for efficient rearrangement in polar aprotic media.

Summary: The optimized conditions for selective formation of the chromono-thiopyran **3G1** involved heating the *S*-propargyl ether in chlorobenzene at reflux ~132 °C for 7 h, whereas selective formation of the chromono-2-methylthiophene **3F1** was best achieved in DMF at 80 °C for 16 h.

Insight: The observed solvent-driven selectivity is unprecedented for thio-Claisen rearrangements of this type. Accessing two distinct fused heterocycles from a common precursor by merely changing the solvent offers a simple yet powerful route for divergent synthesis. This level of solvent control has not been reported for related systems and significantly enhances the method's synthetic utility.

3.4.5 Substrate Scope and Limitations

With the optimized solvent-controlled protocols in hand, the scope and limitations of the thio-Claisen rearrangement of *S*-propargyl ethers were evaluated (**Table 3.6** and **Table 3.7**).

Table 3.6: Synthesis of fused chromono-2-methylthiophene derivatives.[a][b]

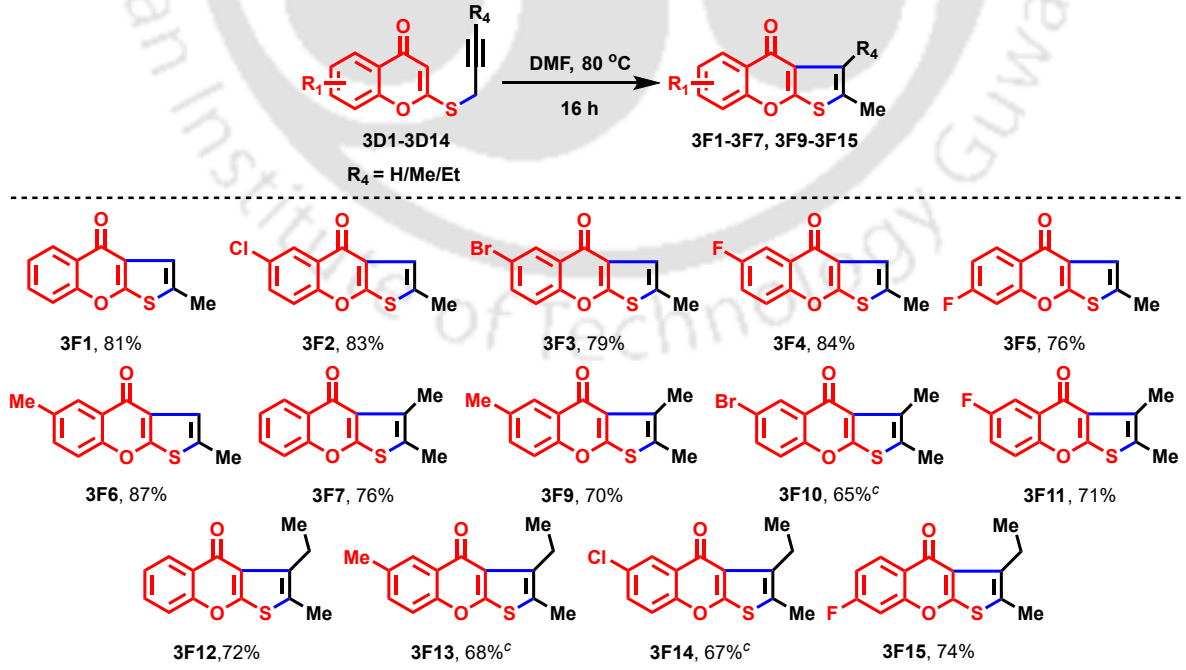

[a]**Reagents and conditions:** 6/7-substituted *S*-propargyl chromene-4-ones (1 equiv), in DMF (1 ml), stirred at 80 °C, 16 h. [b]Isolated yields are provided. [c]Carried out at 120 °C

Substituent effects: *S*-propargyl ethers with various substituents on the chromone ring including electron-donating (–Me, –OMe) or electron-withdrawing (–Cl, –Br, –F), reacted smoothly. Both unsubstituted and alkyl-substituted propargyl groups also rearranged efficiently. In DMF at 80 °C, fused-thiophenes (**3F1**–**3F15**) formed in 65 – 87 % yield; chlorobenzene reflux yielded fused-thiopyrans (**3G1**–**3G14**) in 78 – 96 %, all with high selectivity and minimal side products.

Table 3.7: Synthesis of fused chromono-thipyran derivatives.[a][b]

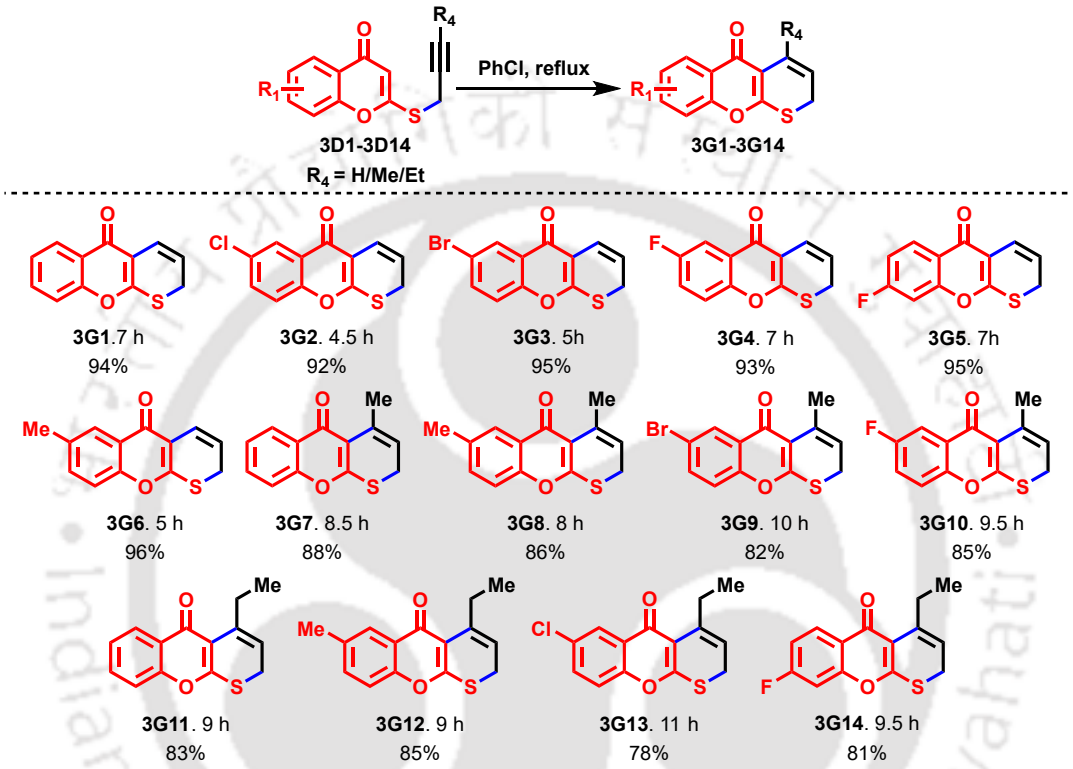

[a]**Reagents and conditions:** 6/7-substituted *S*-propargyl chromene-4-ones (1 equiv), in chlorobenzene (1 ml), stirred at 132 °C. [b]Isolated yields are provided.

Limitations: Substrates with strong electron-withdrawing groups showed slightly reduced yields, possibly due to lower sulfur nucleophilicity. Bulky propargyl groups led to incomplete conversion, indicating steric sensitivity.

3.4.6 Synthesis of Fused Chromono-2,2-dimethyl-thiopyran Derivatives

With the successful development of solvent-dependent thio-Claisen rearrangements for *S*-allyl and *S*-propargyl ethers, attention was turned to the synthesis of fused chromono-2,2-dimethyl-thiopyran derivatives, an important subclass featuring additional substitution at the 2-position of the thiopyran ring.

Reaction design and optimization: Initial attempts to access 2,2-dimethyl-substituted thiopyrans *via* direct propargylation of 4-hydroxythiocoumarin with 3-chloro-3-methylbut-1-yne failed to produce isolable products. Based on literature precedent for thioether formation from tertiary alcohols,[16] a revised approach was attempted: reacting 4-hydroxythiocoumarin

with 2-methylbut-3-yn-2-ol (**3H1**) using 10 mol% *p*-TSA in nitromethane at room temperature, which also did not yield the desired product (**Scheme 3.7**).

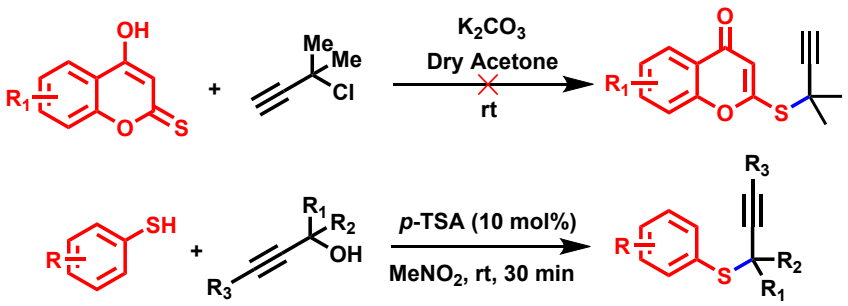

J. Org. Chem., 2021, **86** , 7078–7091

Scheme 3.7: Synthesis of *S*-tert-propargyl-4*H*-chromen-4-one: Initial challenge and revised strategy.

Reaction outcome and scope: Raising the temperature to 80 °C, while keeping other conditions unchanged, converted 4-hydroxythiocoumarin (**1A1**) and 2-methylbut-3-yn-2-ol (**3H1**) smoothly through a one-pot sequence of substitution, thio-Claisen rearrangement, and cyclization, giving fused chromono-2,2-dimethyl-thiopyrans **3I1**–**3I6** in good yields across diverse substrates (**Table 3.8**).

This acid-catalyzed, operationally simple protocol complements the earlier solvent-controlled Claisen methodology and broadens access to chromone-thiopyran hybrids with new substitution patterns.

Table 3.8: Synthesis of fused chromono-2,2-dimethyl-thiopyran derivatives.[a][b]

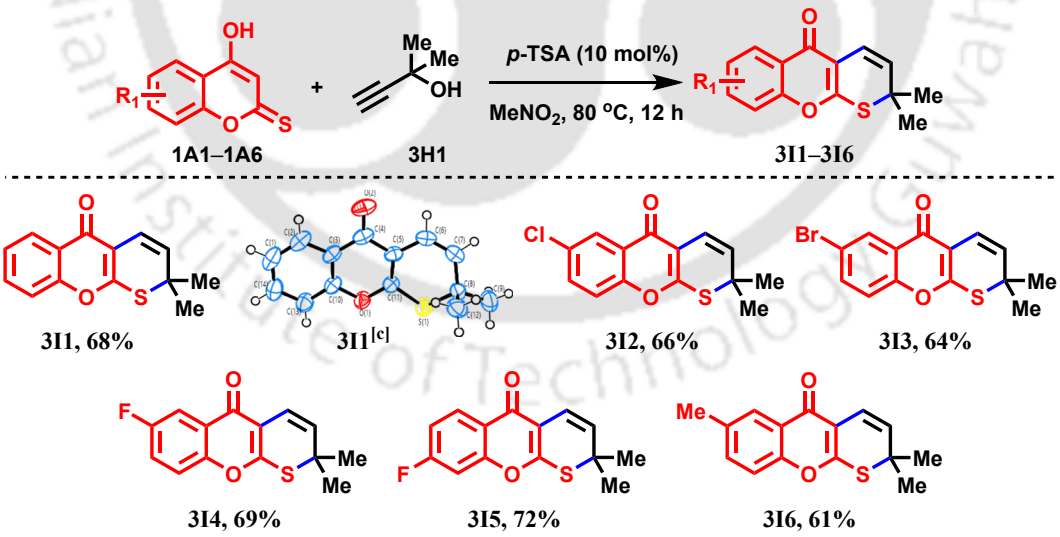

[a]**Reagents and conditions:** 4-hydroxythiocoumarin (1 equiv), 2-methylbut-3-yn-2-ol (1.2 equiv), and *p*-TSA in nitromethane (1 ml), stirred at 80 °C. [b]Isolated yields are provided. [c]ORTEP diagram of **3I1**. CCDC 2266735.

3.4.7 Stepwise Mechanism for the Synthesis of Fused Chromono-2-methyl-2,3-dihydrothiophenes

The transformation of *S*-allyl ethers of 4-hydroxythiocoumarin into fused chromono-2-methyl-2,3-dihydrothiophenes proceeds *via* a nucleophile-assisted thio-Claisen rearrangement. As supported by experimental observations and literature precedent,[15] the mechanistic pathway is outlined below (**Scheme 3.8**).

Step 1- Nucleophile-assisted C—S bond activation: In the initial stage, the nucleophile (DABCO) approaches the allylic carbon from the rear, donating into the C—S σ* orbital. Electron flow toward sulfur generates a 2*p* orbital on the allylic carbon that couples with the adjacent 2*p* orbital to form a new C=C bond, yielding intermediate **A** and regenerating free DABCO.

Step 2- Tautomerization: Intermediate **A** then undergoes tautomerization to generate an enethiol intermediate **B**.

Step 3- Cyclization: The thiol sulfur in **B** attacks the electron-deficient C=C double bond of the chromone core in 5-*exo*-*trig* fashion, leading to ring closure and formation of the fused chromono-2-methyl-2,3-dihydrothiophene.

Role of DABCO: Acting first as a nucleophile and then as a base, DABCO promotes all three stages of the mechanism.

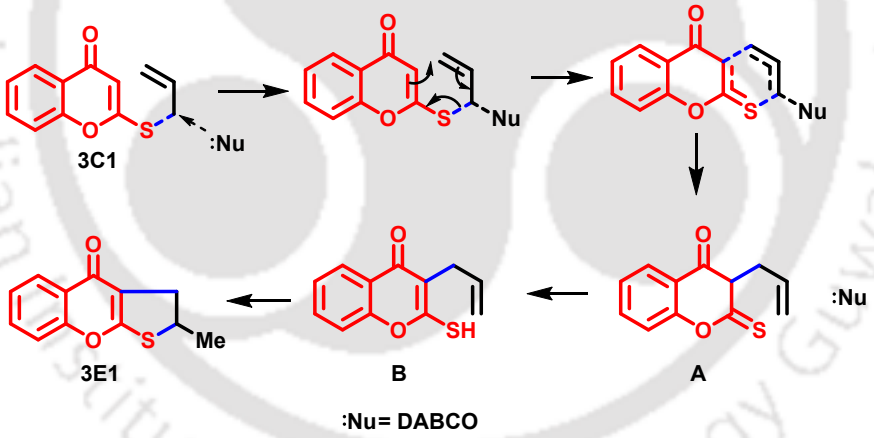

Scheme 3.8: Proposed mechanism for the synthesis of fused chromono-2-methyl-2,3-dihydrothiophene derivatives (**3E1**–**3E12**).

DFT studies and further mechanistic analysis are discussed in later sections

Summary: The mechanism utilizes nucleophile-assisted thio-Claisen rearrangement to efficiently construct sulfur-containing heterocycles with high atom economy.

3.4.8 Mechanistic Elucidation: Solvent-Dependent Formation of Fused Chromono-thiopyran and Chromono-2-methylthiophene

The thio-Claisen rearrangement of *S*-propargyl ethers of 4-hydroxythiocoumarin exhibits a remarkable and unprecedented solvent-dependent selectivity, yielding either fused chromono-

thiopyran or chromono-2-methylthiophene frameworks depending on the reaction medium. The stepwise mechanistic rationale for these divergent outcomes is summarized below (**Scheme 3.9**).

Step 1- [3,3]-Sigmatropic rearrangement and allene formation: Both product pathways begin with a thio-Claisen rearrangement of the *S*-propargyl ether, which forms an allenyl thione intermediate (**C**). This intermediate serves as the pivotal branching point for the reaction.

Step 2A- Pathway to chromono-2-methylthiophene (3F1) in polar aprotic solvents (Pathway A):

- In polar aprotic solvents such as DMF, the nitrogen atom of the solvent acts as a base, abstracting a proton from the intermediate **C**,[17] resulting in the formation of an anionic allenyl sulfide intermediate (**D**).
- This anionic species then undergoes an intramolecular 5-*exo*-*trig* cyclization, leading to the closure of the five-membered thiophene ring, giving the fused chromono-2-methylthiophene (**3F1**), isolated in high yield.

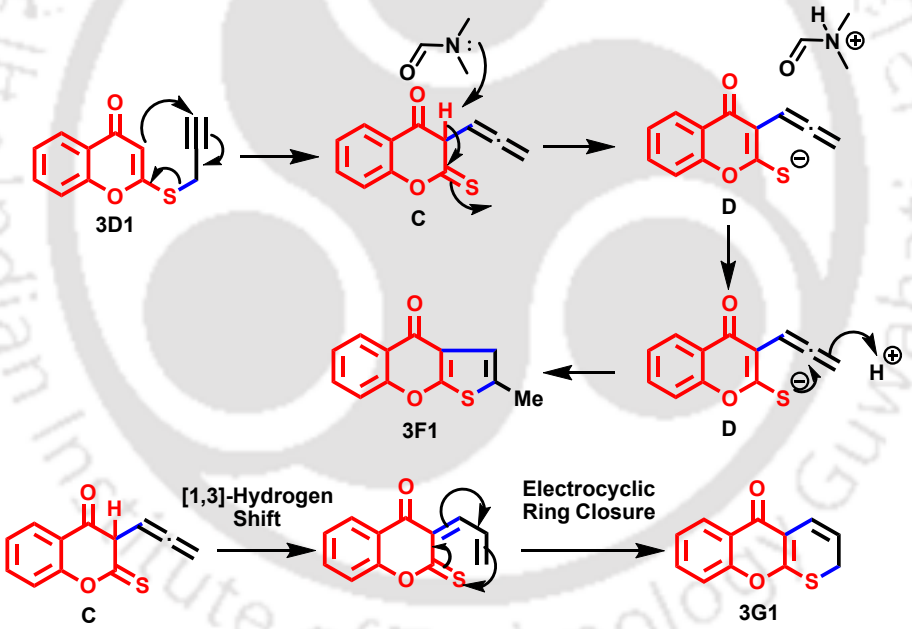

Scheme 3.9: Proposed mechanism for the synthesis of fused chromono-2-methylthiophene (**3F1**–**3F14**) and -thiopyran derivatives (**3G1**–**3G14**).

Step 2B: Pathway to Chromono-thiopyran (3G1) in Nonpolar Aromatic Solvents (Pathway B)

- In nonpolar aromatic solvents, instead of deprotonation of intermediate **C**, a 1,3-hydrogen shift occurs, moving a proton from the terminal position of the allene to the central carbon, generating a new intermediate.
- This intermediate then undergoes electrocyclic ring closure, forming the six-membered thiopyran ring fused to the chromone core, yielding chromono-thiopyran **3G1**.

The proposed mechanisms are illustrated in **Scheme 3.9**

> **Insight:** This mechanistic insight not only rationalizes the observed product divergence but also highlights the critical influence of solvent environment in steering the outcome of the thio-Claisen rearrangement for *S*-propargyl ethers of 4-hydroxythiocoumarin.

3.4.9 DFT Calculations

Mechanistic insights into dihydrothiophene synthesis (*S*-Allyl ether rearrangement)

DFT calculations were performed at the B3LYP-D3/Def2-SVP level to elucidate the nucleophile-assisted thio-Claisen rearrangement of *S*-allyl ethers (**3C1**–**3C12**) to fused chromono-2-methyl-2,3-dihydrothiophenes (**3E1**–**3E12**). The study focused on the role of catalysts in lowering activation barriers for C—S bond cleavage.

Key findings:

Catalyst effects: DABCO significantly reduced the Gibbs free energy barrier ($\Delta G^{\ddagger}$ = 15.8 kcal mol^{-1})(**Figure 3.1a**) compared to triethylamine ($\Delta G^{\ddagger}$ = 20.6 kcal mol^{-1})(**Figure 3.1b**) and imidazole ($\Delta G^{\ddagger}$ = 20.2 kcal mol^{-1})(**Figure 3.1c**), aligning with experimental yields (82 % vs. 58 – 77 %).

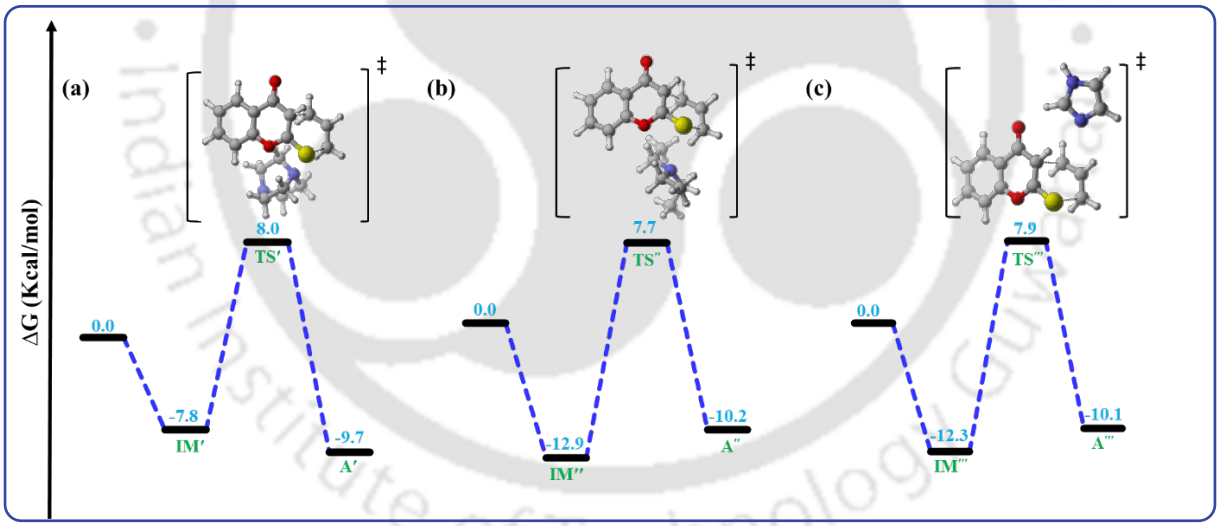

Figure 3.1: Reaction Gibbs free energy profile in the presence of (a) DABCO, (b) Triethylamine (NEt_3), and (c) Imidazole.

Advantages of using DABCO:

- **Balanced reactivity:** Offers an optimal balance of nucleophilicity and basicity, promoting efficient rearrangement.
- **Structural benefits:** The rigid, bicyclic framework minimizes steric hindrance and aids in stabilizing the six-membered transition state.

DFT studies validate the superior catalytic performance of DABCO.

Solvent-Dependent Pathways for Thiophene and Thiopyran Formation (*S*-Propargyl Ether Rearrangement)

DFT studies were conducted to rationalize the solvent-controlled divergence in product formation from *S*-propargyl ethers (**3D1**–**3D14**). Two distinct pathways were identified:

Pathway A–DMF: Fused chromono-thiophene formation (Figure 3.2a):

1. **Deprotonation:** DMF abstracts a proton from the allene intermediate (**C**), forming an anionic species (**D**) *via* **TSI** ($\Delta G^{\ddagger}$ = 17.9 kcal/mol).
   - Polar aprotic solvents stabilize **D** through weak ion-dipole interactions.
2. **Cyclization:** Intramolecular attack by sulfur yields thiophene (**3F1**) *via* **TSII** ($\Delta G^{\ddagger}$ = 37.3 kcal/mol).

> **Insight:** The first transition state involves proton abstraction by the nitrogen atom of DMF, forming an ion-pair-like structure. While a similar interaction *via* the oxygen center is conceivable, DFT calculations suggest that the associated ring-closure barrier is significantly higher, disfavoring this pathway.

Pathway B–Chlorobenzene: fused chromono-thiopyran formation (Figure 3.2b):

1. **1,3-Hydrogen Shift:** Allene undergoes a 1,3-hydrogen shift to intermediate $\mathbf{I^H}$ *via* **TSIII** ($\Delta G^{\ddagger}$ = 49.3 kcal/mol).
   - Nonpolar solvents favor neutral intermediates and viable under the reaction conditions (132 °C).
2. **Electrocyclic closure:** $\mathbf{I^H}$ cyclizes to thiopyran (**3G1**) *via* **TSIV** ($\Delta G^{\ddagger}$ = 12.6 kcal/mol).

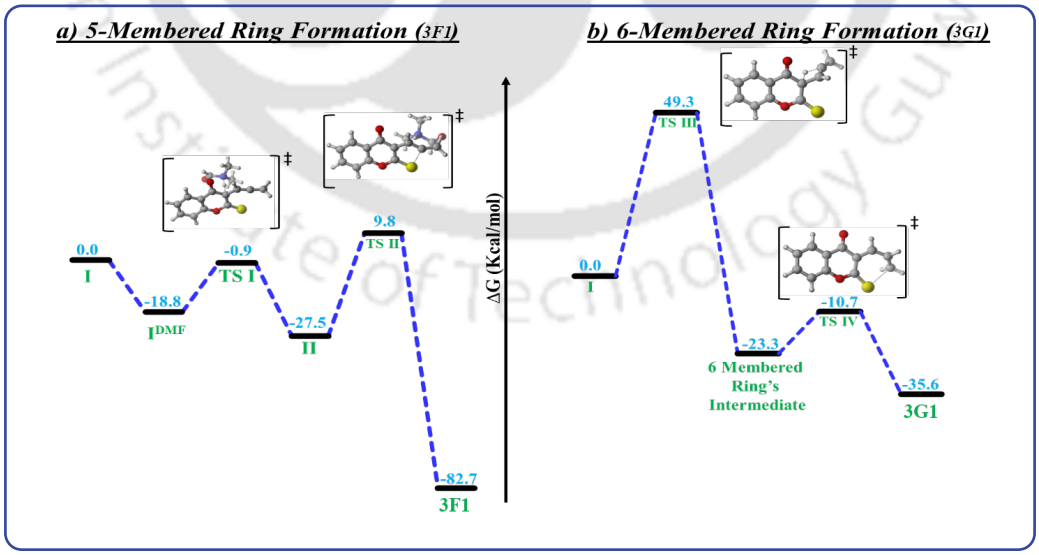

Figure 3.2: Computed free energy profile (ΔG, kcal mol^{-1}) for the formation of (a) **3F1**, and (b) **3G1**. Selected transition states are shown in the panel.

Insight: The calculations confirmed that the solvent environment alters the relative energy barriers, making **Pathway A** kinetically favored in DMF and **Pathway B** thermodynamically favored in chlorobenzene.

3.4.10 Effects of Solvent and Base on The Thio-Claisen Rearrangement: Mechanistic Insights into Thiophene Formation

Experimental design and rationale

To delineate the precise role of DMF in the formation of fused chromono-2-methylthiophene (**3F1**) from *S*-propargyl ether (**3D1**), a series of control experiments were conducted (**Scheme 3.10**). The primary objective was to determine whether the unique reactivity observed in DMF could be replicated in other solvents by the addition of an external base, and to clarify whether DMF's effect was purely basic or also involved specific solvation phenomena.

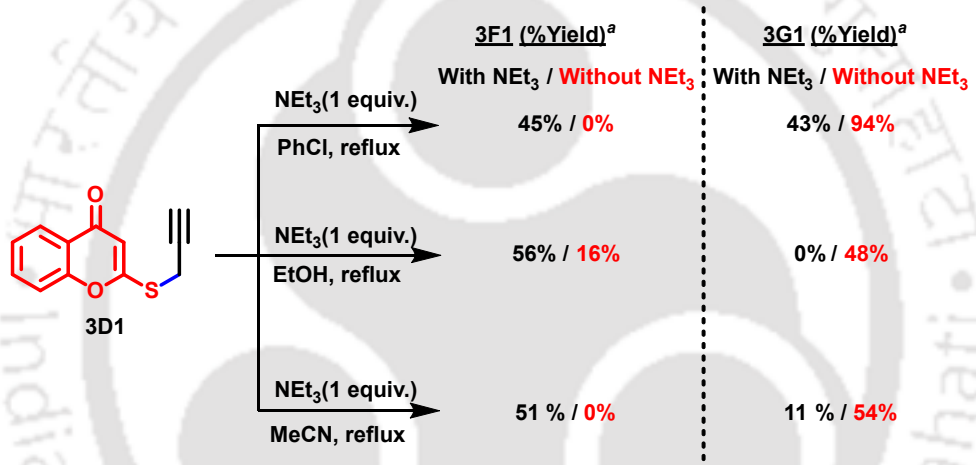

Scheme 3.10: Mechanistic insights into the formation of **3F1**: effects of solvent and base.

Influence of base addition in various solvents

The addition of triethylamine to solvents other than DMF resulted in a marked increase in the formation of **3F1**. This observation confirms that a basic environment, whether provided by DMF or an added base, facilitates the deprotonation of the allene intermediate, thereby promoting the formation of the anionic intermediate **D** (Scheme 3.9), required for cyclization leading to fused-thiophene product **3F1**. However, even with the base present, the selectivity for **3F1** was incomplete, and the overall conversion was lower compared to reactions performed in DMF. This indicates that while proton abstraction is necessary, it is not the sole determinant of the product outcome.

Role of solvent polarity and solvation

A critical finding from these studies is that DMF's role extends beyond simple proton abstraction. As a polar aprotic solvent, DMF is capable of stabilizing the negatively charged intermediate (**D**) through ion-dipole and dipole-dipole interactions.[18] This moderate solvation is sufficient to stabilize the transition state and facilitate smooth progression to **3F1**, without excessively stabilizing the anion and hindering further reactivity.

In contrast, polar protic solvents such as ethanol provide strong solvation through hydrogen-bonding,[19] which over-stabilizes the anionic intermediate and suppresses its further transformation, resulting in poor yields of **3F1**. Nonpolar solvents like chlorobenzene or toluene lack the necessary polarity to stabilize the anionic intermediate, thereby disfavoring the thiophene pathway and instead favoring formation of the alternative product, **3G1** (fused-thiopyran).

Although a polar aprotic solvent, Acetonitrile is less effective than DMF at stabilizing the anionic intermediate, leading to incomplete conversion. This underscores the unique balance of basicity and solvation provided by DMF.

Mechanistic interpretation

The collective results indicate that DMF's dual function, as both a base and a moderate stabilizer of the anionic intermediate, is essential for the efficient and selective formation of **3F1**.

- **Basicity** is required for initial proton abstraction from the allene intermediate.
- **Appropriate solvation** is necessary to stabilize the anionic intermediate without impeding its subsequent cyclization.

Only DMF provides the optimal environment for both steps.

> **Insight:** DMF's unique combination of basicity and moderate solvation enables selective, high-yield synthesis of **3F1**, underscoring the interdependence of solvent effects and the reaction pathway in the current protocol.

3.4.11 Mechanistic Insights: Synthesis of Fused Chromono-2,2-dimethyl-thiopyran Derivatives (3I1–3I6)

The synthesis of fused chromono-2,2-dimethyl-thiopyran derivative (**3I1**–**3I6**) proceeds *via* a stepwise mechanism outlined below:

Step 1: Tertiary carbocation formation: *p*-TSA catalyzes the dehydration of 2-methyl-but-3-yn-2-ol (**3H1**) in nitromethane at 80 °C, forming a stabilized tertiary carbocation.

Step 2: Nucleophilic *S*-alkylation: The sulfur atom of 4-hydroxythiocoumarin acts as a nucleophile, attacking the carbocation to form the corresponding *S*-alkylated intermediate, installing the propargyl unit bearing two methyl groups at the sulfur position.

Step 3: Thio-Claisen Rearrangement: A [3,3]-sigmatropic rearrangement shifts the propargyl group, generating an allene intermediate tethered to the chromone ring.

Step 4: 1,3-Hydrogen shift and ring closure: The allene undergoes a 1,3-hydrogen shift, followed by electrocyclic closure, forming the fused thiopyran system.

The reaction integrates S_N1 substitution, sigmatropic rearrangement, and pericyclic closure in one pot.

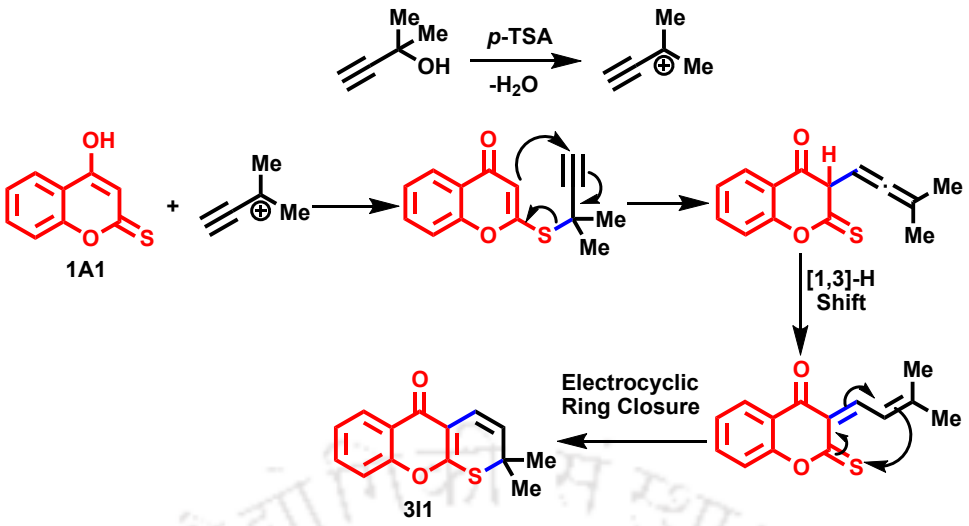

Scheme 3.11: Proposed mechanism for the synthesis of fused chromono-2,2-dimethyl-thiopyran derivatives (**3I1-3I6**).

3.4.12 Product Characterization and Structural Analysis

All synthesized compounds were thoroughly characterized using ^{1}H and ^{13}C NMR, IR, HRMS, and, where applicable, single-crystal X-ray diffraction. The key analytical findings for each class of compounds, using representative substrates (**3C1**, **3D1**, **3E1**, **3F1**, **3G1,** and **3I1**), are summarized below.

***S*-Allyl and *S*-propargyl ethers (3C1–3C12, 3D1–3D14)**

- The ^{1}H NMR spectra of *S*-allyl ethers display characteristic peaks, including vinylic protons between 5.98 – 5.87 ppm, distinct doublets at 5.22 and 5.35 ppm corresponding to the *cis* and *trans* protons, respectively, and a methylene doublet at 3.71 ppm adjacent to sulfur, confirming successful allylation.
- *S*-Propargyl ethers are identified by a methylene doublet at 3.80 ppm (adjacent to sulfur) and a terminal alkyne proton triplet near 2.32 ppm, supporting the presence of the propargyl group.
- The ^{13}C NMR spectrum of **3C1** shows the allylic methylene carbon at 34.02 ppm, while **3D1** displays resonances at 72.88 and 77.20 ppm for the alkyne carbons and 19.67 ppm for the methylene carbon.
- IR spectra exhibit strong C=O stretches at 1635 cm^{-1} (**3C1**) and 1,637 cm^{-1} (**3D1**). Additionally, **3D1** shows characteristic alkyne stretches at 3274 cm^{-1} (C≡C−H) and 2121 cm^{-1} (C≡C).
- HRMS analysis shows $[M+H]^+$ or $[M+Na]^+$ ions in excellent agreement with calculated values, confirming their molecular formulas.

Fused Chromono-2-methyl-2,3-dihydrothiophenes (3E1–3E12)

- The ^{1}H NMR spectra consistently show a methyl doublet near 1.55 ppm, diastereotopic methylene protons at 2.98 and 3.43 ppm, and a methine proton at 4.11 ppm, supporting the formation of the dihydrothiophene ring.
- Aromatic protons appear in the $7.3 - 8.2$ ppm region, consistent with the chromone core.
- The ^{13}C NMR spectrum of **3E1** shows the methyl, methylene, and methine carbons at 22.9, 37.5, and 44.5 ppm, respectively, along with a carbonyl carbon at 172.9 ppm.
- IR spectra of **3E1** display a strong C=O stretch at 1636 cm^{-1} and aromatic C=C bands near 1461 and 1552 cm.
- HRMS for **3E1** ($C_{12}H_{10}NaO_2S$) yields an $[M+Na]^+$ ion at 241.0297, closely matching the calculated value of 241.0294.

Fused Chromono-2-methylthiophenes (3F1–3F14)

- ^{1}H NMR spectra show a methyl singlet around 2.49 ppm and aromatic signals in the $7.3 - 8.2$ ppm range, characteristic of the aromatic thiophene–chromone system.
- The ^{13}C NMR spectrum of **3F1** shows a methyl carbon at 15.6 ppm and expected aromatic carbon resonances.
- IR spectra exhibit a chromone C=O stretch at 1656 cm^{-1}.
- HRMS for **3F1** ($C_{12}H_9O_2S$) gives an $[M+H]^+$ ion at 217.0309, in excellent agreement with the calculated value of 217.0318.

Fused Chromono-thiopyrans (3G1–3G14)

- ^{1}H NMR spectra of **3G1** show a doublet of doublets at approximately 3.74 ppm for the methylene protons adjacent to sulfur, along with aromatic signals in the expected region.
- The ^{13}C NMR spectrum of **3G1** shows a methylene carbon at 27.8 ppm and a carbonyl carbon at 172 ppm.
- IR spectra of **3G1** display a C=O stretch at 1632 cm^{-1}, confirming the chromone core.
- HRMS for **3G1** ($C_{12}H_{10}O_2S$) shows an $[M+H]^+$ ion at 217.0308, closely matching the calculated value of 217.0318.

Fused Chromono-2,2-dimethyl-thiopyran Derivatives (3I1-3I6)

- ^{1}H NMR spectra for **3I1** display a singlet at 1.54 ppm integrating for six protons, confirming the presence of two methyl groups at the 2-position of the thiopyran ring.
- The ^{13}C NMR spectrum of **3I1** shows methyl carbon signals at 30.03 ppm and other signals consistent with the proposed thiopyran scaffold.
- IR spectra of **3I1** reveal a strong C=O stretch at 1637 cm^{-1}.

- HRMS for **3I1** ($C_{14}H_{12}NaO_2S$) yields an $[M+Na]^+$ ion at 267.0454, which closely matches the calculated value of 267.0450.
- Single-crystal X-ray diffraction of **3I1** unequivocally confirms the connectivity and regiochemistry of the fused chromono-2,2-dimethyl-thiopyran scaffold.

3.4.13 Evaluation of the Protocol Against Green Chemistry Principles

The synthetic approaches developed in this chapter demonstrate several green chemistry merits, but also present notable limitations that warrant discussion.

Strengths

- **Atom Economy:** The core thio-Claisen rearrangement and cyclization steps are highly atom-economical, with most reactant atoms incorporated into the final product.
- **Catalysts and Reagents:** The protocols employ catalytic quantities of inexpensive and metal-free catalysts such as DABCO and *p*-TSA, thereby avoiding transition metals and highly toxic reagents.
- **Operational Simplicity:** The protocols are concise, and the main bond-forming steps proceed in a single operation, minimizing the number of synthetic steps and the use of protecting groups.

Limitations and areas for improvement

- **Purification Requirements:** Most products require chromatographic purification on silica gel to achieve analytical purity. This increases solvent consumption and waste, detracting from the ideal of minimal waste generation and operational simplicity.
- **Solvent selection and environmental impact:** The use of chlorobenzene (for fused thiopyran synthesis) and DMF (for fused thiophene synthesis) is a significant limitation.
    - **Chlorobenzene** is a volatile, persistent, and environmentally problematic solvent, and its use at reflux (132 °C) entails considerable energy input and safety considerations.
    - **DMF** is toxic and not readily biodegradable, raising concerns about environmental persistence and health hazards.
    - **Nitromethane**, used for 2,2-dimethyl-thiopyran synthesis, is also of moderate toxicity and volatility.
    - While some steps use greener solvents (e.g., acetone, ethanol), the key selectivity and efficiency depend on less sustainable choices.
- **Energy efficiency:** The high-temperature conditions required for chlorobenzene-mediated reactions compromise energy efficiency.
- **Use of DDQ:** The two-step thiophene synthesis from *S*-allyl ethers involves DDQ, a toxic and non-sustainable oxidant. However, this is not required in the single-step protocol from *S*-propargyl ethers, which is a clear improvement.

- **Scalability and waste:** Although the reactions are robust and reproducible, the reliance on chromatography and non-green solvents could complicate scale-up and increase the environmental burden in large-scale applications.

3.4.14 Summary and Future Directions

These protocols exemplify efficient, metal-free, and atom-economical syntheses of diverse sulfur-containing heterocycles. However, their sustainability remains limited by factors such as solvent choice, purification requirements, and energy-intensive reaction conditions. To address these challenges and enhance the practical utility of the methods, future efforts should focus on:

1. Replacing problematic solvents with greener, more sustainable alternatives to minimize environmental impact.
2. Exploring simplified work-up and purification methods, such as selective precipitation or recrystallization, may reduce reliance on chromatography in specific cases, thereby improving overall process efficiency.
3. While reducing reaction temperatures may not be universally achievable due to mechanistic constraints, optimizing reaction conditions for milder setups where possible could incrementally improve energy efficiency.
4. Extending the scope of these protocols to access additional heterocyclic scaffolds or incorporate diverse substituents will further demonstrate their synthetic versatility.
5. Mechanistic studies, supported by advanced spectroscopic tools, can refine understanding of key bond-forming events and facilitate rational protocol modifications.
6. Preliminary exploration of the biological properties of the synthesized scaffolds may help identify potential functional applications, supporting broader relevance beyond synthetic novelty.

By balancing synthetic efficiency with environmental and operational considerations, these improvements will collectively enhance the sustainability, scalability, and overall impact of the developed methods.

3.5 Conclusion

In this chapter, a comprehensive and systematic approach to the synthesis of fused chromono-thiophene, chromono-thiopyran, and chromono-2,2-dimethyl-thiopyran derivatives was developed, using 4-hydroxythiocoumarin as a versatile starting material. The work established a series of regioselective and operationally straightforward protocols to access a diverse array of sulfur heterocycles.

A key discovery was the unprecedented and highly selective product control achieved through solvent modulation: polar aprotic solvents (e.g., DMF) favored the formation of fused chromono-2-methylthiophenes, whereas nonpolar aromatic solvents (e.g., chlorobenzene) led exclusively to chromono-thiopyrans. Mechanistic insights, supported by experimental results

and DFT calculations, underscored the role of solvent basicity and solvation in stabilizing key transition states and intermediates.

The protocols also enabled the synthesis of fused chromono-2-methyl-2,3-dihydrothiophenes *via* nucleophile-assisted rearrangement of *S*-allyl ethers and the construction of chromono-2,2-dimethyl-thiopyrans through an acid-catalyzed carbocation pathway. All new compounds were thoroughly characterized by NMR, IR, HRMS, and, where possible, X-ray crystallography, confirming their structures and purity.

From a green chemistry standpoint, the protocols exhibit high atom economy, metal-free catalysis, and concise synthetic routes. However, limitations persist, including the reliance on chromatographic purification, the use of environmentally concerning solvents (DMF, chlorobenzene, nitromethane), and elevated reaction temperatures, highlighting areas for further optimization.

Overall, this work advances the field of heterocyclic synthesis by providing efficient, selective, and mechanistically transparent routes to valuable sulfur-containing chromone derivatives. The solvent-controlled divergence demonstrated here not only expands the synthetic toolkit for constructing complex fused heterocycles but also sets the stage for future studies aimed at improving sustainability, broadening substrate scope, and exploring the functional and biological potential of these frameworks.

3.6 Experimental Section

This section details the procedures and analytical methods employed for the synthesis and characterization of the *S*-allyl and *S*-propargyl derivatives, as well as various fused chromono-2-methyl-2,3-dihydrothiophene, fused chromono-2-methylthiophene, and fused chromono-2-methyl-thiopyran derivatives described in this chapter. All chemicals and solvents were purchased from commercial suppliers and used as received unless otherwise specified. The syntheses of 4-hydroxythiocoumarin **1A1**, the key precursor and its derivatives, are described in **Chapter 1, Section 1B**.

General procedure for the synthesis of substituted *S*-allyl and *S*-propargyl thioethers (3C1-3C12 and 3D1-3D14)

To a stirred mixture of 4-hydroxythiocoumarin (**1A1**) (0.5 mmol, 1 equiv) and potassium carbonate (K_2CO_3, 1 mmol, 2 equiv) in anhydrous acetone (2 mL), allyl bromide (**3A1**) or propargyl bromide (**3B1**) (0.6 mmol, 1.2 equiv) was added dropwise at room temperature. The reaction mixture was stirred for 30 min and monitored by TLC. Upon completion, the acetone was evaporated, and the residue was extracted with ethyl acetate (15 mL), then washed with water (2 × 10 mL). The organic layer was dried over anhydrous Na_2SO_4 and concentrated under reduced pressure. The crude product was purified by silica gel (60–120 mesh) column chromatography (1:9 v/v ethyl acetate/hexane) to afford the pure *S*-allyl or *S*-propargyl thioethers, **3C1** and **3D1**, respectively. For derivatives **3C2**–**3C12** and **3D2**–**3D10**, the same procedure was followed. For **3D11**–**3D14**, the reaction was performed at 0 °C instead of room temperature to accommodate more sensitive substrates.

General procedure for the synthesis of fused chromono-2-methyl-2,3-dihydrothiophenes (3E1–3E12)

To a solution of *S*-allyl chromene-4-one (**3C1**, 0.15 mmol) in chlorobenzene (1 mL), DABCO (10 mol%) was added. The mixture was stirred at reflux for 8 h or until complete conversion (monitored by TLC). After completion, the reaction mixture was directly loaded onto a silica gel column. Chlorobenzene was first eluted with hexane, followed by elution with 1:9 ethyl acetate/hexane to collect the product **3E1**. The purified fused chromono-2-methyl-2,3-dihydrothiophene was used for subsequent steps. The same procedure was employed for all derivatives **3E2**–**3E12**.

General procedure for the synthesis of fused chromono-2-methylthiophene derivatives (3F1–3F15)

Method A: From Fused chromono-2-methyl-2,3-dihydrothiophenes *via* dehydrogenation (**3F1**–**3F9**)

A solution of fused chromono-2-methyl-2,3-dihydrothiophene (**3E1**, 0.15 mmol) and DDQ (0.3 mmol, 2.0 equiv) in dry toluene was refluxed under a nitrogen atmosphere for 12 h. The reaction progress was monitored by TLC. Upon completion, the solvent was evaporated under reduced pressure, and the crude residue was purified by silica gel column chromatography using ethyl acetate/hexane (0.3:9.7, v/v) as the eluent to afford the pure product **3F1**. Compounds **3F2**–**3F9** were synthesized analogously following the same procedure.

Method B: From *S*-propargyl chromene-4-ones (**3F1-3F7, 3F9-3F15**)

A solution of *S*-propargyl chromene-4-one (**3D1**, 0.15 mmol) in DMF (1 mL) was stirred at 80 °C in a preheated oil bath for 16 h. Reaction progress was monitored by TLC. After completion, the mixture was cooled to room temperature and diluted with water (5 mL). The aqueous layer was extracted with ethyl acetate (2 × 10 mL), and the combined organic extracts were washed with brine (2 × 7 mL), dried over anhydrous Na_2SO_4, and concentrated under reduced pressure. The resulting crude product was purified by column chromatography using ethyl acetate/hexane (0.3:9.7, v/v) to obtain pure compound **3F1**. Derivatives **3F2-3F7** and **3F9-3F15** were synthesized similarly using this method.

General procedure for the synthesis of fused chromono-thiopyrans (3G1–3G14)

A solution of *S*-propargyl chromene-4-one (**3D1**, 0.15 mmol) in chlorobenzene (1 mL) was refluxed in an oil bath for 5 h with continuous monitoring of the reaction progress by TLC. Upon completion, the reaction mixture was directly loaded onto a silica gel column. Elution with pure hexane was used to remove chlorobenzene, followed by elution with an ethyl acetate/hexane mixture (0.8:9.2, v/v) to isolate the pure product **3G1**. Compounds **3G2**–**3G14** were synthesized using the same general procedure.

General procedure for the synthesis of fused chromono-2,2-dimethyl-thiopyran derivatives (3I1–3I6)

4-Hydroxythiocoumarin, **1A1** (0.15 mmol, 1 equiv) was reacted with 2-methylbut-3-yn-2-ol, **3H1** (1.5 equiv) in nitromethane (1 mL) in the presence of *p*-TSA (10 mol%) as catalyst.

The mixture was stirred at 80 °C until completion (monitored by TLC). Upon completion of the reaction, the mixture was diluted with ethyl acetate (10 mL) and washed twice with water (5 mL). The organic layer was separated, dried over anhydrous sodium sulfate, and concentrated under reduced pressure. The crude product was then purified by silica gel column chromatography using ethyl acetate/hexane (0.3:9.7, v/v) as the eluent to afford the pure compound **3I1**. The remaining derivatives (**3I2**–**3I6**) were synthesized following the same general protocol.

Comprehensive spectroscopic and analytical data for all synthesized *S*-allyl (**3C1**–**3C12**) and *S*-propargyl chromone (**3D1**–**3D12**) fused chromono-2-methyl-2,3-dihydrothiophene (**3E1**–**3E12**), −2-methylthiophene (**3F1**–**3F15**), -thiopyran (**3G1**–**3G14**), and −2,2-dimethyl-thiopyran (**3I1**–**3I6**) derivatives are provided in **Section 3.9**. This includes ^{1}H and ^{13}C NMR, IR, HRMS data, and melting points for each compound. Representative spectra for key examples are also included in **Section 3.9**.

3.7 Crystallographic Analysis

Single crystals suitable for X-ray diffraction were obtained for compound **3I1** by slow evaporation from a mixture of ethyl acetate and hexane. The structure of fused chromono-2,2-dimethyl-thiopyran derivative **3I1** was unambiguously confirmed by single-crystal X-ray diffraction. The crystallographic data clearly established the connectivity, regiochemistry, and three-dimensional arrangement of the fused chromone and thiopyran rings, as well as the presence of the two methyl groups at the 2-position. ORTEP diagram (**Figure 3.3**) was generated using ORTEP-3 for Windows.[20]

The CCDC deposition number **2266735** (for **3I1**) contains the supplementary crystallographic data for this paper, which can be obtained free of charge by the joint Cambridge Crystallographic Data Centre and Fachinformationszentrum Karlsruhe https://www.ccdc.cam.ac.uk/structures/

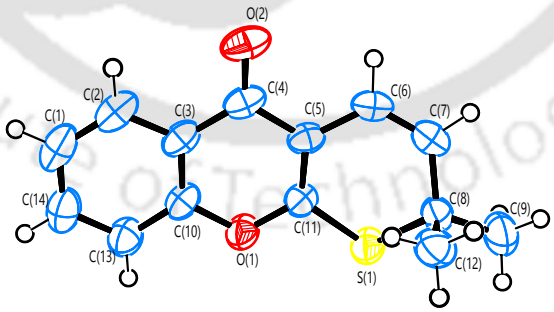

Figure 3.3: ORTEP diagram for compound 3I1.

Table 3.9: Crystallographic data and Structure Refinement for compound **3I1**.[a]

Entry	Identification Code	Compound 3I1
1	Empirical formula	$C_{14}H_{12}O_2S$
2	Formula weight	244.30
3	Temperature	297 K

Entry	Identification Code	Compound 3I1
4	Wavelength	0.71073 Å
5	Radiation type	Mo K\α
6	Radiation system	Fine-focus sealed tube
7	Crystal system	Monoclinic
8	Space group	$P2_1/n$
9	Cell length	a 12.9925 (10) Å b 5.6889 (4) Å c 16.3926 (12) Å
10	Cell angle	α 90° β 102.803 (2)° γ 90°“
11	Cell volume	1181.50 (15) $Å^3$
12	Density	1.373 $Mg\,m^{-3}$
13	Completeness to theta	99.9
14	Absorption correction	multi-scan
15	Refinement method	Full-matrix least-squares on F^2
16	Index ranges	−15≤h≤15, −6≤k≤6, −20≤l≤19
17	Reflection number	2236
18	Theta range	2.6 − 25.6°
19	Cell formula units Z	4
20	CCDC no.	2266735

[a]The full .cif file and additional crystallographic data are available from the CCDC.

3.8 Characterization Data for All New Compounds

2-(Allylthio)-4*H*-chromen-4-one (3C1)

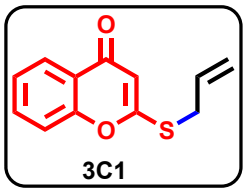

3C1

Brown Liquid (0.079 g, 72%); **^{1}H NMR (500 MHz, $CDCl_3$)** δ 8.16 (d, J = 7.8 Hz, 1H), 7.63 (t, J = 7.7 Hz, 1H), 7.38 (t, J = 9.0 Hz, 2H), 6.30 (s, 1H), 5.98 – 5.87 (m, 1H), 5.35 (d, J = 16.9 Hz, 1H), 5.22 (d, J = 10.0 Hz, 1H), 3.71 (d, J = 6.7 Hz, 2H); **^{13}C{^{1}H} NMR (125 MHz, $CDCl_3$)** δ 175.9, 167.4, 156.9, 133.4, 131.6, 125.9, 125.3, 123.6, 119.5, 117.2, 109.8, 34.0; **IR (KBr)** ν_{max}/cm^{-1} 3075 (C=C−H), 2976, 2926 (C−H), 1635 (C=O), 1612 (C=C), 1546, 1463 (Ar C=C); **HRMS (ESI)** calcd for $C_{12}H_{11}O_2S^+$ 219.0474 M+H^+ found 219.0471.

2-(Allylthio)-6-chloro-4*H*-chromen-4-one (3C2)

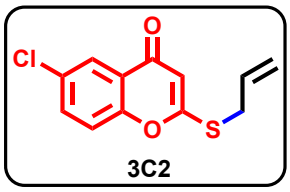

Yellow solid (0.090 g, 71%); **mp** 79 – 81 °C; **^{1}H NMR (500 MHz, $CDCl_3$)** δ 8.12 (d, J = 2.1 Hz, 1H), 7.57 (dd, J = 8.8, 2.2 Hz, 1H), 7.36 (d, J = 8.9 Hz, 1H), 6.29 (s, 1H), 5.97 – 5.87 (m, 1H), 5.36 (d, J = 16.9 Hz, 1H), 5.24 (d, J = 10.1 Hz, 1H), 3.71 (d, J = 6.7 Hz, 2H); **^{13}C{^{1}H} NMR (125 MHz, $CDCl_3$)** δ 174.6, 168.0, 155.2, 133.6, 131.4, 131.3, 125.4, 124.6, 119.7, 118.9, 109.6, 34.1; **IR (KBr)** ν_{max}/cm^{-1} 3070 (C=C–H), 2965, 2924 (C–H), 1639 (C=O), 1612 (C=C), 1542, 1462 (Ar C=C); **HRMS (ESI)** calcd for $C_{12}H_9ClNaO_2S^+$ 274.9904 M+Na$^+$ found 274.9895.

2-(Allylthio)-6-bromo-4*H*-chromen-4-one (3C3)

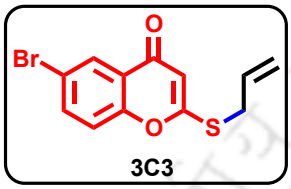

Yellow solid (0.113 g, 76%); **mp** 74 – 75 °C; **^{1}H NMR (500 MHz, $CDCl_3$)** δ 8.27 (d, J = 2.3 Hz, 1H), 7.70 (dd, J = 8.8, 2.3 Hz, 1H), 7.29 (d, J = 8.8 Hz, 1H), 6.29 (s, 1H), 5.91 (ddt, J = 16.8, 10.0, 6.8 Hz, 1H), 5.35 (d, J = 16.9 Hz, 1H), 5.24 (d, J = 10.1 Hz, 1H), 3.70 (d, J = 6.8 Hz, 2H); **^{13}C{^{1}H} NMR (125 MHz, $CDCl_3$)** δ 174.4, 168.0, 155.6, 136.3, 131.4, 128.6, 125.0, 119.7, 119.1, 118.7, 109.6, 34.1; **IR (KBr)** ν_{max}/cm^{-1} 3084 (C=C–H), 2982, 2923 (C–H), 1639 (C=O), 1603 (C=C), 1541, 1460 (Ar C=C); **HRMS (ESI)** calcd for $C_{12}H_9BrNaO_2S^+$ 318.9399 M+Na$^+$ found 318.9388.

2-(Allylthio)-6-fluoro-4*H*-chromen-4-one (3C4)

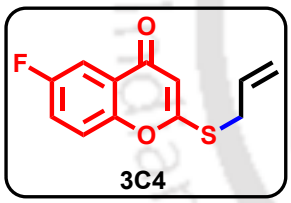

Yellow solid (0.085 g, 72%); **mp** 53 – 55 °C; **^{1}H NMR (500 MHz, $CDCl_3$)** δ 7.80 (dd, J = 8.1, 2.6 Hz, 1H), 7.41 (dd, J = 9.1, 4.1 Hz, 1H), 7.38 – 7.32 (m, 1H), 6.29 (s, 1H), 5.92 (ddt, J = 16.8, 10.1, 6.8 Hz, 1H), 5.36 (d, J = 16.9 Hz, 1H), 5.24 (d, J = 10.0 Hz, 1H), 3.71 (d, J = 6.7 Hz, 2H); **^{13}C{^{1}H} NMR (125 MHz, $CDCl_3$)** δ 175.0 (d, J = 2.1 Hz), 168.0, 159.6 (d, J = 247.1 Hz), 153.0 (d, J = 1.8 Hz), 131.5, 124.9 (d, J = 7.2 Hz), 121.4 (d, J = 25.5 Hz), 119.6, 119.25 (d, J = 8.0 Hz), 111.0 (d, J = 23.8 Hz), 100.0, 34.1; **^{19}F NMR (471 MHz, $CDCl_3$)** δ -114.84; **IR (KBr)** ν_{max}/cm^{-1} 3074 (C=C–H), 2961, 2925 (C–H), 1644 (C=O), 1620 (C=C), 1546, 1475 (Ar C=C); **HRMS (ESI)** calcd for $C_{12}H_{10}FO_2S^+$ 237.0380 M+H$^+$ found 237.0382.

2-(Allylthio)-7-fluoro-4*H*-chromen-4-one (3C5)

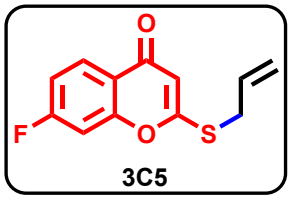

Yellowish White solid (0.084 g, 71%); **mp** 59 – 61 °C; **^{1}H NMR (500 MHz, $CDCl_3$)** δ 8.16 (dd, J = 8.6, 6.4 Hz, 1H), 7.12 (dd, J = 8.4, 2.2 Hz, 1H), 7.08 (dd, J = 8.6, 2.2 Hz, 1H), 6.27 (s, 1H), 5.91 (ddt, J = 16.8, 10.0, 6.8 Hz, 1H), 5.35 (d, J = 16.9 Hz, 1H), 5.23 (d, J = 10.0 Hz, 1H), 3.69 (d, J = 6.7 Hz, 2H); **^{13}C{^{1}H} NMR (125 MHz, $CDCl_3$)** δ 174.9, 167.7, 165.4 (d, J = 255.1 Hz), 157.7 (d, J = 13.1 Hz), 131.4, 128.3 (d, J = 10.6 Hz), 120.4 (d, J = 2.5 Hz), 119.6, 114.0 (d, J = 22.6 Hz), 109.8, 104.2 (d, J = 25.6 Hz), 34.1; **^{19}F NMR (471 MHz, $CDCl_3$)** δ -103.09; **IR (KBr)** ν_{max}/cm^{-1} 3065 (C=C–H),

2961, 2925 (C−H), 1645 (C=O), 1613 (C=C), 1549, 1493 (Ar C=C); **HRMS (ESI)** calcd for $C_{12}H_{10}FO_2S^+$ 237.0380 M+H$^+$ found 237.0386.

2-(Allylthio)-6-methyl-4*H*-chromen-4-one (3C6)

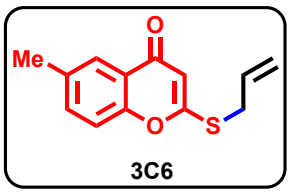

Yellow solid (0.093 g, 80%); **mp** 65 – 66 °C; **^{1}H NMR (500 MHz, $CDCl_3$)** δ 7.92 (s, 1H), 7.42 (dd, J = 8.5, 1.7 Hz, 1H), 7.28 (d, J = 8.5 Hz, 1H), 6.30 (s, 1H), 5.90 (ddt, J = 16.9, 10.0, 6.8 Hz, 1H), 5.34 (d, J = 16.9 Hz, 1H), 5.21 (d, J = 10.6 Hz, 1H), 3.69 (d, J = 6.8 Hz, 2H), 2.42 (s, 3H); **^{13}C{^{1}H} NMR (100 MHz, $CDCl_3$)** δ 176.0, 167.5, 155.2, 135.3, 134.6, 131.6, 125.2, 123.0, 119.5, 116.9, 109.4, 34.0, 20.8; **IR (KBr)** ν_{max}/cm^{-1} 3072 (C=C−H), 2974, 2923 (C−H), 1633 (C=O), 1610 (C=C), 1545, 1465 (Ar C=C); **HRMS (ESI)** calcd for $C_{13}H_{13}O_2S^+$ 233.0631 M+H$^+$ found 233.0633.

2-(But-2-en-1-ylthio)-4*H*-chromen-4-one (3C7)

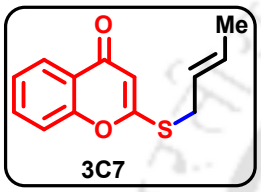

Brown Liquid (0.078 g, 67%); **^{1}H NMR (500 MHz, $CDCl_3$)** δ 8.16 (d, J = 7.9 Hz, 1H), 7.65 – 7.60 (m, 1H), 7.41 – 7.36 (m, 2H), 6.28 (s, 1H), 5.85 – 5.74 (m, 1H), 5.58 – 5.51 (m, 1H), 3.66 (d, J = 7.0 Hz, 2H), 1.70 (d, J = 6.5 Hz, 3H); **^{13}C{^{1}H} NMR (125 MHz, $CDCl_3$)** δ 175.92, 168.17, 156.88, 133.36, 131.24, 125.88, 125.29, 124.07, 123.59, 117.23, 109.35, 33.54, 17.76; **IR (KBr)** ν_{max}/cm^{-1} 3031 (C=C−H), 2964, 2925, 2860 (C−H), 1643 (C=O), 1615 (C=C), 1553, 1470 (Ar C=C); **HRMS (ESI)** calcd for $C_{13}H_{13}O_2S^+$ 233.0631 M+H$^+$ found 233.0642.

2-(But-2-en-1-ylthio)-6-chloro-4*H*-chromen-4-one (3C8)

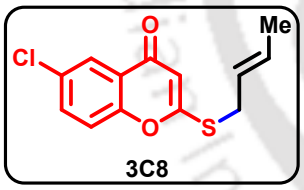

Yellow solid (0.092 g, 69%); **mp** 74 – 75 °C; **^{1}H NMR (500 MHz, $CDCl_3$)** δ 8.12 (d, J = 2.5 Hz, 1H), 7.56 (dd, J = 8.9, 2.6 Hz, 1H), 7.35 (d, J = 8.9 Hz, 1H), 6.26 (s, 1H), 5.84 – 5.76 (m, 1H), 5.58 – 5.49 (m, 1H), 3.65 (d, J = 7.0 Hz, 2H), 1.70 (d, J = 6.5 Hz, 3H); **^{13}C{^{1}H} NMR (125 MHz, $CDCl_3$)** δ 174.56, 168.73, 155.14, 133.49, 131.46, 131.21, 125.37, 124.61, 123.85, 118.92, 109.12, 33.62, 17.77; **IR (KBr)** ν_{max}/cm^{-1} 3043 (C=C−H), 2960, 2921, 2852 (C−H), 1640 (C=O), 1610 (C=C), 1545, 1475 (Ar C=C); **HRMS (ESI)** calcd for $C_{13}H_{12}ClO_2S^+$ 267.0241 M+H$^+$ found 267.0251.

2-(But-2-en-1-ylthio)-6-methyl-4*H*-chromen-4-one (3C9)

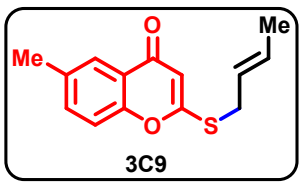

Brown Liquid (0.091 g, 74%); **^{1}H NMR (400 MHz, $CDCl_3$)** δ 7.93 (d, J = 1.5 Hz, 1H), 7.42 (dd, J = 8.5, 2.1 Hz, 1H), 7.28 (d, J = 8.5 Hz, 1H), 6.25 (s, 1H), 5.83 – 5.73 (m, 1H), 5.58 – 5.49 (m, 1H), 3.65 (d, J = 7.0 Hz, 2H), 2.42 (s, 3H), 1.69 (dd, J = 6.4, 1.2 Hz, 3H); **^{13}C{^{1}H} NMR (125 MHz, $CDCl_3$)** δ 176.04, 167.93, 155.21, 135.27, 134.50, 131.16, 125.25, 124.14, 123.20, 116.97, 109.24, 33.53, 20.86, 17.74; **IR (KBr)** ν_{max}/cm^{-1} 3026 (C=C−H), 2959, 2922, 2853 (C−H), 1640 (C=O), 1612 (C=C), 1545, 1480 (Ar C=C); **HRMS (ESI)** calcd for $C_{14}H_{15}O_2S^+$ 247.0788 M+H$^+$ found 247.0787.

6-Bromo-2-((3-methylbut-2-en-1-yl)thio)-4*H*-chromen-4-one (3C10)

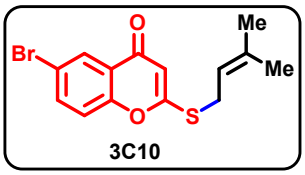

3C10

Yellow solid (0.112 g, 69%); **mp** 84 – 86 °C; **^{1}H NMR (500 MHz, $CDCl_3$)** δ 8.27 (d, J = 2.3 Hz, 1H), 7.70 (dd, J = 8.8, 2.4 Hz, 1H), 7.28 (d, J = 8.9 Hz, 1H), 6.25 (s, 1H), 5.30 (t, J = 7.7 Hz, 1H), 3.69 (d, J = 7.7 Hz, 2H), 1.75 (s, 3H), 1.74 (s, 3H); **^{13}C{^{1}H} NMR (125 MHz, $CDCl_3$)** δ 174.36, 169.24, 155.57, 139.23, 136.23, 128.53, 124.95, 119.18, 118.62, 116.69, 109.01, 29.64, 25.67, 17.96; **IR (KBr)** ν_{max}/cm^{-1} 3035 (C=C–H), 2969, 2925, 2861 (C–H), 1647 (C=O), 1610 (C=C), 1548, 1476 (Ar C=C); **HRMS (ESI)** calcd for $C_{14}H_{14}BrO_2S^+$ 324.9892 M+H$^+$ found 324.9909.

6-Fluoro-2-((3-methylbut-2-en-1-yl)thio)-4*H*-chromen-4-one (3C11)

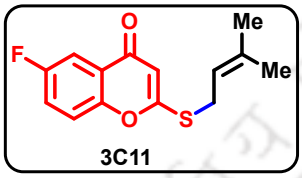

3C11

Yellow solid (0.087 g, 66%); **mp** 77 – 78 °C; **^{1}H NMR (400 MHz, $CDCl_3$)** δ 7.80 (dd, J = 8.2, 3.0 Hz, 1H), 7.40 (dd, J = 9.1, 4.2 Hz, 1H), 7.37 – 7.31 (m, 1H), 6.25 (s, 1H), 5.34 – 5.27 (m, 1H), 3.70 (d, J = 7.7 Hz, 2H), 1.75 (s, 3H), 1.74 (s, 3H); **^{13}C{^{1}H} NMR (125 MHz, $CDCl_3$)** δ 174.96, 169.21, 159.53 (d, J = 246.9 Hz), 153.03 (d, J = 1.8 Hz), 139.15, 124.86 (d, J = 7.3 Hz), 121.31 (d, J = 25.4 Hz), 119.28 (d, J = 8.0 Hz), 116.77, 110.92 (d, J = 23.8 Hz), 108.41, 29.62, 25.67, 17.96; **^{19}F NMR (471 MHz, $CDCl_3$)** δ -115.02; **IR (KBr)** ν_{max}/cm^{-1} 3077 (C=C–H), 2961, 2926, 2858 (C–H), 1646 (C=O), 1623 (C=C), 1548, 1477 (Ar C=C); **HRMS (ESI)** calcd for $C_{14}H_{14}FO_2S^+$ 265.0693 M+H$^+$ found 265.0714.

7-Fluoro-2-((3-methylbut-2-en-1-yl)thio)-4*H*-chromen-4-one (3C12)

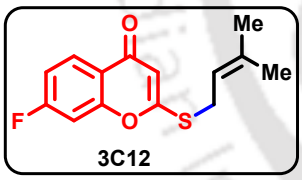

3C12

Yellow solid (0.088 g, 67%); **mp** 50 – 52 °C; **^{1}H NMR (500 MHz, $CDCl_3$)** δ 8.16 (dd, J = 8.7, 6.3 Hz, 1H), 7.13 – 7.05 (m, 2H), 6.23 (s, 1H), 5.33 – 5.27 (m, 1H), 3.68 (d, J = 7.7 Hz, 2H), 1.75 (s, 3H), 1.73 (s, 3H); **^{13}C{^{1}H} NMR (125 MHz, $CDCl_3$)** δ 174.87, 168.96, 165.30 (d, J = 254.9 Hz), 157.63 (d, J = 13.2 Hz), 139.15, 128.26 (d, J = 10.5 Hz), 120.37 (d, J = 2.4 Hz), 116.73, 113.83 (d, J = 22.6 Hz), 109.17, 104.18 (d, J = 25.6 Hz), 29.66, 25.65, 17.94; **^{19}F NMR (471 MHz, $CDCl_3$)** δ -103.24; **IR (KBr)** ν_{max}/cm^{-1} 3071 (C=C–H), 2959, 2925, 2857 (C–H), 1651 (C=O), 1616 (C=C), 1550, 1436 (Ar C=C); **HRMS (ESI)** calcd for $C_{14}H_{14}FO_2S^+$ 265.0693 M+H$^+$ found 265.0705.

2-(Prop-2-yn-1-ylthio)-4*H*-chromen-4-one (3D1)

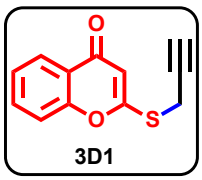

3D1

Orange solid (0.075 g, 69%); **mp** 105 – 107 °C; **^{1}H NMR (400 MHz, $CDCl_3$)** δ 8.18 (dd, J = 7.8, 1.6 Hz, 1H), 7.70 – 7.62 (m, 1H), 7.47 – 7.36 (m, 2H), 6.41 (s, 1H), 3.80 (d, J = 2.5 Hz, 2H), 2.32 (t, J = 2.5 Hz, 1H); **^{13}C{^{1}H} NMR (100 MHz, $CDCl_3$)** δ 176.0, 165.9, 156.9, 133.6, 125.9, 125.5, 123.6, 117.4, 110.2, 77.2, 72.9, 19.7; **IR (KBr)** ν_{max}/cm^{-1} 3274 (C≡C–H), 2959, 2924 (C–H), 2121 (C≡C) 1637 (C=O), 1549, 1462 (Ar C=C); **HRMS (ESI)** calcd for $C_{12}H_9O_2S^+$ 217.0318 M+H$^+$ found 217.0321.

6-Chloro-2-(prop-2-yn-1-ylthio)-4*H*-chromen-4-one (3D2)

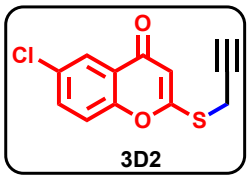

White solid (0.095 g, 76%); **mp** 118 – 120 °C; **^{1}H NMR (400 MHz, $CDCl_3$)** δ 8.14 (d, J = 2.4 Hz, 1H), 7.59 (dd, J = 8.9, 2.4 Hz, 1H), 7.39 (d, J = 8.9 Hz, 1H), 6.41 (s, 1H), 3.79 (d, J = 2.4 Hz, 2H), 2.33 (t, J = 2.4 Hz, 1H); **^{13}C{^{1}H} NMR (125 MHz, $CDCl_3$)** δ 174.6, 166.4, 155.2, 133.7, 131.5, 125.4, 124.6, 119.1, 110.1, 77.1, 73.0, 19.8; **IR (KBr)** ν_{max}/cm^{-1} 3274 (C≡C−H), 3082 (C=C−H), 2963, 2929 (C−H), 2120 (C≡C) 1643 (C=O), 1542, 1463 (Ar C=C); **HRMS (ESI)** calcd for $C_{12}H_8ClO_2S^+$ 250.9928 M+H^+ found 250.9914.

6-Bromo-2-(prop-2-yn-1-ylthio)-4*H*-chromen-4-one (3D3)

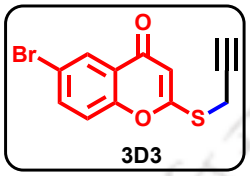

Yellowish white solid (0.117 g, 79%); **mp** 134 – 135 °C; **^{1}H NMR (400 MHz, $CDCl_3$)** δ 8.29 (d, J = 2.5 Hz, 1H), 7.73 (dd, J = 8.9, 2.4 Hz, 1H), 7.32 (d, J = 8.8 Hz, 1H), 6.41 (s, 1H), 3.79 (d, J = 2.6 Hz, 2H), 2.32 (t, J = 2.6 Hz, 1H); **^{13}C{^{1}H} NMR (125 MHz, $CDCl_3$)** δ 174.4, 166.4, 155.6, 136.5, 128.6, 124.9, 119.3, 118.9, 110.1, 77.1, 73.0, 19.8; **IR (KBr)** ν_{max}/cm^{-1} 3296 (C≡C−H), 3073 (C=C−H), 2964, 2924 (C−H), 2121 (C≡C) 1642 (C=O), 1545, 1460 (Ar C=C); **HRMS (ESI)** calcd for $C_{12}H_7BrNaO_2S^+$ 316.9242 M+Na^+ found 316.9232.

6-Fluoro-2-(prop-2-yn-1-ylthio)-4*H*-chromen-4-one (3D4)

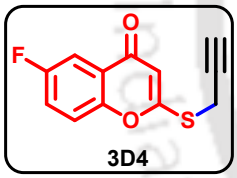

Yellow solid (0.084 g, 72%); **mp** 110 – 112 °C; **^{1}H NMR (400 MHz, $CDCl_3$)** δ 7.80 (dd, J = 8.1, 3.0 Hz, 1H), 7.43 (dd, J = 9.1, 4.2 Hz, 1H), 7.36 (td, J = 9.2, 8.4, 3.1 Hz, 1H), 6.39 (s, 1H), 3.79 (d, J = 2.5 Hz, 2H), 2.32 (t, J = 2.5 Hz, 1H); **^{13}C{^{1}H} NMR (125 MHz, $CDCl_3$)** δ 175.0 (d, J = 2.1 Hz), 166.3, 159.6 (d, J = 247.3 Hz), 153.0 (d, J = 1.8 Hz), 124.8 (d, J = 7.4 Hz), 121.5 (d, J = 25.5 Hz), 119.4 (d, J = 8.0 Hz), 110.9 (d, J = 23.9 Hz), 109.4, 77.2, 73.0, 19.7; **^{19}F NMR (471 MHz, $CDCl_3$)** δ -114.58; **IR (KBr)** ν_{max}/cm^{-1} 3246 (C≡C−H), 3070 (C=C−H), 2960, 2919 (C−H), 2123 (C≡C), 1640 (C=O), 1544, 1473 (Ar C=C); **HRMS (ESI)** calcd for $C_{12}H_8FO_2S^+$ 235.0224 M+H^+ found 235.0226.

7-Fluoro-2-(prop-2-yn-1-ylthio)-4*H*-chromen-4-one (3D5)

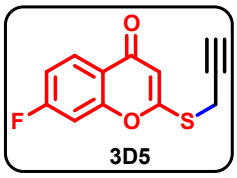

Yellowish white solid (0.082 g, 70%); **mp** 101 – 103 °C; **^{1}H NMR (500 MHz, $CDCl_3$)** δ 8.17 (dd, J = 8.2, 6.5 Hz, 1H), 7.16 – 7.08 (m, 2H), 6.38 (s, 1H), 3.78 (d, J = 2.6 Hz, 2H), 2.33 (t, J = 2.6 Hz, 1H); **^{13}C{^{1}H} NMR (125 MHz, $CDCl_3$)** δ 174.9, 166.1, 165.4 (d, J = 255.4 Hz), 157.7 (d, J = 13.2 Hz), 128.3 (d, J = 10.6 Hz), 120.4 (d, J = 2.4 Hz), 114.1 (d, J = 22.6 Hz), 110.3, 104.3 (d, J = 25.6 Hz), 77.1, 73.0, 19.7; **^{19}F NMR (471 MHz, $CDCl_3$)** δ -102.70; **IR (KBr)** ν_{max}/cm^{-1} 3238 (C≡C−H), 3063 (C=C−H), 2960, 2924 (C−H), 2123 (C≡C), 1639 (C=O), 1550, 1435 (Ar C=C); **HRMS (ESI)** calcd for $C_{12}H_8FO_2S^+$ 235.0224 M+H^+ found 235.0229.

6-Methyl-2-(prop-2-yn-1-ylthio)-4*H*-chromen-4-one (3D6)

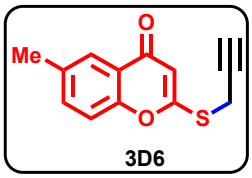

Yellow solid (0.089 g, 77%); **mp** 97 – 98 °C; **^{1}H NMR (500 MHz, $CDCl_3$)** δ 7.93 (s, 1H), 7.44 (dd, J = 8.5, 1.8 Hz, 1H), 7.30 (d, J = 8.5 Hz, 1H), 6.38 (s, 1H), 3.78 (d, J = 2.6 Hz, 2H), 2.42 (s, 3H), 2.31 (t, J = 2.5 Hz, 1H); **^{13}C{^{1}H} NMR (125 MHz, $CDCl_3$)** δ 176.0, 165.7, 155.2, 135.5, 134.7, 125.2, 123.1, 117.1, 110.0, 77.3, 72.8, 20.8, 19.6; **IR (KBr)** ν_{max}/cm^{-1} 3230 (C≡C−H), 3061 (C=C−H), 2958, 2922 (C−H), 2119 (C≡C), 1635 (C=O), 1547, 1480 (Ar C=C); **HRMS (ESI)** calcd for $C_{13}H_{11}O_2S^+$ 231.0474 M+H$^+$ found 231.0477.

2-(But-2-yn-1-ylthio)-4*H*-chromen-4-one (3D7)

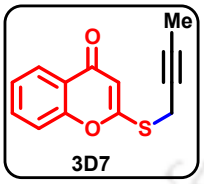

Yellow solid (0.079 g, 69%); **mp** 81 – 83 °C; **^{1}H NMR (400 MHz, $CDCl_3$)** δ 8.16 (dd, J = 7.9, 1.3 Hz, 1H), 7.63 (ddd, J = 8.6, 7.3, 1.7 Hz, 1H), 7.44 – 7.35 (m, 2H), 6.39 (s, 1H), 3.77 (q, J = 2.4 Hz, 2H), 1.81 (t, J = 2.5 Hz, 3H); **^{13}C{^{1}H} NMR (125 MHz, $CDCl_3$)** δ 175.96, 167.17, 156.89, 133.47, 125.86, 125.37, 123.55, 117.34, 109.56, 81.06, 72.19, 20.53, 3.63; **IR (KBr)** ν_{max}/cm^{-1} 3286 (C≡C−H), 3066 (C=C−H), 2958, 2924, 2854 (C−H), 2235 (C≡C), 1642 (C=O), 1548, 1463 (Ar C=C); **HRMS (ESI)** calcd for $C_{13}H_{11}O_2S^+$ 231.0475 M+H$^+$ found 231.0486.

2-(But-2-yn-1-ylthio)-6-methyl-4*H*-chromen-4-one (3D8)

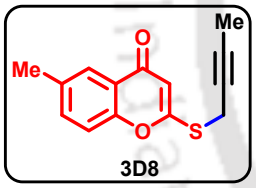

Orange-brown solid (0.093 g, 76%); **mp** 95 – 97 °C; **^{1}H NMR (400 MHz, $CDCl_3$)** δ 7.95 (d, J = 1.6 Hz, 1H), 7.43 (dd, J = 8.5, 2.0 Hz, 1H), 7.39 (d, J = 8.5 Hz, 1H), 6.36 (s, 1H), 3.76 (q, J = 2.5 Hz, 2H), 2.43 (s, 3H), 1.80 (t, J = 2.5 Hz, 3H); **^{13}C{^{1}H} NMR (125 MHz, $CDCl_3$)** δ 176.14, 166.88, 155.23, 135.37, 134.61, 125.25, 123.20, 117.09, 109.47, 81.00, 72.25, 20.87, 20.52, 3.63; **IR (KBr)** ν_{max}/cm^{-1} 3273 (C≡C−H), 3068 (C=C−H), 2960, 2921, 2855 (C−H), 2232 (C≡C), 1643 (C=O), 1549, 1481 (Ar C=C); **HRMS (ESI)** calcd for $C_{14}H_{13}O_2S^+$ 245.0631 M+H$^+$ found 245.0632.

6-Bromo-2-(but-2-yn-1-ylthio)-4*H*-chromen-4-one (3D9)

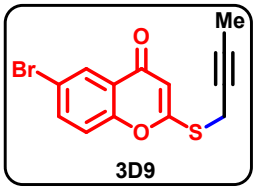

Yellow solid (0.111 g, 72%); **mp** 132 – 133 °C; **^{1}H NMR (500 MHz, $CDCl_3$)** δ 8.28 (d, J = 2.5 Hz, 1H), 7.71 (dd, J = 8.9, 2.5 Hz, 1H), 7.30 (d, J = 8.8 Hz, 1H), 6.39 (s, 1H), 3.76 (q, J = 2.4 Hz, 2H), 1.81 (t, J = 2.5 Hz, 3H); **^{13}C{^{1}H} NMR (125 MHz, $CDCl_3$)** δ 174.48, 167.77, 155.59, 136.39, 128.53, 124.90, 119.27, 118.76, 109.39, 81.24, 71.98, 20.61, 3.64; **IR (KBr)** ν_{max}/cm^{-1} 3259 (C≡C−H), 3061 (C=C−H), 2958, 2925, 2850 (C−H), 2229 (C≡C), 1647 (C=O), 1547, 1480 (Ar C=C); **HRMS (ESI)** calcd for $C_{13}H_{10}BrO_2S^+$ 308.9579 M+H$^+$ found 308.9578.

6-Fluoro-2-(but-2-yn-1-ylthio)-4*H*-chromen-4-one (3D10)

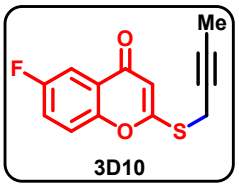

3D10

Yellow solid (0.087 g, 70%); **mp** 118 – 120 °C; **^{1}H NMR (500 MHz, $CDCl_3$)** δ 7.79 (dd, J = 8.1, 3.1 Hz, 1H), 7.41 (dd, J = 9.2, 4.2 Hz, 1H), 7.35 (ddd, J = 9.5, 7.6, 3.1 Hz, 1H), 6.37 (s, 1H), 3.78 – 3.74 (m, 2H), 1.82 – 1.79 (m, 3H); **^{13}C{^{1}H} NMR (125 MHz, $CDCl_3$)** δ 175.04 (d, J = 2.3 Hz), 167.69, 159.57 (d, J = 247.0 Hz), 153.03 (d, J = 1.8 Hz), 124.81 (d, J = 7.4 Hz), 121.46 (d, J = 25.6 Hz), 119.38 (d, J = 8.2 Hz), 110.90 (d, J = 23.9 Hz), 108.77, 81.16, 72.05, 20.57, 3.62; **^{19}F NMR (471 MHz, $CDCl_3$)** δ -114.79; **IR (KBr)** ν_{max}/cm^{-1} 3252 (C≡C−H), 3048 (C=C−H), 2963, 2922, 2848 (C−H), 2232 (C≡C), 1643 (C=O), 1554, 1477 (Ar C=C); **HRMS (ESI)** calcd for $C_{13}H_{10}FO_2S^+$ 249.0380 M+H$^+$ found 249.0382.

2-(Pent-2-yn-1-ylthio)-4*H*-chromen-4-one (3D11)

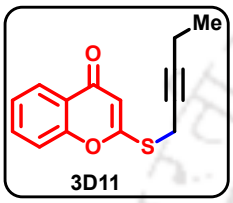

3D11

Yellow solid (0.081 g, 66%); **mp** 60 – 61 °C; **^{1}H NMR (400 MHz, $CDCl_3$)** δ 8.17 (dd, J = 7.9, 1.5 Hz, 1H), 7.64 (ddd, J = 8.6, 7.2, 1.7 Hz, 1H), 7.43 – 7.36 (m, 2H), 6.39 (s, 1H), 3.79 (t, J = 2.3 Hz, 2H), 2.18 (qt, J = 7.5, 2.3 Hz, 2H), 1.08 (t, J = 7.5 Hz, 3H); **^{13}C{^{1}H} NMR (125 MHz, $CDCl_3$)** δ 175.97, 167.14, 156.90, 133.47, 125.87, 125.36, 123.55, 117.33, 109.69, 86.97, 72.39, 20.58, 13.62, 12.43; **IR (KBr)** ν_{max}/cm^{-1} 3289 (C≡C−H), 3007 (C=C−H), 2977, 2925, 2872 (C−H), 2237 (C≡C), 1644 (C=O), 1548, 1463 (Ar C=C); **HRMS (ESI)** calcd for $C_{14}H_{13}O_2S^+$ 245.0631 M+H$^+$ found 245.0632.

6-Methyl-2-(pent-2-yn-1-ylthio)-4*H*-chromen-4-one (3D12)

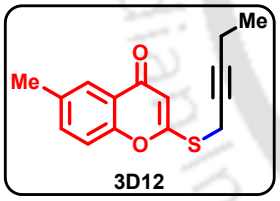

3D12

Yellow solid (0.089 g, 69%); **mp** 65 – 67 °C; **^{1}H NMR (500 MHz, $CDCl_3$)** δ 7.94 (s, 1H), 7.43 (dd, J = 8.4, 2.1 Hz, 1H), 7.30 (d, J = 8.5 Hz, 1H), 6.37 (s, 1H), 3.78 (t, J = 2.2 Hz, 2H), 2.43 (s, 3H), 2.17 (qt, J = 7.5, 2.2 Hz, 2H), 1.08 (t, J = 7.5 Hz, 3H); **^{13}C{^{1}H} NMR (125 MHz, $CDCl_3$)** δ 176.11, 166.85, 155.23, 135.35, 134.60, 125.25, 123.19, 117.08, 109.60, 86.91, 72.46, 20.87, 20.58, 13.62, 12.42; **IR (KBr)** ν_{max}/cm^{-1} 3278 (C≡C−H), 3064 (C=C−H), 2957, 2925, 2855 (C−H), 2239 (C≡C), 1645 (C=O), 1550, 1481 (Ar C=C); **HRMS (ESI)** calcd for $C_{15}H_{15}O_2S^+$ 259.0788 M+H$^+$ found 259.0796.

6-Chloro-2-(pent-2-yn-1-ylthio)-4*H*-chromen-4-one (3D13)

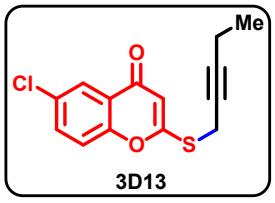

3D13

Yellow solid (0.097 g, 70%); **mp** 94 – 96 °C; **^{1}H NMR (400 MHz, $CDCl_3$)** δ 8.13 (d, J = 2.6 Hz, 1H), 7.58 (dd, J = 8.9, 2.6 Hz, 1H), 7.37 (d, J = 8.9 Hz, 1H), 6.40 (s, 1H), 3.78 (t, J = 2.3 Hz, 2H), 2.18 (qt, J = 7.5, 2.3 Hz, 2H), 1.09 (t, J = 7.5 Hz, 3H); **^{13}C{^{1}H} NMR (125 MHz, $CDCl_3$)** δ 174.65, 167.74, 155.17, 133.62, 131.31, 125.38, 124.57, 119.05, 109.49, 87.15, 72.20, 20.69, 13.62, 12.43; **IR (KBr)** ν_{max}/cm^{-1} 3286 (C≡C−H), 3007 (C=C−H), 2958, 2925, 2870 (C−H), 2239 (C≡C), 1647 (C=O), 1547, 1433 (Ar C=C); **HRMS (ESI)** calcd for $C_{14}H_{12}ClO_2S^+$ 279.0242 M+H$^+$ found 279.0259.

7-Fluoro-2-(pent-2-yn-1-ylthio)-4*H*-chromen-4-one (3D14)

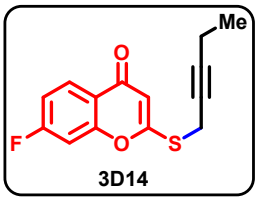

Off white solid (0.084 g, 64%); **mp** 83 – 85 °C; **^{1}H NMR (400 MHz, $CDCl_3$)** δ 8.17 (ddd, J = 8.3, 6.3, 0.9 Hz, 1H), 7.15 – 7.08 (m, 2H), 6.37 (s, 1H), 3.77 (t, J = 2.3 Hz, 2H), 2.17 (qt, J = 7.5, 2.3 Hz, 2H), 1.08 (t, J = 7.5 Hz, 3H); **^{13}C{^{1}H} NMR (125 MHz, $CDCl_3$)** δ 174.98, 167.42, 165.39 (d, J = 255.2 Hz), 157.68 (d, J = 13.3 Hz), 128.31 (d, J = 10.6 Hz), 120.38 (d, J = 2.5 Hz), 113.99 (d, J = 22.6 Hz), 109.79, 104.29 (d, J = 25.6 Hz), 87.11, 72.24, 20.71, 13.61, 12.42; **^{19}F NMR (471 MHz, $CDCl_3$)** δ -102.95; **IR (KBr)** ν_{max}/cm^{-1} 3279 (C≡C−H), 3068 (C=C−H), 2979, 2925, 2852 (C−H), 2239 (C≡C), 1651 (C=O), 1552, 1436 (Ar C=C); **HRMS (ESI)** calcd for $C_{14}H_{12}FO_2S^+$ 263.0537 M+H$^+$ found 263.0535.

2-Methyl-2,3-dihydro-4*H*-thieno[2,3-*b*]chromen-4-one (3E1)

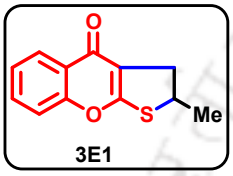

White solid (0.027 g, 82%); **mp** 72 – 74 °C; **^{1}H NMR (500 MHz, $CDCl_3$)** δ 8.19 (dd, J = 7.9, 1.7 Hz, 1H), 7.58 (ddd, J = 8.7, 7.2, 1.7 Hz, 1H), 7.40 (d, J = 3.7 Hz, 1H), 7.39 – 7.35 (m, 1H), 4.11 (h, J = 6.8 Hz, 1H), 3.43 (dd, J = 15.2, 8.5 Hz, 1H), 2.98 (dd, J = 15.2, 5.6 Hz, 1H), 1.55 (d, J = 6.8 Hz, 3H); **^{13}C{^{1}H} NMR (125 MHz, $CDCl_3$)** δ 172.9, 170.6, 157.1, 132.6, 125.8, 125.3, 123.4, 117.3, 116.4, 44.5, 37.5, 22.9; **IR (KBr)** ν_{max}/cm^{-1} 3058 (C=C−H), 2965, 2925 (C−H), 1636 (C=O), 1552, 1461 (Ar C=C); **HRMS (ESI)** calcd for $C_{12}H_{10}NaO_2S^+$ 241.0294 M+Na$^+$ found 241.0297.

6-Chloro-2-methyl-2,3-dihydro-4*H*-thieno[2,3-*b*]chromen-4-one (3E2)

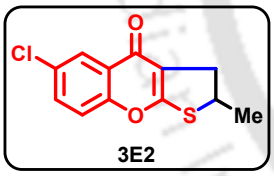

White solid (0.032 g, 85%); **mp** 151 – 152 °C; **^{1}H NMR (400 MHz, $CDCl_3$)** δ 8.16 (s, 1H), 7.54 (dt, J = 8.9, 2.4 Hz, 1H), 7.36 (dd, J = 8.9, 2.0 Hz, 1H), 4.23 – 4.08 (m, 1H), 3.44 (ddd, J = 15.4, 8.5, 2.1 Hz, 1H), 2.99 (ddd, J = 15.4, 5.6, 2.0 Hz, 1H), 1.56 (dd, J = 6.9, 2.0 Hz, 3H); **^{13}C{^{1}H} NMR (100 MHz, $CDCl_3$)** δ 171.6, 171.1, 155.4, 132.7, 131.2, 125.3, 124.6, 119.0, 116.5, 44.7, 37.4, 23.0; **IR (KBr)** ν_{max}/cm^{-1} 3060 (C=C−H), 2963, 2926 (C−H), 1634 (C=O), 1547, 1464 (Ar C=C); **HRMS (ESI)** calcd for $C_{12}H_{10}ClO_2S^+$ 253.0085 M+H$^+$ found 253.0072.

6-Bromo-2-methyl-2,3-dihydro-4*H*-thieno[2,3-*b*]chromen-4-one (3E3)

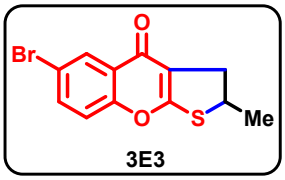

White solid (0.035 g, 79%); **mp** 146 – 148 °C; **^{1}H NMR (500 MHz, $CDCl_3$)** δ 8.32 (d, J = 2.3 Hz, 1H), 7.67 (dd, J = 8.8, 2.4 Hz, 1H), 7.30 (d, J = 8.8 Hz, 1H), 4.13 (dq, J = 13.0, 6.8 Hz, 1H), 3.43 (dd, J = 15.3, 8.5 Hz, 1H), 2.98 (dd, J = 15.3, 5.6 Hz, 1H), 1.56 (d, J = 6.8 Hz, 3H); **^{13}C{^{1}H} NMR (125 MHz, $CDCl_3$)** δ 171.4, 171.1, 155.8, 135.5, 128.5, 124.9, 119.3, 118.7, 116.6, 44.7, 37.4, 22.9; **IR (KBr)** ν_{max}/cm^{-1} 3071 (C=C−H), 2964, 2923 (C−H), 1626 (C=O), 1542, 1456 (Ar C=C); **HRMS (ESI)** calcd for $C_{12}H_{10}BrO_2S^+$ 296.9579 M+H$^+$ found 296.9571.

6-Fluoro-2-methyl-2,3-dihydro-4*H*-thieno[2,3-*b*]chromen-4-one (3E4)

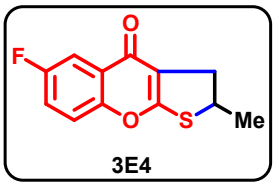

3E4

White solid (0.030 g, 85%); **mp** 111 – 113 °C; **^{1}H NMR (500 MHz, $CDCl_3$)** δ 7.83 (dd, J = 8.3, 3.0 Hz, 1H), 7.40 (dd, J = 9.1, 4.1 Hz, 1H), 7.30 (td, J = 9.1, 8.5, 3.0 Hz, 1H), 4.13 (h, J = 6.7 Hz, 1H), 3.43 (dd, J = 15.3, 8.5 Hz, 1H), 2.98 (dd, J = 15.3, 5.5 Hz, 1H), 1.55 (d, J = 6.8 Hz, 3H); **^{13}C{^{1}H} NMR (125 MHz, $CDCl_3$)** δ 171.9 (d, J = 2.1 Hz), 171.2, 159.7 (d, J = 246.5 Hz), 153.2 (d, J = 1.8 Hz), 124.8 (d, J = 7.2 Hz), 120.4 (d, J = 25.4 Hz), 119.2 (d, J = 8.2 Hz), 116.0, 110.9 (d, J = 24.0 Hz), 44.7, 37.3, 22.9; **^{19}F NMR (471 MHz, $CDCl_3$)** δ -115.27; **IR (KBr)** ν_{max}/cm^{-1} 3063 (C=C−H), 2961, 2925 (C−H), 1635 (C=O), 1556, 1473 (Ar C=C); **HRMS (ESI)** calcd for $C_{12}H_9FNaO_2S^+$ 259.0199 M+Na$^+$ found 259.0202.

7-Fluoro-2-methyl-2,3-dihydro-4*H*-thieno[2,3-*b*]chromen-4-one (3E5)

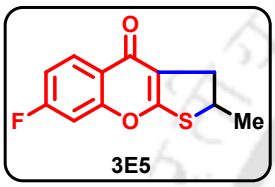

3E5

Off white solid (0.028 g, 78%); **mp** 102 – 104 °C; **^{1}H NMR (500 MHz, $CDCl_3$)** δ 8.20 (dd, J = 8.6, 6.4 Hz, 1H), 7.15 – 7.07 (m, 2H), 4.17 – 4.08 (m, 1H), 3.42 (dd, J = 15.3, 8.5 Hz, 1H), 2.97 (dd, J = 15.3, 5.6 Hz, 1H), 1.55 (d, J = 6.8 Hz, 3H); **^{13}C{^{1}H} NMR (125 MHz, $CDCl_3$)** δ 172.1, 170.7, 164.9 (d, J = 254.0 Hz), 157.8 (d, J = 13.1 Hz), 128.1 (d, J = 10.4 Hz), 120.3 (d, J = 2.5 Hz), 116.4, 113.7 (d, J = 22.5 Hz), 104.4 (d, J = 25.8 Hz), 44.7, 37.3, 22.9; **^{19}F NMR (471 MHz, $CDCl_3$)** δ -104.66; **IR (KBr)** ν_{max}/cm^{-1} 3067 (C=C−H), 2966, 2925 (C−H), 1640 (C=O), 1559, 1434 (Ar C=C); **HRMS (ESI)** calcd for $C_{12}H_{10}FO_2S^+$ 237.0380 M+H$^+$ found 237.0384.

2,6-Dimethyl-2,3-dihydro-4*H*-thieno[2,3-*b*]chromen-4-one (3E6)

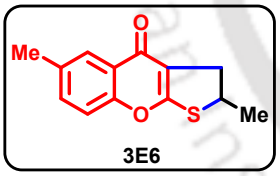

3E6

Off white solid (0.031 g, 88%); **mp** 99 – 101 °C; **^{1}H NMR (500 MHz, $CDCl_3$)** δ 7.98 (s, 1H), 7.39 (dd, J = 8.5, 1.9 Hz, 1H), 7.30 (d, J = 8.5 Hz, 1H), 4.15 – 4.07 (m, 1H), 3.43 (dd, J = 15.2, 8.4 Hz, 1H), 2.98 (dd, J = 15.2, 5.5 Hz, 1H), 2.44 (s, 3H), 1.55 (d, J = 6.8 Hz, 3H); **^{13}C{^{1}H} NMR (125 MHz, $CDCl_3$)** δ 173.1, 170.4, 155.4, 135.2, 133.7, 125.3, 123.1, 117.1, 116.3, 44.5, 37.5, 23.0, 20.9; **IR (KBr)** ν_{max}/cm^{-1} 2961, 2924 (C−H), 1639 (C=O), 1559, 1480 (Ar C=C); **HRMS (ESI)** calcd for $C_{13}H_{13}O_2S^+$ 233.0631 M+H$^+$ found 233.0635.

2,3-Dimethyl-2,3-dihydro-4*H*-thieno[2,3-*b*]chromen-4-one (3E7)

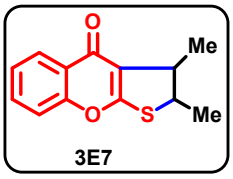

3E7

Brown Liquid (0.026 g, 75%); **^{1}H NMR (400 MHz, $CDCl_3$)** δ 8.21 (dd, J = 7.9, 1.2 Hz, 1H), 7.62 – 7.56 (m, 1H), 7.43 – 7.35 (m, 2H), 3.48 (qd, J = 6.9, 2.6 Hz, 1H), 3.37 (qd, J = 6.8, 2.6 Hz, 1H), 1.51 (d, J = 6.9 Hz, 3H), 1.36 (d, J = 6.8 Hz, 3H); **^{13}C{^{1}H} NMR (125 MHz, $CDCl_3$)** δ 173.06, 169.67, 157.15, 132.53, 125.81, 125.21, 123.81, 120.27, 117.35, 51.52, 45.55, 23.19, 17.65; **IR (KBr)** ν_{max}/cm^{-1} 2965, 2926, 2870 (C−H), 1634 (C=O), 1550, 1460 (Ar C=C); **HRMS (ESI)** calcd for $C_{13}H_{13}O_2S^+$ 233.0631 M+H$^+$ found 233.0635.

6-Chloro-2,3-dimethyl-2,3-dihydro-4*H*-thieno[2,3-*b*]chromen-4-one (3E8)

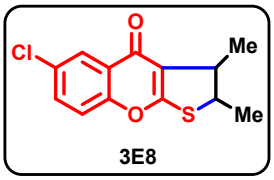

3E8

Off white solid (0.028 g, 71%); **mp** 71 – 72 °C; **^{1}H NMR (400 MHz, $CDCl_3$)** δ 8.17 (d, J = 2.5 Hz, 1H), 7.54 (dd, J = 8.9, 2.5 Hz, 1H), 7.36 (d, J = 8.9 Hz, 1H), 3.50 (qd, J = 6.9, 2.6 Hz, 1H), 3.37 (qd, J = 6.7, 2.4 Hz, 1H), 1.52 (d, J = 6.9 Hz, 3H), 1.36 (d, J = 6.8 Hz, 3H); **^{13}C{^{1}H} NMR (125 MHz, $CDCl_3$)** δ 171.72, 170.20, 155.43, 132.63, 131.18, 125.36, 124.95, 120.39, 118.98, 51.69, 45.52, 23.16, 17.60; **IR (KBr)** ν_{max}/cm^{-1} 2961, 2924, 2852 (C−H), 1637 (C=O), 1550, 1432 (Ar C=C); **HRMS (ESI)** calcd for $C_{13}H_{12}ClO_2S^+$ 267.0242 M+H$^+$ found 267.0242.

2,3,6-Trimethyl-2,3-dihydro-4*H*-thieno[2,3-*b*]chromen-4-one (3E9)

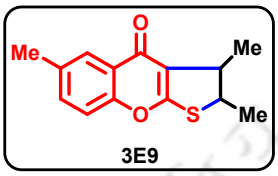

3E9

Yellow solid (0.027 g, 73%); **mp** 54 – 55 °C; **^{1}H NMR (400 MHz, $CDCl_3$)** δ 7.99 (s, 1H), 7.39 (dd, J = 8.5, 1.7 Hz, 1H), 7.30 (d, J = 8.5 Hz, 1H), 3.47 (qd, J = 6.8, 2.4 Hz, 1H), 3.37 (qd, J = 6.7, 2.5 Hz, 1H), 2.44 (s, 3H), 1.51 (d, J = 6.9 Hz, 3H), 1.36 (d, J = 6.8 Hz, 3H); **^{13}C{^{1}H} NMR (125 MHz, $CDCl_3$)** δ 173.21, 169.48, 155.48, 135.14, 133.62, 125.26, 123.45, 120.14, 117.07, 51.49, 45.53, 23.24, 20.89, 17.67; **IR (KBr)** ν_{max}/cm^{-1} 2961, 2925, 2855 (C−H), 1639 (C=O), 1558, 1431 (Ar C=C); **HRMS (ESI)** calcd for $C_{14}H_{15}O_2S^+$ 247.0788 M+H$^+$ found 247.0780.

6-Bromo-2,3,3-trimethyl-2,3-dihydro-4*H*-thieno[2,3-*b*]chromen-4-one (3E10)

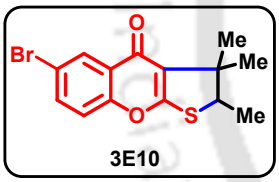

3E10

Off white solid (0.033 g, 69%); **mp** 123 – 125 °C; **^{1}H NMR (400 MHz, $CDCl_3$)** δ 8.29 (d, J = 2.4 Hz, 1H), 7.65 (dd, J = 8.8, 2.5 Hz, 1H), 7.26 (d, J = 8.8 Hz, 1H), 3.82 (q, J = 7.0 Hz, 1H), 1.56 (s, 3H), 1.41 (d, J = 7.0 Hz, 3H), 1.28 (s, 3H); **^{13}C{^{1}H} NMR (125 MHz, $CDCl_3$)** δ 171.23, 170.43, 155.33, 135.35, 128.53, 125.94, 123.75, 119.06, 118.51, 54.68, 48.09, 25.13, 18.52, 13.56; **IR (KBr)** ν_{max}/cm^{-1} 2963, 2925, 2868 (C−H), 1634 (C=O), 1539, 1421 (Ar C=C); **HRMS (ESI)** calcd for $C_{14}H_{14}BrO_2S^+$ 324.9893 M+H$^+$ found 324.9910.

6-Fluoro-2,3,3-trimethyl-2,3-dihydro-4*H*-thieno[2,3-*b*]chromen-4-one (3E11)

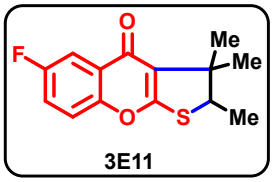

3E11

Yellow solid (0.028 g, 70%); **mp** 101 – 103 °C; **^{1}H NMR (500 MHz, $CDCl_3$)** δ 7.81 (dd, J = 8.4, 3.0 Hz, 1H), 7.37 (dd, J = 9.1, 4.1 Hz, 1H), 7.28 (td, J = 9.1, 3.1 Hz, 1H), 3.82 (q, J = 7.0 Hz, 1H), 1.56 (s, 3H), 1.41 (d, J = 7.0 Hz, 3H), 1.28 (s, 3H); **^{13}C{^{1}H} NMR (125 MHz, $CDCl_3$)** δ 171.76 (d, J = 2.1 Hz), 170.56, 159.61 (d, J = 246.2 Hz), 152.69 (d, J = 1.7 Hz), 125.88 (d, J = 6.9 Hz), 123.15, 120.34 (d, J = 25.5 Hz), 119.05 (d, J = 8.1 Hz), 110.88 (d, J = 24.0 Hz), 54.68, 48.02, 25.14, 18.55, 13.57; **^{19}F NMR (471 MHz, $CDCl_3$)** δ -115.58; **IR (KBr)** ν_{max}/cm^{-1} 2977, 2925, 2873, 2848 (C−H), 1644 (C=O), 1548, 1463 (Ar C=C); **HRMS (ESI)** calcd for $C_{14}H_{14}FO_2S^+$ 265.0694 M+H$^+$ found 265.0711.

7-Fluoro-2,3,3-trimethyl-2,3-dihydro-4*H*-thieno[2,3-*b*]chromen-4-one (3E12)

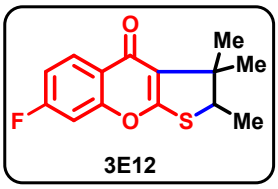

3E12

Off white solid (0.029 g, 72%); **mp** 96 – 98 °C; **^{1}H NMR (400 MHz, $CDCl_3$)** δ 8.18 (dd, J = 8.8, 6.3 Hz, 1H), 7.10 (dd, J = 8.2, 2.4 Hz, 1H), 7.06 (dd, J = 9.0, 2.3 Hz, 1H), 3.81 (q, J = 7.0 Hz, 1H), 1.56 (s, 3H), 1.40 (d, J = 7.0 Hz, 3H), 1.28 (s, 3H); **^{13}C{^{1}H} NMR (125 MHz, $CDCl_3$)** δ 171.91, 170.10, 164.81 (d, J = 253.7 Hz), 157.29 (d, J = 13.1 Hz), 128.02 (d, J = 10.4 Hz), 123.55, 121.25 (d, J = 2.5 Hz), 113.59 (d, J = 22.5 Hz), 104.12 (d, J = 25.7 Hz), 54.70, 48.02, 25.17, 18.53, 13.53; **^{19}F NMR (471 MHz, $CDCl_3$)** δ -104.97; **IR (KBr)** ν_{max}/cm^{-1} 2970, 2925, 2871(C−H), 1640 (C=O), 1545, 1458 (Ar C=C); **HRMS (ESI)** calcd for $C_{14}H_{14}FO_2S^+$ 265.0694 M+H$^+$ found 265.0698.

3-Methyl-4*H*-thieno[2,3-*b*]chromen-4-one (3F1)

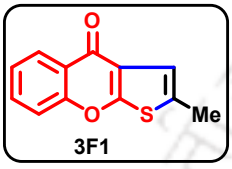

3F1

Yellowish white solid (Method A: 0.029 g, 88%, Method B: 0.026 g, 81%); **mp** 137 – 139 °C; **^{1}H NMR (500 MHz, $CDCl_3$)** δ 8.34 (d, J = 7.9 Hz, 1H), 7.67 (t, J = 7.7 Hz, 1H), 7.50 (d, J = 8.4 Hz, 1H), 7.42 (t, J = 7.5 Hz, 1H), 7.08 (s, 1H), 2.49 (s, 3H); **^{13}C{^{1}H} NMR (125 MHz, $CDCl_3$)** δ 172.6, 166.7, 156.8, 133.2, 130.0, 126.7, 124.7, 123.8, 122.9, 118.2, 117.5, 15.6; **IR (KBr)** ν_{max}/cm^{-1} 3079, 3066 (C=C−H), 2958, 2924 (C−H), 1656 (C=O), 1609, 1463 (Ar C=C); **HRMS (ESI)** calcd for $C_{12}H_9O_2S^+$ 217.0318 M+H$^+$ found 217.0309.

6-Chloro-2-methyl-4*H*-thieno[2,3-*b*]chromen-4-one (3F2)

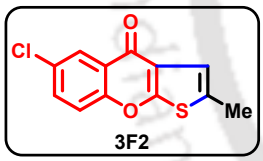

3F2

Yellowish white solid (Method A: 0.032 g, 85%, Method B: 0.030 g, 83%); **mp** 147 – 148 °C; **^{1}H NMR (500 MHz, $CDCl_3$)** δ 8.31 (d, J = 2.2 Hz, 1H), 7.61 (dd, J = 8.9, 2.2 Hz, 1H), 7.46 (d, J = 8.9 Hz, 1H), 7.07 (s, 1H), 2.50 (s, 3H); **^{13}C{^{1}H} NMR (125 MHz, $CDCl_3$)** δ 171.3, 166.8, 155.1, 133.4, 130.7, 130.6, 126.2, 123.9, 123.7, 119.2, 118.2, 15.6; **IR (KBr)** ν_{max}/cm^{-1} 3074 (C=C−H), 2961, 2921 (C−H), 1658 (C=O), 1603, 1459 (Ar C=C); **HRMS (ESI)** calcd for $C_{12}H_8ClO_2S^+$ 250.9928 M+H$^+$ found 250.9919.

6-Bromo-2-methyl-4*H*-thieno[2,3-*b*]chromen-4-one (3F3)

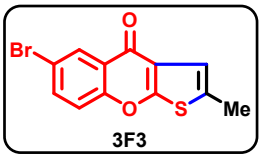

3F3

Yellowish white solid (Method A: 0.039 g, 89%, Method B: 0.035 g, 79%); **mp** 165 – 167 °C; **^{1}H NMR (500 MHz, $CDCl_3$)** δ 8.46 (d, J = 2.4 Hz, 1H), 7.75 (dd, J = 8.9, 2.4 Hz, 1H), 7.40 (d, J = 8.9 Hz, 1H), 7.07 (s, 1H), 2.50 (s, 3H); **^{13}C{^{1}H} NMR (125 MHz, $CDCl_3$)** δ 171.2, 166.7, 155.5, 136.2, 130.7, 129.3, 124.3, 123.7, 119.5, 118.2, 118.1, 15.6; **IR (KBr)** ν_{max}/cm^{-1} 3072 (C=C−H), 2958, 2920 (C−H), 1658 (C=O), 1599, 1459 (Ar C=C); **HRMS (ESI)** calcd for $C_{12}H_7BrNaO_2S^+$ 316.9242 M+Na$^+$ found 316.9246.

6-Fluoro-2-methyl-4*H*-thieno[2,3-*b*]chromen-4-one (3F4)

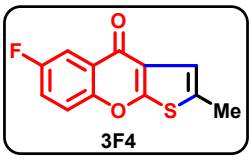

3F4

Yellowish white solid (Method A: 0.031 g, 87%, Method B: 0.030 g, 84%); **mp** 156 – 158 °C; **^{1}H NMR (400 MHz, CDCl$_3$)** δ 7.98 (dd, J = 8.4, 3.1 Hz, 1H), 7.51 (dd, J = 9.1, 4.2 Hz, 1H), 7.43 – 7.37 (m, 1H), 7.07 (d, J = 1.2 Hz, 1H), 2.50 (d, J = 1.2 Hz, 3H); **^{13}C{^{1}H} NMR (100 MHz, CDCl$_3$)** δ 171.7 (d, J = 1.8 Hz), 167.0, 159.2 (d, J = 246.0 Hz), 152.9 (d, J = 1.8 Hz), 130.5, 124.1 (d, J = 7.1 Hz), 123.2, 121.3 (d, J = 25.5 Hz), 119.5 (d, J = 8.0 Hz), 118.0, 111.7 (d, J = 24.0 Hz), 15.7; **^{19}F NMR (376 MHz, CDCl$_3$)** δ -115.94; **IR (KBr)** ν_{max}/cm^{-1} 3077 (C=C−H), 2956, 2923 (C−H), 1653 (C=O), 1624, 1476 (Ar C=C); **HRMS (ESI)** calcd for $C_{12}H_8FO_2S^+$ 235.0224 M+H$^+$ found 235.0217.

7-Fluoro-2-methyl-4*H*-thieno[2,3-*b*]chromen-4-one (3F5)

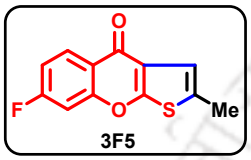

3F5

Yellowish white solid (Method A: 0.032 g, 92%, Method B: 0.027 g, 76%); **mp** 174 – 175 °C; **^{1}H NMR (500 MHz, CDCl$_3$)** δ 8.36 (dd, J = 8.8, 6.4 Hz, 1H), 7.19 (dd, J = 9.0, 2.2 Hz, 1H), 7.15 (td, J = 8.6, 2.3 Hz, 1H), 7.07 (d, J = 1.1 Hz, 1H), 2.50 (d, J = 1.0 Hz, 3H); **^{13}C{^{1}H} NMR (125 MHz, CDCl$_3$)** δ 171.7, 166.6 (d, J = 1.2 Hz), 165.3 (d, J = 255.0 Hz), 157.6 (d, J = 13.3 Hz), 130.4, 129.1 (d, J = 10.7 Hz), 123.8, 119.7 (d, J = 2.5 Hz), 118.2, 113.4 (d, J = 22.6 Hz), 104.4 (d, J = 25.8 Hz), 15.6; **^{19}F NMR (471 MHz, CDCl$_3$)** δ -103.48; **IR (KBr)** ν_{max}/cm^{-1} 3091 (C=C−H), 2958, 2923 (C−H), 1667 (C=O), 1616, 1442 (Ar C=C); **HRMS (ESI)** calcd for $C_{12}H_8FO_2S^+$ 235.0224 M+H$^+$ found 235.0217.

2,6-Dimethyl-4*H*-thieno[2,3-*b*]chromen-4-one (3F6)

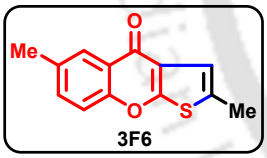

3F6

Yellowish white solid (Method A: 0.029 g, 84%, Method B: 0.030 g, 87%); **mp** 163 – 165 °C; **^{1}H NMR (500 MHz, CDCl$_3$)** δ 8.12 (d, J = 1.6 Hz, 1H), 7.47 (dd, J = 8.5, 1.9 Hz, 1H), 7.39 (d, J = 8.5 Hz, 1H), 7.07 (d, J = 1.3 Hz, 1H), 2.49 (d, J = 1.2 Hz, 3H), 2.47 (s, 3H); **^{13}C{^{1}H} NMR (125 MHz, CDCl$_3$)** δ 172.7, 166.7, 155.1, 134.6, 134.4, 129.8, 126.1, 123.7, 122.5, 118.2, 117.3, 20.9, 15.6; **IR (KBr)** ν_{max}/cm^{-1} 3065 (C=C−H), 2963, 2923 (C−H), 1651 (C=O), 1616, 1476 (Ar C=C); **HRMS (ESI)** calcd for $C_{13}H_{11}O_2S^+$ 231.0474 M+H$^+$ found 231.0478.

2,3-Dimethyl-4*H*-thieno[2,3-*b*]chromen-4-one (3F7)

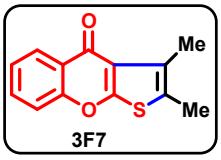

3F7

White solid (Method A: 0.029 g, 85%, Method B: 0.026 g, 76%); **mp** 139 – 140 °C; **^{1}H NMR (500 MHz, CDCl$_3$)** δ 8.33 (dd, J = 8.0, 1.7 Hz, 1H), 7.65 (ddd, J = 8.7, 7.1, 1.7 Hz, 1H), 7.47 (dd, J = 8.4, 1.1 Hz, 1H), 7.40 (ddd, J = 8.1, 7.0, 1.1 Hz, 1H), 2.52 (s, 3H), 2.35 (s, 3H); **^{13}C{^{1}H} NMR (125 MHz, CDCl$_3$)** δ 173.83, 166.31, 156.35, 133.06, 128.91, 126.59, 124.56, 123.48, 122.18, 121.63, 117.34, 13.38, 12.30; **IR (KBr)** ν_{max}/cm^{-1} 3063 (C=C−H), 2963, 2925, 2849 (C−H), 1651 (C=O), 1616, 1480 (Ar C=C); **HRMS (ESI)** calcd for $C_{13}H_{11}O_2S^+$ 231.0474 M+H$^+$ found 231.0476.

6-Chloro-2,3-dimethyl-4*H*-thieno[2,3-*b*]chromen-4-one (3F8)

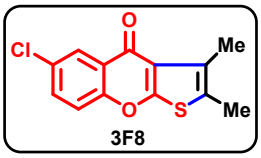

3F8

White solid (Method A: 0.032 g, 82%); **mp** 171 – 172 °C; **^{1}H NMR (500 MHz, $CDCl_3$)** δ 8.28 (d, J = 2.4 Hz, 1H), 7.59 (dd, J = 8.9, 2.6 Hz, 1H), 7.43 (d, J = 8.9 Hz, 1H), 2.51 (s, 3H), 2.36 (s, 3H); **^{13}C{^{1}H} NMR (125 MHz, $CDCl_3$)** δ 172.51, 166.40, 154.65, 133.20, 130.44, 128.87, 126.06, 124.54, 122.20, 122.10, 119.02, 13.36, 12.35; **IR (KBr)** ν_{max}/cm^{-1} 3067 (C=C–H), 2965, 2928, 2852 (C–H), 1654 (C=O), 1618, 1478 (Ar C=C); **HRMS (ESI)** calcd for $C_{13}H_{10}ClO_2S^+$ 265.0085 M+H$^+$ found 265.0098.

2,3,6-Trimethyl-4*H*-thieno[2,3-*b*]chromen-4-one (3F9)

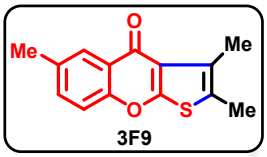

3F9

Off white solid (Method A: 0.030 g, 82%, Method B: 0.026 g, 70%); **mp** 153 – 155 °C; **^{1}H NMR (500 MHz, $CDCl_3$)** δ 8.10 (s, 1H), 7.45 (dd, J = 8.6, 1.6 Hz, 1H), 7.36 (d, J = 8.5 Hz, 1H), 2.52 (s, 3H), 2.47 (s, 3H), 2.34 (s, 3H); **^{13}C{^{1}H} NMR (125 MHz, $CDCl_3$)** δ 173.96, 166.31, 154.68, 134.40, 134.24, 128.92, 125.98, 123.14, 122.10, 121.39, 117.07, 20.92, 13.41, 12.30; **IR (KBr)** ν_{max}/cm^{-1} 3027 (C=C–H), 2959, 2923, 2854 (C–H), 1653 (C=O), 1615, 1478 (Ar C=C); **HRMS (ESI)** calcd for $C_{14}H_{13}O_2S^+$ 245.0631 M+H$^+$ found 245.0635.

6-Bromo-2,3-dimethyl-4*H*-thieno[2,3-*b*]chromen-4-one (3F10)

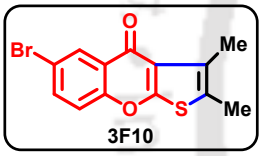

3F10

White solid (Method B: 0.030 g, 65%); **mp** 221 – 222 °C; **^{1}H NMR (500 MHz, $CDCl_3$)** δ 8.43 (d, J = 2.5 Hz, 1H), 7.72 (dd, J = 9.0, 2.5 Hz, 1H), 7.36 (d, J = 8.8 Hz, 1H), 2.51 (s, 3H), 2.35 (s, 3H); **^{13}C{^{1}H} NMR (125 MHz, $CDCl_3$)** δ 172.34, 166.34, 155.11, 135.95, 129.26, 128.92, 124.93, 122.22, 122.15, 119.27, 117.85, 13.33, 12.32; **IR (KBr)** ν_{max}/cm^{-1} 3059 (C=C–H), 2960, 2921, 2848 (C–H), 1655 (C=O), 1612, 1476 (Ar C=C); **HRMS (ESI)** calcd for $C_{13}H_{10}BrO_2S^+$ 308.9579 M+H$^+$ found 308.9580.

6-Fluoro-2,3-dimethyl-4*H*-thieno[2,3-*b*]chromen-4-one (3F11)

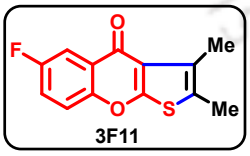

3F11

White solid (Method B: 0.026 g, 71%); **mp** 199 – 201 °C; **^{1}H NMR (500 MHz, $CDCl_3$)** δ 7.95 (dt, J = 8.5, 1.9 Hz, 1H), 7.47 (ddd, 6J = 9.1, 4.2, 1.1 Hz, 1H), 7.37 (dddd, J = 8.8, 7.3, 3.1, 1.1 Hz, 1H), 2.51 (s, 3H), 2.35 (s, 3H); **^{13}C{^{1}H} NMR (125 MHz, $CDCl_3$)** δ 172.85 (d, J = 2.1 Hz), 166.60, 159.21 (d, J = 245.8 Hz), 152.47 (d, J = 1.8 Hz), 128.70, 124.70 (d, J = 7.2 Hz), 122.07, 121.62, 121.08 (d, J = 25.6 Hz), 119.24 (d, J = 8.2 Hz), 111.50 (d, J = 24.0 Hz), 13.33, 12.32; **IR (KBr)** ν_{max}/cm^{-1} 3074 (C=C–H), 2964, 2923, 2859 (C–H), 1652 (C=O), 1623, 1471 (Ar C=C); **HRMS (ESI)** calcd for $C_{13}H_{10}FO_2S^+$ 249.0380 M+H$^+$ found 249.0380.

3-Ethyl-2-methyl-4*H*-thieno[2,3-*b*]chromen-4-one (3F12)

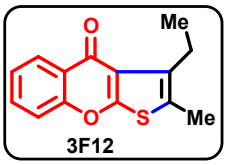

Light yellow solid (Method B: 0.026 g, 72%); **mp** 86 – 88 °C; **^{1}H NMR (400 MHz, $CDCl_3$)** δ 8.33 (dd, J = 8.0, 1.5 Hz, 1H), 7.64 (ddd, J = 8.6, 7.2, 1.7 Hz, 1H), 7.46 (d, J = 8.4 Hz, 1H), 7.42 – 7.37 (m, 1H), 2.99 (q, J = 7.4 Hz, 2H), 2.36 (s, 3H), 1.21 (t, J = 7.4 Hz, 3H); **^{13}C{^{1}H} NMR (125 MHz, $CDCl_3$)** δ 173.28, 166.68, 156.28, 135.51, 133.00, 126.60, 124.52, 123.44, 121.61, 121.44, 117.28, 20.79, 14.83, 12.02; **IR (KBr)** ν_{max}/cm^{-1} 3075 (C=C–H), 2970, 2929, 2872 (C–H), 1649 (C=O), 1610, 1462 (Ar C=C); **HRMS (ESI)** calcd for $C_{14}H_{13}O_2S^+$ 245.0631 M+H$^+$ found 245.0634.

3-Ethyl-2,6-dimethyl-4*H*-thieno[2,3-*b*]chromen-4-one (3F13)

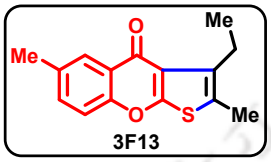

Yellow solid (Method B: 0.026 g, 68%); **mp** 135 – 137 °C; **^{1}H NMR (400 MHz, $CDCl_3$)** δ 8.11 (d, J = 1.4 Hz, 1H), 7.45 (dd, J = 8.5, 2.2 Hz, 1H), 7.36 (d, J = 8.5 Hz, 1H), 2.99 (q, J = 7.4 Hz, 2H), 2.46 (s, 3H), 2.36 (s, 3H), 1.20 (t, J = 7.4 Hz, 3H); **^{13}C{^{1}H} NMR (125 MHz, $CDCl_3$)** δ 173.43, 166.71, 154.61, 135.51, 134.35, 134.18, 126.01, 123.08, 121.51, 121.21, 117.02, 20.91, 20.81, 14.83, 12.03; **IR (KBr)** ν_{max}/cm^{-1} 3032 (C=C–H), 2973, 2928, 2868 (C–H), 1643 (C=O), 1614, 1477 (Ar C=C); **HRMS (ESI)** calcd for $C_{15}H_{15}O_2S^+$ 259.0788 M+H$^+$ found 259.0797.

6-Chloro-3-ethyl-2-methyl-4*H*-thieno[2,3-*b*]chromen-4-one (3F14)

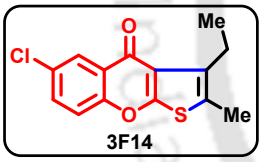

Yellow solid (Method B: 0.028 g, 67%); **mp** 121 – 123 °C; **^{1}H NMR (500 MHz, $CDCl_3$)** δ 8.29 (d, J = 2.6 Hz, 1H), 7.59 (dd, J = 8.9, 2.6 Hz, 1H), 7.43 (d, J = 8.9 Hz, 1H), 2.98 (q, J = 7.4 Hz, 2H), 2.38 (s, 3H), 1.20 (t, J = 7.4 Hz, 3H); **^{13}C{^{1}H} NMR (125 MHz, $CDCl_3$)** δ 172.01, 166.82, 154.61, 135.50, 133.16, 130.43, 126.12, 124.53, 122.03, 121.56, 118.98, 20.78, 14.79, 12.08; **IR (KBr)** ν_{max}/cm^{-1} 3080 (C=C–H), 2961, 2925, 2855 (C–H), 1653 (C=O), 1616, 1440 (Ar C=C); **HRMS (ESI)** calcd for $C_{14}H_{12}ClO_2S^+$ 279.0242 M+H$^+$ found 279.0261.

3-Ethyl-7-fluoro-2-methyl-4*H*-thieno[2,3-*b*]chromen-4-one (3F15)

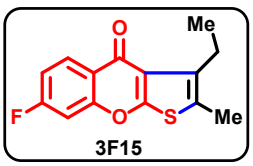

White solid (0.029 g, 74%); **mp** 81 – 83 °C; **^{1}H NMR (500 MHz, $CDCl_3$)** δ 8.34 (dd, J = 8.6, 6.5 Hz, 1H), 7.18 – 7.11 (m, 2H), 2.98 (q, J = 7.4 Hz, 2H), 2.37 (s, 3H), 1.20 (t, J = 7.4 Hz, 3H); **^{13}C{^{1}H} NMR (125 MHz, $CDCl_3$)** δ 172.44, 166.60, 165.20 (d, J = 254.3 Hz), 157.13 (d, J = 13.3 Hz), 135.54, 129.01 (d, J = 10.6 Hz), 121.84, 121.63, 120.31 (d, J = 2.4 Hz), 113.18 (d, J = 22.6 Hz), 104.11 (d, J = 25.7 Hz), 20.78, 14.80, 12.04; **^{19}F NMR (471 MHz, $CDCl_3$)** δ -104.07; **IR (KBr)** ν_{max}/cm^{-1} 3064 (C=C–H), 2967, 2930, 2866 (C–H), 1647 (C=O), 1618, 1453 (Ar C=C); **HRMS (ESI)** calcd for $C_{14}H_{12}FO_2S^+$ 263.0537 M+H$^+$ found 263.0536.

4*H*,5*H*-Thiopyrano[2,3-*b*]chromen-5-one (3G1)

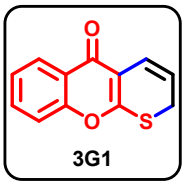

Yellowish White solid (0.031 g, 94%); **mp** 138 – 140 °C; **^{1}H NMR (500 MHz, $CDCl_3$)** δ 8.20 (dd, J = 8.1, 1.8 Hz, 1H), 7.65 – 7.57 (m, 1H), 7.41 – 7.35 (m, 2H), 6.92 – 6.86 (m, 1H), 5.68 (dt, J = 9.9, 4.9 Hz, 1H), 3.74 (dd, J = 4.9, 1.5 Hz, 2H); **^{13}C{^{1}H} NMR (125 MHz, $CDCl_3$)** δ 172.0, 165.8, 156.1, 133.2, 126.3, 125.3, 123.6, 122.8, 117.4, 116.0, 114.4, 27.8; **IR (KBr)** ν_{max}/cm^{-1} 3049 (C=C–H), 2959, 2925 (C–H), 1632 (C=O), 1535, 1462 (Ar C=C); **HRMS (ESI)** calcd for $C_{12}H_9O_2S^+$ 217.0318 M+H$^+$ found 217.0308.

7-Chloro-4*H*,5*H*-thiopyrano[2,3-*b*]chromen-5-one (3G2)

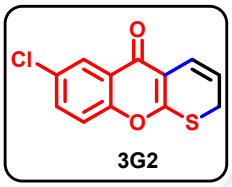

Brown solid (0.035 g, 92%); **mp** 128 – 130 °C; **^{1}H NMR (500 MHz, $CDCl_3$)** δ 8.16 (d, J = 2.6 Hz, 1H), 7.55 (dd, J = 8.9, 2.6 Hz, 1H), 7.34 (dd, J = 8.9, 3.3 Hz, 1H), 6.95 – 6.84 (m, 1H), 5.69 (dt, J = 9.9, 4.9 Hz, 1H), 3.75 (dd, J = 4.9, 1.4 Hz, 2H); **^{13}C{^{1}H} NMR (125 MHz, $CDCl_3$)** δ 170.8, 166.2, 154.4, 133.4, 131.2, 125.8, 124.6, 122.6, 119.1, 116.0, 114.8, 27.8; **IR (KBr)** ν_{max}/cm^{-1} 3071 (C=C–H), 2961, 2923 (C–H), 1636 (C=O), 1527, 1466 (Ar C=C); **HRMS (ESI)** calcd for $C_{12}H_8ClO_2S^+$ 250.9928 M+H$^+$ found 250.9917.

7-Bromo-4*H*,5*H*-thiopyrano[2,3-*b*]chromen-5-one (3G3)

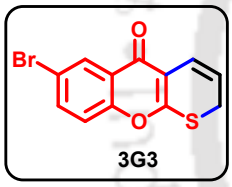

Yellow solid (0.042 g, 95%); **mp** 132 – 134 °C; **^{1}H NMR (500 MHz, $CDCl_3$)** δ 8.32 (d, J = 2.2 Hz, 1H), 7.69 (dd, J = 8.8, 2.3 Hz, 1H), 7.27 (d, J = 8.9 Hz, 1H), 6.86 (d, J = 9.9 Hz, 1H), 5.69 (dt, J = 9.9, 4.9 Hz, 1H), 3.78 – 3.71 (m, 2H); **^{13}C{^{1}H} NMR (125 MHz, $CDCl_3$)** δ 170.6, 166.2, 154.8, 136.2, 129.0, 125.0, 122.6, 119.3, 118.7, 116.1, 114.8, 27.8; **IR (KBr)** ν_{max}/cm^{-1} 3072 (C=C–H), 2959, 2924 (C–H), 1634 (C=O), 1530, 1460 (Ar C=C); **HRMS (ESI)** calcd for $C_{12}H_7BrNaO_2S^+$ 316.9242 M+Na$^+$ found 316.9245.

7-Fluoro-4*H*,5*H*-thiopyrano[2,3-*b*]chromen-5-one (3G4)

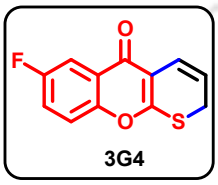

Yellow solid (0.033 g, 93%); **mp** 137 – 139 °C; **^{1}H NMR (500 MHz, $CDCl_3$)** δ 7.84 (dd, J = 8.2, 3.0 Hz, 1H), 7.39 (dd, J = 9.2, 4.2 Hz, 1H), 7.35 – 7.30 (m, 1H), 6.88 (d, J = 9.9 Hz, 1H), 5.69 (dt, J = 10.0, 5.0 Hz, 1H), 3.75 (dd, J = 4.9, 1.5 Hz, 2H); **^{13}C{^{1}H} NMR (100 MHz, $CDCl_3$)** δ 171.2 (d, J = 2.2 Hz), 166.2, 159.6 (d, J = 246.8 Hz), 152.3 (d, J = 1.8 Hz), 124.8 (d, J = 7.3 Hz), 122.6, 121.3 (d, J = 25.5 Hz), 119.4 (d, J = 8.1 Hz), 115.5, 114.8, 111.4 (d, J = 23.9 Hz), 27.8; **^{19}F NMR (471 MHz, $CDCl_3$)** δ -114.96; **IR (KBr)** ν_{max}/cm^{-1} 3073 (C=C–H), 2958, 2925 (C–H), 1635 (C=O), 1537, 1476 (Ar C=C); **HRMS (ESI)** calcd for $C_{12}H_8FO_2S^+$ 235.0224 M+H$^+$ found 235.0213.

8-Fluoro-4*H*,5*H*-thiopyrano[2,3-*b*]chromen-5-one (3G5)

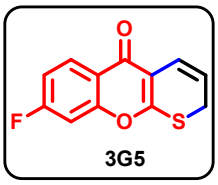

Yellow solid (0.033 g, 95%); **mp** 128 – 130 °C; **^{1}H NMR (500 MHz, $CDCl_3$)** δ 8.21 (dd, J = 8.8, 6.3 Hz, 1H), 7.11 (dd, J = 8.4, 2.4 Hz, 1H), 7.09 – 7.05 (m, 1H), 6.87 (d, J = 9.9 Hz, 1H), 5.68 (dt, J = 10.0, 5.0 Hz, 1H), 3.74 (d, J = 4.2 Hz, 2H); **^{13}C{^{1}H} NMR (125 MHz, $CDCl_3$)** δ 171.2, 165.9, 165.3 (d, J = 254.9 Hz), 156.9 (d, J = 13.2 Hz), 128.8 (d, J = 10.4 Hz), 122.6, 120.4 (d, J = 2.4 Hz), 116.1, 114.6, 113.9 (d, J = 22.6 Hz), 104.3 (d, J = 25.5 Hz), 27.8; **^{19}F NMR (471 MHz, $CDCl_3$)** δ -103.31; **IR (KBr)** ν_{max}/cm^{-1} 3072 (C=C–H), 2957, 2929 (C–H), 1634 (C=O), 1538, 1491 (Ar C=C); **HRMS (ESI)** calcd for $C_{12}H_8FO_2S^+$ 235.0224 M+H$^+$ found 235.0209.

7-Methyl-4*H*,5*H*-thiopyrano[2,3-*b*]chromen-5-one (3G6)

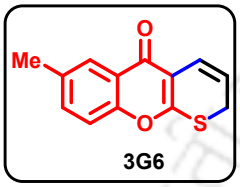

Yellowish White solid (0.033 g, 96%); **mp** 141 – 143 °C; **^{1}H NMR (500 MHz, $CDCl_3$)** δ 7.96 (s, 1H), 7.39 (dd, J = 8.5, 1.8 Hz, 1H), 7.24 (s, 1H), 6.87 (d, J = 9.9 Hz, 1H), 5.65 (dt, J = 9.9, 5.0 Hz, 1H), 3.71 (dd, J = 4.9, 1.3 Hz, 2H), 2.42 (s, 3H); **^{13}C{^{1}H} NMR (125 MHz, $CDCl_3$)** δ 172.2, 165.6, 154.4, 135.3, 134.4, 125.7, 123.2, 122.9, 117.1, 115.9, 114.2, 27.7, 20.9; **IR (KBr)** ν_{max}/cm^{-1} 3055 (C=C–H), 2962, 2925 (C–H), 1634 (C=O), 1553, 1481 (Ar C=C); **HRMS (ESI)** calcd for $C_{13}H_{11}O_2S^+$ 231.0474 M+H$^+$ found 231.0479.

4-Methyl-2*H*,5*H*-thiopyrano[2,3-*b*]chromen-5-one (3G7)

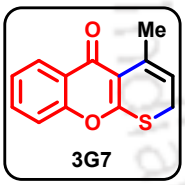

Yellow solid (0.030 g, 88%); **mp** 100 – 102 °C; **^{1}H NMR (500 MHz, $CDCl_3$)** δ 8.18 (dd, J = 8.2, 1.5 Hz, 1H), 7.63 – 7.58 (m, 1H), 7.40 – 7.34 (m, 2H), 5.53 (td, J = 5.5, 1.2 Hz, 1H), 3.45 (d, J = 5.3 Hz, 2H), 2.27 (s, 3H); **^{13}C{^{1}H} NMR (125 MHz, $CDCl_3$)** δ 173.42, 168.45, 155.45, 135.85, 133.11, 126.31, 125.16, 124.65, 118.96, 117.07, 113.46, 26.58, 21.04; **IR (KBr)** ν_{max}/cm^{-1} 3055 (C=C–H), 2962, 2925 (C–H), 1634 (C=O), 1553, 1481 (Ar C=C); **HRMS (ESI)** calcd for $C_{13}H_{11}O_2S^+$ 231.0474 M+H$^+$ found 231.0489.

4,7-Dimethyl-2*H*,5*H*-thiopyrano[2,3-*b*]chromen-5-one (3G8)

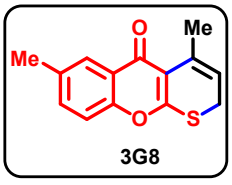

Yellow solid (0.032 g, 86%); **mp** 122 – 123 °C; **^{1}H NMR (400 MHz, $CDCl_3$)** δ 7.96 (d, J = 1.8 Hz, 1H), 7.41 (dd, J = 8.4, 2.0 Hz, 1H), 7.26 (d, J = 8.4 Hz, 1H), 5.55 – 5.50 (m, 1H), 3.44 (dd, J = 5.7, 1.2 Hz, 2H), 2.44 (s, 3H), 2.27 (d, J = 1.4 Hz, 3H); **^{13}C{^{1}H} NMR (125 MHz, $CDCl_3$)** δ 173.57, 168.24, 153.77, 135.98, 135.08, 134.27, 125.72, 124.33, 118.84, 116.83, 113.37, 77.26, 77.00, 76.75, 26.59, 21.04, 20.95; **IR (KBr)** ν_{max}/cm^{-1} 3068 (C=C–H), 2966, 2927, 2872 (C–H), 1647 (C=O), 1543, 1471 (Ar C=C); **HRMS (ESI)** calcd for $C_{14}H_{13}O_2S^+$ 245.0631 M+H$^+$ found 245.0638.

7-Bromo-4-methyl-2*H*,5*H*-thiopyrano[2,3-*b*]chromen-5-one (3G9)

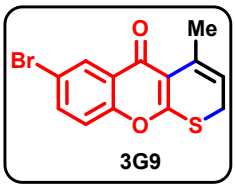

Yellow solid (0.038 g, 82%); **mp** 130 – 132 °C; **^{1}H NMR (500 MHz, $CDCl_3$)** δ 8.29 (d, J = 2.0 Hz, 1H), 7.68 (dd, J = 8.8, 1.9 Hz, 1H), 7.26 (d, J = 8.8 Hz, 1H), 5.53 (t, J = 5.6 Hz, 1H), 3.46 (d, J = 5.7 Hz, 2H), 2.25 (s, 3H); **^{13}C{^{1}H} NMR (125 MHz, $CDCl_3$)** δ 171.94, 168.86, 154.19, 136.01, 135.63, 129.00, 125.99, 119.01, 118.98, 118.49, 113.73, 26.60, 20.92; **IR (KBr)** ν_{max}/cm^{-1} 3073 (C=C–H), 2962, 2923, 2891 (C–H), 1651 (C=O), 1605 (C=C), 1507, 1459 (Ar C=C); **HRMS (ESI)** calcd for $C_{13}H_{10}BrO_2S^+$ 308.9579 M+H$^+$ found 308.9579.

7-Fluoro-4-methyl-2*H*,5*H*-thiopyrano[2,3-*b*]chromen-5-one (3G10)

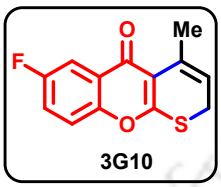

Yellow solid (0.032 g, 85%); **mp** 81 – 83 °C; **^{1}H NMR (500 MHz, $CDCl_3$)** δ 7.81 (dd, J = 8.4, 3.0 Hz, 1H), 7.37 (dd, J = 9.0, 4.2 Hz, 1H), 7.32 (tdd, J = 9.0, 3.1, 1.1 Hz, 1H), 5.57 – 5.51 (m, 1H), 3.46 (d, J = 5.7 Hz, 2H), 2.26 (s, 3H); **^{13}C{^{1}H} NMR (126 MHz, $CDCl_3$)** δ 172.50 (d, J = 2.2 Hz), 168.93, 159.55 (d, J = 246.4 Hz), 151.64 (d, J = 1.6 Hz), 135.65, 125.86 (d, J = 7.3 Hz), 121.15 (d, J = 25.5 Hz), 119.10 (d, J = 8.1 Hz), 118.35, 113.76, 111.33 (d, J = 24.0 Hz), 26.58, 20.98; **IR (KBr)** ν_{max}/cm^{-1} 3074 (C=C–H), 2961, 2929, 2860 (C–H), 1650 (C=O), 1623 (C=C), 1543, 1476 (Ar C=C); **HRMS (ESI)** calcd for $C_{13}H_9FO_2S^+$ 249.0380 M+H$^+$ found 249.0378.

4-Ethyl-2*H*,5*H*-thiopyrano[2,3-*b*]chromen-5-one (3G11)

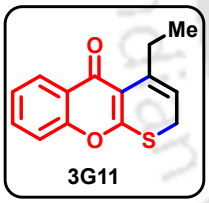

Yellow solid (0.030 g, 83%); **mp** 118 – 119 °C; **^{1}H NMR (400 MHz, $CDCl_3$)** δ 8.19 (dd, J = 8.2, 1.6 Hz, 1H), 7.61 (ddd, J = 8.8, 7.2, 1.7 Hz, 1H), 7.40 – 7.35 (m, 2H), 5.60 (tt, J = 5.8, 1.3 Hz, 1H), 3.45 (d, J = 5.8 Hz, 2H), 2.80 (td, J = 7.4, 0.9 Hz, 2H), 0.99 (t, J = 7.4 Hz, 3H); **^{13}C{^{1}H} NMR (125 MHz, $CDCl_3$)** δ 173.29, 168.82, 155.44, 142.13, 133.10, 126.36, 125.14, 124.64, 118.29, 117.07, 112.37, 26.83, 26.55, 13.67; **IR (KBr)** ν_{max}/cm^{-1} 3073 (C=C–H), 2966, 2925, 2872 (C–H), 1643 (C=O), 1509, 1463 (Ar C=C); **HRMS (ESI)** calcd for $C_{14}H_{13}O_2S^+$ 245.0631 M+H$^+$ found 245.0628.

4-Ethyl-7-methyl-2*H*,5*H*-thiopyrano[2,3-*b*]chromen-5-one (3G12)

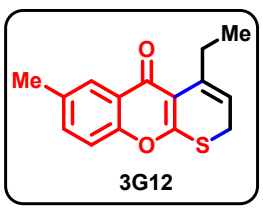

Yellow solid (0.033 g, 85%); **mp** 142 – 144 °C; **^{1}H NMR (400 MHz, $CDCl_3$)** δ 7.96 (d, J = 1.9 Hz, 1H), 7.41 (dd, J = 8.5, 1.9 Hz, 1H), 7.26 (d, J = 8.5 Hz, 1H), 5.59 (tt, J = 5.8, 1.3 Hz, 1H), 3.44 (d, J = 5.8 Hz, 2H), 2.79 (qd, J = 7.3, 0.9 Hz, 2H), 2.44 (s, 3H), 0.98 (t, J = 7.4 Hz, 3H); **^{13}C{^{1}H} NMR (126 MHz, $CDCl_3$)** δ 173.43, 168.64, 153.74, 142.22, 135.05, 134.25, 125.74, 124.29, 118.12, 116.81, 112.30, 77.25, 77.00, 76.75, 26.84, 26.55, 20.94, 13.67; **IR (KBr)** ν_{max}/cm^{-1} 3063 (C=C–H), 2958, 2925, 2854 (C–H), 1638 (C=O), 1614 (C=C), 1519, 1480 (Ar C=C); **HRMS (ESI)** calcd for $C_{15}H_{15}O_2S^+$ 259.0787 M+H$^+$ found 259.0796.

7-Chloro-4-ethyl-2*H*,5*H*-thiopyrano[2,3-*b*]chromen-5-one (3G13)

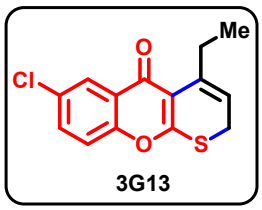

Yellow solid (0.033 g, 78%); **mp** 118 – 120 °C; **^{1}H NMR (500 MHz, $CDCl_3$)** δ 8.15 (d, J = 2.4 Hz, 1H), 7.55 (dd, J = 8.8, 2.5 Hz, 1H), 7.33 (d, J = 8.9 Hz, 1H), 5.61 (t, J = 5.7 Hz, 1H), 3.46 (d, J = 5.7 Hz, 2H), 2.77 (q, J = 7.3 Hz, 2H), 0.98 (t, J = 7.4 Hz, 3H); **^{13}C{^{1}H} NMR (125 MHz, $CDCl_3$)** δ 171.97, 169.26, 153.72, 141.90, 133.25, 131.02, 125.84, 125.59, 118.78, 118.23, 112.66, 26.75, 26.56, 13.62; **IR (KBr)** ν_{max}/cm^{-1} 3075 (C=C–H), 2966, 2926, 2855 (C–H), 1645 (C=O), 1608 (C=C), 1507, 1464 (Ar C=C); **HRMS (ESI)** calcd for $C_{14}H_{12}ClO_2S^+$ 279.0242 M+H$^+$ found 249.0248.

4-Ethyl-8-fluoro-2*H*,5*H*-thiopyrano[2,3-*b*]chromen-5-one (3G14)

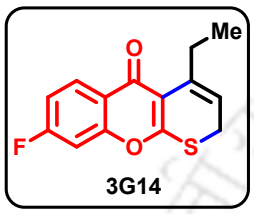

Yellow solid (0.032 g, 81%); **mp** 95 – 97 °C; **^{1}H NMR (500 MHz, $CDCl_3$)** δ 8.19 (dd, J = 8.8, 6.3 Hz, 1H), 7.10 (td, J = 8.6, 2.3 Hz, 1H), 7.06 (dd, J = 8.8, 2.2 Hz, 1H), 5.60 (t, J = 5.8 Hz, 1H), 3.45 (d, J = 5.7 Hz, 2H), 2.77 (q, J = 7.3 Hz, 2H), 0.99 (t, J = 7.4 Hz, 3H); **^{13}C{^{1}H} NMR (125 MHz, $CDCl_3$)** δ 172.41, 169.02, 165.25 (d, J = 254.6 Hz), 156.18 (d, J = 13.3 Hz), 141.94, 128.82 (d, J = 10.5 Hz), 121.42 (d, J = 2.5 Hz), 118.33, 113.78 (d, J = 22.7 Hz), 112.51, 103.91 (d, J = 25.6 Hz), 26.80, 26.58, 13.65; **^{19}F NMR (471 MHz, $CDCl_3$)** δ -103.76; **IR (KBr)** ν_{max}/cm^{-1} 3071 (C=C–H), 2969, 2934, 2877 (C–H), 1645 (C=O), 1613 (C=C), 1507, 1437 (Ar C=C); **HRMS (ESI)** calcd for $C_{14}H_{12}FO_2S^+$ 263.0537 M+H$^+$ found 263.0536.

2,2-Dimethyl-2*H*,5*H*-thiopyrano[2,3-*b*]chromen-5-one (3I1)

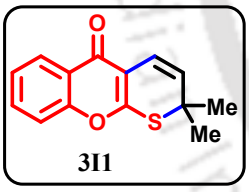

Yellow solid (0.025 g, 68%); **mp** 134 – 135 °C; **^{1}H NMR (500 MHz, $CDCl_3$)** δ 8.22 (d, J = 7.9 Hz, 1H), 7.65 – 7.58 (m, 1H), 7.44 – 7.32 (m, 2H), 6.83 (d, J = 10.0 Hz, 1H), 5.54 (d, J = 10.0 Hz, 1H), 1.54 (s, 6H); **^{13}C{^{1}H} NMR (125 MHz, $CDCl_3$)** δ 172.2, 165.6, 156.2, 133.2, 127.8, 126.3, 125.2, 123.4, 119.3, 117.5, 114.8, 47.4, 30.0; **IR (KBr)** ν_{max}/cm^{-1} 3068 (C=C–H), 2976, 2924 (C–H), 1637 (C=O), 1535, 1463 (Ar C=C); **HRMS (ESI)** calcd for $C_{14}H_{12}NaO_2S^+$ 267.0450 M+Na$^+$ found 267.0454.

7-Chloro-2,2-dimethyl-2*H*,5*H*-thiopyrano[2,3-*b*]chromen-5-one (3I2)

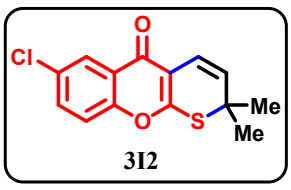

Yellowish white solid (0.028 g, 66%); **mp** 131 – 132 °C; **^{1}H NMR (500 MHz, $CDCl_3$)** δ 8.17 (d, J = 2.5 Hz, 1H), 7.55 (dd, J = 8.9, 2.6 Hz, 1H), 7.35 (d, J = 8.9 Hz, 1H), 6.80 (d, J = 10.0 Hz, 1H), 5.55 (d, J = 10.0 Hz, 1H), 1.54 (s, 6H); **^{13}C{^{1}H} NMR (125 MHz, $CDCl_3$)** δ 171.0, 166.0, 154.5, 133.3, 131.1, 128.2, 125.8, 124.4, 119.2, 119.0, 114.7, 47.6, 30.1; **IR (KBr)** ν_{max}/cm^{-1} 3082 (C=C–H), 2971, 2930 (C–H), 1635 (C=O), 1529, 1461 (Ar C=C); **HRMS (ESI)** calcd for $C_{14}H_{12}ClO_2S^+$ 279.0242 M+H$^+$ found 279.0235.

7-Bromo-2,2-dimethyl-2*H*,5*H*-thiopyrano[2,3-*b*]chromen-5-one (3I3)

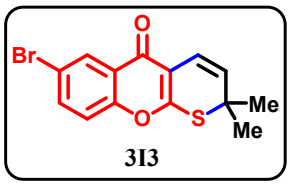

3I3

Yellow solid (0.030 g, 64%); **mp** 148 – 150 °C; **^{1}H NMR (400 MHz, $CDCl_3$)** δ 8.33 (d, J = 2.5 Hz, 1H), 7.70 (dd, J = 8.9, 2.5 Hz, 1H), 7.29 (d, J = 8.9 Hz, 1H), 6.80 (d, J = 10.0 Hz, 1H), 5.55 (d, J = 10.0 Hz, 1H), 1.54 (s, 6H); **^{13}C{^{1}H} NMR (100 MHz, $CDCl_3$)** δ 170.9, 166.0, 154.9, 136.1, 128.9, 128.2, 124.8, 119.4, 119.0, 118.5, 114.8, 47.6, 30.1; **IR (KBr)** ν_{max}/cm^{-1} 3066 (C=C−H), 2968, 2929 (C−H), 1641 (C=O), 1531, 1461 (Ar C=C); **HRMS (ESI)** calcd for $C_{14}H_{11}BrNaO_2S^+$ 344.9556 M+Na$^+$ found 344.9555.

7-Fluoro-2,2-dimethyl-2*H*,5*H*-thiopyrano[2,3-*b*]chromen-5-one (3I4)

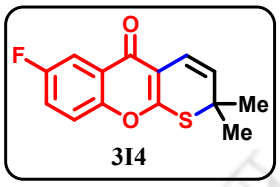

3I4

Yellow solid (0.027 g, 69%); **mp** 118 – 119 °C; **^{1}H NMR (400 MHz, $CDCl_3$)** δ 7.85 (dd, J = 8.3, 3.0 Hz, 1H), 7.40 (dd, J = 9.1, 4.2 Hz, 1H), 7.33 (ddd, J = 9.1, 7.5, 3.1 Hz, 1H), 6.81 (d, J = 10.0 Hz, 1H), 5.56 (d, J = 10.0 Hz, 1H), 1.54 (s, 6H); **^{13}C{^{1}H} NMR (100 MHz, $CDCl_3$)** δ 171.4 (d, J = 2.2 Hz), 166.0, 159.5 (d, J = 246.6 Hz), 152.4 (d, J = 1.7 Hz), 128.2, 124.6 (d, J = 7.4 Hz), 121.2 (d, J = 25.5 Hz), 119.5 (d, J = 8.1 Hz), 119.1, 114.2, 111.3 (d, J = 23.9 Hz), 47.5, 30.1; **^{19}F NMR (471 MHz, $CDCl_3$)** δ -115.15; **IR (KBr)** ν_{max}/cm^{-1} 3074 (C=C−H), 2961, 2925 (C−H), 1644 (C=O), 1546, 1476 (Ar C=C); **HRMS (ESI)** calcd for $C_{14}H_{12}FO_2S^+$ 263.0537 M+H$^+$ found 263.0541.

8-Fluoro-2,2-dimethyl-2*H*,5*H*-thiopyrano[2,3-*b*]chromen-5-one (3I5)

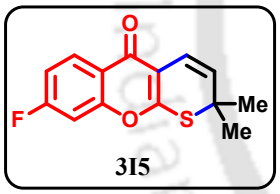

3I5

Yellow solid (0.028 g, 72%); **mp** 104 – 106 °C; **^{1}H NMR (500 MHz, $CDCl_3$)** δ 8.23 (dd, J = 8.7, 6.3 Hz, 1H), 7.14 – 7.07 (m, 2H), 6.80 (d, J = 10.0 Hz, 1H), 5.54 (d, J = 10.0 Hz, 1H), 1.54 (s, 6H); **^{13}C{^{1}H} NMR (125 MHz, $CDCl_3$)** δ 171.4, 165.7, 165.3 (d, J = 254.8 Hz), 157.0 (d, J = 13.1 Hz), 128.8 (d, J = 10.5 Hz), 128.1, 120.2 (d, J = 2.4 Hz), 119.0, 114.8, 113.8 (d, J = 22.6 Hz), 104.4 (d, J = 25.7 Hz), 47.5, 30.0; **^{19}F NMR (471 MHz, $CDCl_3$)** δ -103.47; **IR (KBr)** ν_{max}/cm^{-1} 3078 (C=C−H), 2972, 2924 (C−H), 1642 (C=O), 1536, 1436 (Ar C=C); **HRMS (ESI)** calcd for $C_{14}H_{11}FNaO_2S^+$ 285.0356 M+Na$^+$ found 285.0358.

2,2,7-Trimethyl-2*H*,5*H*-thiopyrano[2,3-*b*]chromen-5-one (3I6)

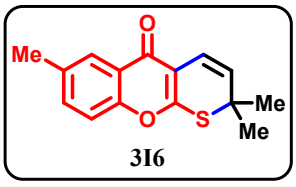

3I6

Yellow solid (0.024 g, 61%); **mp** 95 – 96 °C; **^{1}H NMR (500 MHz, $CDCl_3$)** δ 8.00 (s, 1H), 7.42 (dd, J = 8.8, 1.9 Hz, 1H), 7.29 (d, J = 8.5 Hz, 1H), 6.83 (d, J = 10.0 Hz, 1H), 5.53 (d, J = 10.0 Hz, 1H), 2.44 (s, 3H), 1.54 (s, 6H); **^{13}C{^{1}H} NMR (125 MHz, $CDCl_3$)** δ 172.4, 165.4, 154.5, 135.1, 134.3, 127.7, 125.7, 123.1, 119.4, 117.2, 114.6, 47.3, 30.0, 20.9; **IR (KBr)** ν_{max}/cm^{-1} 3071 (C=C−H), 2958, 2924 (C−H), 1640 (C=O), 1538, 1481 (Ar C=C); **HRMS (ESI)** calcd for $C_{15}H_{15}O_2S^+$ 259.0787 M+H$^+$ found 259.0788.

3.9 Copies of ^{1}H NMR, $^{13}C\{^{1}H\}$ NMR and HRMS spectra of Compounds

Figure 3.4a: ^{1}H NMR (500 MHz, $CDCl_3$) spectrum of compound **3C1**.

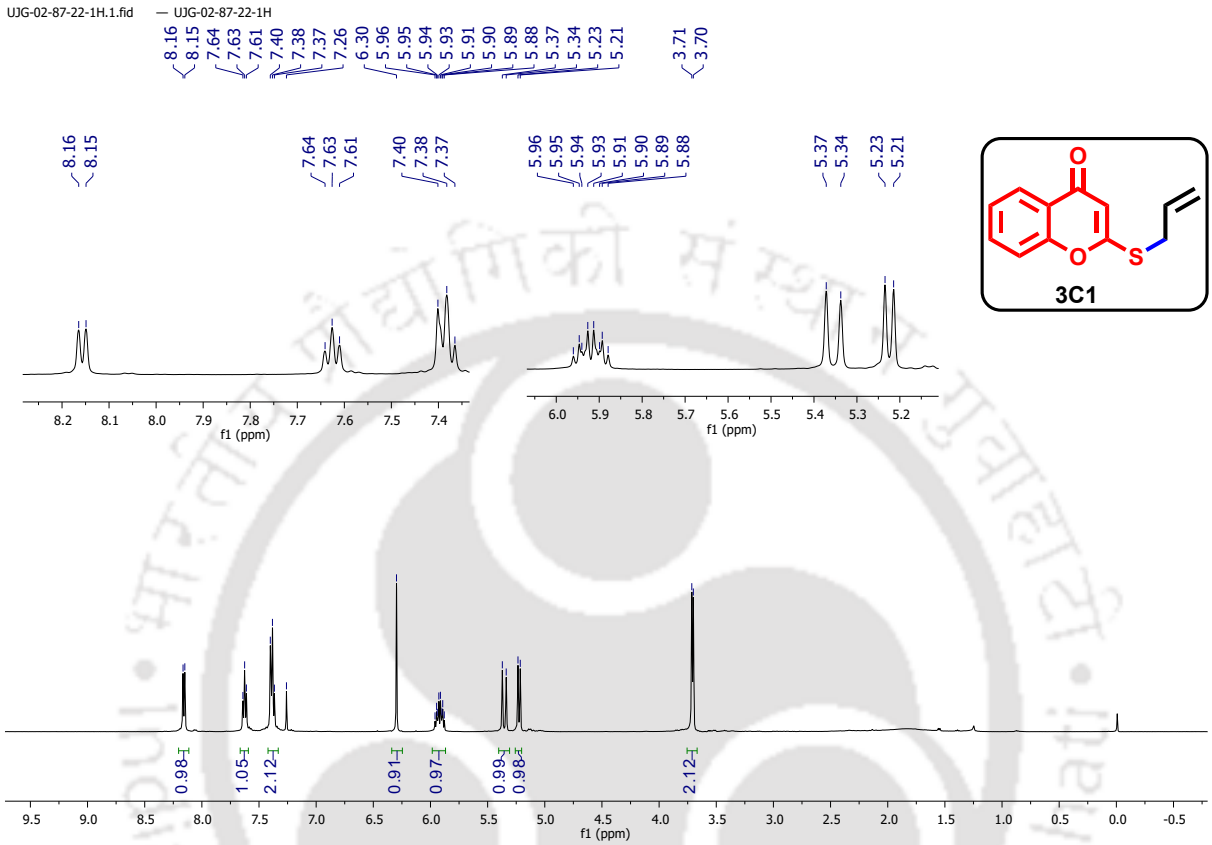

Figure 3.4b: $^{13}C\{^{1}H\}$ NMR (125 MHz, $CDCl_3$) spectrum of compound **3C1**.

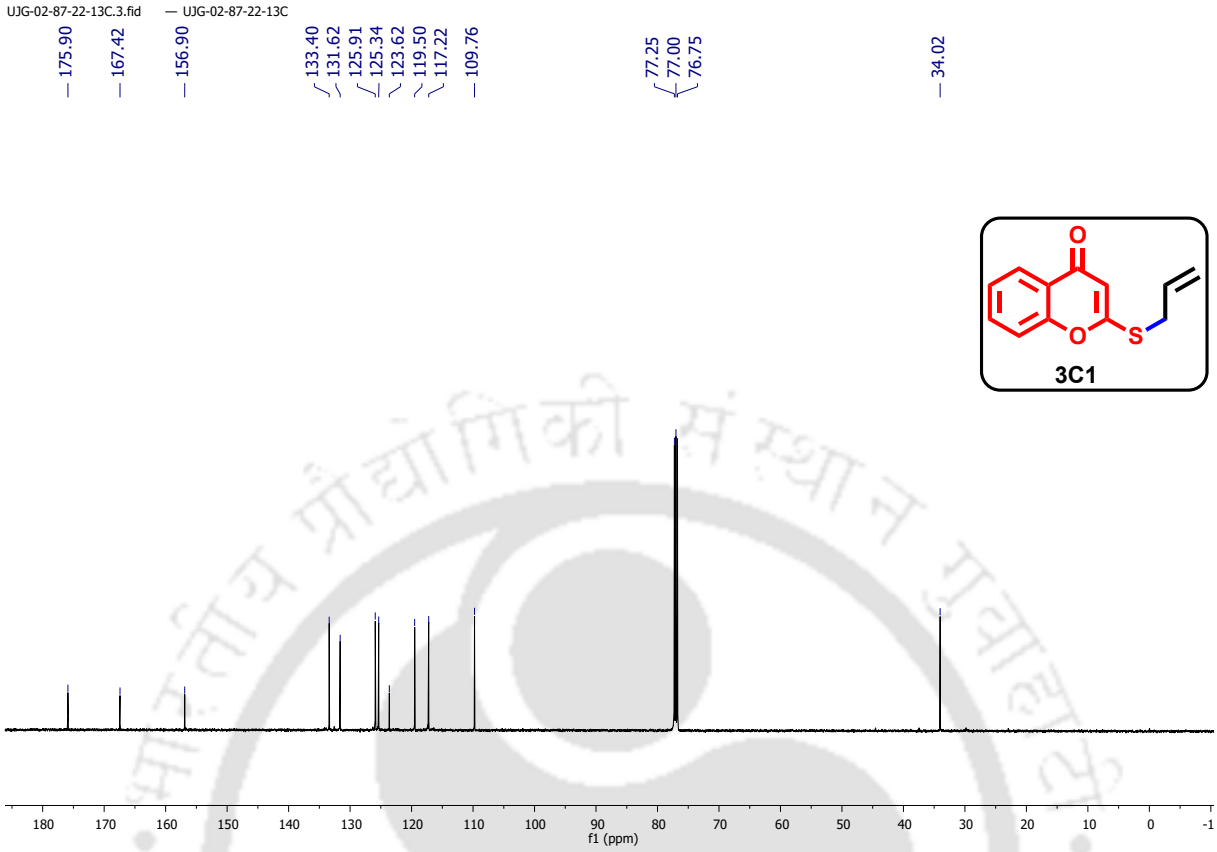

Figure 3.4c: HRMS spectrum of compound **3C1**.

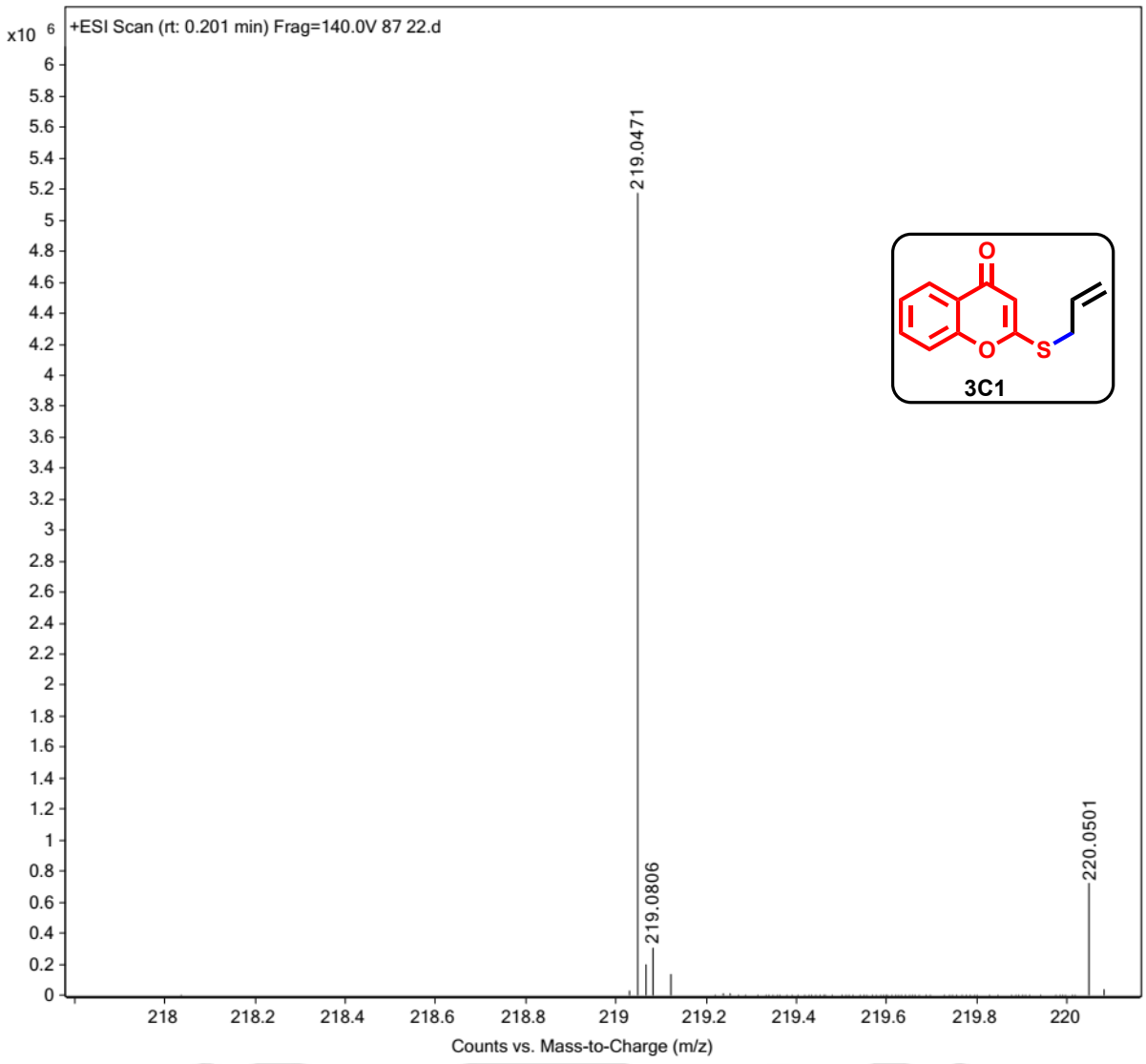

Figure 3.5a: ^{1}H NMR (500 MHz, $CDCl_3$) spectrum of compound **3D9**.

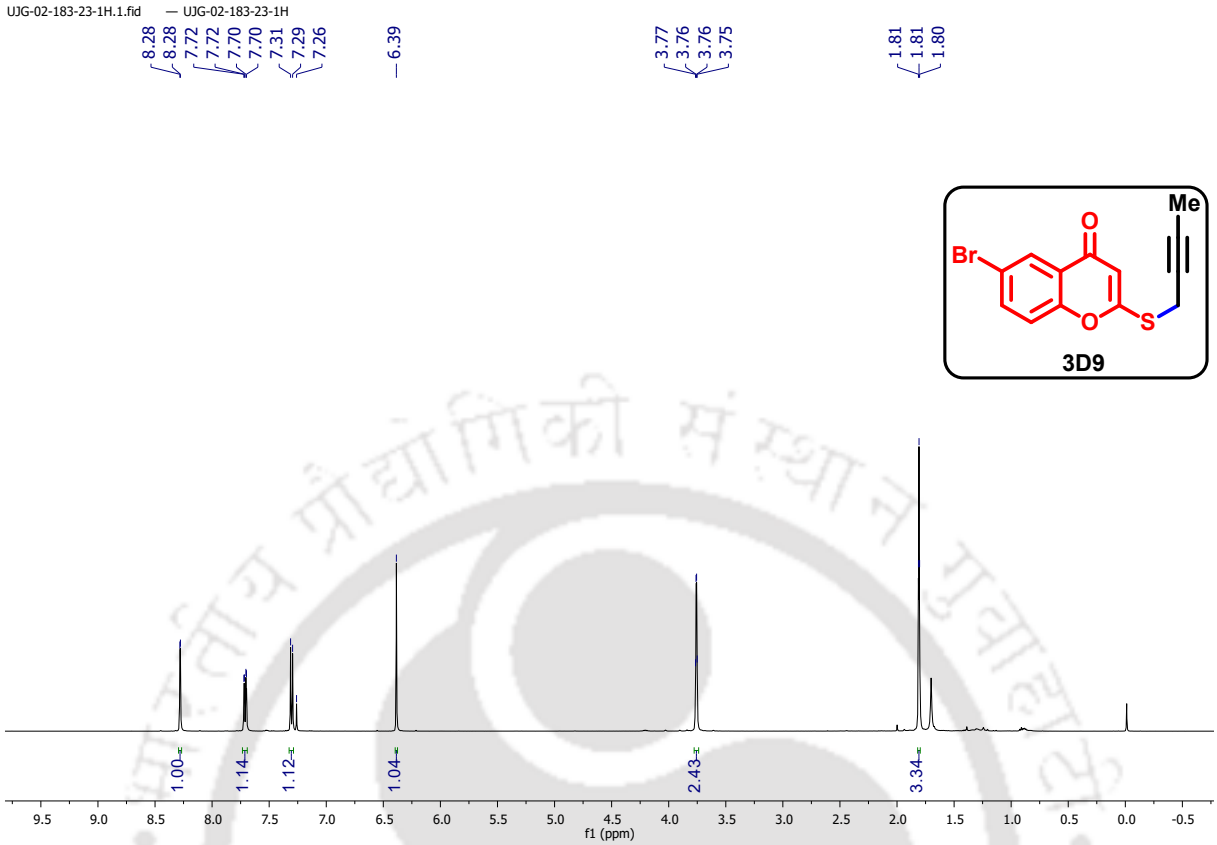

Figure 3.5b: $^{13}C\{^{1}H\}$ NMR (125 MHz, $CDCl_3$) spectrum of compound **3D9**.

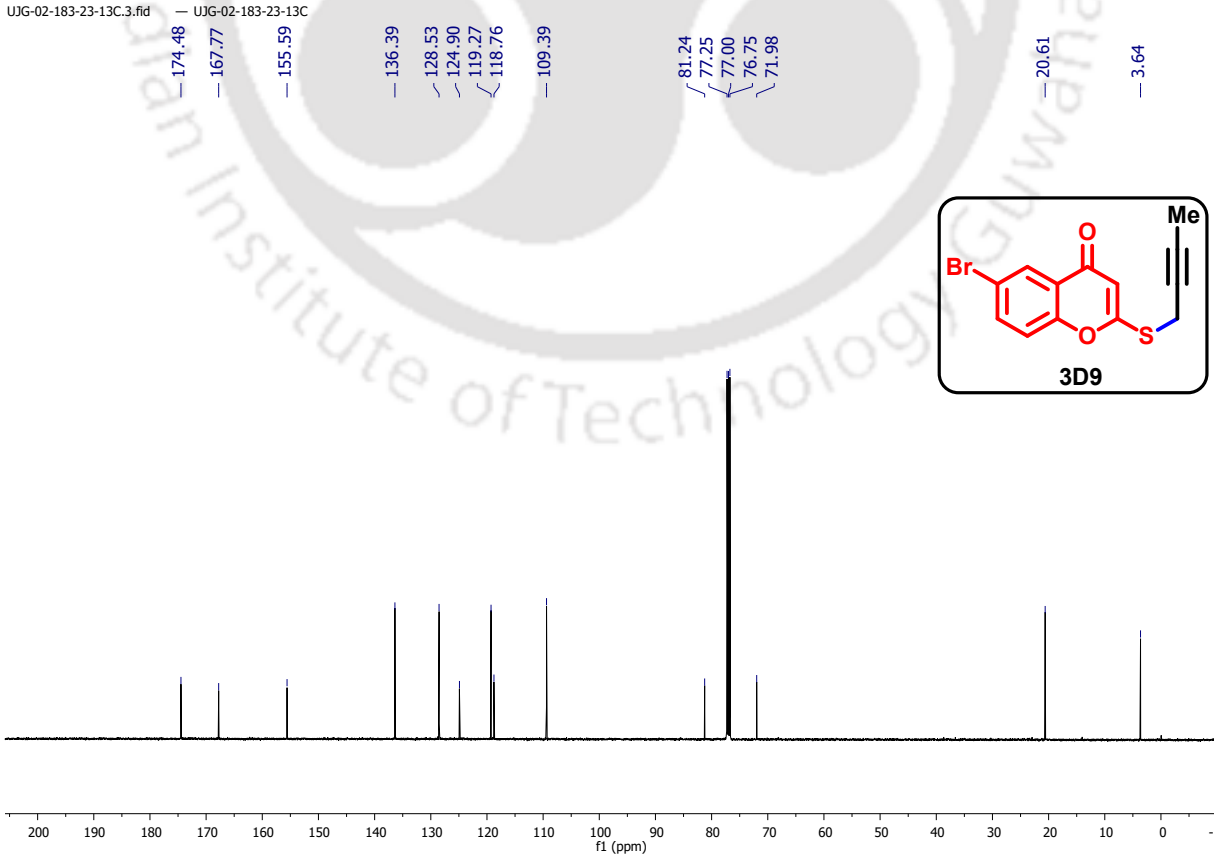

Figure 3.5c: HRMS spectrum of compound **3D9**.

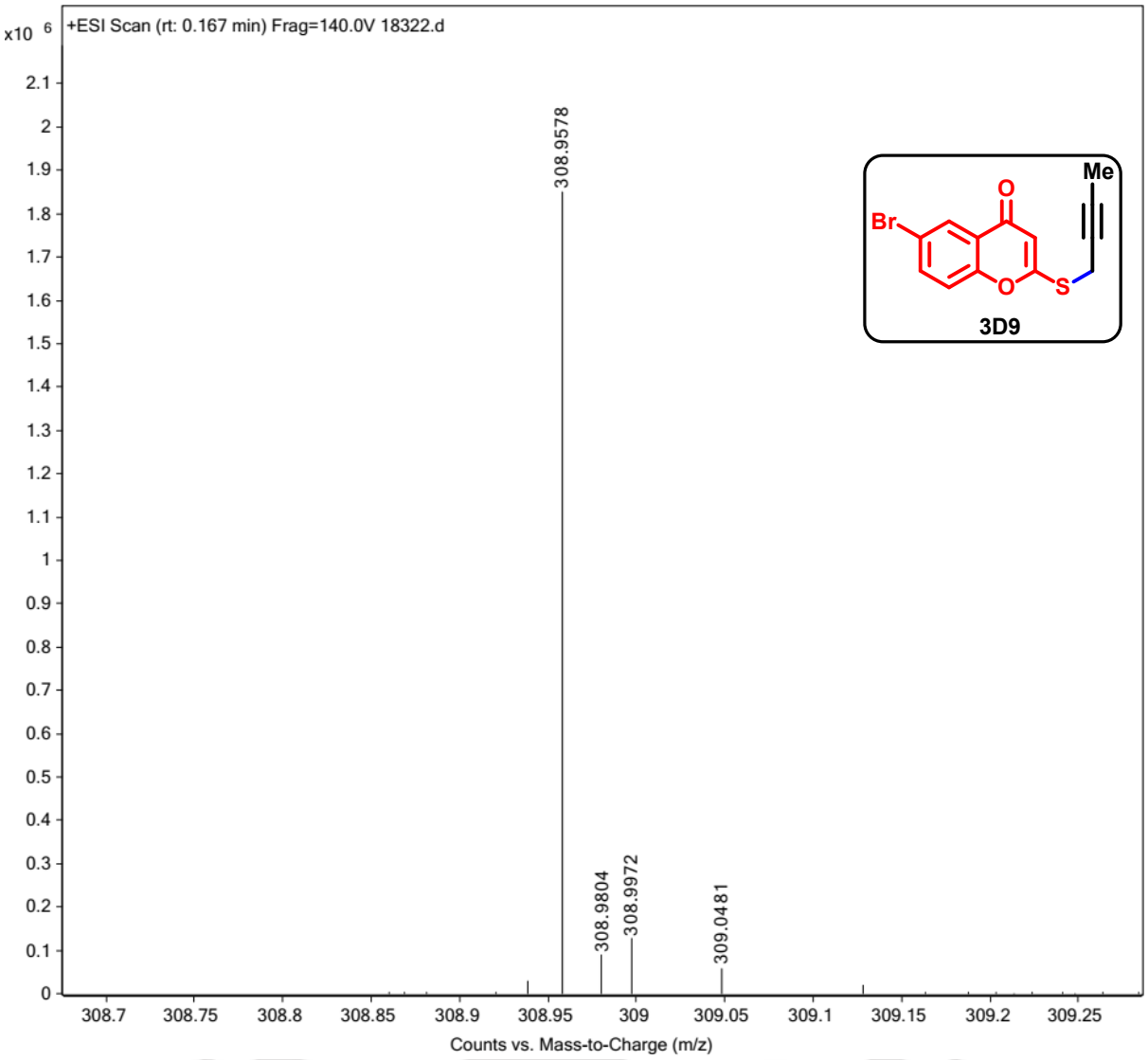

Figure 3.6a: ^{1}H NMR (500 MHz, $CDCl_3$) spectrum of compound **3E5**.

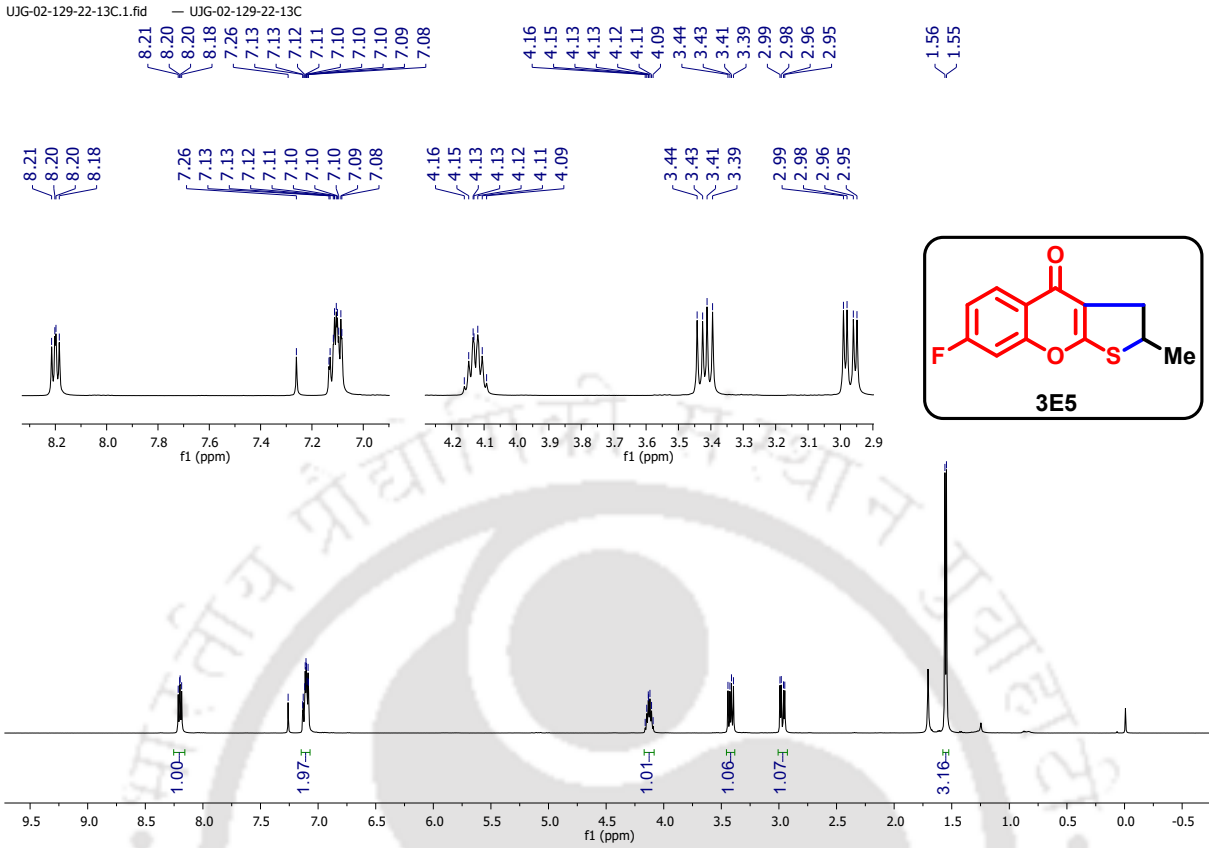

Figure 3.6b: $^{13}C\{^{1}H\}$ NMR (125 MHz, $CDCl_3$) spectrum of compound **3E5**.

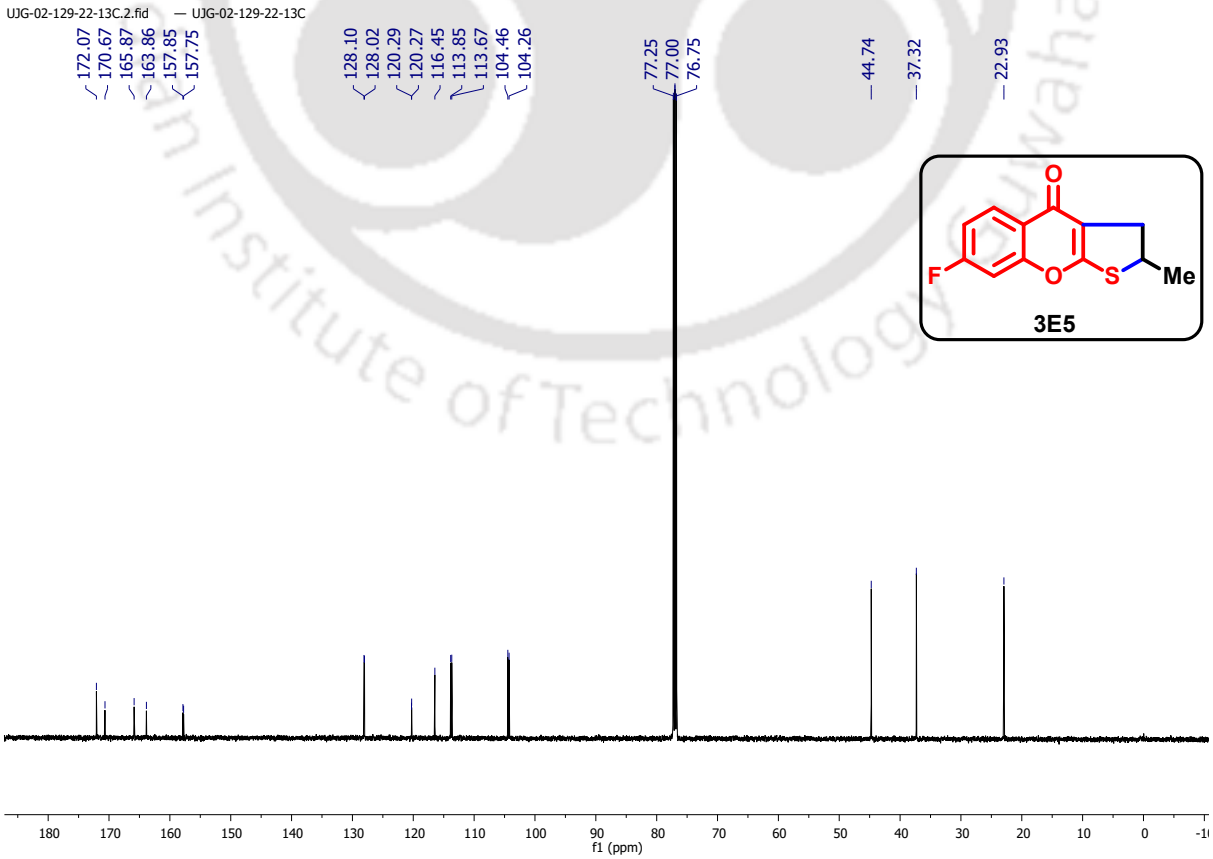

Figure 3.6c: ^{19}F NMR (471 MHz, $CDCl_3$) spectrum of compound **3E5**

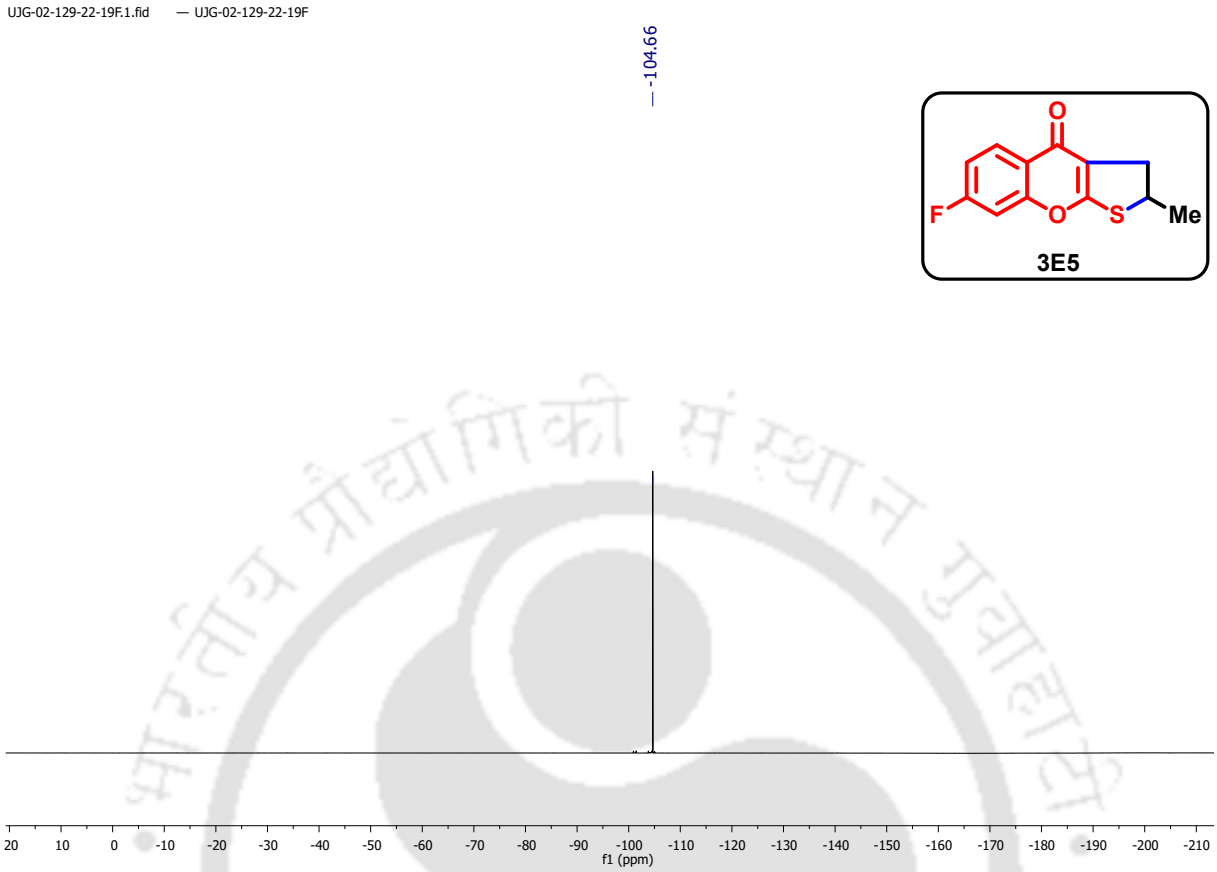

Figure 3.6d: HRMS spectrum of compound **3E5**.

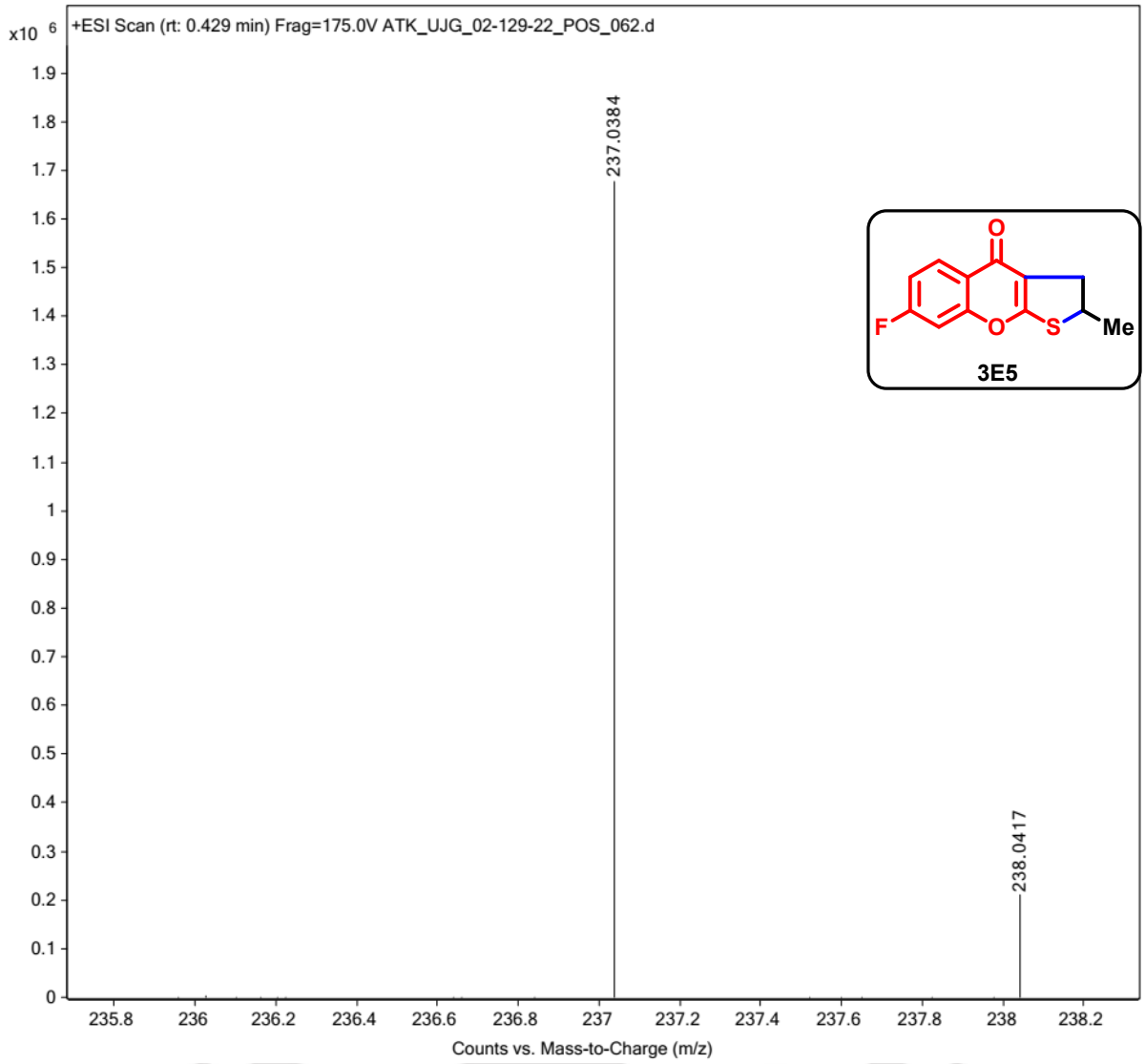

Figure 3.7a: ^{1}H NMR (500 MHz, $CDCl_3$) spectrum of compound **3F6**.

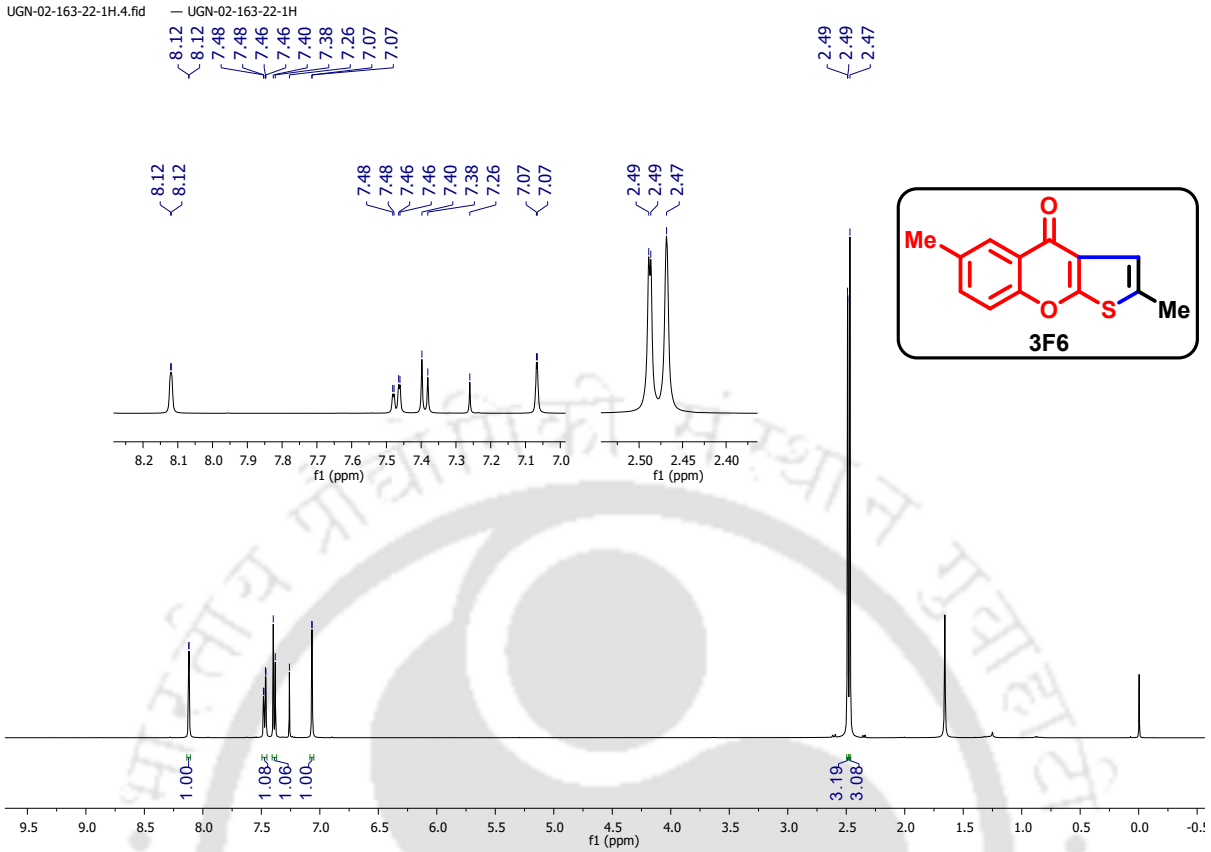

Figure 3.7b: $^{13}C\{^{1}H\}$ NMR (125 MHz, $CDCl_3$) spectrum of compound **3F6**.

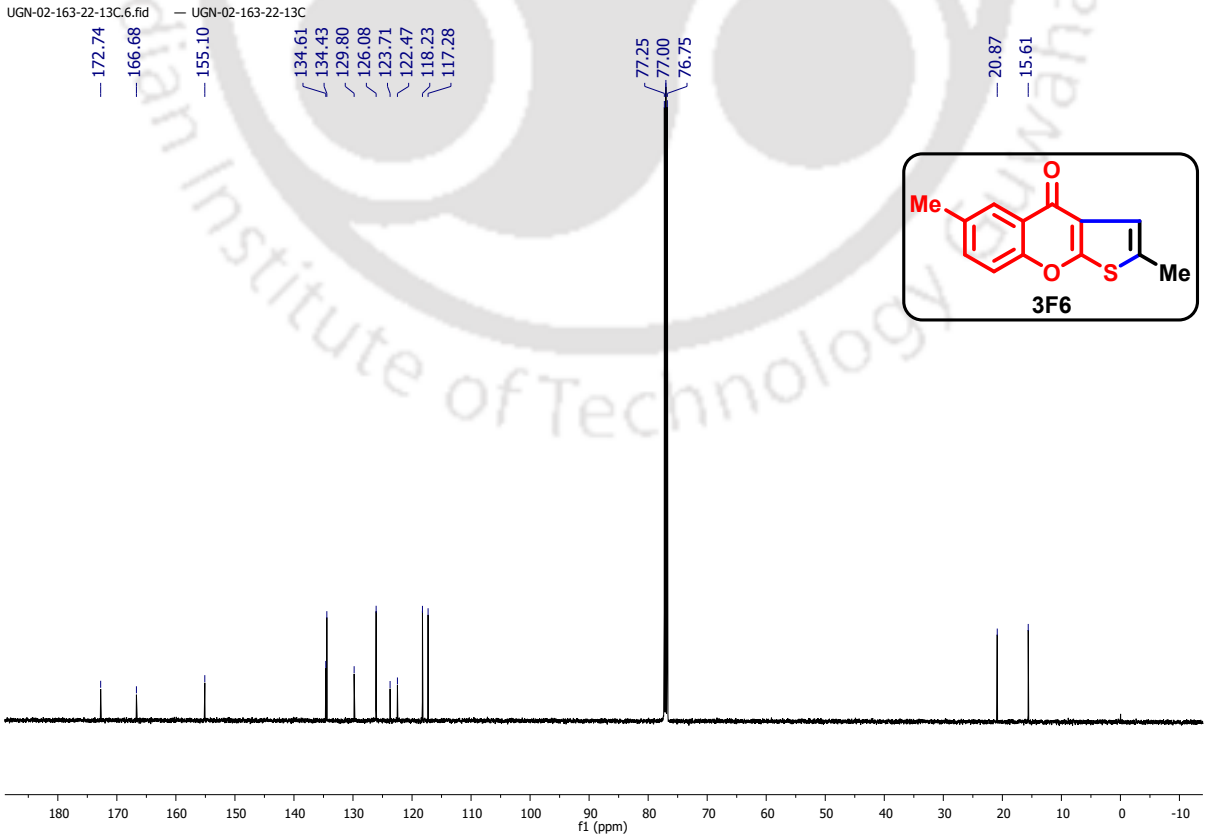

Figure 3.7c: HRMS spectrum of compound **3F6**.

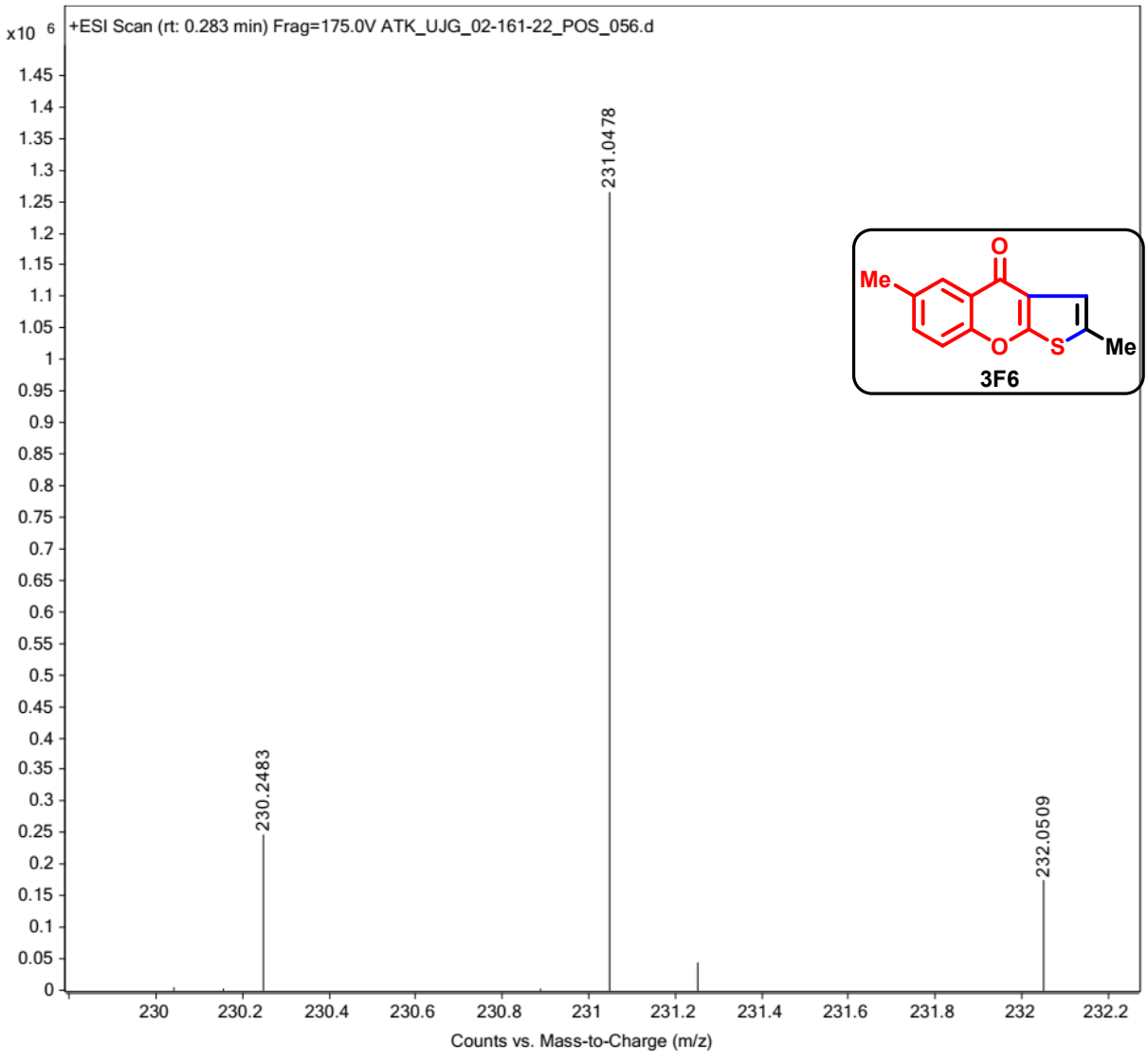

Figure 3.8a: ^{1}H NMR (500 MHz, $CDCl_3$) spectrum of compound **3G1**.

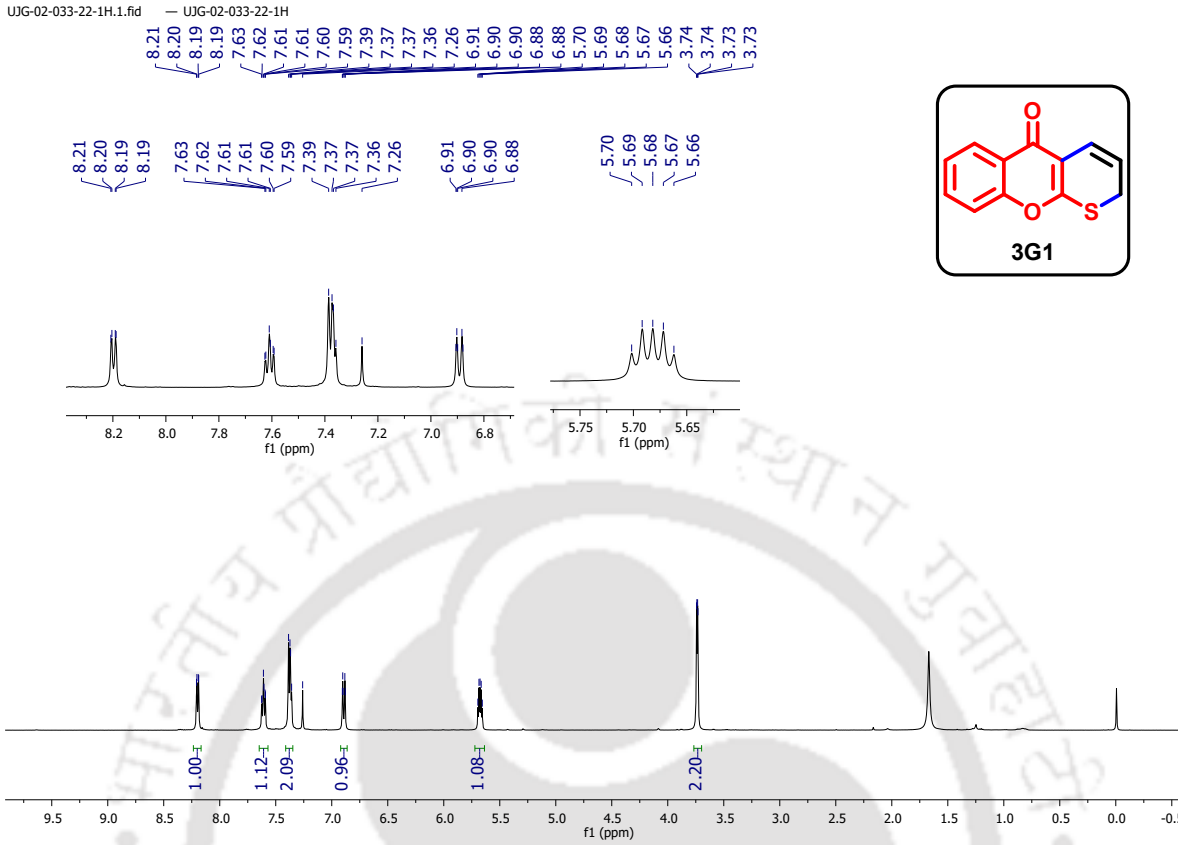

Figure 3.8b: $^{13}C\{^{1}H\}$ NMR (125 MHz, $CDCl_3$) spectrum of compound **3G1**.

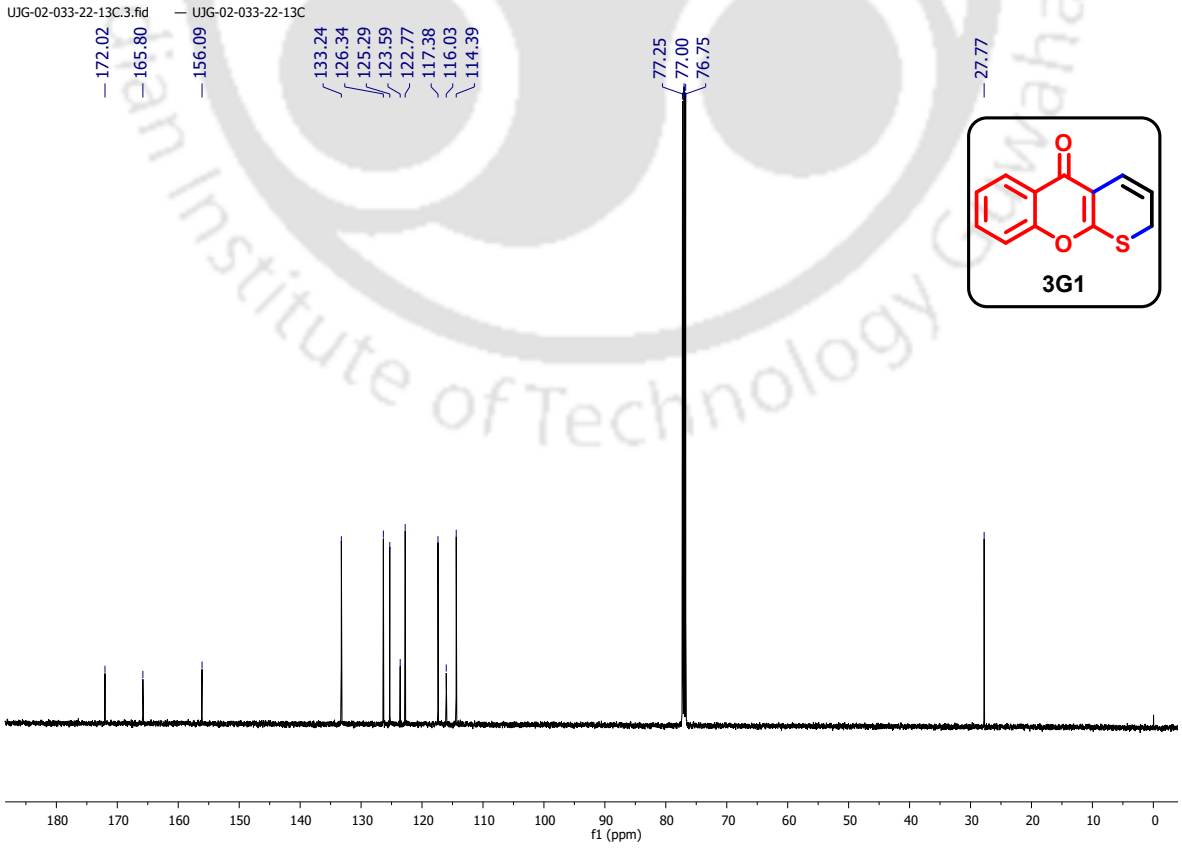

Figure 3.8c: HRMS spectrum of compound **3G1**.

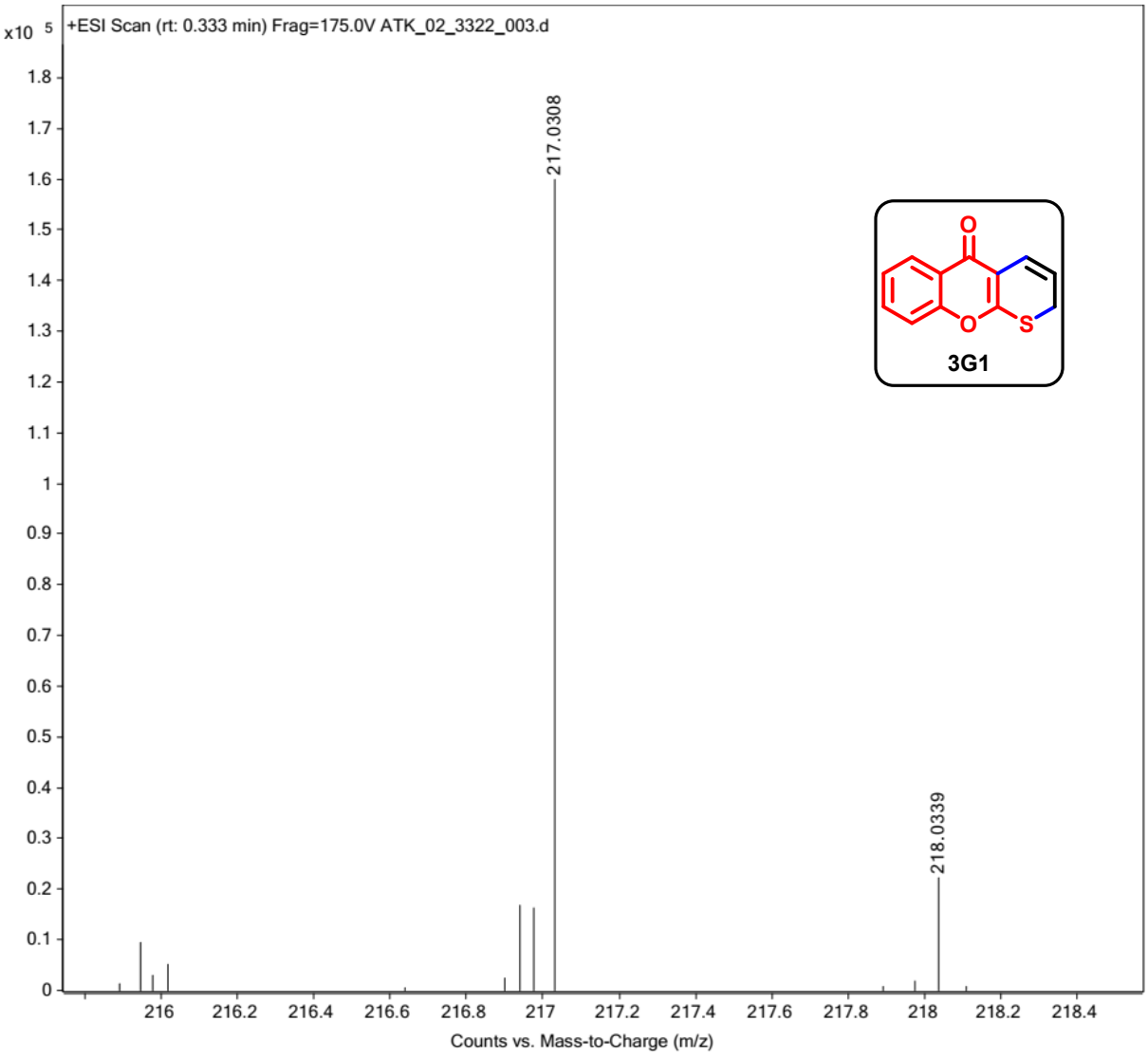

Figure 3.9a: ^{1}H NMR (400 MHz, $CDCl_3$) spectrum of compound **3I3**.

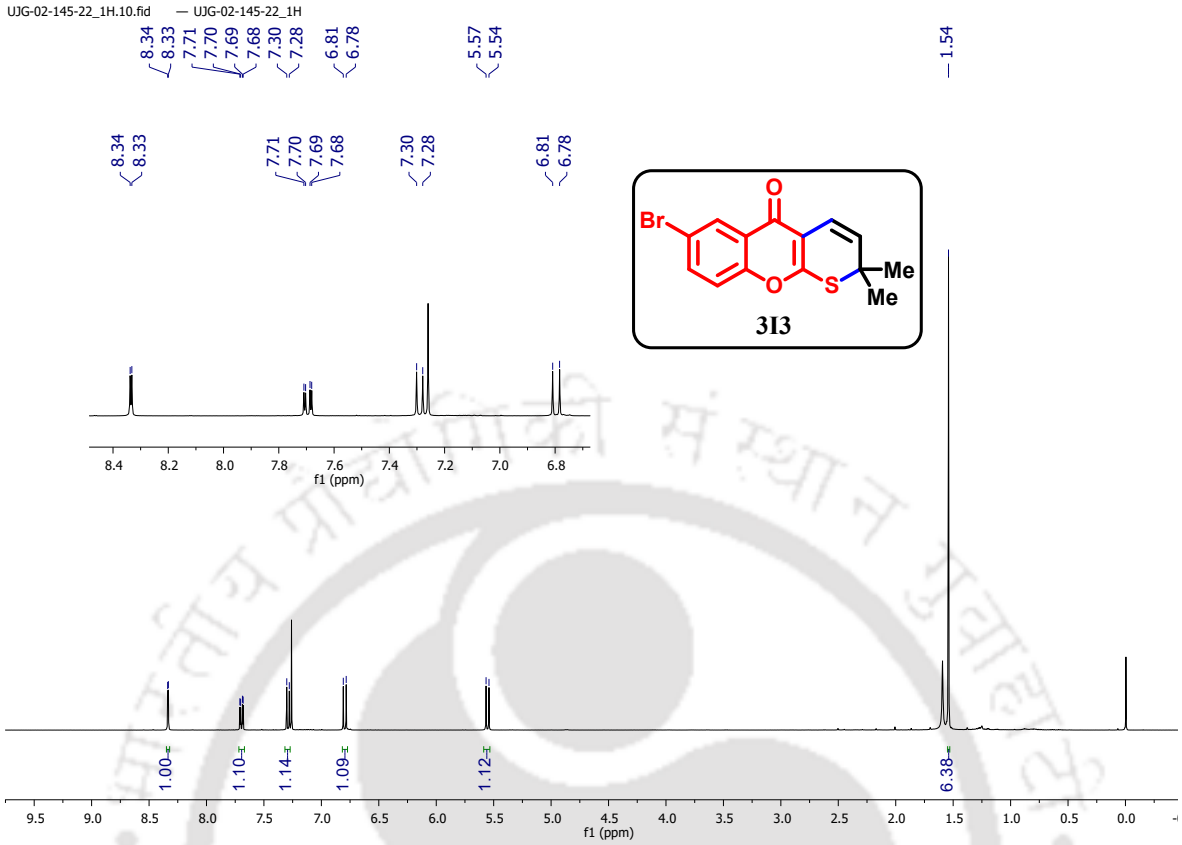

Figure 3.9b: $^{13}C\{^{1}H\}$ NMR (100 MHz, $CDCl_3$) spectrum of compound **3I3**.

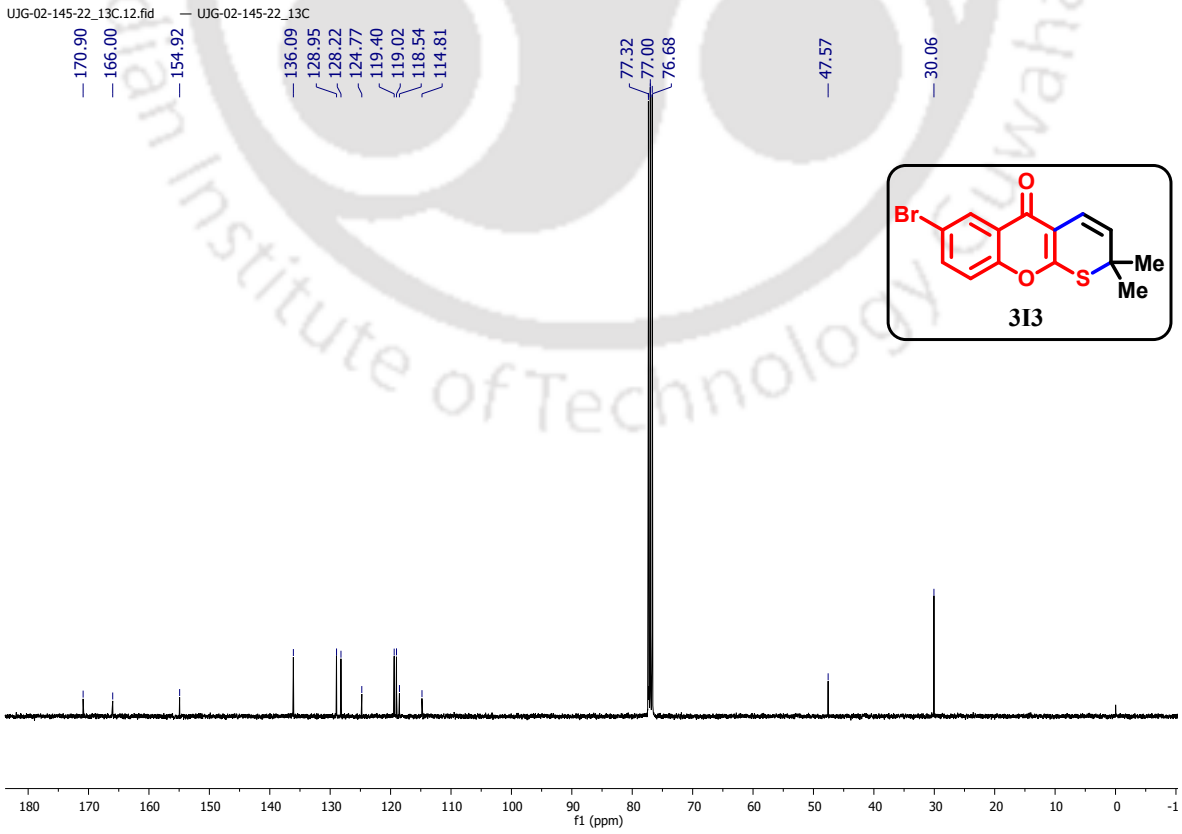

Figure 3.9c: HRMS spectrum of compound **3I3**.

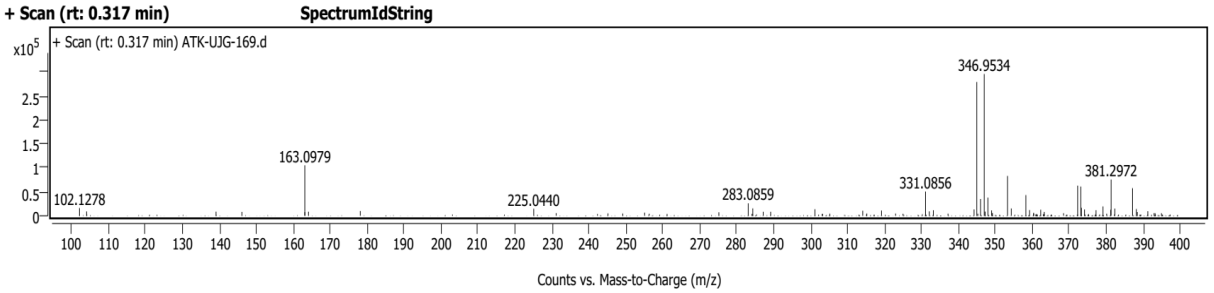

SpectrumIdString

m/z	Z	Abund	Abund %	m/z (Calc)	Diff (ppm)	Ion Species	Formula	Ion Type
102.1278		16143	5.47					
163.0979		105077	35.59					
225.0440		14641	4.96					
283.0859		25913	8.78					
284.3310		15411	5.22					
331.0856		50461	17.09					
344.9555	1	278577	94.36					
345.9587	1	34980	11.85					
346.9534	1	295217	100.00					
347.9564	1	37826	12.81					
353.2660	1	82913	28.09					
354.2696	1	15203	5.15					
358.2273		43118	14.61					
372.2430	1	62719	21.24					
373.0962		60888	20.62					
373.2467	1	16637	5.64					
379.0965		19499	6.61					
381.2972	1	75517	25.58					
382.3005	1	14956	5.07					
387.1117		57482	19.47					

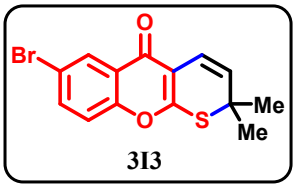

3I3

References

[1] P. S. Auti, S. Jagetiya, A. T. Paul, *Chem. Biodivers.* **2023**, *20*, e202300587.

[2] A. Deepthi, S. S. Leena, D. Krishnan, *Org. Biomol. Chem.* **2024**, *22*, 5676–5717.

[3] W. Wardakhan, O. Abdel-Salam, G. Elmegeed, *Acta Pharmaceut.* **2008**, *58*, 1–14.

[4] J. Reis, A. Gaspar, N. Milhazes, F. Borges, *J. Med. Chem.* **2017**, *60*, 7941–7957.

[5] M. I. Hegab, *Phosphorus, Sulfur, Silicon Relat. Elem.* **2025**, *200*, 1–11.

[6] R. Shah, P. K. Verma, *Chem. Cent. J.* **2018**, *12*, 137.

[7] K. C. Majumdar, A. T. Khan, R. N. De, *Synthetic Commun.* **1988**, *18*, 1589–1595.

[8] K. C. Majumdar, A. T. Khan, S. Saha, *Synlett* **1991**, *1991*, 595–596.

[9] J. W. H. Watthey, M. Desai, *J. Org. Chem.* **1982**, *47*, 1755–1759.

[10] J. Sheng, B. Chao, H. Chen, Y. Hu, *Org. Lett.* **2013**, *15*, 4508–4511.

[11] G. Palmisano, L. Toma, R. Annunziata, S. Tagliapietra, A. Barge, G. Cravotto, *J. Heterocyclic Chem.* **2007**, *44*, 411–418.

[12] K. C. Majumdar, A. K. Pal, *J. Sulfur Chem.* **2009**, *30*, 481–489.

[13] C. Mohan, V. Kumar, M. P. Mahajan, *Tetrahedron Lett.* **2004**, *45*, 6075–6077.

[14] K. Majumdar, S. Ghosh, *Tetrahedron Lett.* **2002**, *43*, 2115–2117.

[15] H. Kwart, J. L. Schwartz, *J. Org. Chem.* **1974**, *39*, 1575–1583.

[16] N. Velasco, A. Suárez, F. Martínez-Lara, M. Á. Fernández-Rodríguez, R. Sanz, S. Suárez-Pantiga, *J. Org. Chem.* **2021**, *86*, 7078–7091.

[17] C. Reichardt, T. Welton, *Solvents and Solvent Effects in Organic Chemistry*, Wiley, **2010**.

[18] W. R. Fawcett, P. Brooksby, D. Verbovy, I. Bakó, G. Pálinkás, *J. Mol. Liq.* **2005**, *118*, 171–178.

[19] A. J. Parker, *Q. Rev. Chem. Soc.* **1962**, *16*, 163.

[20] L. J. Farrugia, *J. Appl. Crystallogr.* **2012**, *45*, 849–854.

Chapter 4

A Regioselective and Sustainable Approach to the Synthesis of Substituted Thieno[2,3-*b*]chromen-4-ones with Pendant Imine Groups *via* Base-Promoted Multicomponent Reaction

Graphical Abstract

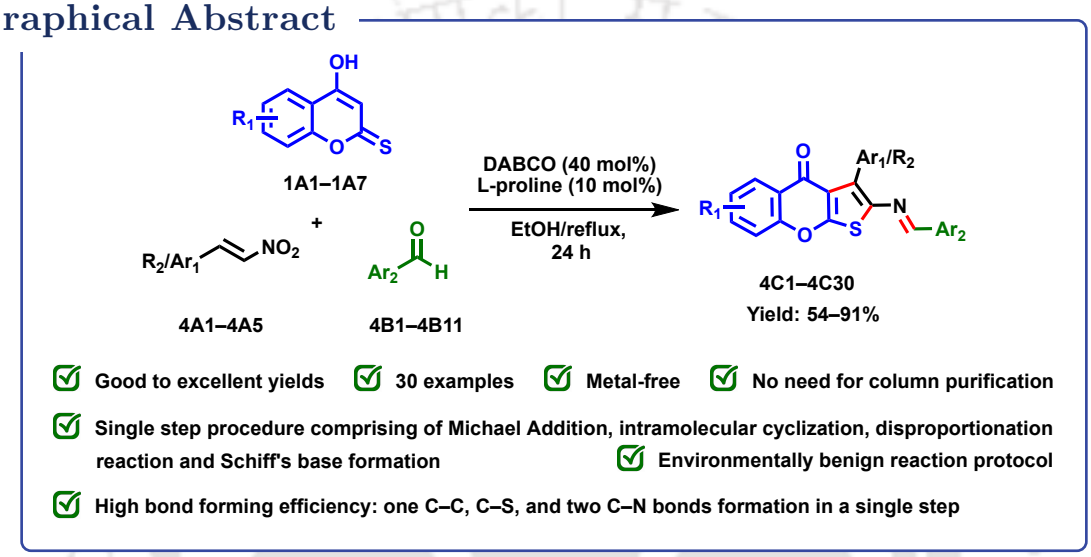

Table of contents

4.1 Context and Significance

Chromone derivatives are well known for their broad spectrum of biological activities, including anti-inflammatory,[1] anticancer,[2] and antimicrobial[3] properties. Similarly, thiophene-containing compounds have found widespread use in medicinal chemistry[4] and materials science,[5,6] owing to their unique electronic and pharmacological properties. The structural features, reactivity, and applications of these heterocycles have been discussed in detail in **Chapter 1, Section 1A.5.1**. Fusing these two motifs yields thieno-chromen-4-one frameworks, which are of particular interest due to their potential for enhanced or novel pharmacological properties.[7,8]

Incorporating imine functionalities into these frameworks further expands their chemical and biological potential.[9,10] Imines are versatile intermediates, valued for their reactivity and as pharmacophores in a wide range of bioactive compounds. Moreover, numerous studies have documented the integration of diverse heterocycles with Schiff base moieties, a structural motif found in several marketed drugs (**Figure 4.1**).[11]

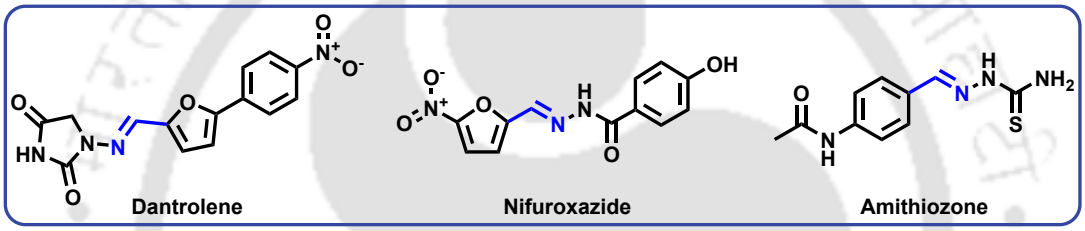

Figure 4.1: Marketed drugs with Schiff base moiety.

The efficient construction of such polycyclic systems remains a synthetic challenge, especially when it comes to achieving high regioselectivity and sustainability.[12,13] Recent developments in multicomponent reactions have enabled the rapid assembly of complex heterocycles from simple and readily available precursors.[14]

In this context, nitrostyrenes serve as highly effective Michael acceptors, facilitating conjugate addition and cyclization processes that are central to the synthesis of fused ring systems.[15–17] Thanks to its ready availability and pronounced reactivity, *trans*-β-nitrostyrene serves as a valuable synthetic building block for a wide range of chromene and chromane derivatives. The strongly electron-withdrawing nitro group activates the β-position toward nucleophilic attack and stabilizes the resulting anion formed upon addition. As a result, *trans*-β-nitrostyrenes readily participate in cascade and multicomponent carbo- and heterocyclization reactions.[18]

To the best of our knowledge, there are no reported methods for the regioselective introduction of imine groups into thieno[2,3-*b*]chromen-4-one scaffolds. This gap in the literature is addressed by the present work, which describes the first sustainable and efficient protocol for constructing these complex heterocycles with pendant imine functionalities under mild conditions.

4.2 Literature Review: Synthesis of Thieno[2,3-*b*]chromenone-Imine Hybrids

The synthesis of fused heterocyclic frameworks combining chromone and thiophene motifs has attracted interest due to their potential biological activities and structural complexity. While chromone and thiophene derivatives have been extensively studied (as discussed in **Chapter 1**), methods for the regioselective construction of thieno[2,3-*b*]chromen-4-one scaffolds remain limited.

4.2.1 Previous Approaches

K_2CO_3-Catalyzed cyclization of 4-hydroxydithiocoumarins: Recently our group have demonstrated that 4-hydroxydithiocoumarin can undergo a K_2CO_3-catalyzed thio[3+2] cyclization with *trans*-β-nitrostyrenes in ethanol, under reflux conditions, affording thieno[2,3-*b*]thiochromen-4-one-oximes with good yields and high regioselectivity (**Scheme 4.1**).[19] This multicomponent protocol efficiently constructs the polycyclic core by leveraging the activated methylene group of the dithiocoumarin and the Michael acceptor character of the nitrostyrene.

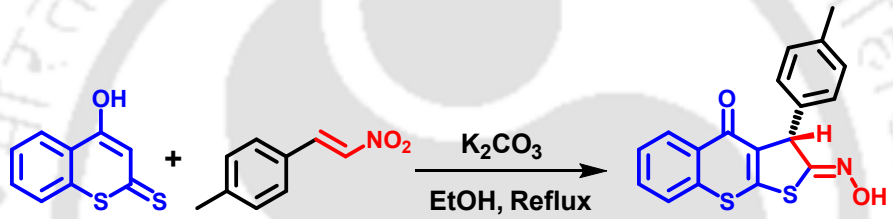

Org. Biomol. Chem. **2017**, *15*, 5625–5634

Scheme 4.1: K_2CO_3-catalyzed thio[3+2] cyclization of 4-hydroxydithiocoumarin with *trans*-β-nitrostyrene.

However, while this strategy is effective for assembling thieno-chromen-4-one-oxime frameworks, it does not provide direct access to imine-functionalized thieno[2,3-*b*]chromen-4-ones.

Four-component furochromone-imine synthesis: Zhou *et al.* developed a four-component protocol for the synthesis of furochromen-4-ones bearing Schiff base moieties, utilizing substituted nitrostyrenes, aromatic aldehydes, 4-hydroxycoumarins, and ammonium acetate (NH_4OAc) (**Scheme 4.2**).[20]

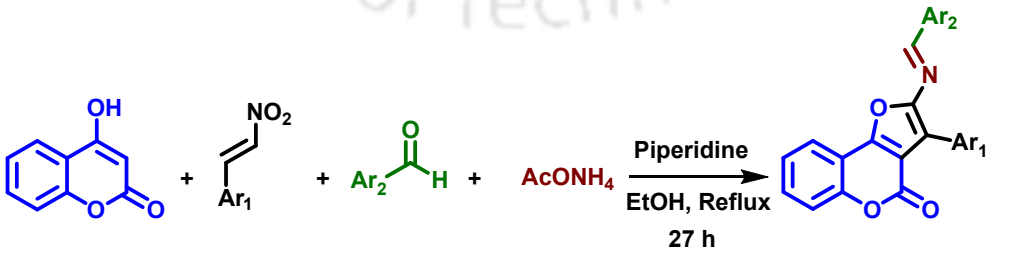

ACS Comb. Sci. **2013**, *15*, 363–369

Scheme 4.2: Four-component synthesis of furochromen-4-one-imine hybrid.

Synthesis of benzofuran-imine: Li *et al.* developed a related approach, using cyclohexane-1,3-diones instead of 4-hydroxycoumarin, affording 3-aryl-2-arylmethyleneamino-4-hydroxybenzofurans under comparable conditions (**Scheme 4.3**).[21]

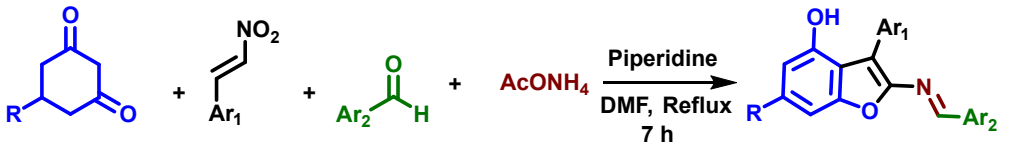

Synlett. **2013**, *24*, 1851–1855

Scheme 4.3: Four-component synthesis of benzofuran-imine hybrid.

4.2.2 Limitations of Existing Methods

- These multicomponent protocols, while efficient for constructing furochromone-imine and benzofuran-imine scaffolds, require an external nitrogen source (NH_4OAc) and stoichiometric reagents (piperidine), increasing operational complexity.
- The direct, regioselective synthesis of sulfur-containing thieno[2,3-*b*]chromenone-imine hybrids has not been reported, leaving a gap in the literature for sustainable and efficient access to these motifs.

4.2.3 Present Strategy

The current study explores a distinct three-component protocol involving 4-hydroxythiocoumarin, 2-hydroxybenzaldehyde, and *trans*-β-nitrostyrene, using DABCO and L-proline as benign, catalytic additives (**Scheme 4.4**).

Notably, this transformation results in the direct formation of a substituted thieno[2,3-*b*]chromenone ring bearing a Schiff base, with the imine nitrogen originating from the nitro group of the nitrostyrene itself, thus *eliminating the need for* NH_4OAc *as a fourth component.*

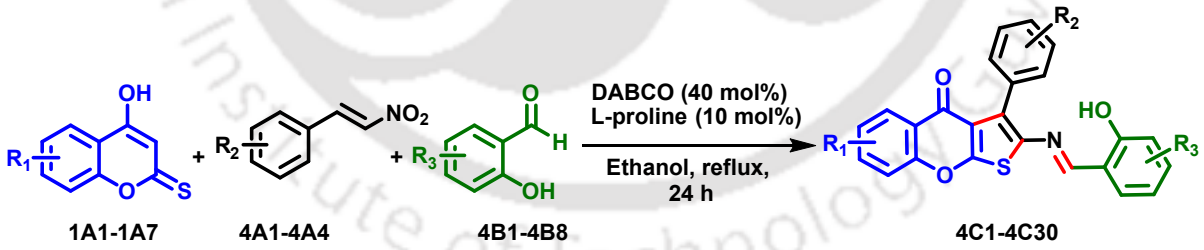

Scheme 4.4: Present catalytic three-component protocol for thieno[2,3-*b*]chromenone-imine hybrids.

Insight: The use of catalytic, rather than stoichiometric, quantities of DABCO and L-proline enhances the sustainability and operational simplicity of the process, setting this protocol apart from previous methods.

Mechanistic distinctions:

In these established protocols, the imine group is introduced *via* external nitrogen sources (e.g., NH_4OAc), and the nitro group on the nitrostyrene is eliminated during the reaction

sequence. This multicomponent approach demonstrates the power of domino processes for generating molecular complexity, but it requires four distinct reactants and stoichiometric use of base piperidine.

In contrast, the present protocol uniquely utilizes the nitro group of the nitrostyrene as the nitrogen source for the imine, eliminating the need for external ammonium acetate and thereby simplifying the process and improving atom economy.

> **Insight:** Although the overall transformations appear similar at first glance, the mechanistic pathways and source of the imine nitrogen are fundamentally distinct. The results of this study establish a new, green route to thieno[2,3-*b*]chromenone-imine hybrids, as detailed herein.

4.3 Green Chemistry Considerations in This Work

The development of this protocol was guided by the following green chemistry goals:

- **Maximize atom economy:** Design the reaction so that all major reactants are incorporated into the final product, minimizing byproduct formation and waste.
- **Employ benign, catalytic additives:** Select inexpensive, readily available, and non-toxic catalysts (such as DABCO and L-proline) to avoid hazardous reagents and reduce environmental impact.
- **Utilize a green solvent:** Choose a renewable and environmentally friendly solvent (ethanol) as the reaction medium, avoiding chlorinated or toxic solvents.
- **Implement a one-pot, multicomponent strategy:** Assemble multiple bonds in a single vessel to reduce the number of synthetic steps, minimize solvent use, and simplify purification.
- **Enable simple product isolation:** Facilitate product purification by designing the process so that products can be isolated by straightforward methods (e.g., filtration and washing), eliminating the need for chromatographic purification.
- **Avoid hazardous reagents and stoichiometric additives:** Exclude the use of metal catalysts, strong acids or bases, and external nitrogen sources such as ammonium acetate to further enhance safety and sustainability.
- **Promote operational simplicity and scalability:** Develop conditions that are robust, straightforward, and amenable to scale-up, making the protocol accessible for both academic and industrial applications.

Note: While green chemistry principles guided the design of this protocol, the actual need for specific reagents or purification methods, such as external nitrogen sources or chromatographic purification, was ultimately dictated by the experimental requirements of the transformation. This reflects the reality that, in developing new synthetic methods, green goals must sometimes be balanced with what is needed to achieve efficient and selective reactions.

A detailed evaluation of the protocol's alignment with green chemistry principles is presented in ***Section 4.5.5****.*

4.4 Research Objectives

This chapter details the development of a novel and sustainable methodology for the synthesis of substituted thieno[2,3-*b*]chromen-4-ones with pendant imine groups. The specific objectives of this research are:

1. To develop a one-pot, three-component reaction protocol for the synthesis of substituted thieno[2,3-*b*]chromen-4-ones from 4-hydroxythiocoumarin, 2-hydroxybenzaldehyde (or aryl aldehyde), and *trans*-β-nitrostyrene.
2. To optimize the reaction conditions by systematically varying parameters such as solvent, catalyst, base, and temperature in order to achieve the best possible outcome.
4. To investigate the substrate scope and limitations of the developed protocol with respect to variations in 4-hydroxythiocoumarin, aldehydes, and *trans*-β-nitrostyrenes.
5. To elucidate a plausible reaction mechanism, including the unique conversion of an oxime intermediate to an amine.
6. To evaluate the developed protocols against green chemistry principles.
7. To characterize the synthesized compounds thoroughly using spectroscopic techniques (NMR, IR, and HRMS) and, where feasible, X-ray crystallography.

4.5 Results and Discussion

4.5.1 Optimization of Reaction Conditions

The optimization of reaction conditions was a pivotal step in establishing an efficient and sustainable protocol for the synthesis of substituted thieno[2,3-*b*]chromen-4-ones bearing imine groups. Using 2 equiv of 4-hydroxythiocoumarin (**1A1**), *trans*-β-nitrostyrene (**4A1**), and 1 equiv 2-hydroxy-5-methyl-benzaldehyde (**4B1**) as model substrates, a systematic investigation was conducted to determine the most effective base, catalyst, solvent, and temperature. In all cases, the reaction time was fixed at 24 hours. The results of these studies are summarized in **Table 4.1**.

Base and catalyst effects: The reaction was first attempted in the absence of any base or catalyst; under these conditions, no product formation was observed, even after extended

heating (**Table 4.1**, entry **1**). This result highlighted the necessity of an activating agent to facilitate the transformation. When inorganic bases such as K_2CO_3 and DBU were evaluated (**Table 4.1**, entries **2** and **3**), no product was detected, indicating insufficient activation. The use of organic bases, including pyrrolidine and pyrimidine (each used in stoichiometric amounts), afforded moderate yields of the desired product **4C1** (**Table 4.1**, entries **4** and **5**; 44% and 53%). When DABCO or triethylamine was used alone, the yields were 57% and 33%, respectively (**Table 4.1**, entries **6** and **7**). These results demonstrate that, while organic bases can promote the reaction to some extent, the efficiency remains limited under these conditions.

A significant enhancement in yield was achieved upon introducing L-proline as an organocatalyst in combination with DABCO (**Table 4.1**, entry **8**), delivering the desired product **4C1** in 82% yield. The use of triethylamine with L-proline was less effective (**Table 4.1**, entry **9**; 51%), underscoring the unique synergy between DABCO and L-proline. L-proline, known for its ability to activate carbonyl compounds *via* enamine or iminium ion formation, likely facilitated key steps in the multicomponent sequence. *The dual catalytic system of* DABCO *and* L-proline *provided a synergistic effect, delivering the product with substantially higher yield and improved reproducibility.*

Solvent and temperature optimization: The choice of solvent proved to be *critical* for both yield and product isolation. Ethanol was identified as the optimal solvent, providing the best yield, operational simplicity, and environmental compatibility (**Table 4.1**, entry **8**). In contrast, when the reaction was attempted in DMF or under neat (solvent-free) conditions, no product formation was observed, even after prolonged heating (**Table 4.1**, entries **10** and **11**). Reactions in acetonitrile gave lower yields (**Table 4.1**, entry **12**), further confirming the superiority of ethanol. Refluxing in ethanol was necessary to achieve the highest yield; lower temperatures were not sufficient for complete reaction within 24 hours (**Table 4.1**, entries **13** and **14**).

Catalyst loading: Reducing the amount of DABCO from 40 mol% to 30, 20, and 10 mol% (**Table 4.1**, entries **15**–**17**) resulted in a gradual decrease in yield (69%, 58%, and 42%, respectively), confirming that 40 mol% DABCO is optimal for this protocol.

Note: Workup and purification: A key advantage of this protocol is the simplicity of product isolation: after completion, the crude solid could be washed with cold ethanol to afford the pure product, eliminating the need for chromatographic purification and further minimizing solvent use.

Summary: The optimal conditions were identified as the reaction of 4-hydroxythiocoumarin **1A1**, *trans*-β-nitrostyrene **4A1**, and 2-hydroxy-5-methyl-benzaldehyde **4B1** in ethanol at reflux for 24 hours, using 40 mol% DABCO and 10 mol% L-proline as catalysts. This method provides high yield and purity, maximizes operational simplicity, and aligns with many of the principles of green chemistry.

Table 4.1: Optimization of the reaction conditions for the synthesis of (*E*)-2-((2-hydroxy-5-methylbenzylidene)amino)-3-phenyl-4*H*-thieno[2,3-*b*]chromen-4-one **4C1**.[a]

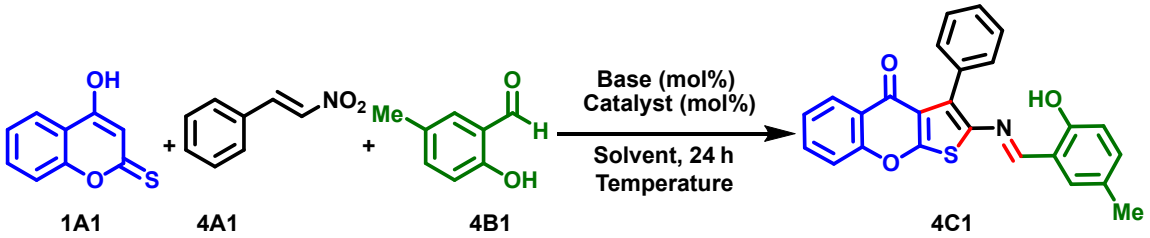

Entry	Base (mol%)	Catalyst (mol%)	Temp (°C)	Solvent	Yield (%)[b]
1	-	-	Reflux	EtOH	NR
2	K_2CO_3 (40)	-	Reflux	EtOH	NR
3	DBU (40)	-	Reflux	EtOH	NR
4	Pyrrolidine (1 eq.)	-	Reflux	EtOH	44
5	Pyrimidine (1 eq.)	-	Reflux	EtOH	53
6	DABCO (40)	-	Reflux	EtOH	57
7	Et_3N (40)	-	Reflux	EtOH	33
8	DABCO (40)	L-proline (10)	Reflux	EtOH	82
9	Et_3N (40)	L-proline (10)	Reflux	EtOH	51
10	DABCO (40)	L-proline (10)	Reflux	DMF	Traces
11	DABCO (40)	L-proline (10)	Reflux	Neat	NR[c]
12	DABCO (40)	L-proline (10)	Reflux	MeCN	21
13	DABCO (40)	L-proline (10)	40	EtOH	72
14	DABCO (40)	L-proline (10)	rt	EtOH	12
15	DABCO (30)	L-proline (10)	Reflux	EtOH	69
16	DABCO (20)	L-proline (10)	Reflux	EtOH	58
17	DABCO (10)	L-proline (10)	Reflux	EtOH	42

[a]Reactions were carried out using 4-hydroxythiocoumarin (2 equiv), *trans*-β-nitrostyrene (2 equiv.), and 2-hydroxy-5-methyl-benzaldehyde (1 equiv). [b]Isolated yields. [c]NR = No Reaction

4.5.2 Substrate Scope and Limitations

The generality and limitations of the optimized protocol were systematically evaluated by employing a diverse array of 4-hydroxythiocoumarins **1A1-1A7**, *trans*-β-nitrostyrenes **4A1-4A4**, and salicylaldehyde derivatives **4B1-4B8** as substrates. The outcomes of these reactions are summarized in **Table 4.2** and **Table 4.3**.

4-Hydroxythiocoumarin variations: A series of 4-hydroxythiocoumarins bearing different substituents on the aromatic ring were subjected to the standard conditions. It was observed that substrates containing electron-donating groups, such as methyl (**Table 4.2**, **4C14-4C16**) or methoxy (**Table 4.2**, **4C24-4C26**), consistently afforded higher yields compared to the unsubstituted parent compound. In contrast, the presence of electron-withdrawing substituents, such as halogens (**Table 4.2**, **4C17-4C22**, **Table 4.3**, **4C28-4C30**), led to a marked decrease in product yield. This trend suggests that electron-rich thiocoumarins are more reactive in the multicomponent sequence, possibly due to increased nucleophilicity or better stabilization of reaction intermediates.

***trans*-β-Nitrostyrene variations:** The influence of substituents on the *trans*-β-nitrostyrene component was also examined. Interestingly, nitrostyrenes bearing electron-donating groups on the aromatic ring (**Table 4.2**, **4C8-4C12**, **4C16**) provided lower yields than the unsubstituted analogues, which in turn gave lower yield than electron-deficient nitrostyrenes (**Table 4.2**, **4C26**) when reacted with the same 4-hydroxythiocoumarin. This result indicates that electron-rich nitrostyrenes may be less effective as Michael acceptors under the optimized conditions, potentially due to decreased electrophilicity at the β-position, while the opposite is true for the electron-deficient ones.

Salicylaldehyde variations: A broad range of salicylaldehyde derivatives, encompassing both electron-donating and electron-withdrawing substituents, were investigated. A clear trend emerged: aldehydes with electron-withdrawing groups afforded the highest yields (**Table 4.2**, **4C2**–**4C3**, **4C7**, **4C10**, **4C25**, **Table 4.3**, **4C29**), followed by unsubstituted derivatives, while electron-donating substituents (**Table 4.2**, **4C1**, **4C5**–**4C6**, **4C9**, **4C12**, **4C19**, **Table 4.3**, **4C27**–**4C28**) led to the lowest yields under otherwise identical conditions. This pattern highlights the beneficial effect of electron-deficient aldehydes in facilitating imine formation.

Expansion to other aldehydes and nitroalkenes: To further probe the versatility of the protocol, aryl aldehydes beyond salicylaldehydes, as well as aliphatic aldehydes and nitroalkenes (prepared from alkyl aldehydes following a literature method[22]), were tested as reaction partners (**Table 4.3**).

Aryl aldehydes (**Table 4.3**, **4C27-4C29**) and nitrobutene (**Table 4.3**, **4C30**) were found to be compatible, furnishing the desired products in moderate to good yields. However, when alkyl aldehydes or longer-chain nitroalkenes were employed, no product formation was observed under the standard conditions. This outcome reveals a limitation of the methodology, restricting its applicability to aromatic and certain short-chain nitroalkene substrates.

Summary: Taken together, these results demonstrate that the developed protocol exhibits broad substrate scope and functional group tolerance among aromatic partners, but is limited in its compatibility with aliphatic aldehydes and extended nitroalkenes.

Table 4.2: Substrate scope for the synthesis of substituted thieno[2,3-*b*]chromen-4-ones from 4-hydroxythiocoumarins, nitrostyrenes, and salicylaldehydes.[a][b]

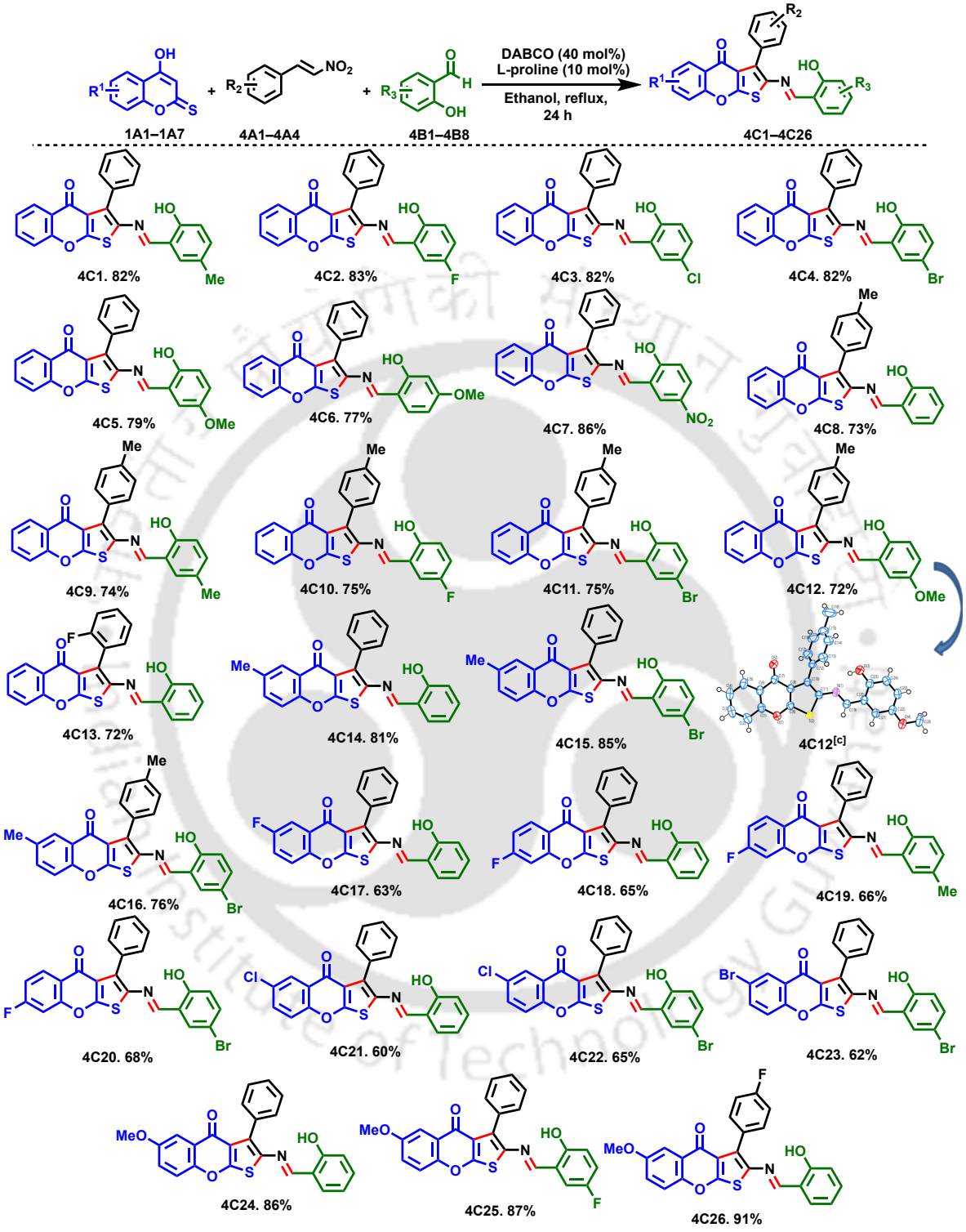

[a]**Reagents and conditions:** 4-hydroxythiocoumarin (0.1 mmol), *trans*-β-nitrostyrene (0.1 mmol), salicylaldehyde (0.5 equiv.), DABCO (40 mol%), and L-proline (10 mol%) in ethanol, stirred at 80 °C. [b]Isolated yields are provided. [c]ORTEP diagram of **4C12** . CCDC 2418286.

Table 4.3: Reactions with aryl and aliphatic aldehydes and nitroalkenes.[a][b]

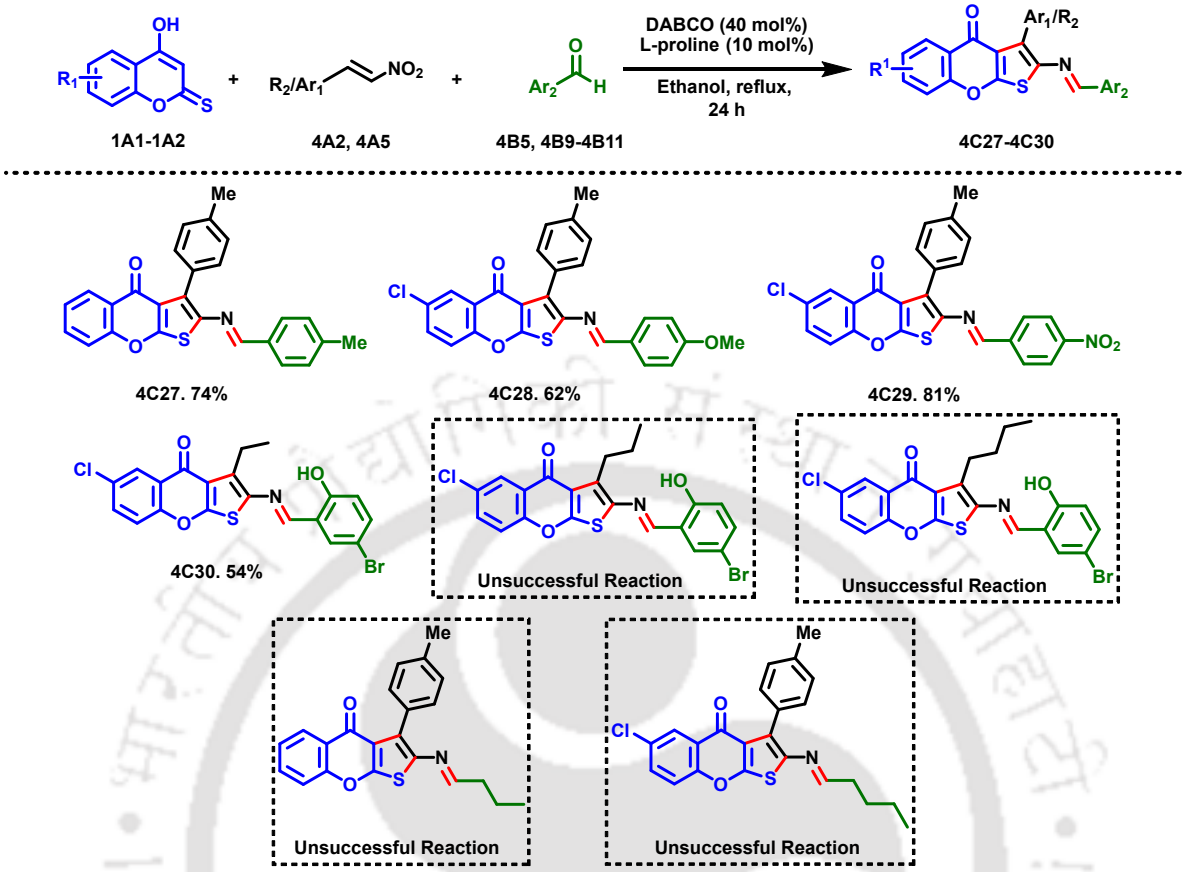

[a]**Reagents and conditions:** 4-hydroxythiocoumarin (0.1 mmol), *trans*-β-nitrostyrene or nitroalkene (0.1 mmol), benzaldehyde or salicylaldehyde (0.5 equiv.), DABCO (40 mol%) and L-proline (10 mol%) in ethanol, stirred at 80 °C. [b]Isolated yields are provided.

4.5.3 Mechanistic Insights

A detailed stepwise mechanism for the formation of compound **4C1** is proposed and illustrated in **Scheme 4.5**. Each stage of the transformation is supported by experimental observation or theoretical reasoning:

Step 1: The process is initiated by deprotonation of 4-hydroxythiocoumarin (**1A1**) by DABCO, resulting in the formation of an anionic intermediate. This anion can be represented by three resonance structures (**I**, **II**, and **III**), each offering distinct nucleophilic sites.

Step 2: Among these, the carbanion resonance structure (**II**) is favored for nucleophilic attack on the *trans*-β-nitrostyrene (**4A1**). This preference is attributed to the relative softness of the nucleophilic center and the stability of the resulting intermediate. The attack leads to the formation of intermediate **A**, establishing the regioselectivity of the process.

Step 3: Intermediate **A** then undergoes *tautomerization*. This process generates intermediate **B**, which features an **enethiol moiety**, i.e., a C=C double bond conjugated to a thiol (–SH) group. The formation of this enethiol is crucial, as it activates the sulfur atom for the subsequent intramolecular cyclization step.

Step 4: Crucially, the sulfur atom of the enethiol moiety in intermediate **B** performs an intramolecular nucleophilic addition to the α-carbon (adjacent to the nitro group) of the nitroalkyl side chain. This cyclization step forms intermediate **C**, establishing the thieno-fused ring system central to the product structure.

Step 5: Intermediate **C** gets protonated to give **D** which features a geminal $N(OH)_2$ group at the 2-position of the thieno[2,3-*b*]chromen-4-one ring system. Dehydration occurs at this site, with the elimination of a molecule of water from the $N(OH)_2$ group, resulting in the formation of the oxime intermediate **E** at the same position. This step establishes the C═N−OH (oxime) functionality, which is essential for the subsequent redox and condensation transformations.

Step 6: The oxime intermediate **E** undergoes a remarkable and unprecedented self-oxidation-reduction process. Two molecules of **E** react with each other, where one acts as a nucleophile

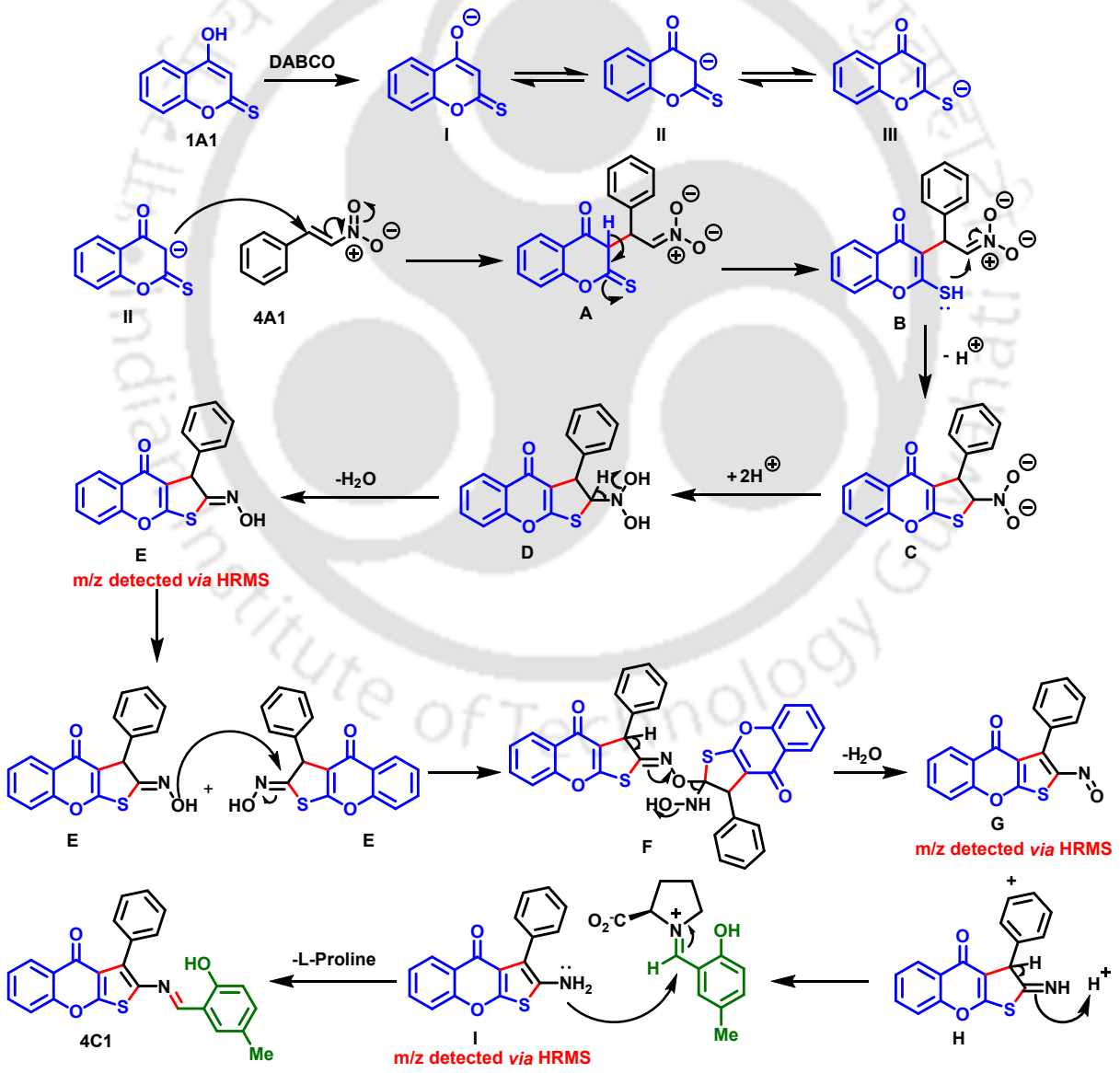

Scheme 4.5: A plausible mechanism for the formation of (*E*)-2-((2-hydroxy-5-methylbenzylidene)amino)-3-phenyl-4*H*-thieno[2,3-*b*]chromen-4-one **4C1**.

and the other as an electrophile at the C=N−OH moiety, resulting in the formation of a dimeric intermediate **F**. This dimer is highly unstable and rapidly fragments, yielding two products: a reduced imine intermediate **H** (which can tautomerize to the amine) and an oxidized nitroso species **G**.

Step 7: The imine intermediate **H** is not stable and rapidly tautomerizes to the corresponding amine **I**. This amine is highly reactive and is efficiently trapped by 5-methylsalicylaldehyde, **4B1**, *via* nucleophilic addition, ultimately forming the final Schiff base product **4C1**.

Insight: This self-disproportionation of oximes to imine and nitroso products, under metal- and radical-free conditions, is highly unusual and represents a unique mechanistic feature of this transformation. The driving force for this process is the instability of the dimer and the favorable formation of both imine/amine and nitroso species. This step is central to the novelty of the mechanism and distinguishes the mechanism from more conventional pathways.

Summary: This sequence of events highlights several crucial features: the regioselectivity of the initial nucleophilic attack, the importance of intramolecular cyclization, and the unusual self-oxidation-reduction step that enables direct formation of the imine and amine intermediates.

Mechanistic confirmation studies

A series of experimental studies were conducted to confirm the validity of the proposed mechanism and to rule out alternative pathways:

- Alternative mechanistic scenarios were considered, particularly for the conversion of oxime **E** to amine **I**. One hypothesis involved the possibility that DABCO could act as a reducing agent, facilitating this transformation. However, HRMS analysis did not reveal any oxidized form of DABCO.
- Stoichiometric experiments provided additional insight– when the reaction was performed with equimolar amounts of 4-hydroxythiocoumarin (**1A1**), *trans*-β-nitrostyrene (**4A1**), and 5-methylsalicylaldehyde (**4B1**), the aldehyde was not completely consumed. In contrast, using twice the equivalents of **1A1** and **4A1** relative to **4B1** resulted in full consumption of the aldehyde. This observation is consistent with a mechanism in which the oxime intermediate undergoes self-oxidation-reduction, rather than relying on external oxidants or reductants.
- To further probe the mechanism, a control experiment was conducted using only 4-hydroxythiocoumarin and *trans*-β-nitrostyrene. Attempts to isolate the amine and nitroso intermediates were unsuccessful due to their instability and the formation of inseparable mixtures. Nonetheless, their transient existence is strongly supported by

mass spectrometric evidence. HRMS analysis confirmed the presence of the oxime (**E**), amine (**I**), and nitroso (**G**) intermediates in the reaction mixture.

Summary: The observed stoichiometric imbalance in the consumption of 5-methylsalicylaldehyde, along with the detection of proposed intermediates and the absence of oxidized DABCO in HRMS, collectively supports the plausibility of the self-oxidation-reduction pathway while effectively ruling out alternative redox processes involving DABCO oxidation or external redox agents.

4.5.4 Product Characterization and Structural Analysis

Comprehensive structural elucidation of the synthesized thieno[2,3-*b*]chromen-4-one-imine derivatives was achieved through an integrated suite of spectroscopic and crystallographic techniques, ensuring unambiguous confirmation of both connectivity and functional group incorporation.

^{1}H NMR spectroscopy: The ^{1}H NMR spectra of the products consistently revealed diagnostic features for the newly formed imine moiety. For compound **4C1**, a distinct singlet at δ 8.38 ppm was observed, attributable to the imine proton (CH═N−C) generated during the final condensation step. The presence of a methyl group on the 2-hydroxy-5-methylphenyl substituent was confirmed by a singlet at δ 2.28 ppm. The aromatic region displayed a complex pattern reflecting the substitution on both the thiocoumarin and salicylaldehyde components, with chemical shifts and integration values matching the proposed structure. The absence of extraneous or unexpected proton signals further supports the product's purity and structural integrity.

^{13}C NMR spectroscopy: ^{13}C NMR spectra provided complementary evidence for the product structure. The imine carbon in **4C1** appeared at δ 157.86 ppm, a chemical shift characteristic of C═N functionalities. The methyl carbon of the 2-hydroxy-5-methylphenyl group was found at δ 20.27 ppm. The remaining carbon signals, including those from the fused heterocyclic core and aromatic rings, were observed in expected regions, confirming the successful assembly of the multi-ring scaffold.

IR spectroscopy: IR analysis revealed several key absorptions that support the proposed functional group composition. For the compound **4C1**, strong bands at 1654 cm^{-1} were assigned to C═N stretching of the imine, while absorptions at 2958 and 2924 cm^{-1} correspond to aliphatic C−H stretching. Aromatic C═C stretches were evident at 1612 and 1575 cm^{-1}, and the band at 1261 cm^{-1} is consistent with C−O stretching, indicative of phenolic or ether functionalities. These features corroborate the presence of the imine, aromatic, and phenolic subunits in the product.

HRMS data: The molecular formula and mass of the synthesized compound were confirmed by HRMS, which showed a $[M + H]^+$ ion consistent with the calculated value for the target structure. For **4C1**, the observed $[M + H]^+$ ion at m/z 412.0994 matches closely with the

calculated value of 412.1002 for $C_{25}H_{18}NO_3S$, supporting the proposed molecular formula of the product.

X-ray Crystallography: For compound **4C12**, unambiguous structural confirmation was obtained *via* single-crystal X-ray diffraction analysis (see **Section 4.8**).

4.5.5 Evaluation of the Current Protocol against Green Chemistry Principles

A critical assessment of the developed protocol reveals its strong alignment with the core principles of green chemistry, as established by Anastas and Warner.[23] The methodology was purposefully designed to minimize environmental impact, maximize efficiency, and simplify operation.

Moderate atom economy through direct nitrogen transfer: The one-pot, three-component reaction directly incorporates the nitrogen atom of the imine from the nitro group of *trans*-β-nitrostyrene, eliminating the need for external amine sources. While this represents an efficient nitrogen transfer, the overall atom economy of the process remains moderate due to the use of excess 4-hydroxythiocoumarin and nitrostyrene, with only a fraction of the total reactant mass contributing to the final product.

Benign catalysts and reagents: Catalyst selection is inherently green. The protocol employs DABCO and L-proline as catalysts, both of which are inexpensive, non-toxic, and readily available organocatalysts. Their use in catalytic (rather than stoichiometric) amounts avoids the hazards and waste associated with metal catalysts or toxic bases, and aligns with the green chemistry principle of safer chemicals and auxiliaries.

Green solvent and moderate thermal conditions: Ethanol, a renewable and relatively benign solvent, is employed as the reaction medium under moderate reflux conditions at 78 °C. No chlorinated or hazardous solvents are required, and the reaction proceeds efficiently at atmospheric pressure, avoiding the need for high-boiling or toxic solvents. While the temperature is moderately elevated, it is significantly lower than many traditional organic syntheses and does not require pressurization. This choice of solvent and conditions reduces both the energy footprint and the risk profile of the process.

Operational simplicity and waste minimization: The reaction products typically precipitate directly from the reaction mixture and are isolated by simple washing with ethanol, eliminating the need for chromatographic purification. This not only reduces solvent consumption and chemical waste but also simplifies the workflow and makes the protocol highly amenable to scale-up. However, the requirement of using two equivalents each of 4-hydroxythiocoumarin and trans-β-nitrostyrene, where approximately half of these quantities end up as by-products, partially offsets the overall efficiency and sustainability of the method.

MCR efficiency: The use of a MCR enables the rapid and convergent formation of complex heterocycles in a single operation, reducing the number of steps, purification procedures, and associated waste. The protocol enables the simultaneous formation of one C—C, one C—S, and two C—N bonds in a single transformation.

No external redox reagents required: The key transformation, conversion of the oxime intermediate to the amine and nitroso products, occurs through an unprecedented self-oxidation-reduction (disproportionation) process, requiring no additional oxidants, reductants, or hazardous additives. This further reduces reagent use and potential waste.

> **Note:** While a detailed quantitative assessment of green metrics such as E-factor or process mass intensity was not performed, a qualitative evaluation of the protocol's alignment with the 12 Principles of Green Chemistry focuses on atom economy, the use of benign and catalytic reagents, avoidance of hazardous solvents, and operational simplicity.

4.5.6 Limitations and future directions

- The reaction exhibits limited scope with aliphatic aldehydes and longer-chain nitroalkenes, which generally fail to provide the desired thieno[2,3-*b*]chromen-4-one-imine products under the optimized conditions due to lower electrophilicity and increased conformational flexibility.
- Direct isolation or spectroscopic observation of all key intermediates remains elusive due to their high reactivity, suggesting the use of advanced techniques such as low-temperature NMR, *in situ* IR, or computational modeling for deeper mechanistic insight.
- The requirement for reflux in ethanol 78 °C is a moderate but not strictly "mild" condition, highlighting the opportunity for catalysts or conditions enabling lower-temperature operation.
- The biological activity and further functionalization of these novel derivatives represent promising avenues for medicinal chemistry or material science applications.
- The requirement for excess 4-hydroxythiocoumarin and *trans*-β-nitrostyrene lowers the theoretical atom economy of the process. Consequently, a substantial portion of the reactant mass does not contribute to the final product, reducing material utilization efficiency and the overall green value of the method.

Post-synthetic modification and coordination prospects

The presence of a pendant imine group in the thieno[2,3-*b*]chromen-4-one scaffold introduces a versatile synthetic handle, opening up numerous opportunities for post-synthetic modification and functional diversification.

- **Reductive transformation to secondary amines:** The imine –C=N– moiety can be selectively reduced to yield secondary amines, enabling further *N*-alkylation or *N*-acylation.
- **Nucleophilic addition to the imine bond:** The electrophilic C=N bond allows nucleophilic addition of thiols, amines, hydrazides, or other nucleophiles to introduce new substituents.

- **N,O-Bidentate chelation and metal complex formation:** The adjacent imine nitrogen and phenolic oxygen can coordinate to transition metals (e.g., Cu, Ni, Zn, Pd) upon deprotonation, forming stable five-membered chelate rings.

4.6 Conclusion

In this chapter, a regioselective and sustainable protocol for the synthesis of substituted thieno[2,3-*b*]chromen-4-one derivatives bearing pendant imine groups has been established using a one-pot, three-component reaction of 4-hydroxythiocoumarin, *trans*-β-nitrostyren, and aryl aldehydes, catalyzed by DABCO and L-proline in ethanol under reflux. The methodology features good atom economy, use of benign reagents, and operational simplicity. The unprecedented self-disproportionation of an oxime intermediate enables imine formation without external redox reagents, and comprehensive spectroscopic and crystallographic analyses confirm product structures. While limitations with certain substrates and reaction temperatures remain, the protocol offers a strong foundation for future mechanistic studies and functional exploration of these heterocyclic hybrids.

A notable feature of this protocol is the unprecedented transformation of the nitro group's nitrogen atom into the imine functionality, achieved through a unique self-oxidation-reduction (disproportionation) of an oxime intermediate without the need for external oxidants or reductants. The reaction proceeds with high regioselectivity, enabling the simultaneous formation of one C—C, C—S, and two C—N bonds in a single step. The broad substrate scope, tolerance for various aromatic substituents, and avoidance of hazardous reagents or labor-intensive purification steps further underscore the practicality and sustainability of this method.

Mechanistic investigations, supported by HRMS detection of key intermediates, provide strong evidence for the proposed pathway and highlight the originality of the disproportionation process. Comprehensive spectroscopic characterization, including NMR, IR, HRMS, and single-crystal X-ray analysis for selected derivatives, unambiguously confirms the structure and purity of the synthesized products.

While the methodology demonstrates significant advantages, certain limitations persist, including reduced efficiency with aliphatic aldehydes and longer-chain nitroalkenes, the need for moderately elevated temperatures during ethanol reflux, and waste generation arising from the use of excess amounts of two reagents. These aspects highlight opportunities for further optimization and mechanistic investigation.

Importantly, the presence of a pendant imine group and a phenolic oxygen in the product scaffold offers versatile avenues for post-synthetic modification, including reductive amination, nucleophilic addition, and N,O-bidentate chelation to transition metals. Such functionalization prospects open new directions for the development of novel materials, catalysts, and bioactive molecules.

Overall, this work shows how green chemistry ideas can be combined with creative synthetic methods to provide a reliable and sustainable way to make and further explore thieno[2,3-

b]chromen-4-one-imine hybrid scaffolds. The findings presented here lay a strong foundation for future studies in synthetic methodology, mechanistic chemistry, and the functional application of these unique heterocyclic frameworks.

4.7 Experimental Section

This section details the procedures and analytical methods employed for the synthesis and characterization of the thieno[2,3-*b*]chromen-4-one-imine derivatives described in this chapter. All chemicals and solvents were purchased from commercial suppliers and used as received unless otherwise specified. The syntheses of 4-hydroxythiocoumarin **1A1**, the key precursor and its derivatives, are described in **Chapter 1, Section 1B**. *trans*-β-Nitrostyrene was synthesized from aryl aldehydes according to a literature procedure.[24]

4.7.1 General Procedure for the Synthesis of Thieno[2,3-*b*]chromen-4-one Imine Derivatives

In a typical experiment, 4-hydroxythiocoumarin (0.1 mmol), *trans*-β-nitrostyrene (0.1 mmol), and the selected salicylaldehyde or aryl aldehyde (0.05 mmol) were placed in a 10 mL round-bottomed flask. DABCO (40 mol%) and L-proline (10 mol%) were added, followed by ethanol (0.5 mL) as the solvent. The reaction mixture was refluxed at 78 °C for 24 h with stirring. The progress of the reaction was monitored by TLC using 9.5:0.5 EtOAc/hexane as the mobile phase. Upon completion, the reaction mixture was cooled to room temperature. The precipitated product was collected by filtration, washed thoroughly with cold ethanol to remove residual starting materials and byproducts, and dried under vacuum. In most cases, the crude product was analytically pure and required no further purification.

4.7.2 Representative Experimental Procedure

Synthesis of (*E*)-2-((2-hydroxy-5-methylbenzylidene)amino)-3-phenyl-4*H*-thieno[2,3-*b*]chromen-4-one (4C1):

A 10 mL round-bottomed flask was charged with 4-hydroxythiocoumarin (**1A1**, 0.1 mmol, 17.82 mg), *trans*-β-nitrostyrene (**4A1**, 0.1 mmol, 14.91 mg), and 2-hydroxy-5-methyl-benzaldehyde (**4B1**, 0.05 mmol, 6.81 mg) in ethanol (0.5). DABCO (40 mol%) and L-proline (10 mol%) were added, and the mixture was refluxed at 78 °C for 24 h. As the reaction progressed, the product precipitated from the solvent. After completion (monitored by TLC), the mixture was cooled to room temperature, and the precipitate was filtered and washed several times with ethanol to yield analytically pure **4C1** as a yellow solid (17 mg, 82% Yield).

Comprehensive spectroscopic and analytical data for all synthesized thieno[2,3-*b*]chromen-4-one-imine derivatives (**4C1**–**4C30**) are provided in **Section 4.9**. This includes ^{1}H and ^{13}C, IR, HRMS data, and melting points for each compound. Representative spectra for key examples are also included in **Section 4.10**.

4.8 Crystallographic Analysis

Single crystals suitable for X-ray diffraction were obtained for compound **4C12** by slow evaporation from a mixture of ethyl acetate and chloroform. The crystallographic data

confirmed the thieno[2,3-*b*]chromen-4-one-imine structure, with bond lengths and angles in agreement with the proposed framework. The ORTEP diagram (**Figure 4.2**) was generated using ORTEP-3 for Windows.[25]

The CCDC deposition number **2418286** (for **4C12**) contains the supplementary crystallographic data for this paper (**Table 4.4**), which can be obtained free of charge by the joint Cambridge Crystallographic Data Centre and Fachinformationszentrum Karlsruhe: https://www.ccdc.cam.ac.uk/structures/

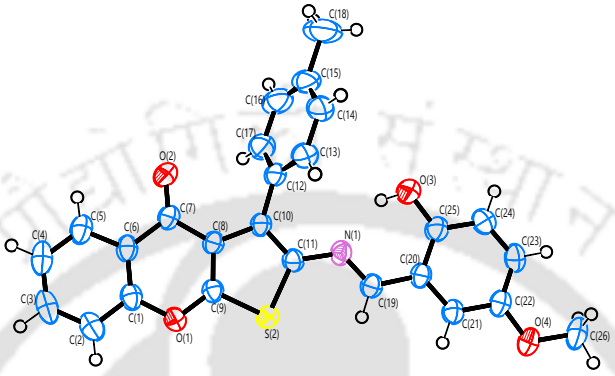

Figure 4.2: ORTEP diagram for compound **4C12**.

Table 4.4: Crystallographic data and Structure Refinement for compound **4C12**.[a]

Entry	Identification Code	Compound 4C12
01	Empirical formula	$C_{26}H_{19}NO_4S$
02	Formula weight	441.48
03	Temperature	295 K
04	Wavelength	0.71073 Å
05	Radiation type	Mo K\α
06	Radiation system	Fine-focus sealed tube
07	Crystal system	Monoclinic
08	Space group	$P2_1/n$
09	Cell length	a 7.1781(12) Å
		b 25.329 (4) Å
		c 11.7749 (18) Å
10	Cell angle	α 90°
		β 92.840 (4)°
		γ 90°“
11	Cell volume	2138.2 (6) $Å^3$
12	Density	1.371 $Mg\,m^{-3}$
13	Completeness to theta	99.6
14	Absorption correction	multi-scan
15	Refinement method	Full-matrix least-squares on F^2

Entry	Identification Code	Compound 4C12
16	Index ranges	−8≤h≤8, −31≤k≤31, −14≤l≤14
17	Reflection number	4187
18	Theta range	2.4 – 27.7°
19	Cell formula units Z	4
20	CCDC no.	2418286

[a]The full .cif file and additional crystallographic data are available from the CCDC.

4.9 Characterization Data for All New Compounds

(*E*)-2-((2-hydroxy-5-methylbenzylidene)amino)-3-phenyl-4*H*-thieno[2,3-*b*]chromen-4-one (4C1)

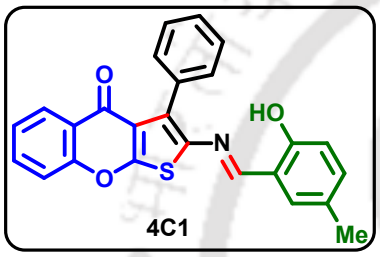

Yellow Solid (17 mg, 82%); **mp** 260 – 262 °C; **^{1}H NMR (400 MHz, $CDCl_3$)** δ 11.34 (s, 1H), 8.38 (s, 1H), 8.27 (dd, J = 7.9, 1.5 Hz, 1H), 7.69 (ddd, J = 8.6, 7.2, 1.7 Hz, 1H), 7.55 – 7.50 (m, 5H), 7.49 – 7.45 (m, 1H), 7.44 – 7.39 (m, 1H), 7.13 – 7.10 (m, 2H), 6.81 (d, J = 9.0 Hz, 1H), 2.28 (s, 3H); **^{13}C{^{1}H} NMR (125 MHz, $CDCl_3$)** δ 172.02, 165.12, 157.86, 157.82, 156.30, 137.17, 134.52, 133.49, 133.31, 133.15, 131.96, 130.23, 128.57, 128.35, 127.79, 126.90, 125.26, 123.56, 121.14, 118.58, 117.35, 117.13, 20.27; **IR (KBr)** ν_{max}/cm^{-1} 2958, 2924, 1654, 1612, 1575, 1460, 1261; **HRMS (ESI)** calcd for $C_{25}H_{18}NO_3S^+$ 412.1002 M+H$^+$ found 412.0994.

(*E*)-2-((5-fluoro-2-hydroxybenzylidene)amino)-3-phenyl-4*H*-thieno[2,3-*b*]chromen-4-one (4C2)

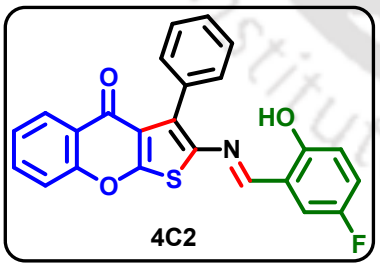

Yellow Solid (17 mg, 83%); **mp** 258 – 260 °C; **^{1}H NMR (400 MHz, $CDCl_3$)** δ 11.34 (s, 1H), 8.36 (s, 1H), 8.27 (dd, J = 8.0, 1.5 Hz, 1H), 7.70 (ddd, J = 8.6, 7.2, 1.7 Hz, 1H), 7.56 – 7.47 (m, 6H), 7.45 – 7.41 (m, 1H), 7.05 – 7.01 (m, 2H), 6.88 – 6.83 (m, 1H); **^{13}C{^{1}H} NMR (125 MHz, $CDCl_3$)** δ 172.00, 165.41, 156.33, 156.26 (d, J = 3.1 Hz), 156.13 (d, J = 1.4 Hz), 155.69 (d, J = 238.0 Hz), 136.47, 134.56, 133.63, 132.99, 130.16, 128.51, 127.87, 126.93, 125.38, 123.54, 121.17, 120.58 (d, J = 23.5 Hz), 118.74 (d, J = 7.4 Hz), 118.51 (d, J = 7.4 Hz), 117.39, 116.67 (d, J = 23.4 Hz); **^{19}F NMR (471 MHz, $CDCl_3$)** δ -124.86; **IR (KBr)** ν_{max}/cm^{-1} 2958, 2924, 1656, 1611, 1459, 1275; **HRMS (ESI)** calcd for $C_{24}H_{15}FNO_3S^+$ 416.0757 M+H$^+$ found 416.0725.

(*E*)-2-((5-chloro-2-hydroxybenzylidene)amino)-3-phenyl-4*H*-thieno[2,3-*b*]chromen-4-one (4C3)

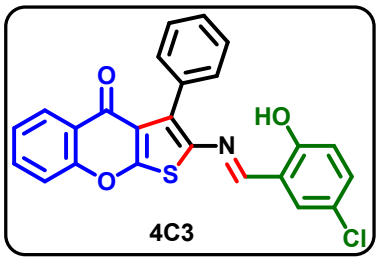

4C3

Yellow Solid (18 mg, 82%); **mp** 286 – 288 °C; **^{1}H NMR (400 MHz, $CDCl_3$)** δ 11.51 (s, 1H), 8.33 (s, 1H), 8.26 (dd, J = 7.9, 1.5 Hz, 1H), 7.69 (ddd, J = 8.6, 7.3, 1.6 Hz, 1H), 7.55 – 7.47 (m, 6H), 7.45 – 7.38 (m, 1H), 7.29 (d, J = 2.5 Hz, 1H), 7.24 (dd, J = 8.8, 2.5 Hz, 1H), 6.84 (d, J = 8.8 Hz, 1H); **^{13}C{^{1}H} NMR (125 MHz, $CDCl_3$)** δ 171.96, 165.40, 158.41, 156.28, 156.03, 136.41, 134.61, 133.63, 133.13, 132.93, 130.81, 130.14, 128.51, 127.87, 126.89, 125.37, 124.09, 123.49, 121.12, 119.75, 118.88, 117.38; **IR (KBr)** ν_{max}/cm^{-1} 2955, 2924, 1655, 1611, 1458, 1276; **HRMS (ESI)** calcd for $C_{24}H_{15}ClNO_3S^+$ 432.0461 M+H$^+$ found 432.0438.

(*E*)-2-((5-bromo-2-hydroxybenzylidene)amino)-3-phenyl-4*H*-thieno[2,3-*b*]chromen-4-one (4C4)

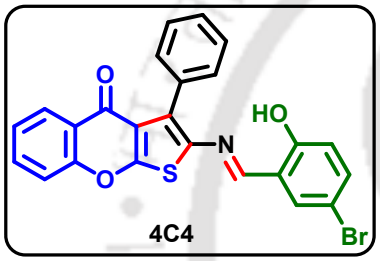

4C4

Yellow Solid (20 mg, 82%); **mp** 279 – 280 °C; **^{1}H NMR (400 MHz, $CDCl_3$)** δ 11.53 (s, 1H), 8.34 (s, 1H), 8.27 (d, J = 7.3 Hz, 1H), 7.70 (t, J = 7.3 Hz, 1H), 7.55 – 7.49 (m, 5H), 7.46 – 7.40 (m, 2H), 7.37 (dd, J = 8.9, 1.9 Hz, 1H), 6.80 (d, J = 8.8 Hz, 1H); **^{13}C{^{1}H} NMR (125 MHz, $CDCl_3$)** δ 172.00, 165.43, 158.88, 156.30, 155.94, 136.40, 135.93, 134.65, 133.84, 133.65, 132.94, 130.14, 128.52, 127.88, 126.91, 125.39, 123.50, 121.14, 120.41, 119.30, 117.39, 110.95; **IR (KBr)** ν_{max}/cm^{-1} 2957, 2924, 1655, 1612, 1459, 1276; **HRMS (ESI)** calcd for $C_{24}H_{15}BrNO_3S^+$ 475.9951 M+H$^+$ found 475.9921.

(*E*)-2-((2-hydroxy-5-methoxybenzylidene)amino)-3-phenyl-4*H*-thieno[2,3-*b*]chromen-4-one (4C5)

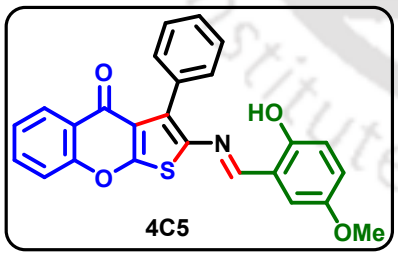

4C5

Yellow solid (17 mg, 79%); **mp** 271 – 272 °C; **^{1}H NMR (400 MHz, $CDCl_3$)** δ 11.15 (s, 1H), 8.37 (s, 1H), 8.26 (dd, J = 8.0, 1.5 Hz, 1H), 7.68 (ddd, J = 8.6, 7.2, 1.7 Hz, 1H), 7.55 – 7.50 (m, 5H), 7.49 – 7.46 (m, 1H), 7.44 – 7.39 (m, 1H), 6.93 (dd, J = 9.0, 3.0 Hz, 1H), 6.84 (d, J = 9.0 Hz, 1H), 6.81 (d, J = 3.0 Hz, 1H), 3.78 (s, 3H); **^{13}C{^{1}H} NMR (125 MHz, $CDCl_3$)** δ 172.00, 165.20, 157.37, 156.31, 154.37, 152.49, 136.99, 133.69, 133.52, 133.13, 130.22, 128.39, 127.82, 126.91, 125.28, 123.57, 121.17, 121.06, 118.56, 118.23, 117.36, 114.73, 55.89; **IR (KBr)** ν_{max}/cm^{-1} 2955, 2924, 1654, 1572, 1459, 1268; **HRMS (ESI)** calcd for $C_{25}H_{18}NO_4S^+$ 428.0951 M+Na$^+$ found 428.0934.

(*E*)-2-((2-hydroxy-4-methoxybenzylidene)amino)-3-phenyl-4*H*-thieno[2,3-*b*]chromen-4-one (4C6)

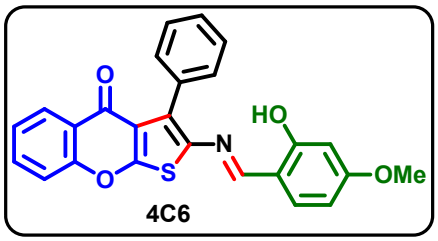

Yellow Solid (16 mg, 77%); **mp** 278 – 279 °C; **^{1}H NMR (400 MHz, $CDCl_3$)** δ 11.95 (s, 1H), 8.33 (s, 1H), 8.27 (dd, J = 8.0, 1.5 Hz, 1H), 7.67 (ddd, J = 8.6, 7.2, 1.7 Hz, 1H), 7.55 – 7.49 (m, 5H), 7.49 – 7.44 (m, 1H), 7.43 – 7.38 (m, 1H), 7.21 (d, J = 8.6 Hz, 1H), 6.47 (dd, J = 8.6, 2.4 Hz, 1H), 6.40 (d, J = 2.4 Hz, 1H), 3.79 (s, 3H); **^{13}C {^{1}H} NMR (125 MHz, $CDCl_3$)** δ 172.02, 164.70, 164.25, 162.30, 157.10, 156.29, 137.46, 133.39, 133.32, 131.84, 130.27, 128.18, 127.75, 126.87, 125.17, 123.56, 121.13, 117.34, 112.85, 107.71, 101.12, 55.46; **IR (KBr)** ν_{max}/cm^{-1} 2955, 2923, 1631, 1600, 1464, 1276; **HRMS (ESI)** calcd for $C_{25}H_{18}NO_4S^+$ 428.0957 M+H$^+$ found 428.0940.

(*E*)-2-((2-hydroxy-5-nitrobenzylidene)amino)-3-phenyl-4*H*-thieno[2,3-*b*]chromen-4-one (4C7)

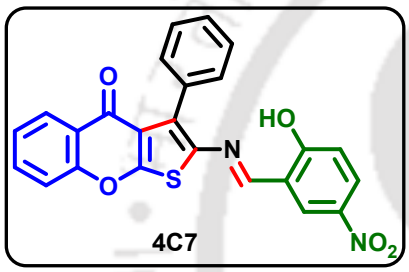

Yellow Solid (19 mg, 86%); **mp** 266 – 267 °C; **^{1}H NMR (600 MHz, $CDCl_3$)** δ 12.44 (s, 1H), 8.49 (s, 1H), 8.33 (d, J = 2.6 Hz, 1H), 8.27 (dd, J = 7.9, 1.3 Hz, 1H), 8.19 (dd, J = 9.1, 2.7 Hz, 1H), 7.74 – 7.71 (m, 1H), 7.56 (d, J = 8.4 Hz, 1H), 7.54 – 7.50 (m, 5H), 7.47 – 7.43 (m, 1H), 6.97 (d, J = 9.1 Hz, 1H); **^{13}C{^{1}H} NMR (150 MHz, $CDCl_3$)** δ 172.00, 156.33, 155.12, 140.36, 135.54, 133.85, 132.74, 130.05, 128.72, 128.27, 128.00, 127.76, 126.92, 125.55, 123.45, 121.15, 118.32, 118.21, 117.45; **IR (KBr)** ν_{max}/cm^{-1} 3055, 2960, 2924, 1651, 1611, 1461, 1275; **HRMS (ESI)** calcd for $C_{24}H_{15}N_2O_4S^+$ 443.0696 M+H$^+$ found 443.0680.

(*E*)-2-((2-hydroxybenzylidene)amino)-3-(*p*-tolyl)-4*H*-thieno[2,3-*b*]chromen-4-one (4C8)

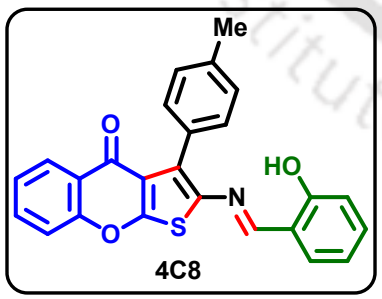

Yellow Solid (15 mg, 73%); **mp** 246 – 247 °C; **^{1}H NMR (500 MHz, $CDCl_3$)** δ 11.63 (s, 1H), 8.43 (s, 1H), 8.27 (d, J = 6.9 Hz, 1H), 7.71 – 7.66 (m, 1H), 7.53 (d, J = 8.3 Hz, 1H), 7.45 – 7.39 (m, 3H), 7.32 (t, J = 9.0 Hz, 4H), 6.92 (dt, J = 7.0, 2.7 Hz, 2H), 2.45 (s, 3H); **^{13}C{^{1}H} NMR (125 MHz, $CDCl_3$)** δ 172.03, 165.21, 159.94, 157.61, 156.29, 138.10, 136.65, 133.70, 133.48, 133.44, 132.01, 130.11, 130.05, 128.57, 126.94, 125.26, 123.61, 121.21, 119.47, 119.00, 117.33, 117.33, 21.53; **IR (KBr)** ν_{max}/cm^{-1} 3053, 2964, 2926, 1656, 1611, 1553, 1461, 1220; **HRMS (ESI)** calcd for $C_{25}H_{18}NO_3S^+$ 412.1002 M+H$^+$ found 412.1002.

(*E*)-2-((2-hydroxy-5-methylbenzylidene)amino)-3-(*p*-tolyl)-4*H*-thieno[2,3-*b*]chromen-4-one (4C9)

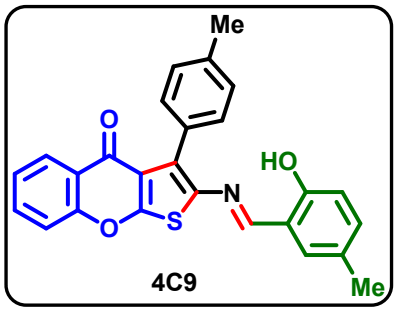

Yellow Solid (16 mg, 74%); **mp** 312 – 314 °C; **^{1}H NMR (400 MHz, $CDCl_3$)** δ 11.41 (s, 1H), 8.38 (s, 1H), 8.26 (dd, J = 8.0, 1.6 Hz, 1H), 7.68 (ddd, J = 8.6, 7.2, 1.7 Hz, 1H), 7.52 (d, J = 8.4 Hz, 1H), 7.46 – 7.38 (m, 4H), 7.31 (d, J = 7.8 Hz, 2H), 7.14 – 7.09 (m, 2H), 6.82 (d, J = 9.0 Hz, 1H), 2.44 (s, 3H), 2.29 (s, 3H); **^{13}C{^{1}H} NMR (125 MHz, $CDCl_3$)** δ 172.00, 165.14, 157.81, 157.68, 156.27, 138.04, 136.86, 134.43, 133.45, 133.43, 131.94, 130.11, 130.08, 128.57, 128.54, 126.92, 125.22, 123.61, 121.20, 118.63, 117.32, 117.09, 21.53, 20.27; **IR (KBr)** ν_{max}/cm^{-1} 2961, 2923, 1654, 1611, 1460, 1276; **HRMS (ESI)** calcd for $C_{26}H_{20}NO_3S^+$ 426.1158 M+H$^+$ found 426.1167.

(*E*)-2-((5-fluoro-2-hydroxybenzylidene)amino)-3-(*p*-tolyl)-4*H*-thieno[2,3-*b*]chromen-4-one (4C10)

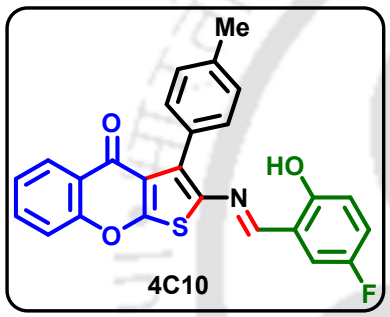

Yellow Solid (16 mg, 75%); **mp** 254 – 256 °C; **^{1}H NMR (400 MHz, $CDCl_3$)** δ 11.41 (s, 1H), 8.34 (s, 1H), 8.26 (dd, J = 7.9, 1.5 Hz, 1H), 7.72 – 7.65 (m, 1H), 7.52 (d, J = 8.3 Hz, 1H), 7.44 – 7.39 (m, 3H), 7.31 (d, J = 7.9 Hz, 2H), 7.02 (d, J = 8.2 Hz, 2H), 6.86 (dd, J = 8.5, 4.4 Hz, 1H), 2.45 (s, 3H); **^{13}C{^{1}H} NMR (125 MHz, $CDCl_3$)** δ 171.97, 165.42, 156.26, 156.08 (d, J = 2.9 Hz), 156.04 (d, J = 1.4 Hz), 155.68 (d, J = 237.8 Hz), 138.26, 136.15, 134.65, 133.56, 130.04, 129.89, 128.60, 126.91, 125.32, 123.56, 121.18, 120.46 (d, J = 23.4 Hz), 118.78 (d, J = 7.4 Hz), 118.43 (d, J = 7.5 Hz), 117.34, 116.65 (d, J = 23.5 Hz), 21.53; **^{19}F NMR (471 MHz, $CDCl_3$)** δ -124.86; **IR (KBr)** ν_{max}/cm^{-1} 2958, 2925, 1661, 1612, 1460, 1248; **HRMS (ESI)** calcd for $C_{25}H_{17}FNO_3S^+$ 430.0908 M+H$^+$ found 430.0915.

(*E*)-2-((5-bromo-2-hydroxybenzylidene)amino)-3-(*p*-tolyl)-4*H*-thieno[2,3-*b*]chromen-4-one (4C11)

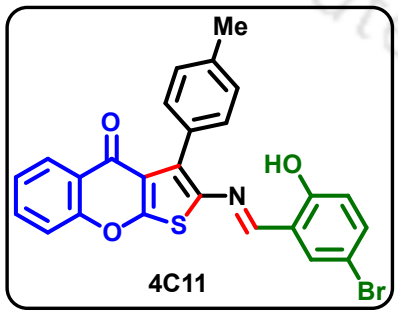

Yellow Solid (18 mg, 75%); **mp** 270 – 272 °C; **^{1}H NMR (400 MHz, $CDCl_3$)** δ 11.61 (s, 1H), 8.33 (s, 1H), 8.26 (dd, J = 7.9, 1.4 Hz, 1H), 7.72 – 7.66 (m, 1H), 7.52 (d, J = 8.3 Hz, 1H), 7.45 (d, J = 2.3 Hz, 1H), 7.41 (d, J = 8.0 Hz, 3H), 7.37 (dd, J = 8.9, 2.4 Hz, 1H), 7.31 (d, J = 7.9 Hz, 2H), 6.80 (d, J = 8.8 Hz, 1H), 2.45 (s, 3H); **^{13}C{^{1}H} NMR (125 MHz, $CDCl_3$)** δ 171.97, 165.45, 158.82, 156.25, 155.77, 138.29, 136.08, 135.84, 134.77, 133.81, 133.59, 130.03, 129.85, 128.61, 126.91, 125.35, 123.54, 121.16, 120.45, 119.24, 117.35, 110.95, 77.25, 77.00, 76.75, 21.54; **IR (KBr)** ν_{max}/cm^{-1} 2958, 2925, 2854, 1662, 1612, 1460, 1277; **HRMS (ESI)** calcd for $C_{25}H_{17}BrNO_3S^+$ 490.0107 M+H$^+$ found 490.0091.

(*E*)-2-((2-hydroxy-5-methoxybenzylidene)amino)-3-(*p*-tolyl)-4*H*-thieno[2,3-*b*]chromen-4-one (4C12)

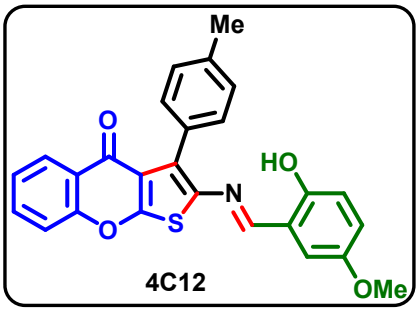

Yellow Solid (16 mg, 72%); **mp** 230 – 232 °C; **^{1}H NMR (400 MHz, $CDCl_3$)** δ 11.22 (s, 1H), 8.39 (s, 1H), 8.27 (dd, J = 8.0, 1.6 Hz, 1H), 7.69 (ddd, J = 8.6, 7.1, 1.7 Hz, 1H), 7.53 (d, J = 7.8 Hz, 1H), 7.45 – 7.40 (m, 3H), 7.31 (d, J = 7.9 Hz, 2H), 6.94 (dd, J = 9.0, 3.0 Hz, 1H), 6.86 (d, J = 9.0 Hz, 1H), 6.82 (d, J = 3.0 Hz, 1H), 3.80 (s, 3H), 2.44 (s, 3H); **^{13}C{^{1}H} NMR (125 MHz, $CDCl_3$)** δ 172.02, 165.24, 157.22, 156.27, 154.27, 152.46, 138.12, 136.65, 133.83, 133.49, 130.08, 130.02, 128.56, 126.93, 125.26, 123.59, 121.20, 120.94, 118.59, 118.19, 117.33, 114.66, 55.88, 21.54; **IR (KBr)** ν_{max}/cm^{-1} 2962, 2924, 2855, 1653, 1610, 1571, 1458, 1267; **HRMS (ESI)** calcd for $C_{26}H_{20}NO_4S^+$ 442.1108 M+H$^+$ found 442.1109.

(*E*)-3-(2-fluorophenyl)-2-((2-hydroxybenzylidene)amino)-4*H*-thieno[2,3-*b*]chromen-4-one (4C13)

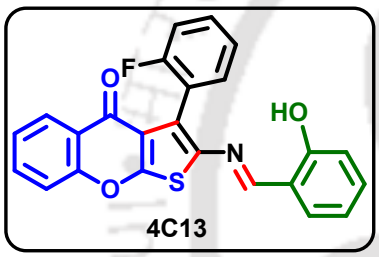

Yellow Solid (15 mg, 72%); **mp** 239 – 240 °C; **^{1}H NMR (600 MHz, $CDCl_3$)** δ 11.54 (s, 1H), 8.45 (s, 1H), 8.27 (d, J = 7.8 Hz, 1H), 7.70 (t, J = 7.8 Hz, 1H), 7.54 (d, J = 8.4 Hz, 1H), 7.49 (t, J = 6.9 Hz, 2H), 7.43 (t, J = 7.5 Hz, 1H), 7.35 (d, J = 7.3 Hz, 1H), 7.32 (d, J = 8.8 Hz, 1H), 7.30 (d, J = 7.5 Hz, 1H), 7.23 (d, J = 9.3 Hz, 1H), 6.94 – 6.90 (m, 2H); **^{13}C{^{1}H} NMR (150 MHz, $CDCl_3$)** δ 171.99, 164.64, 160.21 (d, J = 247.5 Hz), 160.14, 158.28, 156.46, 137.91, 133.65 (d, J = 19.7 Hz), 132.17, 131.82 (d, J = 2.9 Hz), 130.57 (d, J = 8.3 Hz), 126.85, 126.55, 125.32, 123.74 (d, J = 3.4 Hz), 123.41, 121.56, 121.37 (d, J = 16.0 Hz), 119.55, 118.82, 117.40 (d, J = 11.7 Hz), 115.55 (d, J = 21.7 Hz); **^{19}F NMR (471 MHz, $CDCl_3$)** δ -112.68; **IR (KBr)** ν_{max}/cm^{-1} 2963, 2924, 2853, 1659, 1615, 1553, 1461, 1275; **HRMS (ESI)** calcd for $C_{24}H_{15}FNO_3S^+$ 416.0757 M+H$^+$ found 416.0751.

(*E*)-2-((2-hydroxybenzylidene)amino)-6-methyl-3-phenyl-4*H*-thieno[2,3-*b*]chromen-4-one (4C14)

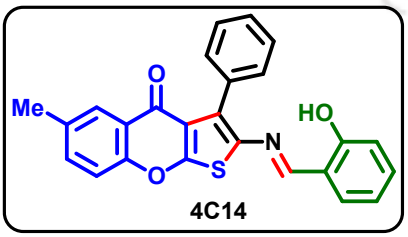

Yield Solid (17 mg, 81%); **mp** 233 – 235 °C; **^{1}H NMR (400 MHz, $CDCl_3$)** δ 11.55 (s, 1H), 8.37 (s, 1H), 8.02 (d, J = 1.0 Hz, 1H), 7.54 – 7.50 (m, 3H), 7.50 – 7.48 (m, 1H), 7.47 – 7.46 (m, 1H), 7.44 (d, J = 2.0 Hz, 1H), 7.39 (d, J = 8.5 Hz, 1H), 7.30 (ddd, J = 7.3, 3.8, 1.6 Hz, 2H), 6.92 – 6.87 (m, 2H), 2.41 (s, 3H); **^{13}C{^{1}H} NMR (125 MHz, $CDCl_3$)** δ 172.11, 165.14, 159.90, 157.51, 154.56, 136.76, 135.22, 134.65, 133.55, 133.42, 133.13, 131.98, 130.23, 128.33, 127.76, 126.24, 123.13, 120.95, 119.43, 118.93, 117.30, 117.07, 20.91; **IR (KBr)** ν_{max}/cm^{-1} 2961, 2925, 2856, 1660, 1618, 1471, 1276; **HRMS (ESI)** calcd for $C_{25}H_{18}NO_3S^+$ 412.1002 M+H$^+$ found 412.1005.

(*E*)-2-((5-bromo-2-hydroxybenzylidene)amino)-6-methyl-3-phenyl-4*H*-thieno[2,3-*b*]chromen-4-one (4C15)

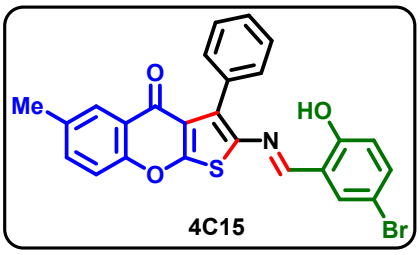

Yellow Solid (21 mg, 85%); **mp** 274 – 275 °C; **^{1}H NMR (400 MHz, $CDCl_3$)** δ 11.52 (s, 1H), 8.26 (s, 1H), 8.01 (d, J = 1.0 Hz, 1H), 7.51 (d, J = 1.8 Hz, 2H), 7.50 (s, 2H), 7.49 – 7.46 (m, 1H), 7.45 (d, J = 2.0 Hz, 1H), 7.41 – 7.37 (m, 2H), 7.35 (dd, J = 8.8, 2.4 Hz, 1H), 6.78 (d, J = 8.8 Hz, 1H), 2.41 (s, 3H); **^{13}C{^{1}H} NMR (125 MHz, $CDCl_3$)** δ 172.08, 165.41, 158.82, 155.76, 154.57, 136.23, 135.84, 135.35, 134.76, 134.65, 133.80, 132.97, 130.17, 128.46, 127.83, 126.27, 123.10, 120.97, 120.41, 119.25, 117.09, 110.93, 20.93; **IR (KBr)** ν_{max}/cm^{-1} 2960, 2924, 1656, 1616, 1469, 1276; **HRMS (ESI)** calcd for $C_{25}H_{17}BrNO_3S^+$ 490.0107 M+H$^+$ found 490.0080.

(*E*)-2-((5-bromo-2-hydroxybenzylidene)amino)-6-methyl-3-(*p*-tolyl)-4*H*-thieno[2,3-*b*]chromen-4-one (4C16)

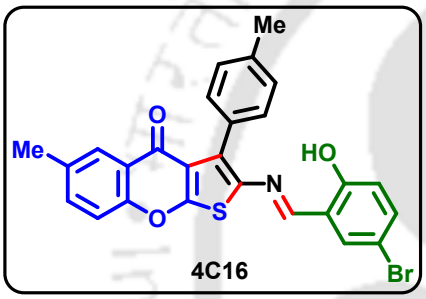

Yellow Solid (19 mg, 76%); **mp** 272 – 273 °C; **^{1}H NMR (400 MHz, $CDCl_3$)** δ 11.61 (s, 1H), 8.31 (s, 1H), 8.03 (s, 1H), 7.48 (d, J = 8.3 Hz, 1H), 7.43 (dd, J = 10.7, 1.6 Hz, 3H), 7.40 – 7.36 (m, 2H), 7.30 (d, J = 7.7 Hz, 2H), 6.80 (d, J = 8.8 Hz, 1H), 2.44 (s, 3H), 2.44 (s, 3H); **^{13}C{^{1}H} NMR (125 MHz, $CDCl_3$)** δ 172.10, 165.46, 158.83, 155.65, 154.59, 138.24, 135.93, 135.79, 135.31, 134.86, 134.71, 133.80, 130.07, 129.93, 128.59, 126.34, 123.22, 121.07, 120.51, 119.25, 117.08, 110.94, 21.53, 20.96; **IR (KBr)** ν_{max}/cm^{-1} 2961, 2924, 1658, 1616, 1470, 1275; **HRMS (ESI)** calcd for $C_{26}H_{19}BrNO_3S^+$ 504.0264 M+H$^+$ found 504.0236.

(*E*)-6-fluoro-2-((2-hydroxybenzylidene)amino)-3-phenyl-4*H*-thieno[2,3-*b*]chromen-4-one (4C17)

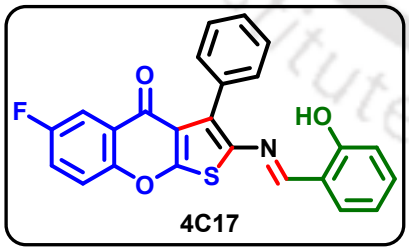

Yellow Solid (13 mg, 63%); **mp** 237 – 239 °C; **^{1}H NMR (400 MHz, $CDCl_3$)** δ 11.51 (s, 1H), 8.41 (s, 1H), 7.89 (dd, J = 8.2, 3.0 Hz, 1H), 7.56 – 7.47 (m, 6H), 7.43 – 7.36 (m, 1H), 7.34 – 7.28 (m, 2H), 6.93 – 6.88 (m, 2H); **^{13}C{^{1}H} NMR (125 MHz, $CDCl_3$)** δ 171.09, 165.39, 160.00, 159.52 (d, J = 246.9 Hz), 157.98, 152.40 (d, J = 1.7 Hz), 137.24, 133.63, 133.20, 132.90, 132.07, 130.19, 128.49, 127.85, 124.81 (d, J = 7.1 Hz), 121.53 (d, J = 25.6 Hz), 120.52, 119.50, 119.35 (d, J = 8.1 Hz), 118.86, 117.37, 111.87 (d, J = 24.2 Hz); **^{19}F NMR (471 MHz, $CDCl_3$)** δ -114.87; **IR (KBr)** ν_{max}/cm^{-1} 3060, 2956, 2925, 1659, 1622, 1469, 1277; **HRMS (ESI)** calcd for $C_{24}H_{15}FNO_3S^+$ 416.0757 M+H$^+$ found 416.0734.

(*E*)-7-fluoro-2-((2-hydroxybenzylidene)amino)-3-phenyl-4*H*-thieno[2,3-*b*]chromen-4-one (4C18)

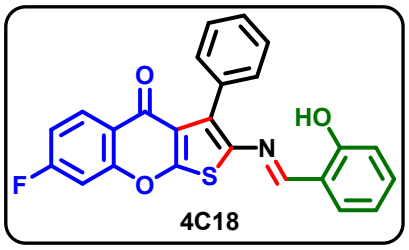

Yellow Solid (14 mg, 65%); **mp** 278 – 280 °C; **^{1}H NMR (400 MHz, $CDCl_3$)** δ 11.52 (s, 1H), 8.44 (s, 1H), 8.28 (dd, J = 8.8, 6.3 Hz, 1H), 7.54 – 7.45 (m, 5H), 7.35 – 7.30 (m, 2H), 7.23 (dd, J = 8.8, 2.3 Hz, 1H), 7.15 (td, J = 8.7, 2.3 Hz, 1H), 6.95 – 6.89 (m, 2H); **^{13}C{^{1}H} NMR (125 MHz, $CDCl_3$)** δ 171.11, 165.40 (d, J = 255.8 Hz), 165.02, 160.04, 157.96, 157.10 (d, J = 13.2 Hz), 137.26, 133.64, 133.41, 132.96, 132.08, 130.19, 129.33 (d, J = 10.6 Hz), 128.47, 127.85, 121.18, 120.39 (d, J = 2.4 Hz), 119.50, 118.88, 117.40, 113.93 (d, J = 22.5 Hz), 104.34 (d, J = 25.9 Hz); **^{19}F NMR (471 MHz, $CDCl_3$)** δ -102.77; **IR (KBr)** ν_{max}/cm^{-1} 3057, 2958, 2925, 2854, 1662, 1615, 1567, 1436, 1277; **HRMS (ESI)** calcd for $C_{24}H_{15}FNO_3S^+$ 416.0757 M+H$^+$ found 416.0727.

(*E*)-7-fluoro-2-((2-hydroxy-5-methoxybenzylidene)amino)-3-phenyl-4*H*-thieno[2,3-*b*]chromen-4-one (4C19)

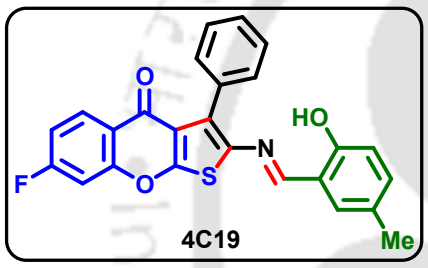

Yellow Solid (14 mg, 66%); **mp** 266 – 267 °C; **^{1}H NMR (500 MHz, $CDCl_3$)** δ 11.30 (s, 1H), 8.26 (dd, J = 8.4, 6.5 Hz, 1H), 7.53 – 7.43 (m, 5H), 7.20 (dd, J = 8.8, 1.8 Hz, 1H), 7.16 – 7.10 (m, 2H), 7.09 (s, 1H), 6.79 (d, J = 8.1 Hz, 1H), 2.27 (s, 3H); **^{13}C{^{1}H} NMR (125 MHz, $CDCl_3$)** δ 171.07, 165.34 (d, J = 255.8 Hz), 164.94, 157.97, 157.85, 157.03 (d, J = 13.2 Hz), 137.46, 134.62, 133.08, 132.96, 131.98, 130.19, 129.26 (d, J = 10.6 Hz), 128.60, 128.41, 127.81, 121.10, 120.33 (d, J = 2.6 Hz), 118.46, 117.11, 113.86 (d, J = 22.5 Hz), 104.30 (d, J = 26.0 Hz), 20.24; **IR (KBr)** ν_{max}/cm^{-1} 3062, 2961, 2925, 2860, 1660, 1615, 1576, 1434, 1278; **HRMS (ESI)** calcd for $C_{25}H_{17}FNO_3S^+$ 430.0908 M+H$^+$ found 430.0911.

(*E*)-2-((5-bromo-2-hydroxybenzylidene)amino)-7-fluoro-3-phenyl-4*H*-thieno[2,3-*b*]chromen-4-one (4C20)

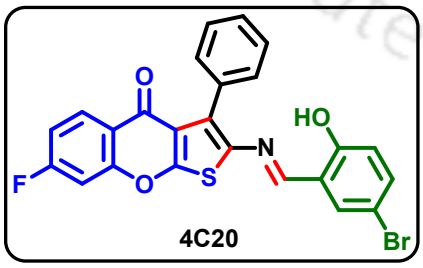

Yellow Solid (17 mg, 68%); **mp** 284 – 285 °C; **^{1}H NMR (500 MHz, $CDCl_3$)** δ 11.49 (s, 1H), 8.34 (s, 1H), 8.30 – 8.24 (m, 1H), 7.54 – 7.47 (m, 5H), 7.45 (s, 1H), 7.38 (d, J = 8.7 Hz, 1H), 7.22 (d, J = 8.7 Hz, 1H), 7.15 (t, J = 8.2 Hz, 1H), 6.79 (d, J = 8.8 Hz, 1H); **^{13}C{^{1}H} NMR (125 MHz, $CDCl_3$)** δ 171.08, 165.48 (d, J = 255.8 Hz), 165.30, 158.96, 157.12 (d, J = 14.0 Hz), 156.20, 136.73, 136.08, 134.52, 133.91, 132.81, 130.14, 129.37 (d, J = 10.6 Hz), 128.62, 127.93, 121.20, 120.37, 119.35, 114.05 (d, J = 22.9 Hz), 111.01, 104.41 (d, J = 25.9 Hz); **^{19}F NMR (471 MHz, $CDCl_3$)** δ -102.48; **IR (KBr)** ν_{max}/cm^{-1} 3053, 2961, 2924, 1658, 1615, 1571, 1435, 1276; **HRMS (ESI)** calcd for $C_{24}H_{14}BrFNO_3S^+$ 493.9856 M+H$^+$ found 493.9830.

(*E*)-6-chloro-2-((2-hydroxybenzylidene)amino)-3-phenyl-4*H*-thieno[2,3-*b*]chromen-4-one (4C21)

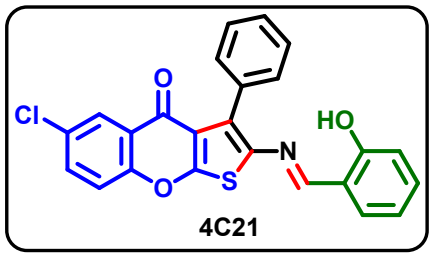

Yellow Solid (13 mg, 60%); **mp** 224 – 226 °C; **^{1}H NMR (400 MHz, $CDCl_3$)** δ 11.52 (s, 1H), 8.44 (s, 1H), 8.22 (d, J = 2.6 Hz, 1H), 7.63 (dd, J = 8.9, 2.6 Hz, 1H), 7.52 – 7.50 (m, 4H), 7.49 (t, J = 2.5 Hz, 1H), 7.32 (td, J = 6.7, 5.9, 1.7 Hz, 3H), 6.94 – 6.88 (m, 2H); **^{13}C{^{1}H} NMR (125 MHz, $CDCl_3$)** δ 170.78, 165.24, 160.03, 158.09, 154.58, 137.33, 133.69, 133.65, 133.28, 132.83, 132.10, 131.21, 130.20, 128.51, 127.86, 126.34, 124.56, 121.00, 119.53, 119.04, 118.86, 117.40; **IR (KBr)** ν_{max}/cm^{-1} 3053, 2963, 2926, 2855, 1661, 1611, 1465, 1277; **HRMS (ESI)** calcd for $C_{24}H_{15}ClNO_3S^+$ 432.0461 M+H$^+$ found 432.0436.

(*E*)-2-((5-bromo-2-hydroxybenzylidene)amino)-6-chloro-3-phenyl-4*H*-thieno[2,3-*b*]chromen-4-one (4C22)

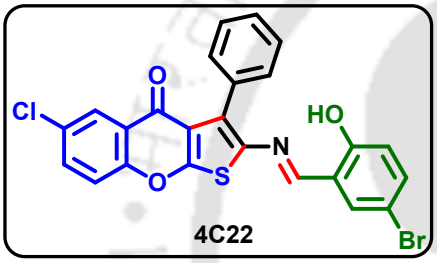

Yellow Solid (17 mg, 65%); **mp** 227 – 229 °C; **^{1}H NMR (400 MHz, $CDCl_3$)** δ 11.49 (s, 1H), 8.34 (s, 1H), 8.21 (d, J = 2.5 Hz, 1H), 7.63 (dd, J = 8.9, 2.6 Hz, 1H), 7.53 – 7.47 (m, 6H), 7.45 (d, J = 2.4 Hz, 1H), 7.38 (dd, J = 8.8, 2.4 Hz, 1H), 6.80 (d, J = 8.8 Hz, 1H); **^{13}C{^{1}H} NMR (125 MHz, $CDCl_3$)** δ 170.72, 165.47, 158.93, 156.31, 154.56, 136.77, 136.10, 134.35, 133.91, 133.76, 132.66, 131.33, 130.13, 128.64, 127.92, 126.34, 124.52, 120.99, 120.32, 119.33, 119.06, 111.01; **IR (KBr)** ν_{max}/cm^{-1} 3055, 2957, 2924, 2854, 1658, 1604, 1460, 1275; **HRMS (ESI)** calcd for $C_{24}H_{14}BrClNO_3S^+$ 509.9561 M+H$^+$ found 509.9530.

(*E*)-6-bromo-2-((5-bromo-2-hydroxybenzylidene)amino)-3-phenyl-4*H*-thieno[2,3-*b*]chromen-4-one (4C23)

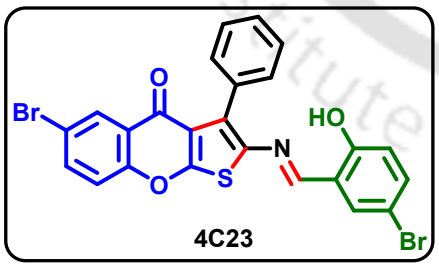

Yellow Solid (17 mg, 62%); **mp** 285 – 287 °C; **^{1}H NMR (400 MHz, $CDCl_3$)** δ 11.49 (s, 1H), 8.36 (d, J = 2.4 Hz, 1H), 8.33 (s, 1H), 7.77 (dd, J = 8.8, 2.4 Hz, 1H), 7.50 (s, 5H), 7.44 (d, J = 2.4 Hz, 1H), 7.43 (d, J = 9.0 Hz, 1H), 7.38 (dd, J = 8.8, 2.2 Hz, 1H), 6.79 (d, J = 8.8 Hz, 1H); **^{13}C{^{1}H} NMR (125 MHz, $CDCl_3$)** δ 170.59, 165.43, 158.92, 156.33, 155.02, 136.78, 136.54, 136.11, 134.35, 133.91, 132.63, 130.13, 129.53, 128.64, 127.91, 124.85, 121.03, 120.31, 119.33, 119.29, 118.73, 111.01; **IR (KBr)** ν_{max}/cm^{-1} 3060, 2956, 2925, 2854, 1656, 1611, 1464, 1277; **HRMS (ESI)** calcd for $C_{24}H_{14}Br_2NO_3S^+$ 553.9056 M+H$^+$ found 553.9042.

(*E*)-2-((2-hydroxybenzylidene)amino)-6-methoxy-3-phenyl-4*H*-thieno[2,3-*b*]chromen-4-one (4C24)

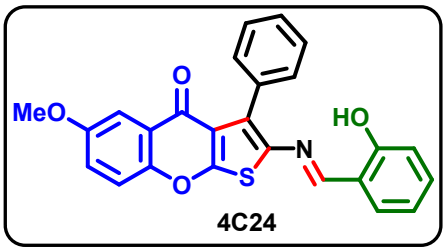

Yellow Solid (18 mg, 86%); **mp** 274 – 275 °C; **^{1}H NMR (400 MHz, $CDCl_3$)** δ 11.58 (s, 1H), 8.42 (s, 1H), 7.65 (d, J = 3.1 Hz, 1H), 7.54 – 7.51 (m, 4H), 7.49 – 7.45 (m, 2H), 7.33 (d, J = 7.7 Hz, 2H), 7.28 (d, J = 3.1 Hz, 1H), 6.90 (d, J = 7.7 Hz, 2H), 3.85 (s, 3H); **^{13}C{^{1}H} NMR (150 MHz, $CDCl_3$)** δ 171.96, 165.15, 159.99, 157.66, 156.95, 151.14, 136.87, 133.51, 133.48, 133.19, 132.01, 130.22, 128.33, 127.78, 124.11, 123.24, 120.54, 119.46, 118.97, 118.69, 117.36, 106.25, 55.85; **IR (KBr)** ν_{max}/cm^{-1} 3059, 2959, 2925, 2854, 1653, 1618, 1473, 1276; **HRMS (ESI)** calcd for $C_{25}H_{18}NO_4S^+$ 428.0951 M+H$^+$ found 428.0950.

(*E*)-2-((5-fluoro-2-hydroxybenzylidene)amino)-6-methoxy-3-phenyl-4*H*-thieno[2,3-*b*]chromen-4-one (4C25)

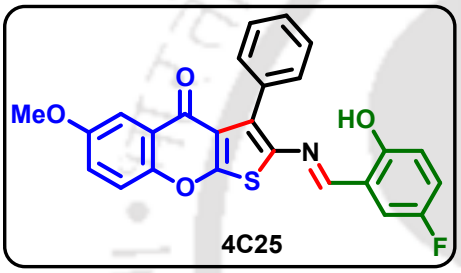

Yellow Solid (19 mg, 87%); **mp** 268 – 269 °C; **^{1}H NMR (400 MHz, $CDCl_3$)** δ 11.35 (s, 1H), 8.33 (s, 1H), 7.65 (d, J = 3.1 Hz, 1H), 7.52 (s, 2H), 7.51 (s, 2H), 7.48 (t, J = 2.2 Hz, 1H), 7.45 (s, 1H), 7.28 (d, J = 3.1 Hz, 1H), 7.02 (d, J = 8.2 Hz, 2H), 6.85 (dd, J = 9.0, 4.4 Hz, 1H), 3.85 (s, 3H); **^{13}C{^{1}H} NMR (125 MHz, $CDCl_3$)** δ 171.95, 165.37, 156.97, 156.15 (d, J = 3.0 Hz), 156.08 (d, J = 1.3 Hz), 155.67 (d, J = 237.8 Hz), 151.12, 136.37, 134.46, 133.03, 130.15, 128.45, 127.82, 124.05, 123.34, 120.63, 120.48 (d, J = 8.2 Hz), 118.76, 118.71, 118.48 (d, J = 7.5 Hz), 116.65 (d, J = 23.5 Hz), 106.19, 55.85; **^{19}F NMR (471 MHz, $CDCl_3$)** δ -124.85; **IR (KBr)** ν_{max}/cm^{-1} 3059, 2958, 2925, 2853, 1655, 1613, 1471, 1274; **HRMS (ESI)** calcd for $C_{25}H_{17}FNO_4S^+$ 446.0857 M+H$^+$ found 446.0851.

(*E*)-3-(4-fluorophenyl)-2-((2-hydroxybenzylidene)amino)-6-methoxy-4*H*-thieno[2,3-*b*]chromen-4-one (4C26)

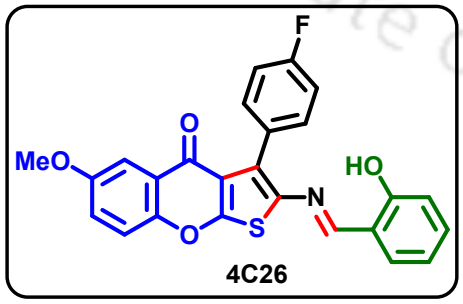

Yellow Solid (18 mg, 81%); **mp** 255 – 256 °C; **^{1}H NMR (400 MHz, $CDCl_3$)** δ 11.57 (s, 1H), 8.42 (s, 1H), 7.64 (d, J = 3.1 Hz, 1H), 7.51 (dd, J = 8.7, 5.4 Hz, 2H), 7.46 (d, J = 9.1 Hz, 1H), 7.36 – 7.31 (m, 2H), 7.28 (d, J = 3.2 Hz, 1H), 7.20 (t, J = 8.7 Hz, 2H), 6.91 (d, J = 7.9 Hz, 2H), 3.86 (s, 3H); **^{13}C{^{1}H} NMR (125 MHz, $CDCl_3$)** δ 172.04, 165.10, 162.67 (d, J = 247.9 Hz), 159.96, 157.98, 156.97, 151.09, 137.02, 133.66, 132.13 (d, J = 8.4 Hz), 132.08, 128.97 (d, J = 3.4 Hz), 123.98, 123.36, 120.34, 119.56, 118.85, 118.71, 117.31, 114.87 (d, J = 21.7 Hz), 106.09, 55.84; **^{19}F NMR (471 MHz, $CDCl_3$)** δ -113.06; **IR (KBr)** ν_{max}/cm^{-1} 2960, 2925, 2853, 1650, 1612, 1473, 1276; **HRMS (ESI)** calcd for $C_{25}H_{17}FNO_4S^+$ 446.0857 M+H$^+$ found 446.0852.

(*E*)-2-((4-methylbenzylidene)amino)-3-phenyl-4*H*-thieno[2,3-*b*]chromen-4-one (4C27)

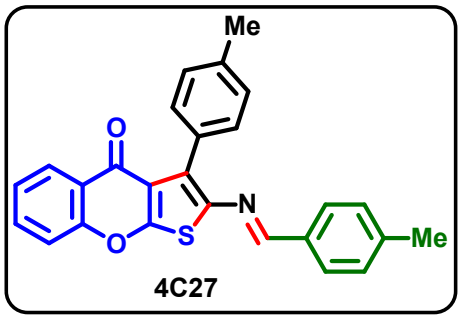

Yellow Solid (15 mg, 74%); **mp** 251 – 253 °C; **^{1}H NMR (600 MHz, $CDCl_3$)** δ 8.35 (s, 1H), 8.29 (d, J = 7.4 Hz, 1H), 7.70 – 7.64 (m, 1H), 7.60 (dd, J = 18.7, 7.1 Hz, 4H), 7.51 (d, J = 8.1 Hz, 1H), 7.49 – 7.44 (m, 2H), 7.44 – 7.38 (m, 2H), 7.20 (d, J = 7.1 Hz, 2H), 2.37 (s, 3H); **^{13}C{^{1}H} NMR (150 MHz, $CDCl_3$)** δ 172.09, 165.35, 156.21, 155.87, 142.12, 139.48, 133.35, 133.25, 133.07, 133.01, 131.49, 129.53, 128.98, 127.61, 126.88, 125.04, 123.65, 121.09, 117.28, 21.65; **IR (KBr)** ν_{max}/cm^{-1} 2956, 2925, 2853, 1662, 1605, 1473, 1267; **HRMS (ESI)** calcd for $C_{25}H_{18}NO_2S^+$ 396.1053 M+H$^+$ found 396.1050.

(*E*)-6-chloro-2-((4-methoxybenzylidene)amino)-3-(*p*-tolyl)-4*H*-thieno[2,3-*b*]chromen-4-one (4C28)

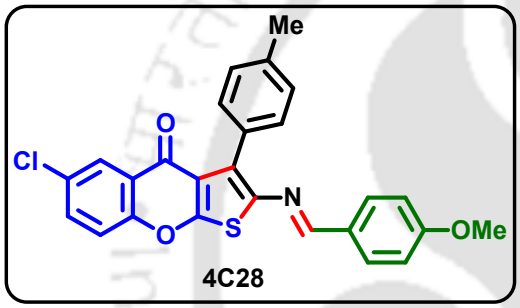

Yellow Solid (14 mg, 62%); **mp** 235 – 236 °C; **^{1}H NMR (400 MHz, $CDCl_3$)** δ 8.30 (s, 1H), 8.22 (d, J = 2.5 Hz, 1H), 7.69 (d, J = 8.7 Hz, 2H), 7.60 (dd, J = 8.9, 2.6 Hz, 1H), 7.46 (d, J = 7.2 Hz, 3H), 7.28 (s, 2H), 6.91 (d, J = 8.7 Hz, 2H), 3.84 (s, 3H), 2.45 (s, 3H); **^{13}C{^{1}H} NMR (125 MHz, $CDCl_3$)** δ 170.80, 165.24, 162.43, 155.38, 154.43, 139.74, 137.37, 133.27, 131.32, 130.80, 130.15, 128.56, 127.73, 126.31, 124.69, 120.96, 118.93, 114.27, 55.41, 21.48; **IR (KBr)** ν_{max}/cm^{-1} 3069, 2954, 2924, 2852, 1676, 1603, 1462, 1257; **HRMS (ESI)** calcd for $C_{26}H_{19}ClNO_3S^+$ 460.0769 M+H$^+$ found 460.0760.

(*E*)-6-chloro-2-((4-nitrobenzylidene)amino)-3-(*p*-tolyl)-4*H*-thieno[2,3-*b*]chromen-4-one (4C29)

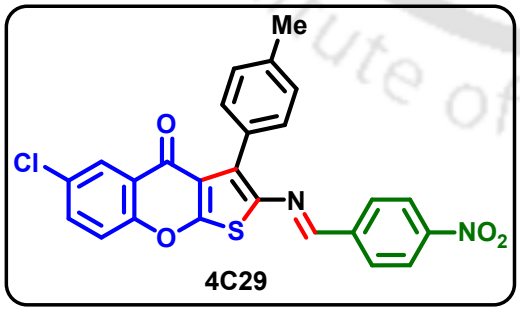

Yellow Solid (19 mg, 81%); **mp** 241 – 243 °C; **^{1}H NMR (400 MHz, $CDCl_3$)** δ 8.41 (s, 1H), 8.26 (d, J = 8.6 Hz, 2H), 8.23 (d, J = 2.4 Hz, 1H), 7.88 (d, J = 8.6 Hz, 2H), 7.63 (dd, J = 8.8, 2.5 Hz, 1H), 7.49 (d, J = 8.9 Hz, 1H), 7.46 (d, J = 7.9 Hz, 2H), 7.30 (d, J = 7.9 Hz, 2H), 2.47 (s, 3H); **^{13}C{^{1}H} NMR (125 MHz, $CDCl_3$)** δ 170.78, 166.43, 154.48, 152.30, 149.04, 141.01, 138.20, 136.67, 133.69, 131.26, 129.67, 129.35, 127.90, 126.42, 124.65, 124.07, 121.06, 119.00, 21.51; **IR (KBr)** ν_{max}/cm^{-1} 3092, 2957, 2924, 2855, 1660, 1605, 1520, 1455, 1344; **HRMS (ESI)** calcd for $C_{25}H_{16}ClN_2O_4S^+$ 475.0514 M+H$^+$ found 475.0513.

(*E*)-2-((5-bromo-2-hydroxybenzylidene)amino)-6-chloro-3-ethyl-4*H*-thieno[2,3-*b*]chromen-4-one (4C30)

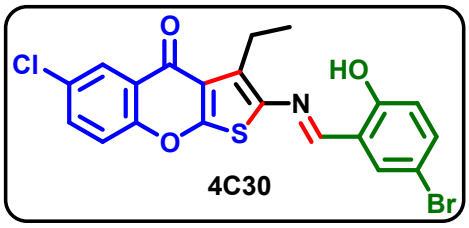

Yellow Solid (12 mg, 54%); **mp** 212 – 213 °C; **^{1}H NMR (600 MHz, $CDCl_3$)** δ 12.21 (s, 1H), 8.29 (s, 1H), 8.28 (d, J = 2.5 Hz, 1H), 7.63 (dd, J = 8.9, 2.5 Hz, 1H), 7.50 (d, J = 2.3 Hz, 1H), 7.47 (d, J = 8.8 Hz, 1H), 7.45 (dd, J = 8.8, 2.3 Hz, 1H), 6.93 (d, J = 8.8 Hz, 1H), 3.25 (q, J = 7.5 Hz, 2H), 1.30 (t, J = 7.5 Hz, 3H); **^{13}C{^{1}H} NMR (150 MHz, $CDCl_3$)** δ 171.62, 165.91, 159.17, 155.27, 154.69, 138.01, 135.85, 134.63, 133.81, 133.68, 131.21, 126.22, 124.46, 121.44, 120.42, 119.21, 119.12, 111.14, 21.23, 14.77; **IR (KBr)** ν_{max}/cm^{-1} 2957, 2925, 2854, 1646, 1605, 1460, 1297, 1278; **HRMS (ESI)** calcd for $C_{20}H_{14}BrClNO_3S^+$ 461.9561 M+H$^+$ found 461.9547.

4.10 Copies of ^{1}H NMR, $^{13}C\{^{1}H\}$ NMR and HRMS spectra of Compounds

Figure 4.2a: ^{1}H NMR (400 MHz, $CDCl_3$) spectrum of compound **4C1**.

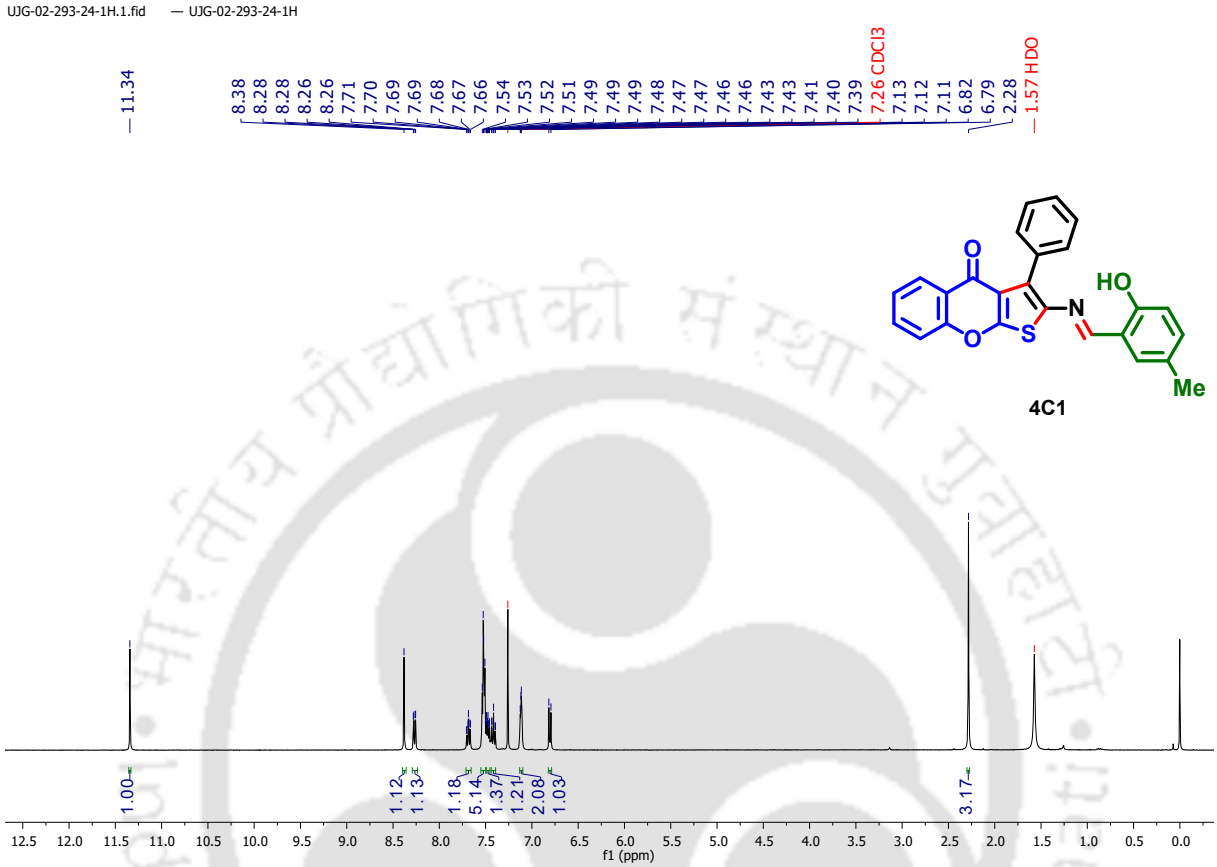

Figure 4.2b: $^{13}C\{^{1}H\}$ NMR (125 MHz, $CDCl_3$) spectrum of compound **4C1**.

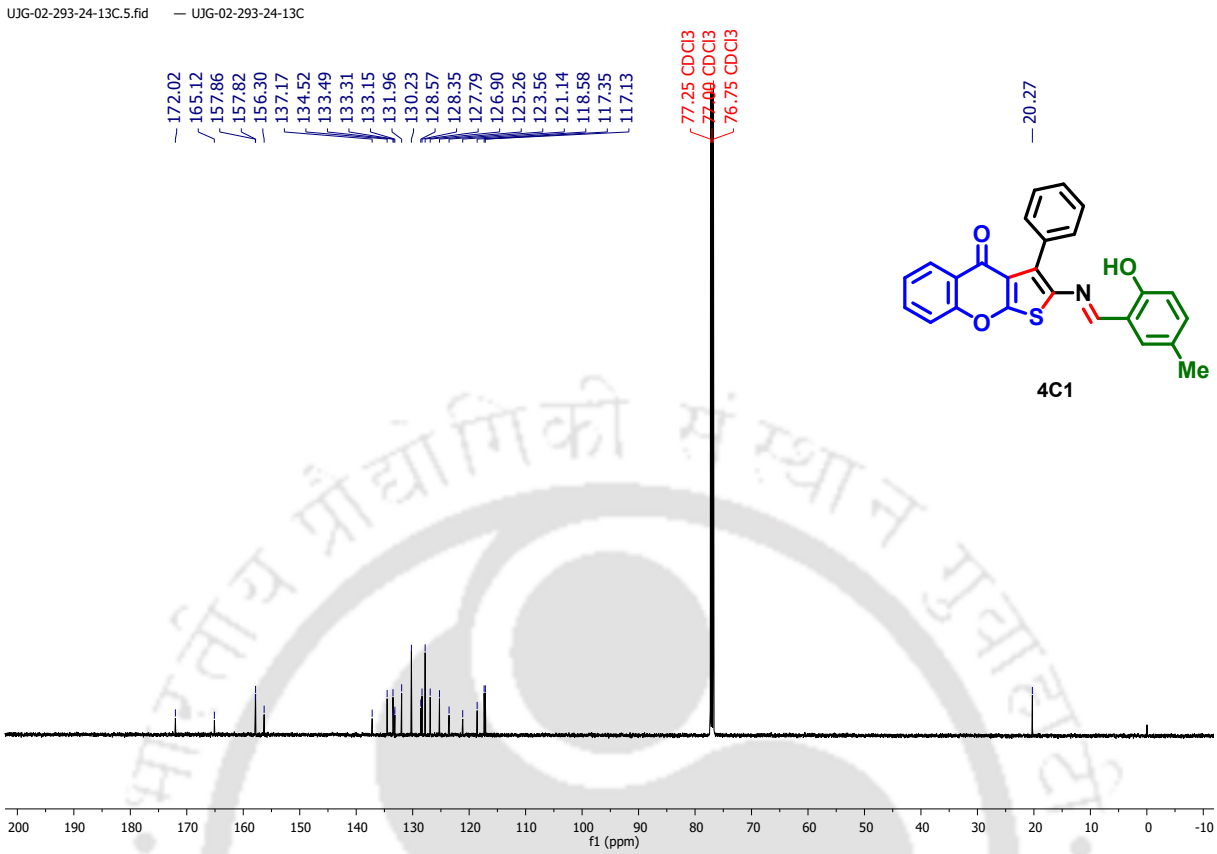

Figure 4.2c: HRMS spectrum of compound **4C1**.

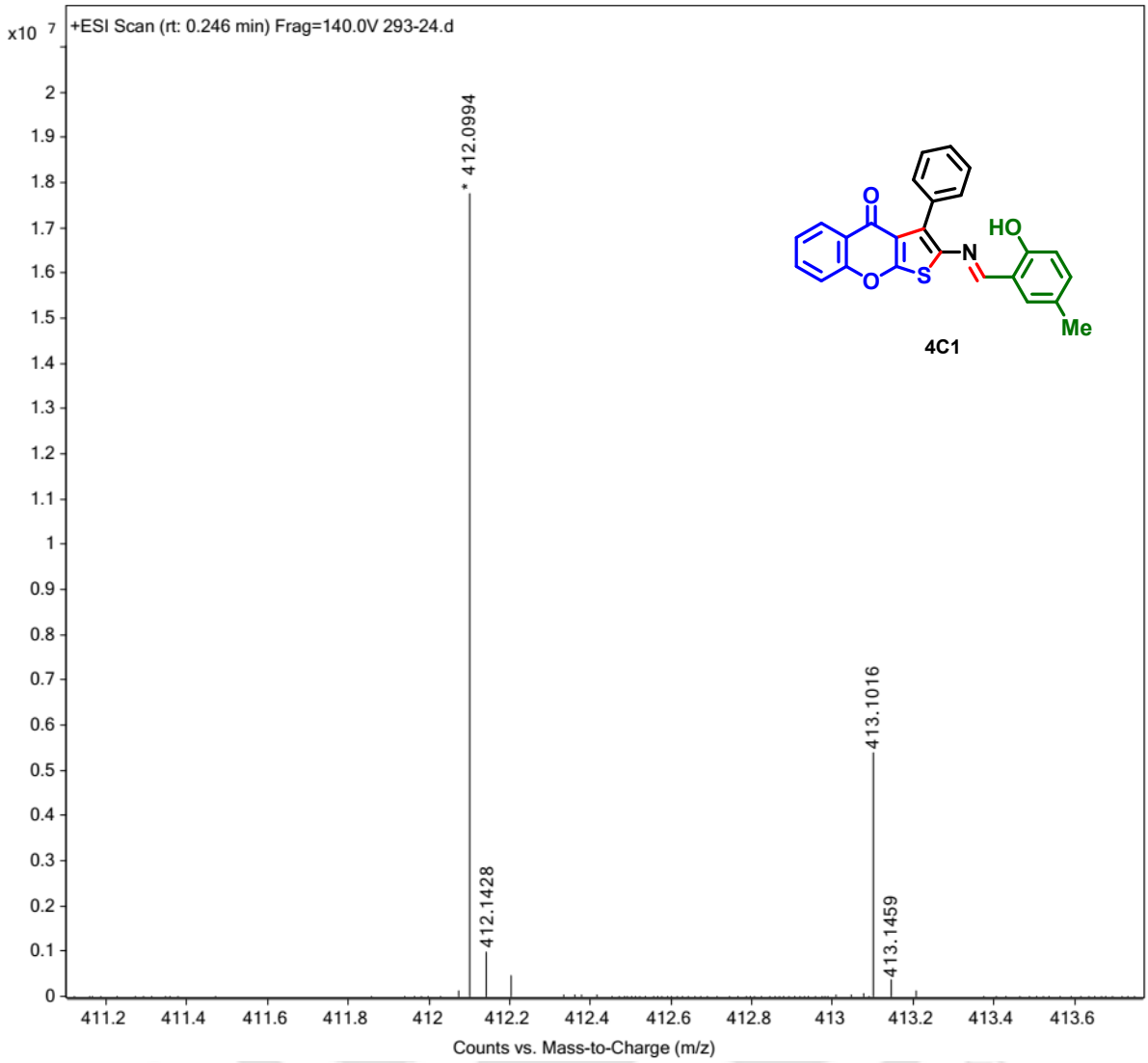

Figure 4.3a: ^{1}H NMR (400 MHz, $CDCl_3$) spectrum of compound **4C9**.

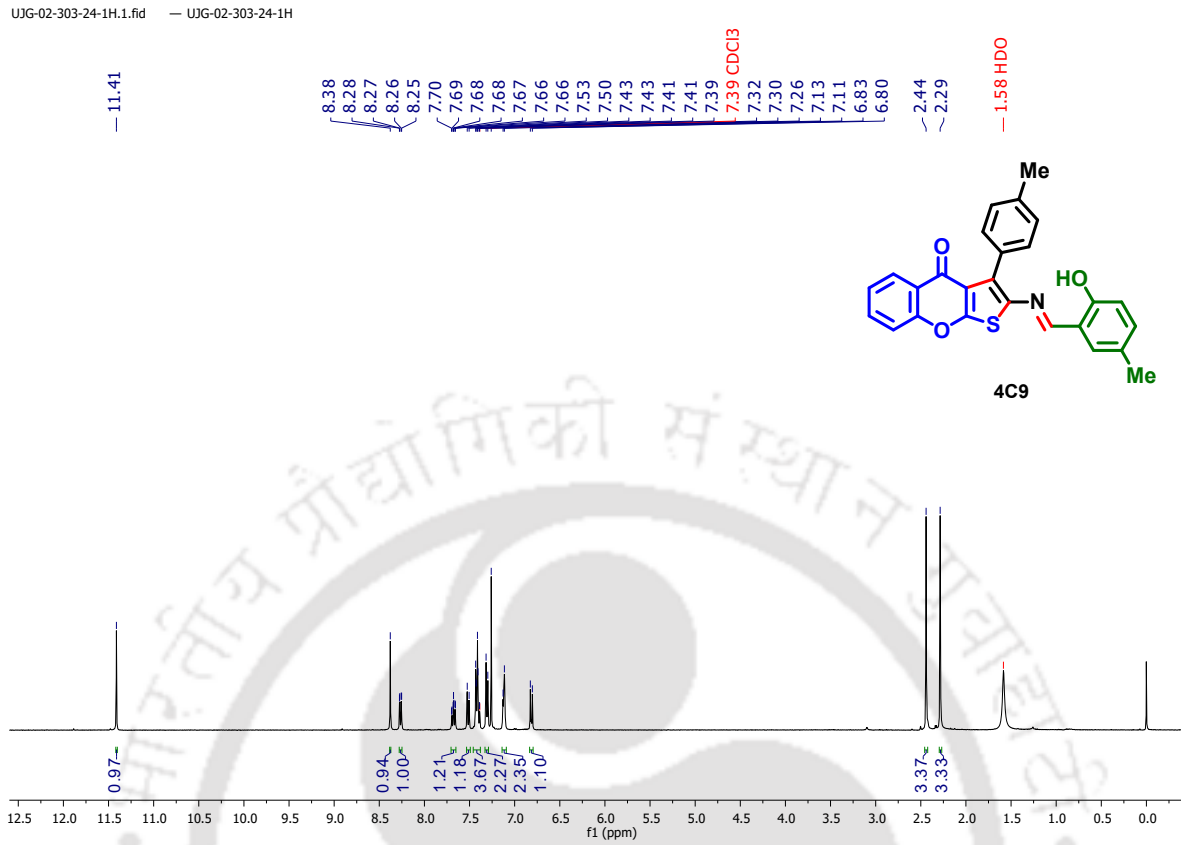

Figure 4.3b: $^{13}C\{^{1}H\}$ NMR (125 MHz, $CDCl_3$) spectrum of compound **4C9**.

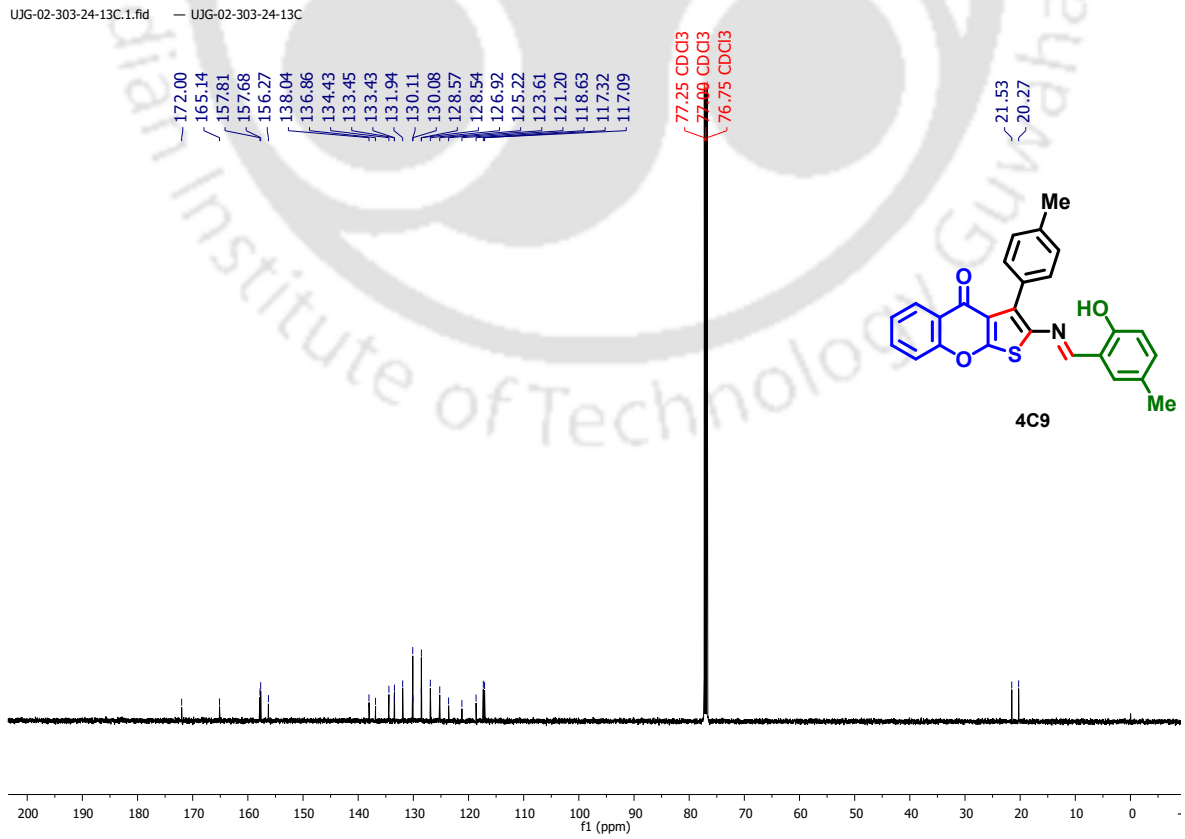

Figure 4.3c: HRMS spectrum of compound **4C9**.

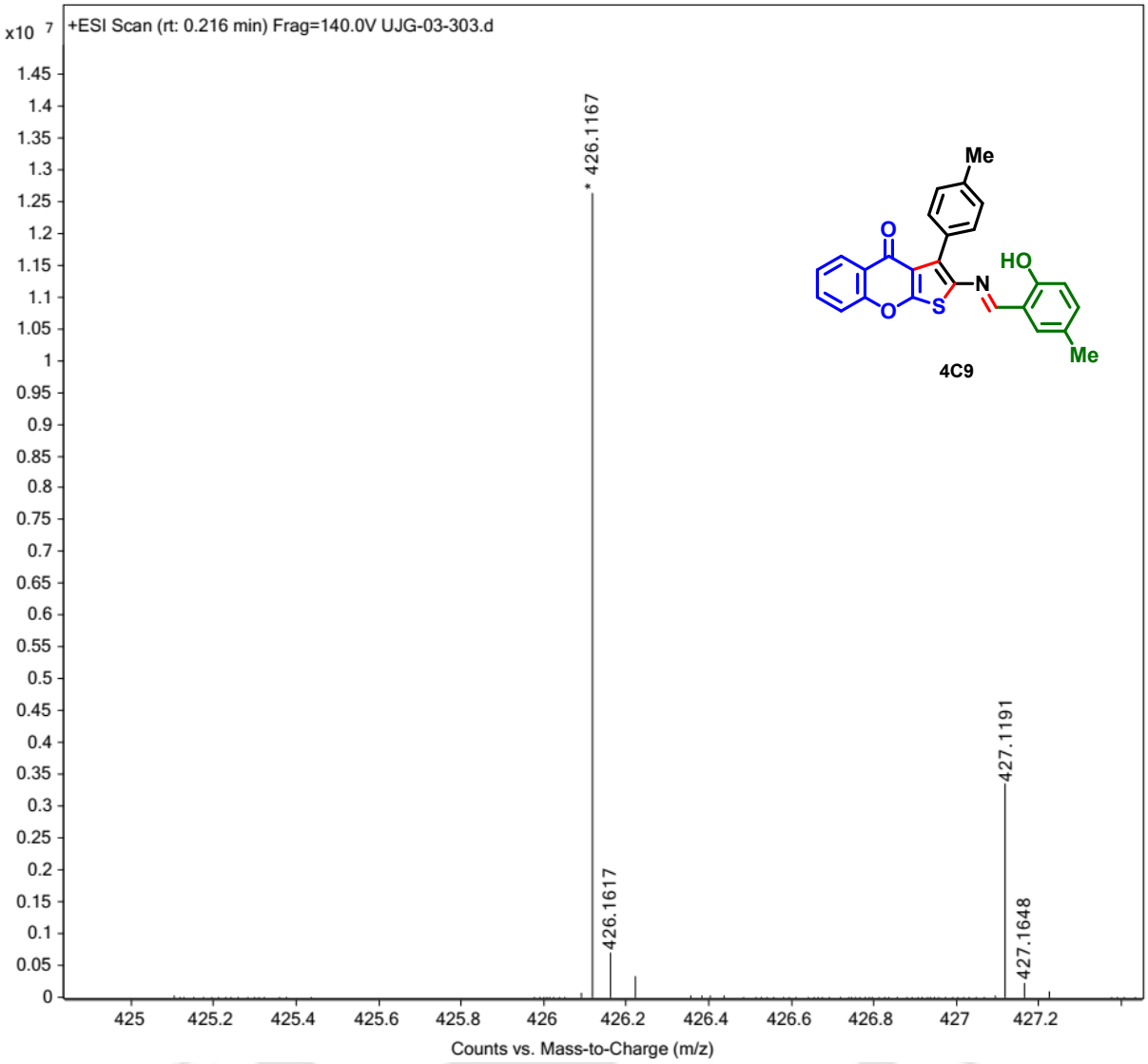

Figure 4.4a: ^{1}H NMR (400 MHz, $CDCl_3$) spectrum of compound **4C14**.

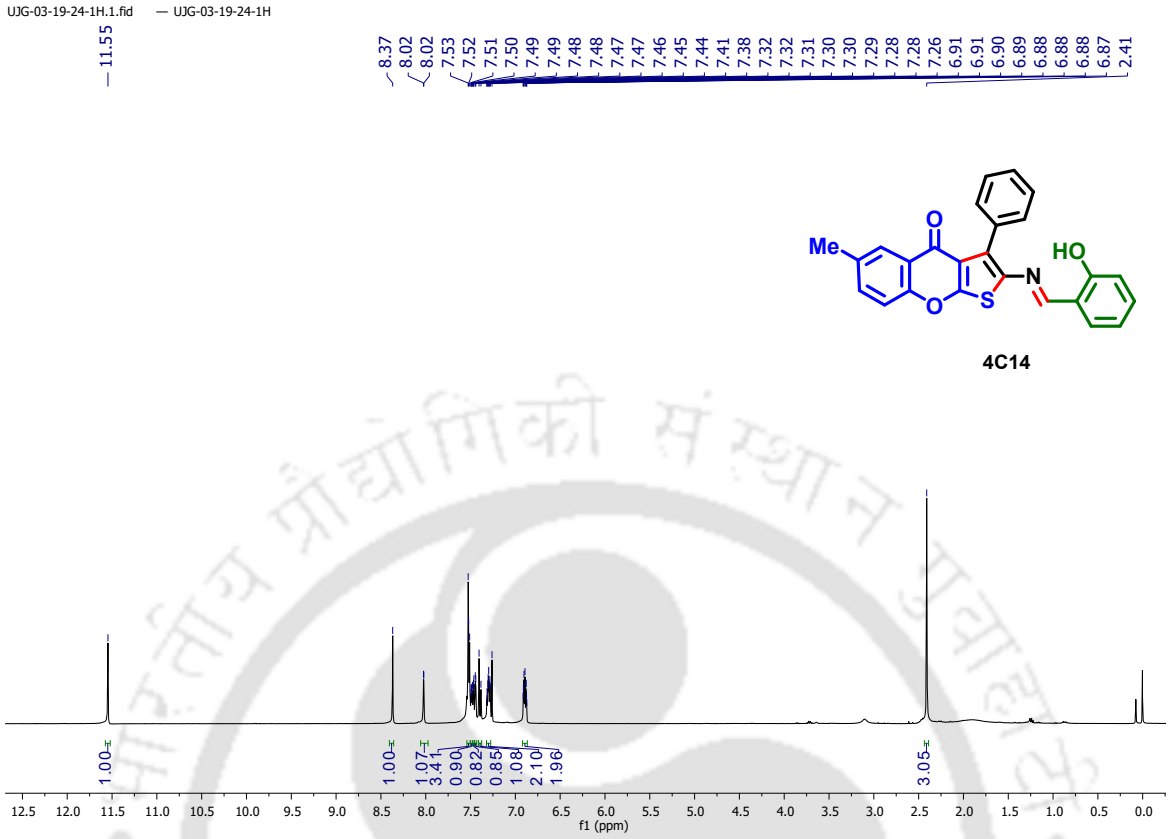

Figure 4.4b: $^{13}C\{^{1}H\}$ NMR (125 MHz, $CDCl_3$) spectrum of compound **4C14**.

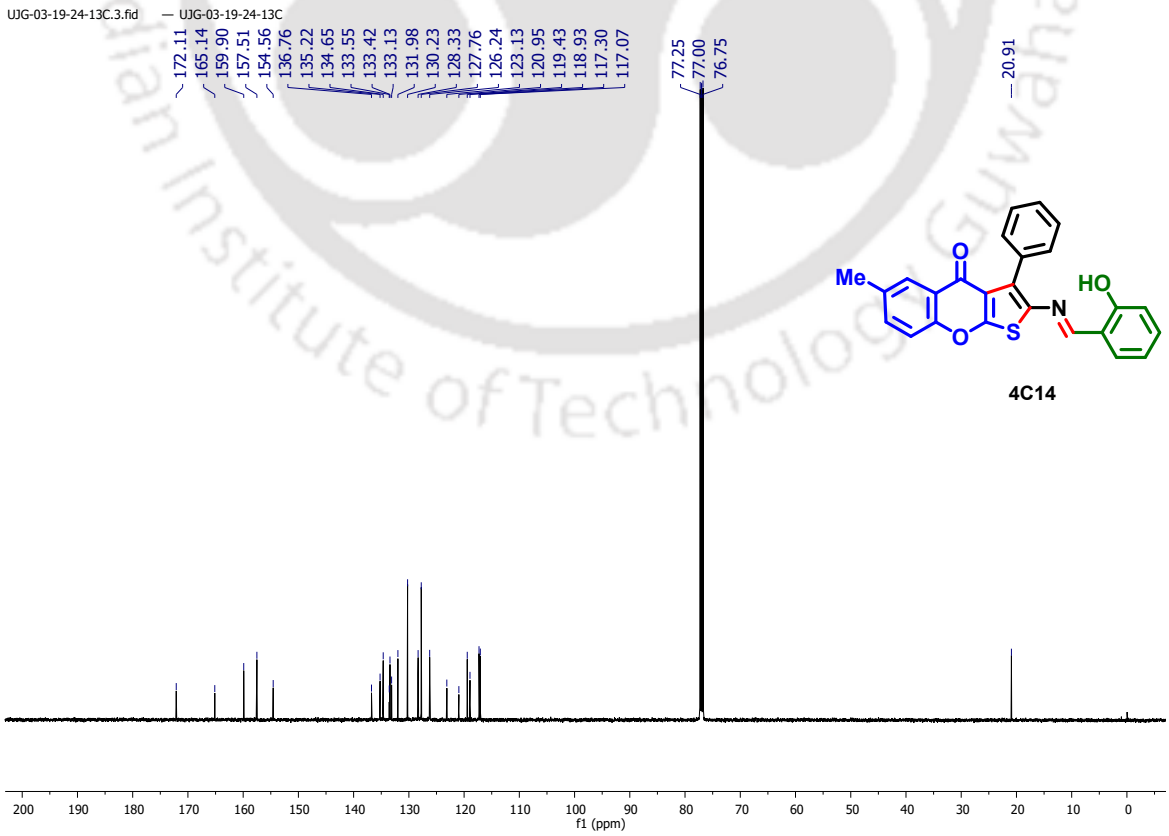

Figure 4.4c: HRMS spectrum of compound **4C14**.

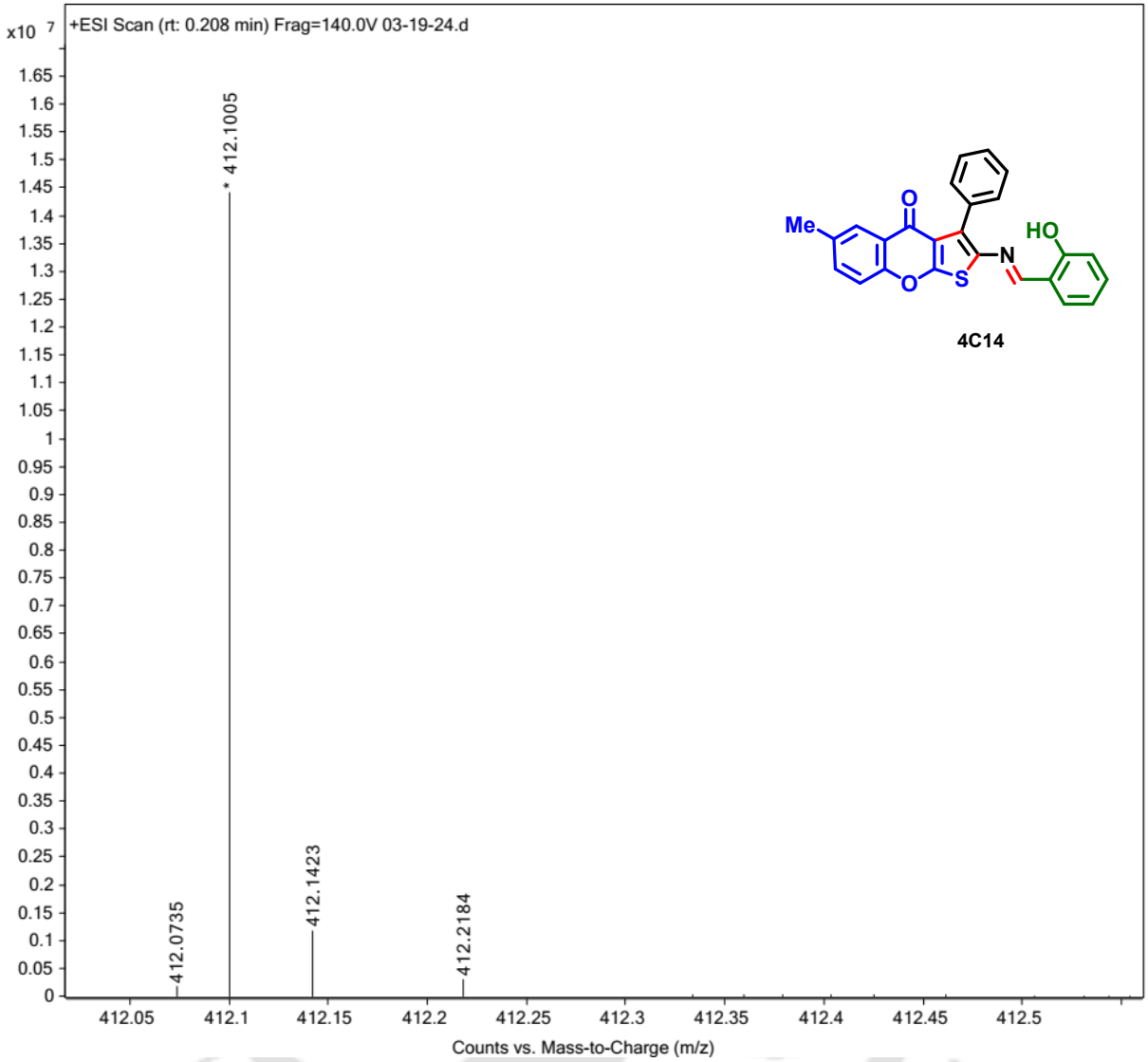

Detection of intermediates in HRMS

0.1 mmol of 4-hydroxythiocoumarin **1A1** and *trans*-β-nitrostyrene **4A1** and 0.05 mmol of 2-hydroxy-5-methyl-benzaldehyde **4B1** was stirred in Ethanol in a 10 mL round bottom flask at reflux temperature. After 5.5 h. the reaction mixture was subjected to ESI-MS mass experiment, and the intermediates **E**, **G**, **H** and **I** were detected by HRMS values. The observed m/z values are as follows: intermediate **E**: 310.0530 (expected 310.0532); intermediate **G**: 308.0369 (expected 308.0376); intermediate **H** or **I**: 294.0577 (expected 294.0583).

Figure 4.5a: HRMS spectrum of intermediate **E**.

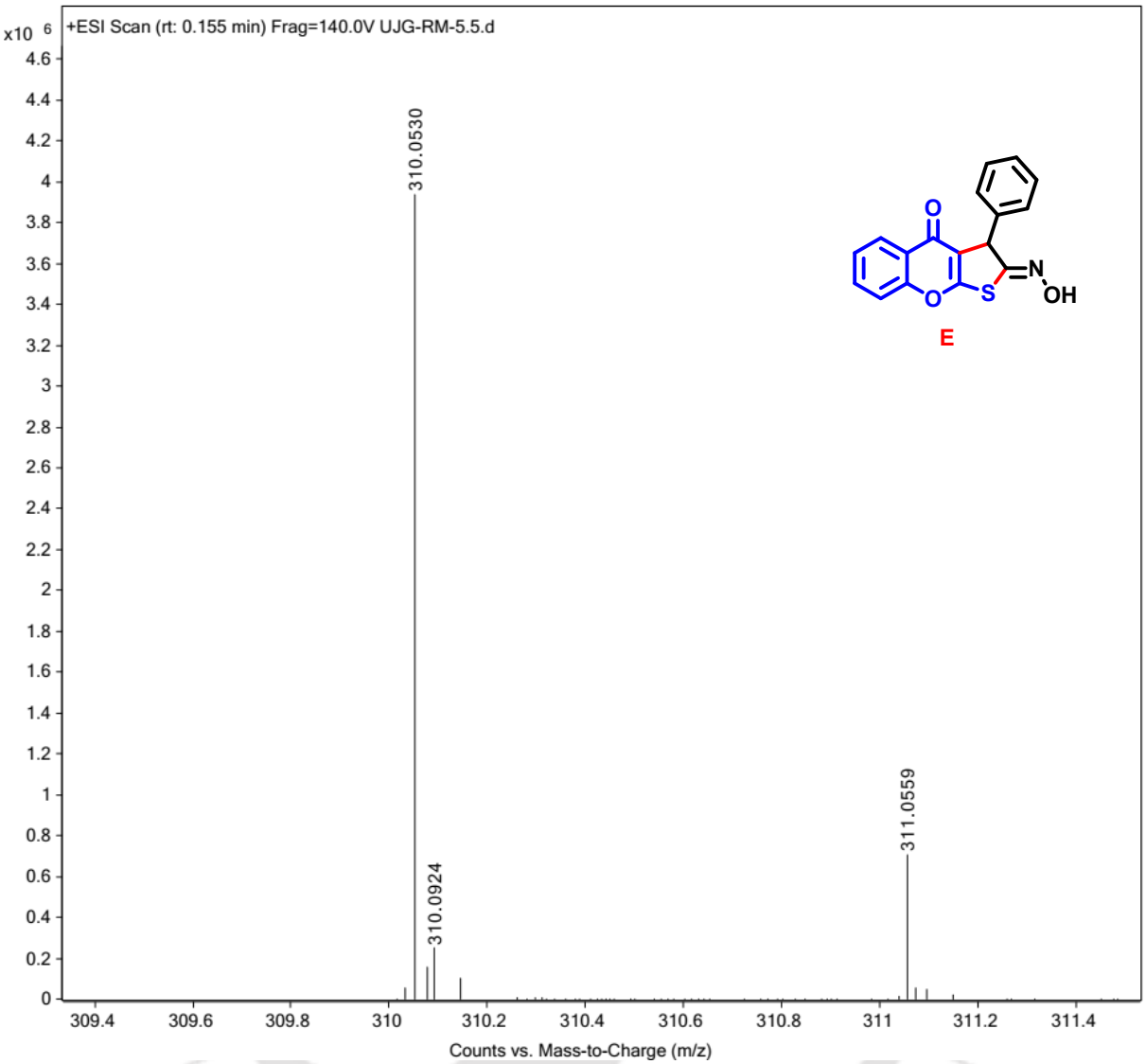

Figure 4.5b: HRMS spectrum of intermediate **G**.

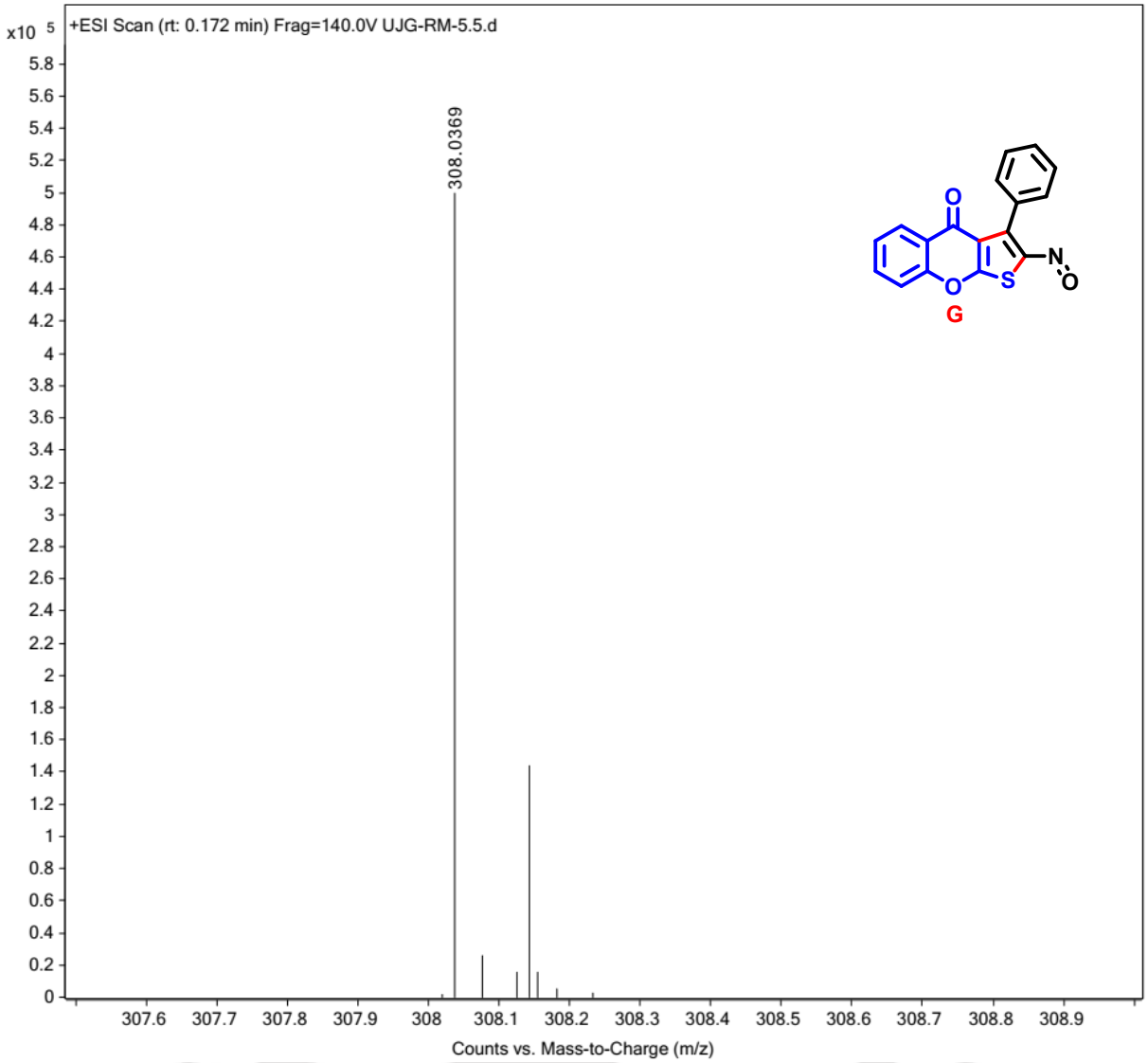

Figure 4.5c: HRMS spectrum of compound **H** or **I**.

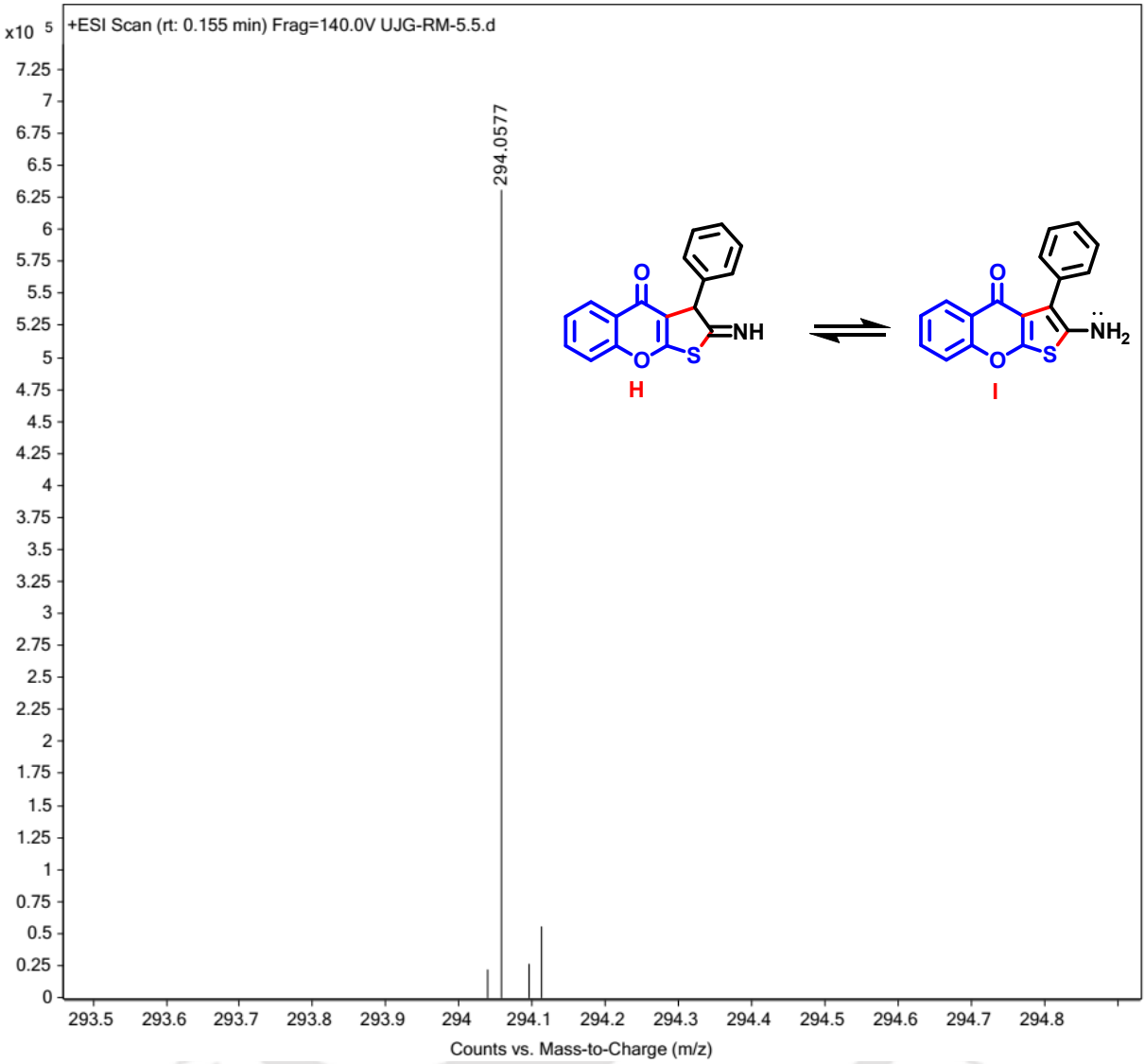

References

[1] C. F. M. Silva, D. C. G. A. Pinto, A. M. S. Silva, *ChemMedChem* **2016**, *11*, 2252–2260.

[2] V. M. Patil, N. Masand, S. Verma, V. Masand, *Chem. Biol. Drug Des.* **2021**, *98*, 943–953.

[3] B. O. Do Nascimento, O. C. Da Silva Neto, M. T. Teodoro, E. De Oliveira Silva, M. L. S. Guedes, J. M. David, *Phytochem. Lett.* **2020**, *39*, 124–127.

[4] S. Thakur, D. Kumar, S. Jaiswal, K. K. Goel, P. Rawat, V. Srivastava, S. Dhiman, H. R. Jadhav, A. R. Dwivedi, *RSC Med. Chem.* **2025**, *16*, 481–510.

[5] M. Benabdellah, A. Aouniti, A. Dafali, B. Hammouti, M. Benkaddour, A. Yahyi, A. Ettouhami, *Appl. Surf. Sci.* **2006**, *252*, 8341–8347.

[6] C. Kim, K. S. Choi, J. H. Oh, H.-J. Hong, S.-H. Han, S. Y. Kim, *Sci. Adv. Mater.* **2015**, *7*, 2401–2409.

[7] K. Wittine, I. Ratkaj, K. Benci, T. Suhina, L. Mandić, N. Ilić, S. K. Pavelić, K. Pavelić, M. Mintas, *Med. Chem. Res.* **2016**, *25*, 728–737.

[8] F. Havaldar, S. Bhise, S. Burudkar, *J. Serb. Chem. Soc.* **2004**, *69*, 527–532.

[9] M. Gaber, N. El-Wakiel, K. El-Baradie, S. Hafez, *J. Iran. Chem. Soc.* **2019**, *16*, 169–182.

[10] S. Nayab, A. Alam, N. Ahmad, S. W. Khan, W. Khan, D. F. Shams, M. I. A. Shah, M. Ateeq, S. K. Shah, H. Lee, *ACS Omega* **2023**, *8*, 17620–17633.

[11] A. Kajal, S. Bala, S. Kamboj, N. Sharma, V. Saini, *J. Catal.* **2013**, *2013*, 1–14.

[12] J. Sheng, B. Chao, H. Chen, Y. Hu, *Org. Lett.* **2013**, *15*, 4508–4511.

[13] J. W. H. Watthey, M. Desai, *J. Org. Chem.* **1982**, *47*, 1755–1759.

[14] R. C. Cioc, E. Ruijter, R. V. A. Orru, *Green Chem.* **2014**, *16*, 2958–2975.

[15] W. Ye, Y. Li, L. Zhou, J. Liu, C. Wang, *Green Chem.* **2015**, *17*, 188–192.

[16] H. Rostami, L. Shiri, *ChemistrySelect* **2020**, *5*, 11197–11220.

[17] T. Wang, X. Qing, C. Dai, Z. Su, C. Wang, *Org. Biomol. Chem.* **2018**, *16*, 2456–2463.

[18] C. Li, X. Zhou, F. Zhang, Z. Shen, *Curr. Org. Chem.* **2023**, *27*, 108–118.

[19] K. Mahato, P. R. Bagdi, A. T. Khan, *Org. Biomol. Chem.* **2017**, *15*, 5625–5634.

[20] Z. Zhou, H. Liu, Y. Li, J. Liu, Y. Li, J. Liu, J. Yao, C. Wang, *ACS Comb. Sci.* **2013**, *15*, 363–369.

[21] Y. Li, H. Liu, L. Sun, J. Liu, Z. Xue, J. Yao, C. Wang, *Synlett* **2013**, *24*, 1851–1855.

[22] S. Ali, R. Gattu, V. Singh, S. Mondal, A. T. Khan, G. Dubey, P. V. Bharatam, *Org. Biomol. Chem.* **2020**, *18*, 1785–1793.

[23] P. T. Anastas, J. C. Warner, *Green Chemistry: Theory and Practice*, Oxford University Press, Oxford, **2000**.

[24] J.-T. Liu, C.-F. Yao, *Tetrahedron Lett.* **2001**, *42*, 6147–6150.

[25] L. J. Farrugia, *J. Appl. Crystallogr.* **2012**, *45*, 849–854.

Chapter 5

Thesis Overview and Future Perspectives

5.1 Thesis Overview

This thesis is structured into five chapters, beginning with an introductory chapter that establishes the scientific background, followed by three experimental chapters, each presenting a distinct research project rooted in the reactivity of 4-hydroxythiocoumarin. Collectively, the work explores novel synthetic methodologies to generate diverse sulfur-containing heterocyclic scaffolds with potential therapeutic relevance.

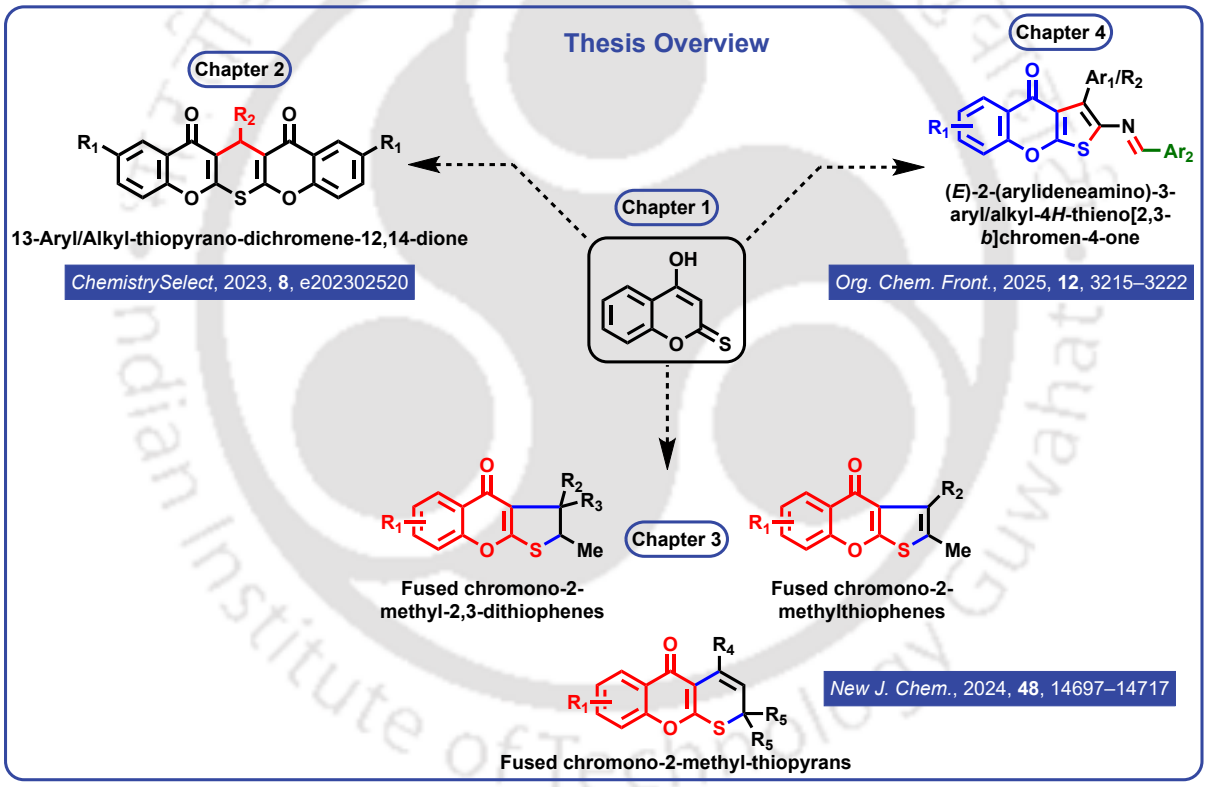

A brief outline of each chapter is as follows:

Chapter 1 introduces 4-hydroxythiocoumarin as a key sulfur-based scaffold, highlighting its relevance as a bioisosteric analog of 4-hydroxycoumarin. It reviews structural features, reactivity patterns, and medicinal significance, and includes a discussion on the design of hybrid heterocycles. The chapter also outlines synthetic approaches to 4-hydroxythiocoumarin, including literature precedents, a revised strategy, and characterization of derivatives, thereby establishing the foundation for the synthetic work detailed in subsequent chapters.

Chapter II describes a catalyst- and solvent-free synthesis of pentacyclic-dione derivatives *via* a pseudo-three-component reaction with aldehydes. The method features mild conditions,

broad substrate scope, and high atom economy, aligning with green chemistry principles. Optimization, characterization, and mechanistic aspects are also discussed.

Chapter III investigates the thermal reactivity of *S*-allyl or *S*-propargyl derivatives of 4-hydroxythiocoumarin, leading to solvent-dependent thio-Claisen rearrangements that yield fused chromono-thiophene and thiopyran derivatives *via* a cascade process. DFT studies provide mechanistic insights into the rearrangement pathways.

Chapter IV describes a regioselective multicomponent synthesis of substituted thieno[2,3-*b*]chromen-4-ones with pendant imine groups. The transformation involves Michael addition, intramolecular cyclization, and an unusual oxime-to-amine conversion *via* disproportionation. The method is regioselective and efficient and it forms multiple bonds in a single step.

5.2 Future Perspectives

The findings presented in this thesis open several avenues for further exploration and application. Key future directions are outlined below:

1. **Pharmacological Exploration:** The synthesized hybrid molecules, particularly the chromone-thiopyran and chromone-thiophene derivatives, warrant extensive biological evaluation. Screening for anticancer, antimicrobial, or anti-inflammatory activities could reveal promising candidates for therapeutic development.

2. **Structural Modifications for Drug Design:** The privileged scaffolds developed in this work can serve as valuable templates for medicinal chemistry. Tailored structural modifications may enhance key pharmacokinetic parameters such as aqueous solubility, metabolic stability, and membrane permeability, thereby improving their suitability for pharmaceutical applications.

3. **Scale-Up and Industrial Applications:** The synthetic methodologies employed herein, especially those demonstrating catalyst- and solvent-free conditions or mild base-promoted multicomponent reactions, offer significant potential for scale-up. Optimization for industrial settings may enable the efficient and sustainable production of pharmaceutically relevant compounds or specialty chemicals.

4. **Post-Synthetic Diversification *via* Pendant Imines:** The presence of a pendant imine group in the thieno[2,3-*b*]chromen-4-one framework (**Chapter 4**) presents versatile opportunities for chemical diversification:
    - *Reduction to Secondary Amines:* The imine (–C=N–) functionality can be reduced to secondary amines, allowing further derivatization (e.g., *N*-alkylation or acylation) to modulate solubility, bioavailability, or biological target affinity.

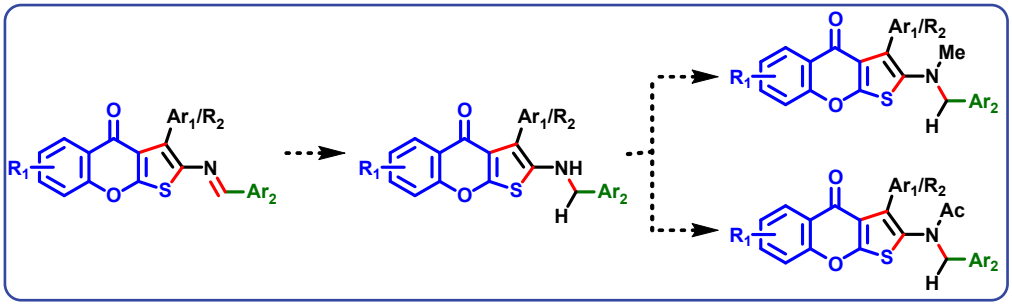

- *MCR Compatibility:* Imines are known to participate actively in multicomponent reactions due to their ambident nature. The electron-rich nitrogen can act as a nucleophile, while the imine carbon functions as an electrophilic center, akin to a masked carbonyl group. This dual reactivity enables the formation of Mannich-type products when combined with suitable carbon nucleophiles.
- *Electrophilic Activation:* The electrophilicity of the imine carbon can be further enhanced *via* Brønsted acid protonation of the nitrogen atom, facilitating reactivity with a broader range of nucleophiles.
- *Cycloaddition Pathways:* Imines can also function as azadienes or dienophiles in cycloaddition reactions, offering pathways to construct complex nitrogen-containing heterocycles.
- *Bidentate Chelation:* The imine functionality enables bidentate coordination through both the nitrogen lone pair and the adjacent phenolic oxygen. Upon deprotonation of the phenolic hydroxyl group, these ligands form stable six-membered chelate rings with transition metals (e.g., Cu, Zn), facilitating the formation of metal complexes with potential applications in catalysis, photophysics, or as metallodrugs.

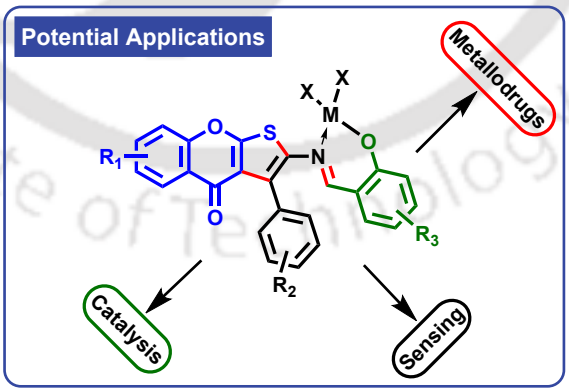

These future directions collectively aim to enhance the utility and translational relevance of the synthesized scaffolds in both academic and industrial contexts.

5.3 Concluding Remarks

The studies presented in this thesis highlight the untapped synthetic potential of 4-hydroxythiocoumarin as a modular and sustainable core for the generation of structurally complex

heterocycles. The work demonstrates that sulfur substitution at the coumarin framework not only imparts unique reactivity but also enables access to novel scaffolds *via* efficient multicomponent and rearrangement-based transformations. Through a combination of diverse reactivity patterns, mechanistic novelty, and alignment with green chemistry principles, this study lays the groundwork for future advances in organosulfur drug design and heterocyclic synthesis.

Appendix

Peer-Reviewed Publications and Conference Presentations

Publications in Peer-Reviewed Journals Based on the Thesis Work

1. **Ujjwal Jyoti Goswami**, Anjela Xalxo, and Abu Taleb Khan*, Catalyst- and solvent-free synthesis of pentacyclic-dione derivatives from 4-hydroxythiocoumarin and aldehyde using pseudo-three-component reaction, *ChemistrySelect* **2023**, *8*, e202302520. DOI: 10.1002/slct.202302520.

2. **Ujjwal Jyoti Goswami**, Anjela Xalxo, Kusum, Mapleleaf Basumatary, Kaushik Soni, Kalishankar Bhattacharyya, and Abu Taleb Khan*, Reactivity study of 4-hydroxythiocoumarin: A novel synthetic route to fused chromono-thiophene and -thiopyran derivatives through solvent-dependent thio-Claisen rearrangement, *New J. Chem.* **2024**, *48*, 14697–14717. DOI: 10.1039/D4NJ02617A.

3. **Ujjwal Jyoti Goswami**, Anjela Xalxo, and Abu Taleb Khan*, A regioselective and sustainable approach for the synthesis of substituted thieno[2,3-*b*]chromen-4-ones with pendant imine groups *via* a base-promoted multicomponent reaction, *Org Chem. Front.* **2025**, *12*, 3215–3222. DOI: 10.1039/D5QO00228A.

Additional Publications in Peer-Reviewed Journals Not Included in This Thesis

1. Anjela Xalxo, **Ujjwal Jyoti Goswami**, Shilpi Sarkar, Thirukumaran Kandasamy, Kriti Mehta, Siddhartha S. Ghosh, Prasad V. Bharatam, and Abu Taleb Khan*, Synthesis of 3-sulfenylindole derivatives from 4-hydroxy-2*H*-chromene-2-thione and indole using oxidative cross-dehydrogenative coupling reaction and anti-proliferative activity study of some of their sulfone derivatives, *Bioorg. Chem.* **2023**, *141*, 106900. DOI: 10.1016/j.bioorg.2023.106900.

2. Anjela Xalxo, **Ujjwal Jyoti Goswami**, Chiranjit Das, Kriti Mehta, Prasad V. Bharatam, and Abu Taleb Khan*, A reactivity study of 4-hydroxy-2*H*-chromene-2-thione and 4-hydroxy-2*H*-thiochromene-2-thione with *tert*-butyl nitrite and aromatic amines: an environmentally benign synthesis of new hydrazone derivatives, *Synthesis* **2025**, *57*, 616–628. DOI: 10.1055/a-2434-9481.

3. Anjela Xalxo, **Ujjwal Jyoti Goswami**, and Abu Taleb Khan*, Regioselective synthesis of 3-benzoyl-4-phenyl-4*H*,5*H*-thiopyrano[2,3-*b*]chromen-5-one derivatives through one-pot domino reaction using aromatic aldehyde, β-enaminone, and 4-hydroxy-2*H*-chromene-2-thione, *Eur. J. Org. Chem* **2025**, *00*, e202500788. DOI: 10.1002/ejoc.202500788.

Posters Presented in International Conferences

1. **Ujjwal Jyoti Goswami** and Abu Taleb Khan*. *A regioselective and sustainable approach for the synthesis of substituted thieno[2,3-b]chromen-4-ones with pendant imine groups via a base-promoted multicomponent reaction.*

Conference: Innovation and Advances in Chemical Sciences – 2025.
Venue: Cotton University, Guwahati-781001, Assam, India.

2. **Ujjwal Jyoti Goswami** and Abu Taleb Khan*. *Condition Dependent Thio-Claisen Rearrangement: Easy Access to Thiopyran and Thiophene Fused Chromen-4-ones Derived from 4-Hydroxythiocoumarin.*

   Conference: Frontiers in Chemical Sciences – 2022.
   Venue: Indian Institute of Technology Guwahati, Guwahati-781039, Assam, India.